ISBN: 978-3-95450-197-7 doi:10.18429/JACoW-RUPAC2018-MOXMH01

DAΦNE COLLIDER WITH CRAB WAIST SCHEME: FROM KLOE-2 TO SIDDHARTA-2 EXPERIMENT

M. Zobov†, D. Alesini, S. Bini, O. R. Blanco-García, M. Boscolo, B. Buonomo, S. Cantarella, S. Caschera, A. De Santis, G. Delle Monache, C. Di Giulio, G. Di Pirro, A. Drago, A. D'Uffizi, L. G. Foggetta, A. Gallo, R. Gargana, A. Ghigo, S. Guiducci, S. Incremona, F. Iungo, C. Ligi, M. Maestri, A. Michelotti, C. Milardi, L. Pellegrino, R. Ricci, U. Rotundo, L. Sabbatini, C. Sanelli, G. Sensolini, A. Stecchi, A. Stella, A. Vannozzi, LNF-INFN, Frascati, Italy
J. Chavanne, G. Le Bec, P. Raimondi, ESRF, Grenoble, France
G. Castorina, Roma1-INFN, Roma, Italy

Abstract

In March 2018 DAΦNE, the Italian electron-positron Φ-factory based on the Crab Waist (CW) collision concept, has successfully completed the challenging experimental run for the KLOE-2 detector. At present, installation of the SIDDHARTA-2 detector is underway in order to start data acquisition with the new experimental apparatus in the year 2019. In this paper we review the collider performances during the KLOE-2 run in terms of the achieved beam currents, the peak and integrated luminosity and encountered beam dynamics challenges. The design and development work done in view of the SIDDHARTA-2 operation is presented and discussed.

INTRODUCTION

DAΦNE [1, 2] is an accelerator complex consisting of a double ring lepton collider working at the c.m. energy of the Φ-resonance (1.02 GeV) and an injection system. The collider includes two independent rings, each ~ 97 m long. The two rings share a common interaction region (IR), where the detector on duty is installed. A full energy injection system, including an S-band linac, 180 m long transfer lines and an accumulator/damping ring, provides fast and high efficiency electron–positron injection also in topping-up mode while delivering luminosity.

DAΦNE became operational in 2001 and it is still an attractive collider to perform relevant high energy and nuclear physics experiments. This has been possible due to a continuous effort aimed at improving collider performances, which culminated with the realization of a new approach to the beam-beam interaction, Crab Waist (CW) collision scheme [3, 4], during DAΦNE operation with the SIDDHARTA apparatus [5, 6]. Such developments paved the way to a new run with a revised KLOE detector, KLOE-2 [7], which in view of a higher luminosity extended its physics search program.

Presently DAΦNE, after having successfully completed the KLOE-2 run in March 2018, is facing the preparatory phase for a new operational period aimed at delivering data to the SIDDHARTA-2 detector [8], an upgraded version of the old apparatus. The new experimental program aims at performing the first kaonic deuterium measurement by improving its measurement resolution. The experiment aims at integrating a sample of data of the order of 1.0 fb^{-1}. This target should be achieved in one year operations.

† Mikhail.Zobov@lnf.infn.it

KLOE-2 INTERACTION REGION

Using the Crab Waist collision scheme the highest DAΦNE peak luminosity of 4.5×10^{32} $cm^{-2}s^{-1}$ was achieved with the SIDDHARTA apparatus that is a small detector without solenoidal field [5]. For the KLOE-2 run the high luminosity IR was modified to host a large detector with a strong solenoidal field which significantly perturbs beam dynamics introducing new design challenges in terms of interaction region optics design, beam transverse coupling control and beam stay clear requirements [9]. Figure 1 shows a schematic drawing of the KLOE-2 interaction region.

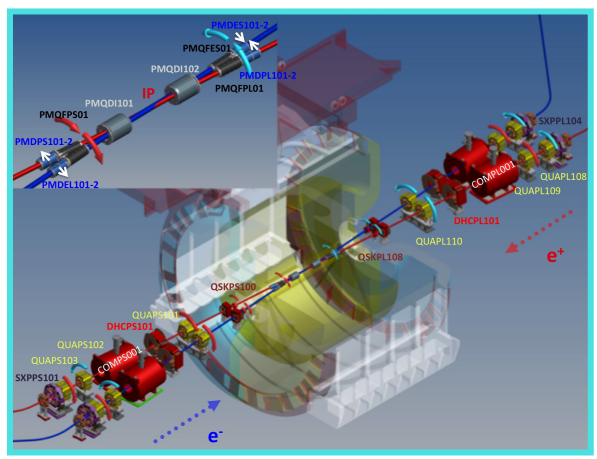

Figure 1: Schematic drawing of the KLOE-2 IR.

The KLOE-2 detector superconducting solenoid has an intense 2.3 Tm integrated magnetic field which, due to the low collider energy, results in the beam transverse oscillation plane rotation by an angle of about 39 degrees. The field integral introduced by the solenoidal detector is almost cancelled by means of two anti-solenoids, installed in each ring symmetrically with respect to the interaction point (IP), which provide compensation also for off-energy particles. The rotation of the beam transverse plane is compensated by co-rotating the IR quadrupoles. Only the first low beta quadruples have been kept in the upright position in order to avoid a significant displacement of the vertical beam trajectory. In addition, in order to keep the vertical trajectory within reasonable values a

ISBN: 978-3-95450-197-7 doi:10.18429/JACoW-RUPAC2018-MOXMH02

VEPP-2000 COLLIDER OPERATION IN FULL ENERGY RANGE WITH NEW INJECTOR

D. Shwartz†[1], V. Anashin, A. Batrakov, O. Belikov, D. Berkaev, D. Burenkov, K. Gorchakov, A. Kasaev, A. Kirpotin, I. Koop[1], A. Krasnov[1], G. Kurkin, A. Lysenko, S. Motygin, A. Otboyev, A. Pavlenko, E. Perevedentsev[1], V. Prosvetov, D. Rabusov, Yu. Rogovsky[1], A. Semenov, A. Senchenko[1], D. Shatilov, P. Shatunov, Yu. Shatunov[1], O. Shubina, M. Timoshenko, S. Vasichev, V. Yudin, I. Zemlyansky, Yu. Zharinov

Budker Institute of Nuclear Physics, Novosibirsk, 630090, Russia
[1]also at Novosibirsk State University, Novosibirsk, 630090, Russia

Abstract

VEPP-2000 is the only electron-positron collider operating with round beams that allow to enhance beam-beam limit. VEPP-2000 with SND and CMD-3 detectors carried out two successful data-taking runs after new BINP injection complex was commissioned. The 2016/2017 run was dedicated to high energy range (640-1000 MeV per beam) while the 2017/2018 run was focused at 275-600 MeV/beam energies. With sufficient positron production rate and upgraded full-energy booster the collider luminosity was limited by beam-beam effects, namely flip-flop effect. Thorough machine tuning together with new ideas introduced to suppress flip-flop allowed to establish new world record for beam-beam parameter and bunch-by-bunch luminosity values at specific beam energies. The achieved luminosity increased 2-5 times in a whole energy range in comparison to phase-1 operation (2010-2013).

VEPP-2000 OVERVIEW

VEPP-2000 is a small 24 m perimeter single-ring collider operating in one-by-one bunch regime in the energy range below 1 GeV per beam [1-4]. Its layout is presented in Fig. 1. Collider itself hosts two particle detectors [5, 6], Spherical Neutral Detector (SND) and Cryogenic Magnetic Detector (CMD-3), placed into dispersion-free low-beta straights. The final focusing (FF) is realized using superconducting 13 T solenoids. The main design collider parameters are listed in Table 1.

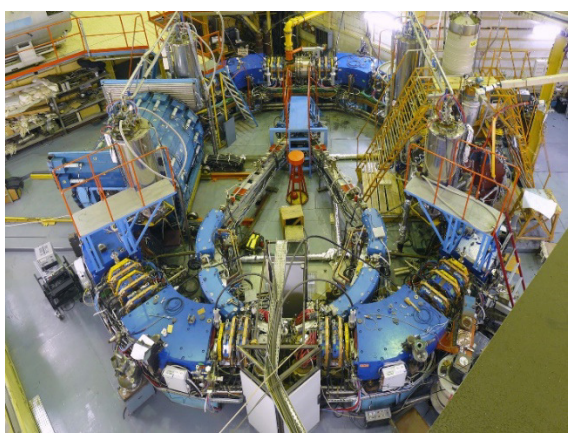

Figure 1: VEPP-2000 collider photo.

Table 1: VEPP-2000 Design Parameters (at E = 1 GeV)

Parameter	Value
Circumference, C	24.39 m
Energy range, E	150–1000 MeV
Number of bunches	1 × 1
Number of particles per bunch, N	1×10^{11}
Betatron functions at IP, $\beta^*_{x,y}$	8.5 cm
Betatron tunes, $\nu_{x,y}$	4.1, 2.1
Beam emittance, $\varepsilon_{x,y}$	1.4×10^{-7} m rad
Beam–beam parameters, $\xi_{x,z}$	0.1
Luminosity, L	1×10^{32} cm^{-2} s^{-1}

Injection Chain Upgrade

During commissioning and first operation phase in 2010–2013 VEPP-2000 used old positron production and injection chain that restricted available positron beam intensity and limited the luminosity at energy range above 500 MeV. Since 2016, VEPP-2000 is linked to the new BINP injection complex (IC) [7, 8] via long transfer channel. In addition, the booster BEP was upgraded in order to increase top energy up to 1 GeV and perform top-up injection [9]. Minor changes were made in addition at VEPP-2000 storage ring [10, 11].

SND and CMD-3 Physics Program

Experimental program at VEPP-2000 includes:

1. Precise measurement of $R = \sigma(e^+e^- \to \text{hadrons})/\sigma(e^+e^- \to \mu^+\mu^-)$ to achieve less than 1% systematic for major channels. Contribution to magnetic anomaly of muon $(g-2)/2$ comes mainly from low energy ranges.
2. Study of exclusive hadronic channels of e^+e^- annihilation, ~ 30 channels in total.
3. Study of the "excited" vector mesons: ρ', ρ'', ω', ϕ'.
4. Study of G_E/G_M for nucleons near threshold.
5. CVC tests: comparison of isovector part of cross section to hadrons with τ-decay spectra.
6. Measurement of the cross-sections using ISR.
7. Diphoton physics, e.g. η, η' production.

† d.b.shwartz@inp.nsk.su

ISBN: 978-3-95450-197-7 doi:10.18429/JACoW-RUPAC2018-MOXMH03

STATUS OF ACCELERATOR COMPLEX NICA

E. Syresin, O. Brovko, A. Butenko, E. Donets, E. Gorbachev, A. Govorov, V. Karpinsky, V. Kekelidze, H. Khodzhibagiyan, S. Kostromin, A. Kovalenko, O. Kozlov, K. Levterov, I. Meshkov, A. Sidorin, V. Slepnev, A. Smirnov, G. Trubnikov, A. Tuzikov, V. Volkov, JINR, Dubna, Moscow Region, Russia
V. Parkhomchuk, A. Tribendis, A. Zhuravlev, BINP SB RAS, Novosibirsk, Russia

Abstract

The Nuclotron-based Ion Collider fAcility (NICA) is under construction in JINR. The NICA goals are providing of colliding beams for studies of hot and dense strongly interacting baryonic matter and spin physics. The accelerator facility of collider NICA consists of following elements: acting Alvarez-type linac LU-20 of light ions at energy 5 MeV/u, constructed a new light ion linac at ion energy 7 MeV/u with additional acceleration section for protons at energy 13 MeV, acting heavy ion linac HILAC with RFQ and IH DTL sections at energy 3.2 MeV/u, superconducting booster synchrotron at energy up 600 MeV/u, acting superconducting synchrotron Nuclotron at gold ion energy 4.5 GeV/n and two collider storage rings with two interaction points. The status of acceleration complex NICA is under discussion.

INTRODUCTION

The NICA accelerator complex (Fig. 1) [1] is constructed and commissioned at JINR. NICA experiments shall be performed in search of the mixed phase of baryonic matter and nature of nucleon/particle spin. The new NICA accelerator complex will permit implementing experiments in the following modes: with the Nuclotron ion beams extracted at a fixed target; with colliding ion beams in the collider; with colliding ion-proton beams; with colliding beams of polarized protons and deuterons.

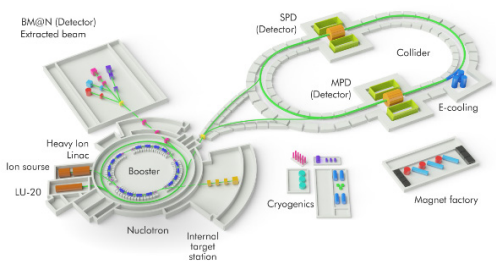

Figure 1: Layout of the NICA Accelerator complex.

The NICA complex (Fig. 1) includes the following main elements: an injection complex; a Booster; the superconducting synchrotron Nuclotron; a Collider composed of two superconducting rings with two beam interaction points; two detectors a Multi-Purpose Detector (MPD) and a detector for experiments in particle spin physics, the Spin Physics Detector (SPD); channels for beam transportation.

INJECTION ACCELERATOR COMPLEX NICA

The injection complex [2] includes a set of ion sources and two linear accelerators. The first one, the LU-20 linear accelerator, which is under operation since 1974, accelerates protons and ions from few sources: the laser source and the source of polarized ions (SPI) - protons and deuterons. SPI was constructed by JINR-INR RAS collaboration. The beam current of polarized deuterons corresponds to 2 mA. At the LU-20 exit, the energy of ions is 5 MeV/n. At present time, the LU-20 beam is injected directly into the Nuclotron. The HV injector of linac LU-20 has been replaced in 2016 by RFQ [2,3] with beam matching channels. The RFQ was constructed by JINR, ITEP of NRC "Kurchatov Institute", NRNU MEPHI, VNIITF collaboration. The new buncher constructed by ITEP of NRC "Kurchatov Institute" was installed between RFQ and LU20 in 2017. Installation of new buncher permits to increase the heavy ion beam current in 5 times in Nuclotron 55 run in 2018.

The design of new Light Ion Linac (LILAc) was started in 2017 to replace the LU-20 in NICA injection complex. LILAc consists of three sections: warm injection section applied for acceleration of light ions and protons up to energy 7 MeV/n [2,4], warm medium energy section used for proton acceleration up to energy 13 MeV [3] and superconducting HWR sections [2, 5], which provides proton acceleration up to energy 20 MeV. The LILAC should provide beam current of 5 emA. The construction of first light ion section [4] at ion energy 7 MeV/n was started in 2018 by Bevatech GmbH (Germany), it should be delivered in JINR in 2021. The next step of the LILAc project – design of a middle energy section [3] and HWR superconducting sections [2, 5]. The increased beam energy of LILAc is required for future researches with polarized proton beams. The operating frequency of the LILAc is equal to 162.5 MHz for first two sections and 325 MHz for HWR section. The superconducting HWR are designed and constructed by Russian-Belarusian collaboration with participation of JINR, NRNU MEPhI, ITEP of NRC "Kurchatov Institute", INP BSU, PTI NASB, BSUIR and SPMRC NASB.

The second accelerator of NICA injection complex— a new heavy-ion linear accelerator (Heavy Ion Linac, HILAc) [2] (Fig. 2) constructed by JINR-Bevatech collaboration is under exploitation since 2016. It will accelerate heavy ions ($^{197}Au^{31+}$ ions have been chosen as the base ions) injected from KRION-6T, a superconducting electron-string heavy ion source, constructed by JINR. At present time KRION-6T produces $5 \cdot 10^{8}$ Au^{31+} ions. This ion

ISBN: 978-3-95450-197-7 doi:10.18429/JACoW-RUPAC2018-TUXMH01

STATUS AND DEVELOPMENT PROSPECTS OF CHARGED-PARTICLE ACCELERATORS IN RFNC-VNIIEF

N.V. Zavyalov#, S.V. Vorontsov, V.S. Gordeev, , A.V. Grunin, L.N. Generalov, S.L. Glushkov, A.A. Devyatkin, S.A. Lazarev, G.A. Myskov, S.T. Nazarenko, V.S. Pavlov, V.I. Smerdov, M.L. Smetanin, K.V. Strabykin, A.V. Telnov, I.V. Shorikov, S.L. Elyash, V.A. Yukhnevich

Since the sixties of the twentieth century, a large experimental and test base of facilities and complexes have been developed in RFNC-VNIIEF. It allows studies of radiation hardness for electronic component base and electronic radio equipment (ERE), radiographic examinations of fast processes, nuclear physics researches. Experimental and test base of RFNC-VNIIEF is a federal importance base and provides needs of enterprises: state corporation (SC) "Rosatom", Department of Defence, Department of Industry and Trade and SC "Roscosmos". The base involves pulse high-current electron accelerators, pulsed nuclear reactors (PNR), linear resonance electron accelerators, electrostatic tandem accelerator EGP-10, plasma pulsed neutron radiation generators. Irradiation complexes are developed on the basis of linear induction electron accelerators (LIA) and PNR.

Accelerator LIU-30 [1-3], which is a basic facility for a multipurpose irradiation complex PULSAR [4, 5], was put into operation in 1988. The accelerator allows to produce accelerated electrons with the energy up to 40 MeV (record for its facility class) and beam current ~ 100 kA with pulse width ~ 20 ns. Furthermore, the facility is one of the most high-power sources of bremsstrahlung (BR) short pulses in the world. The common view of LIU-30 accelerator is given in Fig. 1.

Figure 1: Overall view of LIU-30 accelerator.

At present LIU-30 acceleration system is arranged as a 32-module structure with an independent power supply and module control for each module. Each module of the accelerating path contains one unit comprised of four inductors with on water insulated radial lines, possessing a common accelerating tube.

Besides 32 modules, the accelerator structure comprises transport system and output device with a target providing stable beam transport and BR field formation in the irradiation hall of PULSAR complex. The accelerating system length ~ 23 m, both with transport system ~ 30 m, width ~ 9.5 m, height ~ 4 m.

The most steady BR generation mode is optimized at beam current amplitude 70 kA, when BR dose per a pulse at a distance 1 m from the target is ~ 4.5 kR, average dose rate ~ $2.5 \cdot 10^{11}$ R/s at BR pulse half-height duration ~ 18 ns.

The system of electron beam compression at the output of the transport guide can be attached for a radial beam compressed by a magnet field enhancing along the axis, what allows generation of a dose ~ 240 krad (thermoluminescent detector) and BR dose rate ~ $1.5 \cdot 10^{13}$ prad/s in a spot with the area of ~ 100 cm^2 with irradiation heterogeneity 50 % at radiation pulse length $\tau_{1/2} \approx 16$ ns [6].

In the period from 2006 to 2015 without stops in facility operation accelerating units of inductors and transport guide section have been sequentially upgraded; as a result the reliability and functioning steadiness of LIU-30 accelerator [7, 8] have significantly grown.

Basic facility of the irradiation complex LIU-10M-GIR2 is a linear induction accelerator LIU-10M [9, 10]. The accelerator is manufactured on the basis of VNIIEF developed step-like forming lines. As a result of wave processes, output accelerating voltage a several times higher compared to the line charge voltage. The accelerating system (Fig. 2) consists of injector, 16 typical accelerating modules, each involving one inductor, the transport electron beam guide of 4 m length and the output device with a target unit. Dimensions of the accelerating system without the transport guide – (12×3.5×2.4) m^3. Diameter of inductors – 1.1 m, axis dimension – 0.58 m.

At a 1 m distance from the target the BR pulse dose rate, generated by the accelerator is $4 \cdot 10^{10}$R/s at half-height duration from 10 up to 20 ns. At the electron beam compression mode near the accelerator target the obtained BR dose rate is ~ $4 \cdot 10^{12}$R/s in the spot of diameter 8 cm at pulse length (15 ± 3) ns. In this case BR dose approaches ~ 60 kR. Boundary energy of accelerated electrons and, respectively, BR quantum approaches 25 MeV.

Zavyalov@expd.vniief.ru

ISBN: 978-3-95450-197-7 doi:10.18429/JACoW-RUPAC2018-TUXMH02

THE MAIN PROBLEMS AND ITS SOLUTIONS IN MODERN SR SOURCES

V.N.Korchuganov, National Research Center Kurchatov Institute, Moscow, 123182, Russia

Abstract

This report is an attempt to consider the basic accelerator problems arising in connection with the requirements of the SR experiment in modern synchrotron radiation sources based on electron storage rings, and the technological solutions available today.

INTRODUCTION

Half a century has passed since the targeted use of synchrotron radiation in experiments in the various areas of knowledge. During this period of time SR sources were turned into factories of photons with high intensity and brightness.

Development of accelerator technologies over the past twenty years has also led to many important results. Successfully tested new magnets designs and fabrication technologies, the innovative vacuum technology, new RF generators for solid state amplifiers, a revolution in digital beam monitoring systems and in feedback systems for orbit correction.

These new technologies will ultimately determine the possible outstanding options for future new accelerator complexes and boundaries moved in experiments.

EVOLUTION OF SR SOURCES

Brightness and Coherence

The pursuit of high stability and high brightness, the desire to increase the coherent radiation fraction has defined crucially perfection of dedicated synchrotron radiation sources based on the electron storage rings.

The average and pick values of the spectral brightness - photon density in 6D phase volume depend on SR intensity and phase spaces of electron beam and radiation phase space of separate electron - are given by the formulae (eq.1).

$$B_{avg}(\lambda) \propto \frac{N_{ph}(\lambda)}{\Sigma_x(\lambda)\cdot\Sigma_y(\lambda)(s\cdot\%BW)},\quad B_{pk}(\lambda) \propto \frac{N_{ph}(\lambda)}{\Sigma_x(\lambda)\cdot\Sigma_y(\lambda)(\sigma_t\cdot\%BW)} \quad (1)$$

The coherence plays an important role in experiments. Uniform phase wave front of transversely coherent X-rays permits to make coherent imaging, holography, speckle, etc.; the possibility to be focused to smallest spot size – nano-focus; the availability of high flux (~ 10^{14}-10^{15} photon/sec) in small spot – slits may not be required, etc; round beams mean symmetric optics, circular zone plates, flexibility in optics.

According with definition the radiation coherent fraction at a given wavelength equals to the relation of the phase volume of the diffraction - limited source to the phase volume of the real source (eq. 2).

$$f_{cog}(\lambda) = \frac{\lambda/4\pi}{\Sigma_x(\lambda)}\cdot\frac{\lambda/4\pi}{\Sigma_y(\lambda)} \quad (2)$$

Here: $\Sigma_{x,y}(\lambda) = \sqrt{\sigma_r^2(\lambda)+\sigma_{x,y}^2}\cdot\sqrt{\sigma'^2_r(\lambda)+\sigma'^2_{x,y}}$, σ_τ – bunch length, $\varepsilon_r(\lambda) = \lambda/4\pi$ – the diffraction limited emittance for coherent Gaussian photon distribution (laser beam) and $\varepsilon_r(\lambda) \approx \frac{\lambda}{2\pi}$ - the diffraction limited emittance for undulator radiation from single electron filament, $\varepsilon_{x,y}$ are the horizontal and vertical emittances of the electron beam, $\sigma_{x,y} = \sqrt{\varepsilon_{x,y}\cdot\beta_{x,y}}$, $\sigma'_{x,y} = \sqrt{\varepsilon_{x,y}/\beta_{x,y}}$ -standard horizontal and vertical sizes and the angles of electron bunch, $\sigma_r = \frac{\sqrt{2\lambda L}}{2\pi}$ and $\sigma'_r = \sqrt{\frac{\lambda}{2L}}$ – the size and the angle of photon beam from single electron filament in a undulator with length of L.

We note the absolute value of the coherent part of the total flux is important too. Optimize trade-off between low of emittance vs stored electron current value is necessary.

SR sources Optical Structures Evolution

Electron SR sources that worked with large emittances in spurious mode are considered as SR sources of the 1st generation. The 2-nd generation - 10-100 nm-rad specialized SR sources working mainly on radiation from bending magnets.

The 3-rd generation, 10-1 nm rad specialized SR sources operating on radiation from Insertion Devices. First - 1994: ESRF (France); ALS (USA); Elettra (Italy); next decades: ALBA (Spain), APS (USA), Bessy II (Germany), DIAMOND (UK), MAX III (Sveden), PETRA II (Germany), PLS (South Korea), SLS (Swiss), SOLEIL (France), SPRING-8 (Japan), TLS (Тайвань) and others).

According to the formulae (3), connecting main optics and structure parameters with natural emittance ε,

$$\varepsilon \propto E_0^2\frac{\langle\mathcal{H}/\rho^3\rangle}{\langle 1/\rho^2\rangle},\quad \varepsilon = F(\nu_x, lattice)\cdot\frac{E_0^2}{J_x\cdot N_d^3} \quad (3)$$

to decrease the natural emittance, we can: a) to reduce the energy E_0, b) to increase the bending radius ρ - this leads to larger circumference; c) to decrease so called dispersion invariant $\mathcal{H}=\gamma\eta^2+2\alpha\eta\eta'+\beta\eta'^2$ and, as the consequence, we have to have stronger and more frequent focusing; d) to increase damping - J_x, that is additional damping wigglers to be installed.

Almost all possible kinds of magneto-optical structures were investigated: from structures of type DBA (Double-Bend Achromat or Chasman-Green Achromat) and TBA (Triple-Bend Achromat) to so-called

ISBN: 978-3-95450-197-7 doi:10.18429/JACoW-RUPAC2018-TUYMH02

FOUR-BEAM COMPENSATION WITH TWO BEAMS*

N. A. Vinokurov†[1], Budker Institute of Nuclear Physics SB RAS, 630090, Novosibirsk, Russia
[1]also at Novosibirsk State University, 630090, Novosibirsk, Russia

Abstract

A figure-8 scheme of a storage-ring collider with zero-angle collision and electron and positron beams of equal currents but different energies is considered. In the common straight section, both electrons and positrons move in both directions. Outside the common straight section, electrons and positrons circulate in separated loops (which "reflect" both beams to the common straight section). Therefore, in a multi-bunch mode one can provide collision of four bunches and space charge compensation. This configuration can be considered as the combination of an electron storage ring with electron-electron collisions and a positron storage ring with positron-positron collisions. The new scheme can solve the well-known problem of separating instabilities of compensation in the case of four beams.

INTRODUCTION

Compensating for non-linear focusing in the storage ring colliders due to an opposite-charge beam circulating in another storage ring was proposed and tested many years ago (see [1] and references there). Ya.S. Derbenev had shown first [2] that the scheme suffers from tune shifts of coherent betatron oscillations, which move betatron frequencies toward the nearest integer or half-integer resonance. In this paper we will revisit the stability condition in a simple model of hard short bunches and discuss other configurations of colliders with beam compensation.

CONVENTIONAL SCHEME

Consider first a collider with four rings (see Fig. 1) of revolution periods of $2\pi q_1/\omega_{RF}$ - $2\pi q_4/\omega_{RF}$, described by 2×2 matrices $M_1 - M_4$ (no coupling is assumed).

As the energies of the rings may be different, we will describe the particle state using the dimensionless momentum $\beta\gamma x'$, not the angle x, as the second variable in the column. In the model of hard bunches, coherent betatron oscillations in such a collider with compensation for four beams are described with the following $2(q_1 + q_2 + q_3 + q_4) \times 2(q_1 + q_2 + q_3 + q_4)$ matrices (see, e. g., [1, 2]):

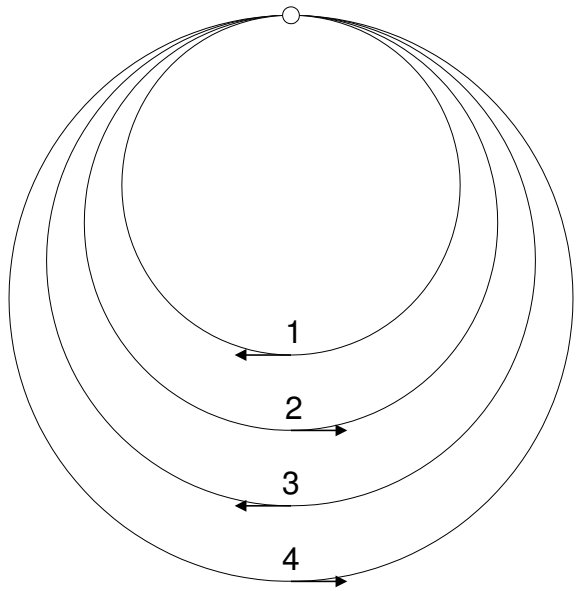

Figure 1: Scheme of four-ring collider.

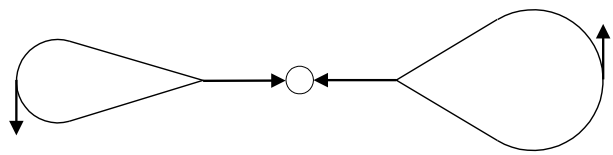

Figure 2: Scheme of electron-electron collider.

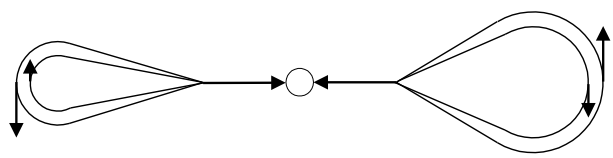

Figure 3: Scheme of two-beam compensated electron-positron collider.

* Work supported by the Russian Science Foundation (project No. 14-50-00080).
† vinokurov@inp.nsk.su

ISBN: 978-3-95450-197-7 doi:10.18429/JACoW-RUPAC2018-TUCBMH01

OPTIMUM LUMINOSITY OF PROTON-ION COLLIDER

I.N. Meshkov, Joint Institute for Nuclear Research, 141980 Dubna, Russia and
St Petersburg University, 199034, St. Petersburg

Abstract

The problem of optimal parameters of proton-ion collider is considered. It is shown that the maximum luminosity of the p-i collider is achieved when the Laslett tune shifts of the ion and proton bunches are equal. As an example, the luminosity of the NICA collider in three different collision mode – ion-ion (symmetric), proton-ion (asymmetric) and proton-proton (symmetric) are presented. These calculations are based on the results of the article [1].

LUMINOSITY OF SYMMETRIC AND ASYMMETRIC CIRCULAR COLLIDERS

Luminosity of Symmetric Colliders

Luminosity of a circular collider in so called symmetric mode of the parameters of the colliding particles and the bunches are identical. Then, the collider luminosity is described by the well-known formula:

$$L = \frac{n_{bunch}N_1N_2f_0}{4\pi\sqrt{\varepsilon_x\varepsilon_y}B^*}\cdot F_{HG},\ F_{HG}(\alpha) = \frac{1}{\sqrt{\pi}}\int_0^\infty \frac{e^{-u^2}du}{1+(\alpha u)^2},\ \alpha = \frac{\sigma_s}{B^*} \quad (1)$$

Here $\varepsilon_{x,\,y}$ - x, y - emittances of the bunches of colliding beams, B* - value of the beta function at the meeting point, n_{bunch} - number of bunches in the beam, $N_{1,2}$ - number of particles in the cluster of the 1st and 2nd beams, σ_s is the length (σ-parameter) of a Gaussian bunch.

Luminosity of an Asymmetric Colliders with a Common Final Focus System

The luminosity of such a collider is described by the formula [1]

$$L = \frac{n_{bunch}N_1N_2f_0}{(2\pi)^2\sigma_{s1}\sigma_{s2}}\cdot Int\,, \quad (2)$$

$$Int = \int_{-\infty}^{\infty}d\xi\int_{-\infty}^{\infty}d\eta\,\frac{f_s(\xi,\eta)}{\sqrt{f_x(\xi,\eta)\cdot f_y(\xi,\eta)}},$$

where

$$f_s(\xi,\eta) = exp\left\{-\frac{1}{2}\left[\frac{\eta^2}{\sigma_{s1}^2}+\left(\frac{\eta+V\xi}{\sigma_{s2}}\right)^2\right]\right\}$$

$$f_x(\xi,\eta) = \left(\varepsilon_{x1}B_{x1}(\xi,\eta)+\varepsilon_{x2}B_{x2}(\xi,\eta)\right)$$

$$f_y(\xi,\eta) = \left(\varepsilon_{y1}B_{y1}(\xi,\eta)+\varepsilon_{y2}B_{y2}(\xi,\eta)\right)$$

Here $V = 1 + v_1 / v_2$. The indices 1 and 2 indicate the parameters of the bunches of the first and second colliding beams and the values of the beta functions $B_{x1,2}$ for them. The particle velocity of the second beam for colliding beams is negative, $v_2 < 0$, whereas for merging beams both velocities are positive, i.e. $v_{1,2} > 0$. The latter do not coincide if the lenses of the final focus of the collider are common for both beams, and the particles of the beams 1 and 2 differ in at least one of the parameters - charge, mass or energy. Beta functions depend on two parameters - the longitudinal coordinates of the colliding particles ξ and η in the moving system of one of the two colliding clusters (see details in [1]). Since the values of the betatron functions $B_{x1,2}$ are proportional to the magnetic rigidity of the particles, it is possible to introduce the relative magnetic stiffness parameter λ of the colliding particles:

$$\lambda_x = \frac{B^*_{x1}}{B^*_{x2}} = \frac{p_1}{Z_1}\cdot\frac{Z_2}{p_2}, \quad (3)$$

where $B^*_{x1,2}$ are the beta function values in the interaction points (IP). $p_{1,2}$ are the momenta of colliding particles, $Z_{1,2}$ are their charges in units of electron charge. It follows that

$$\lambda_y = \lambda_x \equiv \lambda.$$

Formula (3) is simplified if the perimeters of the rings are the same. Then from the collision synchronization condition it follows that $v_1 = v_2$ and

$$\lambda = \frac{p_1}{Z_1}\cdot\frac{Z_2}{p_2} = \frac{A_1m_N\gamma_1v_1}{Z_1}\cdot\frac{Z_2}{A_2m_N\gamma_2v_2} = \frac{A_1}{Z_1}\cdot\frac{Z_2}{A_2}, \qquad \gamma_{1,2} = \frac{1}{\sqrt{1-\beta_{1,2}^2}},\ \beta_{1,2} = \frac{v_{1,2}}{c}, \quad (4)$$

Thus, the values of $\lambda_{x,\,y}$ do not depend on the velocity of the colliding particles.

We shall confine our attention to the case of identical values of the parameters of two beams and *focusing systems of two rings:*

$$C_1 = C_2 \equiv C_{Ring}, Q_{x1} = Q_{y1} = Q_{x2} = Q_{y2} \equiv Q. \quad (5)$$

$$v_1 = v_2, \varepsilon_{x1} = \varepsilon_{x2} = \varepsilon_{y1} = \varepsilon_{y2} \equiv \varepsilon,\ \sigma_{s1} = \sigma_{s2}. \quad (6)$$

The luminosity formula (2) for such an asymmetric collider takes the form (see Appendix):

$$L = \frac{n_{bunch}N_1N_2f_0}{4\pi^{3/2}\varepsilon B_1^*}\cdot Int_{asym}\,,$$

$$Int_{asym} == \int_{-\infty}^{\infty}\frac{e^{-\chi^2}\cdot d\chi}{\left[1+\left(\frac{\sigma_s}{B_1^*}\chi\right)^2\right]+\frac{1}{\lambda}\left[1+\left(\lambda\cdot\frac{\sigma_s}{B_1^*}\chi\right)^2\right]} \quad (7)$$

HOW TO FIND OPTIMAL VALUES OF THE COLLIDER PARAMETERS

Limitation of Collider Parameters by Space-Charge Effects

The choice of the parameters of the collider is determined to a large extent by the stability conditions of the beams circulating in the rings of the collider. The strongest limitations are the effects of the space charge of the beams - the so-called "Laslett effect" and the "beam-beam effect". Both of them lead to shifts in the frequencies of betatron oscillations of particles in the collider focusing system, bringing them closer to the

ISBN: 978-3-95450-197-7 doi:10.18429/JACoW-RUPAC2018-TUCBMH02

STATUS OF THE 2.5 MeV ELECTRON COOLING SYSTEM FOR NICA COLLIDER

V. Parkhomchuk, M. Bryzgunov, A. Bubley, A. Denisov, A. Goncharov, N. Kremnev, V. Panasyuk, A. Putmakov, D. Skorobogatov, BINP SB RAS, Novosibirsk, Russia
Vladimir Reva, BINP SB RAS, Novosibirsk, Russia and NSU, Novosibirsk, Russia

Absract

Status of the development of the 2.5 MV electron cooling system for the NICA collider is reported. The goal of the system is to cool both ion beams during experiment. Cooling of beams during collision prevents grows of beam emittance by compensation of heating effects (intra-beam scattering, beam-beam effects etc.) that increases luminosity of the NICA collider. The system consists of two independent electron coolers in order to meet the requirement of cooling of two independent beams. Each cooler contains high voltage system, transport channels and cooling section. Construction of main parts of the cooling system, results of testing of some prototypes and status of production are described in the article.

INTRODUCTION

Electron cooling was proposed 62 years ago by G.I. Budker at 1966 in BINP [1,2]. As it is generally known, the first estimation of the electron cooling was made with the plasma model of the temperature relaxation and the first experimental results confirmed this fact. But after modernization of the experimental setup the cooling time was decreased significantly from 10 s to 0.1 s. The theoretical and experimental investigation show that the reason is difference in the collision dynamics of electrons and ion at the presence of the strong longitudinal magnetic field that distinguish it from the usual relaxation of two-component plasma. The ion doesn't interact with a single electron but with a blur Larmor circle. The initial temperature of Au ion beam in NICA is about $3 \cdot 10^9$ degree of Kelvin. The electron cooling should suppress IBS, noise at NICA system heats ion beams. There are many the electron cooling devices, which operate now at low and middle energy (SIS-18, CSRm, CSRe, LEIR, ESR, etc). The 2 MeV electron cooling system for COSY-Juelich has the highest energy from all coolers that were made with using idea of the magnetized intensive electron beam. Figure 1 demonstrates cooling of 1.66 GeV proton beam by 0.908 MeV electron beam with current 0.8 A. The initial temperature 10^7 degree of Kelvin dropped down at 10 times and beam size decreased from 3 mm to 1 mm. The experience of COSY cooler used for designing and construction of 2.5 MV electron cooling system for NICA [3]. The biggest problem was design of the cooling section with two counters solenoids with only 32 cm between centres of electron beams with low electric power consumption.

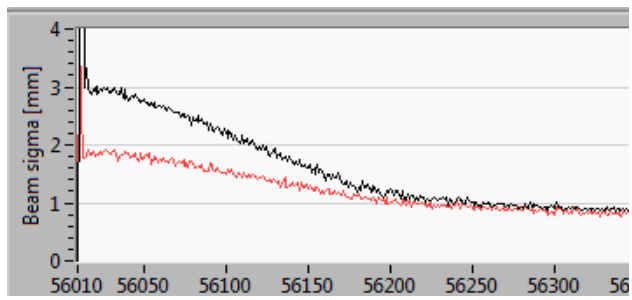

Figure 1: The proton beam cooling at COSY (Julich). The cooling time is about 100 s.

Basic ideas for cooler design:

1. An electron gun was put into a solenoid producing the longitudinal guiding magnetic field, which accompanies the beam until it reaches the collector. The all operated coolers have solenoid field at cooling section. The strong magnet field suppressed transverse motion of electrons.
2. The effect of magnetization the own transverse motion of the electrons help to reach the Kelvin range of the ion beam temperature [4-7]. The nice features solenoid field is the free motion of the light electrons along magnet lines. It help to have the fast cooling by absorbing the kinetic energy of the moving ions. The kinematic suppression of longitudinal motion of electrons after acceleration gives temperature close to 0 at the cooling section. The transverse motion by the space charge of

$$V_{drift} = c\frac{2\pi e n_e}{B} r \qquad (1)$$

the electron beam should be suppressed by the high longitudinal field (B).

The vessel for 2.5 MV electrostatic column p<10bar SF6. The electron gun and collector inside HV terminal. The electron gun with low energy bending for protection the cathode from secondary ion beam bombarding.

The collector equipped filter with crossing electrostatic and magnet fields for suppression reflected from collector electrons (see Fig. 2).

The first 3 high voltage sections were produced and tested at air for corona current and sparking (see Fig. 3). Maximum voltage was obtained near 20 kV. If SF6 gas increase voltage by a factor of 2 and pressure is 4 bar, for 40 section it corresponds to full maximum voltage 6.4 MV. This estimation gives hope to reach working voltage of cooler 2.5 MeV.

ISBN: 978-3-95450-197-7 doi:10.18429/JACoW-RUPAC2018-TUZMH02

VEPP-5 INJECTION COMPLEX PERFORMANCE IMPROVEMENT FOR TWO COLLIDER OPERATION

Yu.I. Maltseva*, A. Andrianov[1], K. Astrelina, V. Balakin[1], A. Batrakov, O. Belikov, D. Berkaev, M. Blinov, D. Bolkhovityanov, A. Butakov, E. Bykov, N. Dikansky, F. Emanov[1], A. Frolov, V. Gambaryan, K. Gorchakov, Ye. Gusev, S. Karnaev, G. Karpov, A. Kasaev, E. Kenzhbulatov, V. Kiselev, S. Kluschev, A. Kondakov, Ivan Koop[1], I. Korenev, N. Kot, V. Kozak, A. Krasnov[1], S. Krutikhin, I. Kuptsov, G. Kurkin, N. Lebedev[1], A. Levichev[1], P. Logatchov, A. Mickailov[1], A. Murasev, V. Muslivets, D. Nikiforov[1], An. Novikov, A. Ottmar, A. Pavlenko[1], I. Pivovarov, V. Rashchenko, Yu. Rogovsky[1], S. Samoylov, N. Sazonov, D. Shwartz[1], A. Skrinsky, A. Starostenko[1], D. Starostenko, A. Tribendis[2], A. Tsyganov, S. Vasichev, S. Vasiliev, V. Yudin, I. Zemlyansky, A. Zhuravlev,
Budker Institute of Nuclear Physics SB RAS, Novosibirsk, Russian Federation
[1]also at Novosibirsk State University, Novosibirsk, Russian Federation
[2]also at Novosibirsk State Technical University, Novosibirsk, Russian Federation

Abstract

VEPP-5 Injection Complex (IC) is designed to supply BINP RAS colliders with high energy electron and positron beams. Recently constructed K-500 beam transfer line connects IC to both VEPP-4M and VEPP-2000 colliders. IC two collider operation was successfully started in 2016. Nowadays, research on improvement of IC performance is carried out, in particular 10.94 MHz RF cavity was installed instead of 700 MHz one and a new 10 A electron gun installation is expected to be in winter 2018-2019. Moreover, streak-camera based longitudinal beam profile measurements in IC damping ring were carried out and BPM system in the damping ring was upgraded. Operation experience of IC and results of longitudinal beam profile measurements are reported.

INTRODUCTION

VEPP-5 Injection Complex (IC) [1–4] supplies VEPP-2000 [5–7] and VEPP-4M [8] colliders with high energy electron and positron beams via recently constructed K-500 beam transfer line [9]. VEPP-2000 switched to IC as its main injector in 2015, VEPP-4M - in summer 2016. Since that time IC has shown the ability to support operation of both colliders routinely. The layout of BINP accelerator facilities is presented in Fig. 1.

IC consists of electron gun, 270 MeV electron linac, isochronous achromatic U-turn, optional conversion system, 510 MeV positron linac and dumping ring. Damping ring (DR) stores both electron and positron beams for further extraction to the K-500 beam transfer line.

Current IC parameters are presented in Table 1. Number of particles of $1.2 \cdot 10^{11}$ corresponds to 200 mA circulating beam in the 27.4 m long DR, which is more than twice project parameters [3, 10]. However, our research is aimed to improve operational stability of the facility.

* yu.i.maltseva@inp.nsk.su

Table 1: IC Beam Production Parameters

Parameter	Value
Energy (2017/2018 runs)	385-420 MeV
Inj./extr. repetition rate	up to 12.5 Hz / 1 Hz
e- storage rate @ 12.5 Hz	$2 \cdot 10^{10}$ /s
e+ storage rate @ 12.5 Hz	$3 \cdot 10^{9}$ /s
Max e-/e+ extraction	up to $1.2 \cdot 10^{11}$

BEAM USER REQUIREMENTS

Since IC supplies both BINP colliders simultaneously, it must fulfill their requirements imposed on beam current, injection repetition rate and collider operation cycles.

VEPP-4M facility has two operating modes: HEP program and SR experiments. For the HEP program 5-10 minutes injection time in the booster is enough to obtain 120-160 mA current for both types of beam ($I_{DR} \approx 2.72\ I_{V3} \approx 13.36\ I_{V4M}$), which is sufficient to reach the desired luminosity. VEPP-3 booster cycle takes 10-15 minutes and after that it is ready for another sort of particles. HEP experiments take 1-2 hours. While SR experiments require 10 minutes electron injection every 5 hours.

VEPP-2000 collider constantly requires beam injection due to small beam lifetime (500 sec) caused mostly by Touschek effect in 24.18 m ring. To achieve the desired luminosity beam current must be 200 mA ($I_{DR} \approx 0.81\ I_{BEP} \approx 0.88\ I_{V2}$) in VEPP-2000 ring, it should not be reduced more than 10%. Thus, adding new portion of 10^{10} particles at least every 50 sec is needed.

While electron storage rate in the DR is not an issue, the requirement to supply 10^{10} positrons every 50 sec was challenging due to small conversion efficiency for positron production. It was required to minimize polarity switching

ISBN: 978-3-95450-197-7 doi:10.18429/JACoW-RUPAC2018-TUZMH03

A FAMILY OF GAZ IONIZATION CHAMBERS AND SEM FOR BEAM LOSS MONITORING OF LHC AND OTHER ACCELERATORS

V. Grishin, European Spallation Source, Lund, Sweden
B. Dehning, E. Effinger, J. Emery, B. Holzer, T.Medvedeva, W. Vigano, C. Zamantzas, CERN, Geneva, Switzerland
A. Koshelev, A. Larionov, V. Seleznev, M. Sleptsov, Institute for High Energy Physics, Protvino, Russian Federation

Abstract

A serious problem for high current accelerators is the high density of the beam, which is able to destroy the equipment and to make a quench of super conductive magnets. Loss of even a small fraction of this intense beam equipment. The Beam Loss Monitor (BLM) system must be sensitive to different levels of losses in different accelerator locations. BLM system protection should limit the losses to a level, which ensures hands-on-maintenance or intervention. On the other side, the BLM system should be sensitive enough to enable the fine tuning and studies by machine with the help of BLM signals. Beam-loss monitoring is the cornerstone element in the accelerator protection and beam setup.

INTRODUCTION

The main beam loss detector type is ionization chamber (IC). The detector is originally designed for CERN Large Hadron Collider (LHC) [1-5] and 4250 nitrogen filled ionization chambers were produced in the Institute for High Energy Physics, Protvino, Russia, in 2006-2008, and currently are widely used in almost all accelerators at CERN, in IHEP (same Protvino) and other accelerators (Fig. 1).

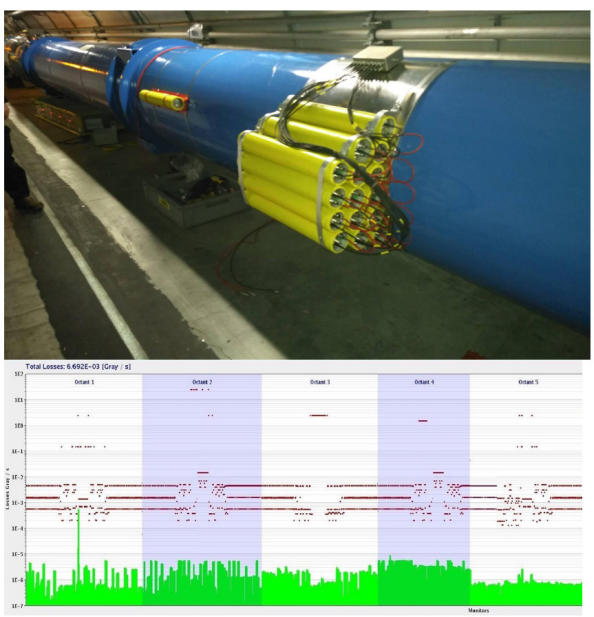

Figure 1: BLM at LHC and control room beam loss display.

In 2014-2017 a new production of 830 IC was performed to replenish spares for LHC and to make series for ESS (Sweden), GSI (Germany) (Fig. 2).

Figure 2: IC at ESS and GSI.

Apart from the IC, the 378 secondary emission monitors (SEM) for LHC, BNL (USA), 300 little ionization chambers (LIC) and 50 flat ionization chambers (FIC) have been manufactured and tested at IHEP in Protvino following their development at CERN (IC, SEM, LIC) [6-8] and IHEP (LIC, FIC).

FAMILIES OF BLM

There are different families of beam loss monitors, produced in CERN-IHEP collaboration (Fig. 3):

a) Ionization chambers (IC), which are installed at local aperture minimum and loss locations,
b) SEM - at very high dose rates locations,
c) LIC - designed to reduce the sensitivity to saturate for higher losses,
d) FIC -detectors designed to geometry considerations.

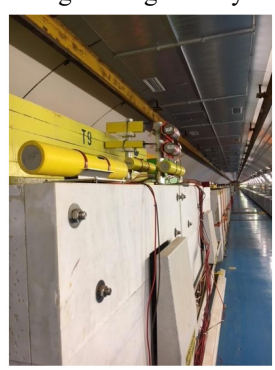

Figure 3: Family of BLM.

Signal speed and robustness against aging were the main design criteria. Each monitor is permanently sealed inside

ISBN: 978-3-95450-197-7 doi:10.18429/JACoW-RUPAC2018-TUZMH04

STATUS OF THE NUCLOTRON

A. Sidorin[1], N. Agapov, A. Alfeev, V. Andreev, A. Baldin, A. Belov, O. Brovko, V. Bugaev, A. Butenko, E.D. Donets, E.E. Donets, D.E. Donets, A. Eliseev, V. Fimushkin, E. Gorbachev, A. Govorov, E. Ivanov, V. Karpinsky, H. Khodzhibagiyan, A. Kirichenko, S. Kostromin[1], A. Kovalenko, O. Kozlov, K. Levterov, V. Mikhailov, V. Monchinsky, A. Nesterov, A. Osipenkov, A. Philippov, S. Romanov, P. Rukoyatkin, A. Shurygin, V. Slepnev, A. Smirnov, E. Syresin, A. Tuzikov, B. Vasilishin, V. Volkov, JINR, Dubna, Moscow Region, Russia
[1]also at Saint Petersburg State University, Saint Petersburg, Russia

Abstract

Since last RuPAC two runs of the Nuclotron operation were performed. The run #54 performed in February – March of 2017 was dedicated to polarized beam acceleration. One of the achievements was the acceleration of polarized proton beam performed at the Nuclotron for the first time. During the run #55 in February- April of 2018 the Nuclotron provided heavy ion beams for first fixed target experiments in the frame of the NICA scientific program. These and other results of the facility operation and development are presented.

INTRODUCTION

The Nuclotron is the basic facility of the Veksler and Baldin laboratory for high energy physics (VBLHEP). The accelerator complex consists of Alvarez-type linac LU-20, superconducting synchrotron Nuclotron equipped with an internal target station, slow extraction system and facilities for fixed target experiments. The program includes experimental studies on relativistic nuclear physics, spin physics and physics of flavours. At the same time, the Nuclotron beams are used for research in radiobiology and applied research. In future the Nuclotron will be main synchrotron of the NICA facility being constructed at JINR [1].

The Nuclotron operational time is optimizing in accordance with the JINR topical plans with account the plan of the NICA construction. The Nuclotron run #53 started 26 of October 2016 was successfully completed 25 of December. It was longest (about 1400 h) run in the Nuclotron history. This and the next run (#54, provided at the beginning of 2017) were dedicated to spin physics experiments with polarized deuteron beams and test of the BM@N detector elements with deuteron and light ion beams. BM@N (Baryonic Matter at Nuclotron) is the fixed target experiment with heavy ions realizing as a first stage of the NICA experimental program. In the frame of machine development works during the run #54 the acceleration of polarized proton beam was performed at the Nuclotron for the first time. Preparation for the heavy ion run #55, started just after completion of the run #54, included development and tuning of the Nuclotron injection complex [see in details in 2], development of low intensive beam diagnostics, improvement of power supply of optic elements in the extracted beam lines. During the run #55 provided in February – April of 2018 the experiments for relativistic nuclear physics at BM@N and radiobiology researches were performed with carbon, argon and krypton beams.

In September 2018 assembly of the Nuclotron Booster was started.

STATISTICS OF OPERATION

Main task of the run #53 (26.10-25.12.2016) was experimental investigations in spin physics in few body nuclear systems (with polarized deuterons). Unpolarized deuteron beams were used for test of BM@N and MPD elements. Development of the diagnostics, investigations of dynamic behaviors of the Booster power supply prototypes with the beam acceleration, test of new current source for optic elements in the extracted beam lines, investigations of stochastic cooling were the main goals of the machine development. The run was provided using the source of polarized ions (SPI). Optimization of the SPI regimes and polarimetry were methodical tasks of the run. 77.6% from 1400 hours of the run duration were spending for experiments with the beams at energy up to 4.6 GeV/u. Intensity of polarizes beams was obtained at the level of $2\div5*10^8$ particles per cycle (Fig. 1).

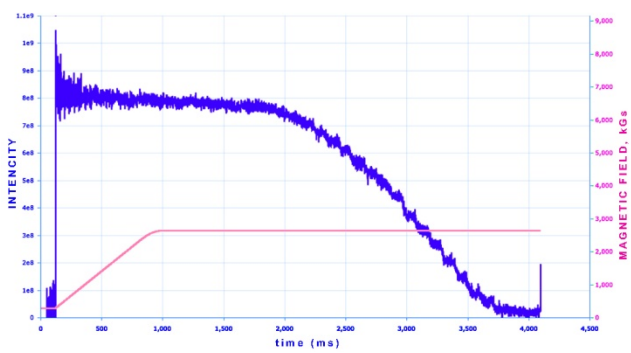

Figure 1: Intensity of polarized deuteron beam (blue curve) and magnetic field (pink curve) during acceleration cycle. Deuteron Spin Structure experiment provided at the Nuclotron internal target

Run #54 provided from 10.02 till 24.03.2017 was dedicated to acceleration of polarized and unpolarized deuterons and protons from the SPI, carbon and lithium ions from the laser source. Maximum achieved extracted beam energy was 5.2 GeV/u (that corresponds to 1.85 T of the dipole magnetic field). In the total energy range an acceptable quality of the slow extraction was achieved. Further optimization of the SPI and routine operation with

ISBN: 978-3-95450-197-7 doi:10.18429/JACoW-RUPAC2018-TUCDMH01

HEAVY ION INJECTION CHAIN OF NICA COLLIDER

A. Tuzikov, A. Butenko, D. Donets, A. Govorov, K. Levterov, I. Meshkov, A. Smirnov, E. Syresin, V. Volkov, Joint Institute for Nuclear Research, Dubna, Russia
A. Zhuravlev, V. Kiselev, I. Okunev, S. Sinyatkin,
Budker Institute of Nuclear Physics, Novosibirsk, Russia
O. Tasset-Maye, SigmaPhi, Vannes, France

Abstract

New accelerator complex is constructed by Joint Institute for Nuclear Research (Dubna, Russia) in frame of Nuclotron-based Ion Collider fAcility (NICA) project. The NICA layout includes new 600 MeV/u Booster and existing Nuclotron synchrotrons as parts of the heavy ion injection chain of the NICA Collider as well as transport beam lines which are the important link for the whole accelerator facility. Designs and current status of beam transfer systems of the NICA complex are presented in this paper.

INTRODUCTION

The NICA project [1] intends the construction of new accelerator complex based on existing superconducting synchrotron Nuclotron. In frame of NICA project the existing accelerators such as Nuclotron and linac LU-20 were modernized to match the project specifications. The following facilities are being included: the heavy ion source KRION of ESIS type, the source of polarized protons and deutrons, the heavy ion linear accelerator (HILAC), the superconducting Booster synchrotron [2], the Collider having two superconducting storage rings, and transport beam lines.

In the paper, designs and current status of three beam transport channels connecting the primary elements of the heavy ion injection chain of the NICA Collider are detailed:

1) beam line from the HILAC to the Booster;
2) beam line from the Booster to the Nuclotron;
3) beam line from the Nuclotron to the Collider.

Main parameters of ion beams along the Collider injection chain and working modes of the beam transfer systems are given in Table 1.

BEAM TRANSFER FROM HILAC TO BOOSTER

The beam transfer in the HILAC-Booster transport channel [3] involves beam debunching, betatron matching of ion beam of the target charge state with the Booster, separation and collimation of neighbor parasitic charge states of ions. The ion-optical system of the transport channel and the beam injection system of the Booster provide multi-variant injection for accumulation of beams in the Booster with required intensity [4]. Main methods of beam injection into the Booster are single-turn, multi-turn and multiple injections. Ions are accumulated on the horizontal phase plane of the Booster.

Table 1: Main Parameters of Beam Transfers

Ions	Au^{30+}, Au^{31+}, Au^{32+} (from HILAC); Au^{31+} (inside Booster); Au^{78+}, Au^{79+} (at the exit of Booster); Au^{79+} (at the entry of Nuclotron and further)
Intensity:	
HILAC-Booster	up to $2.5\cdot10^9$ (Au^{31+}); up to $6\cdot10^9$ (total);
Booster-Nuclotron	up to $1.3\cdot10^9$ (Au^{79+}); up to $1.5\cdot10^9$ (total);
Nuclotron-Collider	up to $1\cdot10^9$ (Au^{79+}).
Energy, MeV/amu:	
HILAC-Booster	3.2
Booster-Nuclotron	572
Nuclotron-Collider	1000 ÷ 4000
Repetition rate of beam transfer, Hz	up to 0.25
Transverse 95% emittance, π·mm·mrad:	
at the exit of HILAC	10
at the entry of Booster	15
Booster-Nuclotron	0.2 ÷ 3 (hor.) / 0.2 ÷ 1.5 (vert.)
Nuclotron-Collider	up to 3 (hor.) / up to 1.5 (vert.)
Transverse acceptances, π·mm·mrad:	
HILAC-Booster	38
Booster-Nuclotron	8 (hor.) / 6 (vert.)
Nuclotron-Collider	13 (hor.) / 10 (vert.)
R.m.s. longitudinal momentum spread:	
at the exit of HILAC	$2.5\cdot10^{-3}$
at the entry of Booster	$5\cdot10^{-4}$
Booster-Nuclotron	$1.1\cdot10^{-4} \div 2.1\cdot10^{-4}$
Nuclotron-Collider	up to $2\cdot10^{-4}$

Layout of the channel is shown in Figure 1. The beam transport channel provides the beam transfer only in the horizontal plane as the HILAC axis is located on the median plane of the Booster.

The beam transport channel contains 2 dipole magnets, 7 quadrupole lenses, a debuncher (produced by Bevatech company) and a set of steerers. At present all the transport

ISBN: 978-3-95450-197-7 doi:10.18429/JACoW-RUPAC2018-WEXMH01

STATUS OF U70

S. Ivanov, A. Afonin, Yu. Antipov, D. Hmaruk, N. Ignashin, V. Kalinin, I. Kuzmin, V. Lapygin, O. Lebedev, A. Maksimov, Yu. Milichenko, A. Minchenko, A Soldatov, S. Sytov, N. Tyurin, D. Vasiliev, A. Zaitsev, NRC "Kurchatov Institute" – IHEP, 142281 Protvino, Russia

Abstract

The report overviews present status of the Accelerator Complex U70 at IHEP of NRC "Kurchatov Institute" (Protvino). The emphasis is put on the recent activity and upgrades implemented since the previous conference RuPAC-2016, in a run-by-run chronological ordering.

History of the foregoing activity is recorded sequentially in Refs. [1].

GENERALITIES

The entire Accelerator Complex U70 comprises four machines — 2 linear (I100, URAL30) and 2 circular (U1.5, U70) accelerators. Proton mode (default) employs a cascade of URAL30–U1.5–U70, while the light-ion (carbon) one — that of I100–U1.5–U70.

Since the previous conference RuPAC-2016, the U70 complex operated for four runs in total. Table 1 lists their calendar data. The second run of 2018 is being planned for October–November of 2018.

Details of the routine operation and upgrades through years 2016–18 are reported in what follows, run by run.

RUN 2016-2

The run lasted from October 03 till December 27 2016 in the two modes sequentially: with 50 GeV protons (see Fig. 1), and 455 MeV/u carbon beams.

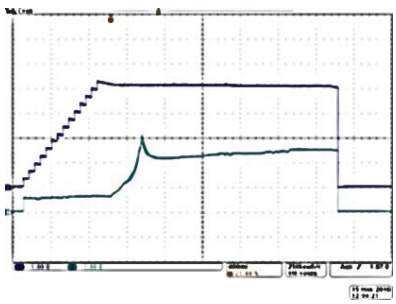

Figure 1: Acceleration of protons in U70. Traces from top to bottom: beam DC current (14 bunches (of 29 feasible) injected); bunch peak current (spike occurs at γ-transition 7.96 GeV).

During the 1st half of the run, 50 GeV proton beam was directed to applied research at the radiographic facility.

To this end, the facility was fed with the fast-extracted bunched beam with equal bunches of $3–4\cdot10^{11}$ ppb. To attain electric energy conserving operation, the flattop length was cut short to 0.6 sec.

During the 2nd half of the run, the azimuthally uniform (de-bunched) 50 GeV proton beam was used for 672 hr for fundamental physics at seven experimental facilities. Typically, slow extraction took 2.5 sec with $7.7\cdot10^{12}$ protons per a spill, refer to Figs. 2, 3.

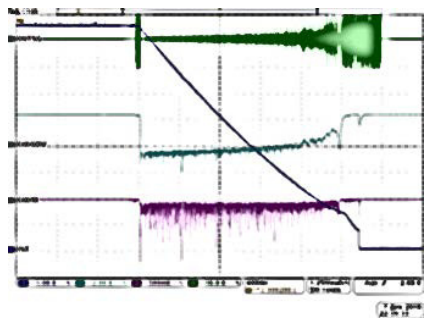

Figure 2: Slow stochastic extraction of protons from U70. Traces from top to bottom: waiting beam DC current, AM-modulated noise, beam feedback signal to modulate amplitude of noise, and a slow stochastic spill as such.

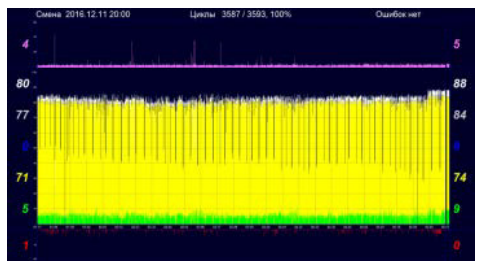

Figure 3: Numerical data at the intensity monitor screen during run 2016-2 for physics: The upper trace is overall beam loss during the cycle (5%). Beam intensity delivered is $8.0\cdot10^{12}$ ppp (average), or $8.8\cdot10^{12}$ ppp (instantaneous).

Some of the fixed-target experiments were run with secondary particles from internal targets under a parallel beam splitting see Fig. 4.

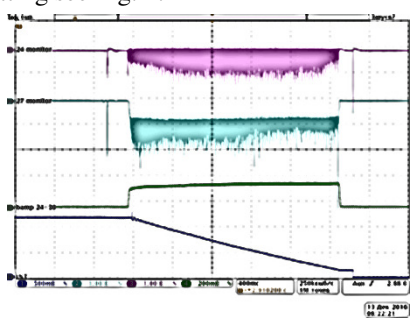

Figure 4: Traces from top to bottom. Spill of secondary particles beam from internal targets ## 24 and 27. Driving current of the enclosing orbit bump between straight sections ## 24 and 30, DC current of the waiting circulating beam.

ISBN: 978-3-95450-197-7 doi:10.18429/JACoW-RUPAC2018-WEXMH02

HEAVY ION CYCLOTRONS OF FLNR JINR – STATUS AND PLANS

I.V. Kalagin*, G.G. Gulbekian, S.N. Dmitriev, Yu.Ts. Oganessian, B.N. Gikal, S.L. Bogomolov, I.A.Ivanenko, N.Yu.Kazarinov, V.A. Semin, G.N. Ivanov, N.F.Osipov
Joint Institute for Nuclear Research, FLNR, Dubna, Moscow region, Russia

Abstract

Status of JINR FLNR cyclotrons and plans of their modernization together with plans on creation of new facilities are reported. At present, three cyclotrons: U400, U400M and IC100 and MT-25 microtron are under operation at the JINR FLNR. U400 and U400M are the basic FLNR facilities that both are under operation is about 12000 hours per year. The U400 (pole diameter of D=4 m) was designed to accelerate ions from B to Bi up to 19 MeV/u. U400 reconstruction is planned. The U400M cyclotron (D=4 m) is used to accelerate ions from Li to Bi up to 60 MeV/u. U400M modernization is planned. The IC100 accelerator (D=1m) is used for applied researches with Ar, Kr and Xe ions at energy of 1.2 MeV/u. Creation of the dedicated DC130 cyclotron (D=2m) with ion energies of 4.5 and 2 MeV/u is planned on the base of U200 cyclotron. The Super Heavy Element Factory (SHE factory) is the new FLNR JINR project. The DC280 cyclotron (D=4 m) is the basic facility of the SHE factory, which will accelerate ions with energies 4 - 8 MeV/u cyclotron at intensities up to 10 pμA for ion masses over A=50. The main systems of the DC280 were assembled and tested, the cyclotron is preparing for commissioning.

INTRODUCTION

The scientific program of the Flerov Laboratory of Nuclear Reactions of the Joint Institute for Nuclear Research (FLNR JINR) consists of experiments on synthesis of heavy and exotic nuclei using ion beams of stable and radioactive isotopes and studies of nuclear reactions, acceleration technology and applied research.

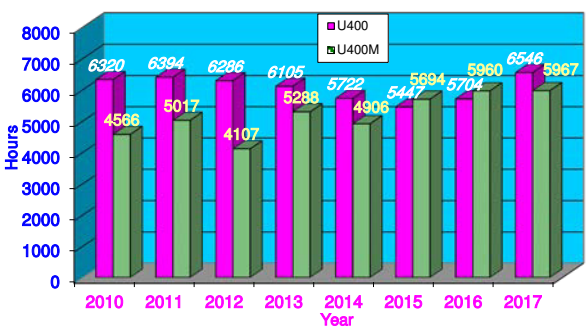

Figure 1: U400 and U400M operation in 2010-2017.

Presently, the FLNR JINR has four cyclotrons of heavy ions: U400, U400M, IC100 (IC-100), that provide performance of the basic and applied researches (Fig.3). Total annual operating time of the U400 and U400M cyclotrons is more than 10000 for many years (Fig.1).

The old U200 cyclotron will be reconstructed to the DC130 cyclotron for applied research.

At present time, the project of Super Heavy Element Factory is being performed at the FLNR JINR [1]. The project implies design and creation of the new experimental building with new DC280 cyclotron which has to provide intensities of ion beams with middle atomic masses (A~50) up to 10 pμA.

U400 CYCLOTRON

The isochronous U400 cyclotron has been in operation since 1978 [2]. The cyclotron produces ion beams of atomic masses 4÷209 with energies of 3÷29 MeV/nucleon. Before 2017 about 66% of the total time has been used for acceleration of $^{48}Ca^{5+}$ ions with intensities up to 1.2 pμA for synthesis of super heavy elements. New prospects for the synthesis of super heavy elements may appear to be connected with the usage of the intense beam of neutron-rich ^{50}Ti. The beam of $^{50}Ti^{5+}$ ions has been accelerated into the U400 cyclotron with extracted beam intensity is about 0.5 pμA [3]. In 2017, about 40% of the total time was used for $^{50}Ti^{5+}$ acceleration.

Figure 2: The sketch of the new U400 experimental hall.

The U-400 modernization is planned to begin in 2021. The aims of the modernization are increasing the total acceleration efficiency and possibility to vary ion energy fluently at factor 5 for every mass to charge ratio (A/Z). The width of ion energy region will be 0.8÷27 MeV/nucleon. The project of U400 modernization intends decreasing the magnetic field level at the cyclotron center from 1.93÷2.1T to 0.8÷1.8T. The axial injection and ion extraction systems will be changed. For the ion extraction both the stripping foil and the deflector methods are considered.

* kalagin@jinr.ru

ISBN: 978-3-95450-197-7 doi:10.18429/JACoW-RUPAC2018-WEXMH03

THE STATUS OF THE ACCELERATOR COMPLEX NRC KI - PNPI

D.A. Amerkanov, S.A. Artamonov, E.M. Ivanov, V.I. Maximov, G.F. Mikheev, G.A. Riabov, V.A. Tonkikh, NRC KI-PNPI, Gatchina, Russia

Abstract

The main accelerators are concentrated in the accelerator department of PNPI. First of all this is the 1000 MeV synchrocyclotron (SC). It is widely used for fundamental research in the field of elementary particle physics, nuclear physics, and the physics of nuclear reactions, in solid state physics and in radiobiology. The role of the SC is also wide in a variety of applied research on radiation and nuclear tests, including specific medical research.

Second of all this is the isochronous cyclotron C-80. It allows obtaining proton beams with energy from 40 to 80 MeV and current up to 100 μA. The cyclotron is intended for production of a wide assortment of radioisotopes including radiation generators (Sr - Rb, Ge - Ga) for medicine, proton therapy of ophthalmic diseases, tests of radioelectronic components for radiation resistance and studies in the field of nuclear physics and radiation material science.

SYNCHROCYCLOTRON SC-1000

Since the start-up of the SC in 1970, a new generation of the intermediate-energy accelerators has appeared in the world. These are in particular modernized synchrocyclotrons after cardinal reconstruction of all their systems and meson factories. Thanks to intensive and original improvements programs at the SC, about the same beam intensities were obtained at the SC, as in other synchrocyclotrons after their reconstruction. In spite of the fact that modern "meson factories" exceed considerably the PNPI SC in the beam intensity, nevertheless, due to some accelerator features, mainly due to the higher energy, which is important in a number of cases for experiments on proton, meson and neutron beams, and an extensive and successful application program, there is a significant area for the research at the SC which is not overlapped by other facilities.

Simultaneously with physical experiments on SC, an intensive program was carried out to improve the beam parameters and to develop new experimental capabilities. Briefly the main features of 1000 MeV synchrocyclotron facility can be formulated as follows.

1. *Long burst operation system* [1]. To increase the effectiveness of electronic methods of registration, an original long burst operation system using a Cee-electrode was developed. Unlike similar systems, the SC uses a ¾ wave resonance line with ferrite frequency variation and synchronization of the Cee–voltage in frequency and phase with the main dee voltage. The use of a resonance scheme made it possible to reduce the Cee power supply and to increase the beam macro duty cycle from 1.4 to 50 % and more. The originality of the technical solutions is confirmed by an author's certificate.

2. *Electrostatic focusing system in the SC centre* [2]. In the central region of the accelerator, a new three-electrode focusing system was put into operation to increase the vertical focusing and to compensate the space-charge forces that limit the accelerator intensity. The new focusing system made it possible to increase the intensity by about 5 times and to reach 3.5 μA beam inside the vacuum chamber, and the intensity of the extracted beam to 1 μA. The originality of the technical solutions is also confirmed by an author's certificate.

3. *New variators*. To improve the reliability of the accelerator and to facilitate the maintenance work of the HF system, new variator rotors with Al plates, manufactured at PNPI, were introduced instead of the old ones with stainless steel plates. After installation of the new two variators, the accelerator operating time achieved 6000 hours per year.

4. *The experimental complex of the PNPI SC* consists of the accelerator, buildings and experimental halls with the systems of engineering maintenance (power supplies, water cooling, and ventilation), beam transport lines P1, P2, P3 and P4, biological protection, beam dampers and the experimental installations. When the proton mode is in operation, the extracted beam is transported through the accelerator hall and then directed by the bending magnet SP-40 into the experimental hall through one of the collimators. The beam for the proton therapy is transported by the beam line P2 in the special medical building [3]. The magnetic spectrometer with 10^{-3} energy resolution [4] is using the P1 beam. Its effective use became possible after an invention of a way of monochromatization of the SC proton beam. With this spectrometer, an extensive series of researches on the study of the nuclear matter structure by means of elastic and quasi-elastic proton-nucleus scattering was performed. The beam line P3 provides the proton beam to the IRIS laboratory where short-lived isotopes are investigated by using a mass-separator and the laser technique [5]. There is second proton beam with small intensity P4 (about 1 %) that acts in parallel with a main beam. It can be used as for physical so for applied purposes. For an example using this beam for proton therapy will essentially decrease the cost of patient irradiation.

5. *All meson beams at the PNPI SC* are generated at the same target installed in the accelerator hall behind a thick wall. It is possible to perform two experiments simultaneously. In total, there are three meson channels: π1-channel, π2-channel of lower energy, and μ^- channel. The π1-channel selects $\pi^{\pm}$ mesons generated in the

ISBN: 978-3-95450-197-7 doi:10.18429/JACoW-RUPAC2018-WECAMH02

LIGHT ION LINEAR ACCELERATOR UP TO 7 AMEV FOR NICA

H. Höltermann*, M. Basten, B. Koubek, H. Podlech, U. Ratzinger,
A. Schempp, R. Tiede, Bevatech GmbH, Frankfurt am Main, Germany
A. M. Bazanov, A. V. Butenko, B. V. Golovenskiy, D.E. Donets, V. V. Kobets,
A. D. Kovalenko, A.V. Butenko, A. I.Govorov, B. V. Golovenskiy, D. E. Donets,
K. A. Levterov, D. A. Lyuosev, A. A. Martynov, V. A. Monchinskiy, D. O. Ponkin,
K.V. Shevchenko, A. O. Sidorin, I. V. Shirikov, E. M. Syresin, JINR, Dubna, Russia
C. Kampmeyer, H. Schlarb, DESY, Hamburg, Germany

Abstract

In the frame of the NICA ion collider upgrade a new light ion frontend linac (LILac) for protons and ions with a mass to charge ratio of up to 3 will be built. The LILac will consist of 3 parts: 1. a normal conducting Linac up to 7 AMeV, 2. a normal conducting energy upgrade up to 13 AMeV, 3. a superconducting section. The normal conducting Linac up to 7 AMeV will be built in collaboration between JINR and Bevatech GmbH. The technical design of LILac up to 7 AMeV is discussed in this paper.

INTRODUCTION

In the frame of the NICA ion collider upgrade [1] a new light ion frontend Linac (LILac) for polarised particles, protons and ions with a mass to charge ration of up to 3 will be built. Behind the ion source and LEBT, LILac will consist of 3 parts:

1. a normal conducting Linac up to 7 MeV/u
2. a normal conducting energy upgrade up to 13 MeV/u
3. a superconducting section from 13 MeV/u up to a final energy to be determined

In this paper only the Part 1 of LILac up to 7 MeV/u is discussed. This normal conducting Linac will be built in collaboration between JINR and Bevatech GmbH.

The Linac will be located in LU20 hall at JINR and provides a beam energy of 7 MeV/u to be injected into the Nuclotron ring for further acceleration as a first stage of the project. Protons and light ions up to a mass to charge ratio of up to 3 will be used for either fixed target experiments to study baryonic matter or will be injected into the NICA collider ring for hadron matter and its phase transition experiments and to study spin physics on polarised particles.

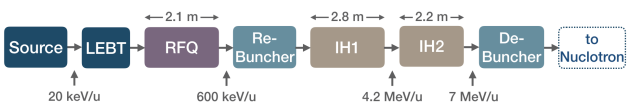

Figure 1: Scheme of the LILac cavities.

The Linac consists of 5 cavities, an RFQ followed by a rebuncher, 2 IH-DTL structures and a de-buncher as shown in Fig. 1. It is operating at 162.5 MHz with a beam repetition rate of 5 Hz and a duty cycle of 0.15 % [2]. The main parameters of the LILac are summarised in Table 1. The length of the Linac comprising the cavities, the beam diagnostic devices and focusing magnets but excluding the de-buncher will be realised within a length of 9 m. A scheme of the LILac cavities is shown in Table1.

Table 1: LILac Main Parameters

Parameter	Protons	C^{4+}
Mass to Charge Ratio	1	3
Injection Energy	30 keV	60 keV
Exit Energy	7 MeV	21 MeV
Beam Current	5 mA	15 mA
Repetition Rate Limit	≤5 Hz	
Current Pulse Duration	30 μs	
RF Pulse Length	200 μs	
RF Frequency	162.5 MHz	
Transmission	≥80 %	
Full Length of the Linac	<9 m	

Each cavity will be fed by a dedicated high power solid state amplifier to provide the corresponding power for the accelerating fields in the cavities. The LLRF control soft- and hardware based on the MicroTCA.4 standard will be developed together with Bevatech and the MicroTCA Technology Lab at DESY.

ARCHITECTURE

Ion Source and LEBT

At the LILAC two different ion sources, a laser ion source (LIS) and a source of polarized ions (SPI), will be used. From the LIS it is planned to receive light ions, while the SPI will generate polarised and non-polarised protons [3]. The ion sources are placed on a high-voltage terminal (up to 150 kV) [4]. The LEBT channel with a length of about 1.8 m is split into two main parts. The first part is an electrostatic section with ion optics and an electrostatic tube, and the second part uses two magnetic solenoids with a maximum magnetic field of 1.2 T. This channel will be similar to the existing which works at the LU-20 pre-injector.

* holger.hoeltermann@bevatech.com

ISBN: 978-3-95450-197-7 doi:10.18429/JACoW-RUPAC2018-WECAMH04

STATUS REPORT OF DEVELOPMENT OF HIGH POWER BEAM CW ELECTRON ACCELERATOR

A.V. Telnov#, N.V. Zavyalov, A.N. Belyaev, Ya.V. Bodryashkin, I.V. Zhukov, V.V. Kuznetsov, N.N. Kurapov, I.A. Mashin, A.M. Opekunov, L.E. Polyakov, G.P. Pospelov, S.A. Putevskoj, M.L. Smetanin, S.M. Treskov, A.N. Shein, I.V. Shorikov, RFNC-VNIIEF, Sarov, Russia

Abstract

The present paper describes the current status of CW resonance electron accelerator design at RFNC-VNIIEF. The range of output electron energy is from 1.5 MeV to 7.5 MeV. The average power of electron beam is up to 300 kW.

Parameters of basic accelerator components (RF power supply system, RF injector, accelerating structure, beam transport system) are presented. The electron acceleration scheme is displayed in this paper.

First experiments were carried out. As a result, 1.5 and 3 MeV electron beams were obtained. The average beam current is up to 100 μA. Derived beam characteristics confirm physical principles of designed accelerator.

INTRODUCTION

The accelerator has been designed for technological process testing required high values of beam power and absorbed dose of electron radiation and bremsstrahlung.

Basic design objectives of the installation are as follows [1]:

- output electron energy – 1.5, 4.5, 7.5 MeV;
- maximal average power of electron beam - 300 kW;
- operating resonance frequency – 100 MHz;
- average current – up to 40 mA;
- operating modes – continuous and pulse-periodic.

The principle of acceleration is based on multiple passes of electron beam through the accelerating gaps of coaxial half-wavelength cavity on the level of median plane where the magnetic component of RF field is entirely absent (Fig. 1) [2].

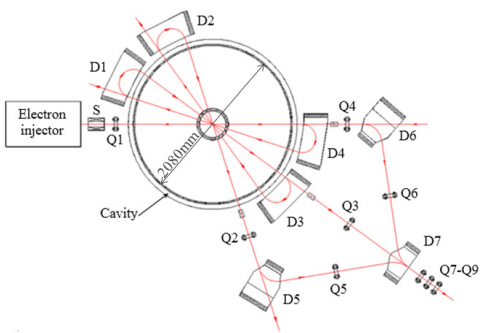

Figure 1: Scheme of the acceleration: → – beam propagation trajectory; D1 – D7 – bending dipole electromagnets; S – focusing solenoid; Q1 – Q9 – quadrupole magnet lenses.

The maximal electron energy of 7.5 MeV is achieved after five passes of electron beam through the accelerating cavity.

Multiple passes of electrons through accelerating gaps is being provided with the help of bending electromagnets arranged outside the cavity (Fig. 1, D1 – D4). With the help of of electromagnets D5 – D7 the accelerated beams with different electron energies is being transported to the output device.

ACCELERATOR COMPOUND SYSTEMS

Accelerating Cavity

The accelerating cavity is a half-wavelength coaxial cavity (a tube surrounding a central conductor, both tubes having coincident axes), shorted at both ends and resonating in metric waves at 100 MHz (Fig. 2).

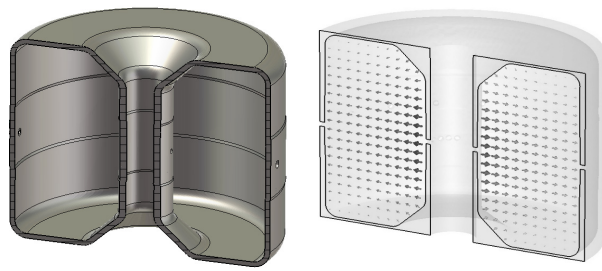

(a) (b)

Figure 2: 3D-model of the cavity (a) and electric field distribution (b).

RF Power Supply System

To get the average value of beam power equal to 300 kW it is required to provide the accelerating cavity with the RF power of 540 kW. Such system is composed of three typical generators with the output power 180 kW of each of them and RF power summator [3].

RF power enters the accelerating cavity by a coaxial feeder through RF power input unit. T_1-mode electromagnetic waves are being exited in the cavity with the amplitude of electrical field which provides 1.5 MeV electron energy gain per one pass through the cavity.

Electron Injector

Electron injector is located at the outer wall of the accelerating cavity (Fig. 1). The injector is a grid-controlled thermo-cathode electron RF gun based on a quarter-wavelength coaxial cavity (100 keV, 40 mA, 100 MHz) [4]. Electron bunches enter the accelerating cavity through the injection channel for the subsequent energy gain.

Telnov@expd.vniief.ru

ISBN: 978-3-95450-197-7 doi:10.18429/JACoW-RUPAC2018-WECAMH06

PROGRESS OF THE NICA COMPLEX INJECTION FACILITY DEVELOPMENT

A.V. Butenko, A.I. Govorov, B.V. Golovenskiy, D.E. Donets, A.D. Kovalenko, K.A. Levterov, D.A. Lyuosev, A.A. Martynov, V.V. Mialkovsky, V.A. Monchinskiy , D.O. Ponkin, K.V. Shevchenko, A.O. Sidorin, I.V. Shirikov, A.V. Smirnov, G.V. Trubnikov
Joint Institute for Nuclear Research, Dubna, Moscow Region, Russia
T.V. Kulevoy
Institute of Theoretical and Experimental Physics NRC "Kurchatov Institute", Moscow, Russia
S.M. Polozov
National Research Nuclear University – Moscow Engineering Physics Institute, Moscow, Russia
H.Höltermann, U.Ratzinger, A.Schempp, H.Podlech
BEVATECH GmbH, Frankfurt, Germany

Abstract

The new accelerator complex Nuclotron-based Ion Collider fAcility (NICA) is under development and construction at JINR, Dubna now. This complex is assumed to operate using two injectors: the Alvarez type linac LU-20 as injector of light ions, polarized protons and deuterons and a new linac HILAc - injector of heavy ions beams. The modernization of Alvarez-type linac began in 2016 by commissioning of new RFQ foreinjector, and in 2017 the new buncher in front of linac has been installed. The first Nuclotron run with new buncher was performed in January 2018 with beams of Xe+, Ar+ and Kr+. The beam produced by KRION-6T ion source were successfully injected and accelerated in the Nuclotron ring during the last run #55. Main results of the last Nuclotron run and plans for future development of NICA injection complex are presented in this paper.

INTRODUCTION

Nuclotron-based Ion Collider fAcility (NICA) (Fig. 1.) is new accelerator complex developing and constructing at JINR [1] for ion collision and high-density matter study.

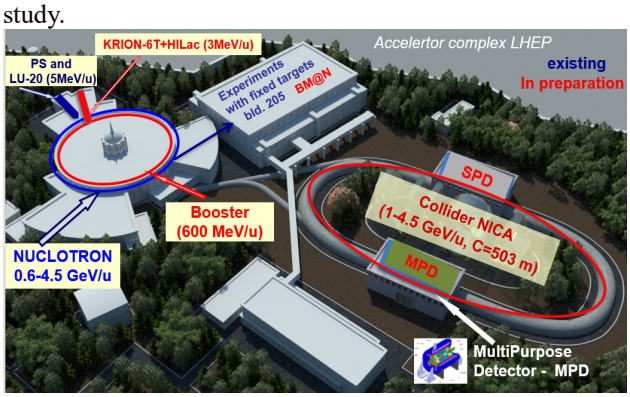

Figure 1: The NICA complex.

For the NICA collider ion beams from p to Au ions with energies from a few hundred MeV/u up to a few GeV/u will be provided by two injection LINACs and two superconducting synchrotrons: the Booster and the Nuclotron. The beams are generated by three new ion sources: SPI (Source of Polarized Ions), LIS (Laser Ion Source) and Krion (ESIS type heavy ion source). The ion sources feed two LINACs: the existing linac LU-20 with a new RFQ as pre-injector and the new heavy ion linac – HILAc. Design and development of RFQ, MEBT and two IH sections of the HILAc was performed by Bevatech GmbH (Frankfurt, Germany) [2] and described in detail in [3].

HILAC

The main parameters of the HILAc (Fig. 2) are given in the Table 1.

Table 1: HILAc Parameters

A/q	6.25
Current	< 10 emA
Pulse length	10 μs – 30 μs
Rep. rate	< 10 Hz
RFQ energy	300 keV/u
LINAC max. energy	3.2 MeV/u

The HILAc RFQ is a 4-rod structure operating at 100.625 MHz. The RFQ tank is a 3.16 m stainless steel tank of 0.35 m in diameter which is copper-plated inside. The RFQ is powered by a 140 kW solid state amplifier.

The first IH tank contains an internal quadrupole triplet lens. The IH1 and IH2 have 2.42 m and 2.15 m outer length correspondingly. For the design A/q – value of 6.5 the sum voltage gain is 20.8 MV. Both IH cavities are powered by 340 kW solid state amplifiers, one for each cavity.

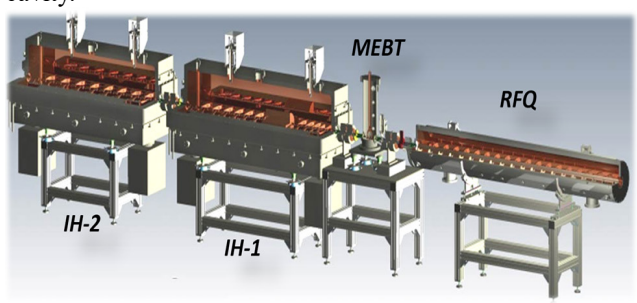

Figure 2: HILAC scheme.

ISBN: 978-3-95450-197-7 doi:10.18429/JACoW-RUPAC2018-WECBMH03

DEVELOPMENT OF HED@FAIR QUADRUPOLES*

L. Tkachenko, A. Ageyev, Y. Altukhov, I. Bogdanov, E. Kashtanov, S. Kozub, P. Slabodchikov, M. Stolyarov, S. Zinchenko, NRC "Kurchatov Institute" - IHEP, Protvino, Moscow region, 142281

Abstract

Novel experiments to study fundamental properties of high-energy-density states in matter, generated by intense heavy ion beams, will be carried out by the HED@FAIR collaboration at FAIR. For strong transverse focusing a special final focus system, consisted of four superconducting large-aperture high-gradient quadrupole magnets, will be installed at the end of the HED@FAIR beam line. Design and main characteristics of the quadrupole are discussed. Results of mechanical and thermal calculations of main parts of the quadrupole are presented.

INTRODUCTION

The HED@FAIR collaboration novel experiments [1, 2] to study thermos-physical, transport and radiation properties of high-energy-density matter that is generated by the impact of intense heavy ion beams on dense targets were proposed at FAIR [3]. For strong transverse focusing, a special final focus system (FFS) has to be installed at the end of the HED@FAIR beam line. In order to provide a focal spot of the order of 1 mm, a large focal angle is needed and consequently, four large-aperture high-gradient quadrupole magnets have to be used in the FFS, which IHEP develops at present [4]. This work examines the main characteristics of four wide-aperture quadrupoles, which will be used for focusing the heavy ion beams in these experiments.

A geometry optimization at the infinite permeability approximation μ and a cylindrical inner radius of the iron yoke was done, using the computer code HARM-3D [5]. Basically, this program uses analytical formulae. In the magnet design, a computer code MULTIC [6] has been employed. This code allows calculating a 3D geometry, taking into account the real dependence of $\mu(B)$ in the iron yoke.

MAIN REQUIREMENTS TO THE QUADRUPOLE

The required specifications of the quadrupoles are:

- The central integral gradient (G_0^{int}) is equal to 36 T;
- The inner diameter of the coil is 260 mm;
- The minimal distance between quadrupole centers of two nearby magnets is 2500 mm;
- The operating mode is DC;
- The radius of the good field quality is r_0 = 110 mm;
- The lowest 6-th, 10-th and 14-th harmonics of the field and b_6^{int} of the integral field should not exceed $\pm 2\times10^{-4}$ in geometry optimization; The radius of the good field quality for a geometry optimization is 110 mm;
- The field multipoles b_n, n = 6, 10, 14 in the custom magnet are $<2\times10^{-3}$;
- The integral multipole b_6^{int} in the custom magnet is $<2\times10^{-3}$;
- The operating temperature is about 4.4 K;
- The temperature margin has to be about 1 K.

2D GEOMETRY

General Description

A two-layer quadrupole has a number of advantages over the single-layer one. In particular, it is more technological in manufacturing, easier to manufacture [7] and has half as much a lower operating current. An inter-turn spacer is inserted in the first layer, so the three coil blocks allow one to suppress the first lower multipoles b_6, b_{10} and b_{14} in the approximation of the infinitely high magnetic permeability in the iron yoke with a cylindrical internal surface. The coils are enclosed in stainless steel collars that hold all the magnetic forces. The inner iron radius is 160 mm. In order to balance all the forces, acting on the coil and the support system, and to ensure that the offset of any point in the coil is allowed no more than 50 μm, the thickness of the collar should be 35 mm. The cross section of the quadrupole is shown in Figure 1 and the main geometric parameters are presented in Table 1.

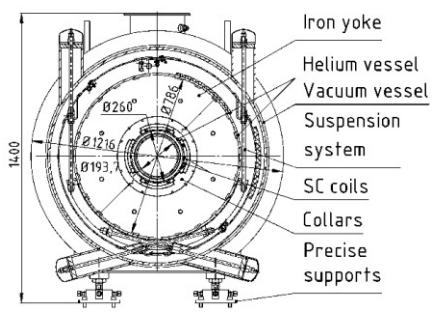

Figure 1: Cross section of the quadrupole.

Table 1: Main Parameters of the Coil Blocks

Coil blocks	1	2	3
Inner radius, mm	130	130	143.75
Initial angle, deg.	0.2101	26.1493	0.0572
Final angle, deg.	19.5735	34.0521	30.7269
Turn number	27	11	47
Maximal field, T	5.12	5.87	5.46
Critical temperature, K	6.44	5.84	6.16

*Work supported by the contract between FAIR and IHEP from 19.12.2016.

ISBN: 978-3-95450-197-7 doi:10.18429/JACoW-RUPAC2018-WEZMH01

STATUS OF THE KURCHATOV SYNCHROTRON RADIATION SOURCE

V. Korchuganov, A. Belkov, Y. Fomin, E. Kaportsev, Yu. Krylov, V. Moiseev, K. Moseev, N. Moseiko, D. Odintsov, S. Pesterev, A. Smygacheva, A. Stirin, V. Ushakov, V. Ushkov, A. Valentinov, A. Vernov,
NRC Kurchatov Institute, Akademika Kurchatova Sq., 1, Moscow, 123182 Russia

Abstract

The Kurchatov synchrotron radiation source goes on to operate in the range of synchrotron radiation from VUV up to hard X-ray. An electron current achieved 200 mA at 2.5 GeV, up to 12 experimental stations may function simultaneously. An improvement of an injection process allowed to minimize injection time and to increase injection efficiency. A production of two new superconducting wigglers is now in progress in BINP (Novosibirsk). They will be installed on the main ring in next year. Great modernization of the whole facility is planned for 2020. The present status and future plans of the Kurchatov synchrotron radiation source is presented in the report.

INTRODUCTION

Kurchatov synchrotron radiation source (KSRS) consists of 80 MeV linac, 450 MeV small storage ring Siberia-1 and 2.5 GeV main storage ring Siberia-2 [1]. Siberia-1 serves as a booster ring for Siberia-2 while Siberia-2 supplies experimental stations by synchrotron radiation. Siberia-2 magnetic structure provides 98 nm horizontal emittance at 2.5 GeV. As a result of facility modernization Siberia-2 achieved electron current level of 200 mA. Now electron current is limited by RF system power. Further enhancement of the beam current is possible only after introducing of an additional RF generator. This is provided in Federal Program of the KSRS modernization in 2018 – 2020. The Federal Program also includes modernization of other facility systems such as vacuum, power supplies, water and air cooling, control system and so on. Two new 3 T superconducting wigglers will be installed on the main ring and several experimental stations will be constructed.

OPERATIONAL STATISTICS

As a rule Siberia-2 operates for SR users from the middle of September till the beginning of July. It works during 3 or 4 weeks in around-the-clock mode from Monday to Saturday. Then one week of preventive maintenance and machine tuning follows. Usually there is one beam storing per day (depends on beam lifetime). Storing of 200 mA takes approximately one hour, then energy ramping occurs for 3 minutes with 2 - 3 % current losses. During a day of operation beam current slowly decreases down to 40 – 50 mA so new storing is needed. Beam lifetime at 2.5 GeV depends on vacuum level and beam integral accumulated from the moment of last vacuum chamber violation.

Operational time and integral of the beam current of Siberia-2 have grown during last two years because of machine systems improvements (see Table 1). Three additional experimental stations and beamlines were installed. Number of simultaneously operating beamlines can reach 12. Shortage of the machine stuff prevents further operational time growing. Also facility cannot operate in summer time because of insufficient water and air cooling of the equipment.

Table 1: Statistics of Siberia-2 operation for last 4 years. Data for 2018 correspond to the beginning of September. Planned values for whole year are given in round brackets.

Parameter	2015	2016	2017	2018
Time for users, hours	2115	2755	2724	1680 (2700)
Beam integral, A·hours	115.5	178.8	200.3	127.6 (200)
Average number of stations in use	5.5	6.7	7.6	8.3
Average current, mA	54.6	64.9	73.5	76.0

BEAM CURRENT ENHANCING

A maximum value of Siberia-2 stored current depends on many parameters. Two main groups can be specified: stable work of the injection complex (that is storing rate in Siberia-1 and injection efficiency for Siberia-2) and beam stability in Siberia-2.

The Injection Complex Operation

In order to improve the operation of the injection complex following actions were taken:

- High voltage cables in klystron station “Olivin” feeding linac were replaced for modern ones. So risk of breakdowns at klystron’s anode was eliminated.
- New generator for “Olivin” station was put into operation. It not need multiplication of master frequency and operates at linac frequency of 2.8 GHz.
- In order to control short “Olivin” pulses modern digital oscillograph was put into operation. Thus the

ISBN: 978-3-95450-197-7 doi:10.18429/JACoW-RUPAC2018-WEZMH02

KURCHATOV SYNCHROTRON RADIATION SOURCE – FROM THE 2ND TO THE 4TH GENERATION*

Ye. Fomin†, V. Korchuganov, NRC «Kurchatov Institute», Moscow, Russia

Abstract

The inauguration of the only dedicated synchrotron radiation source in Russia was held at NRC "Kurchatov Institute" in 1999. At present according to its main parameters it is a "2+" generation synchrotron radiation facility. In this article we consider the possibility of the Kurchatov synchrotron radiation source upgrade up to compact 3rd generation facility with keeping of all experimental stations at the same places. Also we present the conceptual design of the new diffraction limited synchrotron radiation source (4th generation facility) for NRC "Kurchatov Institute".

INTRODUCTION

Kurchatov synchrotron radiation source is dedicated synchrotron light facility and works for the experiments in the range of synchrotron radiation from VUV up to hard X-ray. It consists of 80 MeV linac, 450 MeV booster synchrotron and 2.5 GeV main storage ring. Synchrotron radiation from bending magnets of the main storage ring overlapping the spectral range of 0.1-2000 Å.

The lattice of the main storage ring consists of 6 superperiods with two types of 3 m straight sections [1]. Dispersion free straight sections are used for installation of wigglers and RF cavities. And straight sections with nonzero dispersion function are used for injection, for installation of diagnostic, feedback systems and undulators.

The main storage ring has only one user operation mode with 98 nm·rad electron beam emittance. Its main parameters are given in Table 1, lattice functions of one of superperiods – in Fig. 1 and dynamic aperture in the centre of dispersion straight section – in Fig. 2.

Table 1: The Main Parameters of the Main Storage Ring

Parameter	Value
Energy	2.5 GeV
Circumference	124.13 m
Number of superperiods	6
Beam current	100 – 150 mA
Beam lifetime	15-20 h
Horizontal emittance	98 nm·rad
Horizontal/vertical tune	7.775 / 6.695
Horizontal/vertical chromaticity	-16.9 / -12.9

According to its main parameters Kurchatov synchrotron radiation source is a "2+" generation facility. But due the facility was initially designed to have some space for improvement in the future now it is possible to upgrade it up to a compact 3rd generation synchrotron light source.

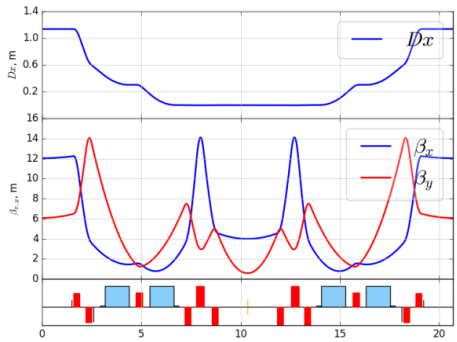

Figure 1: Lattice functions in user operation mode.

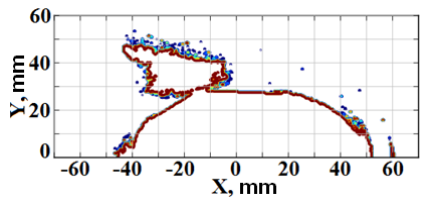

Figure 2: Dynamic aperture.

TO THE 3RD GENERATION LIGHT SOURCE

Currently a lot of work is carried out to improve facility performance and extend its experimental capabilities. Namely new photon beamlines are comissionning, next year two superconducting wiggers will be installed at the main storage ring, many facility systems are under upgrade and so on.

The research carried out in ref. [2, 3] show that it is possible to reduce electron beam emittance by varying excitation currents into quadrupoles and, most importantly, without any changings of geometric sizes or positions of all magnetic elements. So if the beam current and lifetime will remain at the same level then the intensity and brightness of synchrotron radiation will be increased.

If the size of the dynamic aperture is kept sufficient for an electron beam injection from the existing booster synchrotron, storing and acceleration up to working energy then there are two options with completely different main storage ring lattices. The first option is the lattice with 60-65 nm·rad emittance and dispersion free into one of two straight sections. Lattice functions and dynamic aperture of lattice tuning to achieve 67 nm·rad emittance are shown in Fig. 3 and Fig. 4. The second option is the lattice with 15-20 nm·rad emittance and nonzero dispersion into both two straight sections. Lattice

* Work supported by the Ministry of Science and Education of Russian Federation, Agreement No 14.616.21.0086 from 24.12.2017, ID RFMEFI61617X0086
†yafomin@gmail.com

ISBN: 978-3-95450-197-7 doi:10.18429/JACoW-RUPAC2018-THCAMH02

SOLITARY AND SHOCK WAVES IN FREE AND MAGNETIZED QUASI-NEUTRAL LASER INDUCED PLASMAS*

Stephan I. Tzenov†, Extreme Light Infrastructure - Nuclear Physics, 077125, Magurele, Bucharest, Ilfov County, Romania

Abstract

Starting from the Vlasov-Maxwell equations, an exact relativistic hydrodynamic closure for a special type of water-bag distributions satisfying the Vlasov equation has been derived. In the case of magnetized quasi-neutral plasma, the hydrodynamic substitution has been used to derive the hydrodynamic equations for the plasma density and current velocity, coupled to the wave equations for the self-consistent electromagnetic fields. Based on the method of multiple scales, a system comprising a vector nonlinear Schrodinger equation for the transverse envelopes of the self-consistent plasma wakefield, coupled to a scalar nonlinear Schrodinger equation for the electron current velocity envelope for free plasma, has been derived. In the case of magnetized plasma, it has been shown that the whistler wave envelopes of the three basic modes satisfy a system of three coupled nonlinear Schrodinger equations. Numerical examples for typical plasma parameters have been presented. It has been shown that in the case of magnetized plasma, the whistler waves facilitate the transverse confinement considerably.

INTRODUCTION

In the mid 1950s, Budker and Veksler [1, 2] proposed utilizing plasma collective fields to accelerate charged particles more compactly. Twenty years later this idea was further developed by the late John Dawson and his collaborators [3, 4]. Several mechanisms to generate large amplitude electron plasma waves are presently put into practice. The first one dates back to 1956, when V.I. Veksler's [2] suggestion of acceleration by means of collective fields was further elaborated by G.I. Budker [1], who proposed the concept of a self-stabilized ring beam. In recent years the beat wave mechanism [5], the laser-driven wakefield generation, and last but not least excitation of plasma wave structures by charged particle beams propagating in the plasma medium have attracted much attention. More recent numerical simulations and experimental investigations show that ultra-intense laser-matter interactions and laser-induced plasma wakefields can be used for new type of laser-driven positron sources [6] and acceleration of ion beams [7] with narrow energy spread.

Whistler waves are one of the first plasma waves observed and studied for more than a century. The first analytical approach to the linear dispersion properties of whistler waves is the one suggested by Appleton [8] and Hartree [9], who proposed the famous Appleton-Hartree dispersion equation. While the linear stability properties of the electromagnetic waves in the whistler mode are relatively well studied [10,11], there is a serious gap in the understanding of their nonlinear behaviour. The general theory of nonlinear waves in a cold, collisionless relativistic plasma was initiated by Akhiezer and Polovin [12]. The study of the nonlinear behaviour of whistler waves has been initiated by Taniuti and Washimi [13], who obtained a nonlinear Schrodinger equation for the slowly varying wave amplitude.

We first review and summarize some basic properties of laser driven plasmas. Then, following Refs. 14 and 15, we reduce the Vlasov-Maxwell system to an *exact closure* of relativistic warm fluid dynamic equations for the plasma species, which are coupled to the wave equations for the radiation field. Using the method of multiple scales, we outline how a vector nonlinear Schrodinger equation describing the evolution of the slowly varying amplitude of the transverse plasma wakefield, coupled to a scalar nonlinear Schrodinger equation for the amplitude of the electron current velocity can be derived. Next, the derivation of the cold hydrodynamic picture by using the so-called hydrodynamic substitution has been outlined. We then obtain a system of coupled nonlinear Schrodinger equation describing the evolution of the slowly varying amplitudes of the three basic whistler modes. The analysis of an approximate traveling wave solution to the coupled nonlinear Schrodinger equations in both the relativistic and the non relativistic case concludes Section 4. Finally, we draw some conclusions in the last Section.

BASIC PROPERTIES OF LASER PLASMAS

To gain insight into the basic properties of laser induced plasmas, we consider a simple non-relativistic model

$$\partial_t n + \partial_x (n v_x) = 0, \tag{1}$$

$$\partial_t \mathbf{v} + v_x \partial_x \mathbf{v} = -\frac{e}{m}[\mathbf{E} + \mathbf{e}_x (\mathbf{v} \cdot \partial_x \mathbf{A}) - v_x \partial_x \mathbf{A}], \tag{2}$$

$$\partial_x E_x = -\frac{e}{\epsilon_0}\left(n - \overline{Z} n_i\right). \tag{3}$$

This model describes the plasma response to an external perturbation propagating longitudinally along the x-axis with a unit direction vector $\mathbf{e}_x$ and specified by the electromagnetic vector potential $\mathbf{A}$. Here, n and $\mathbf{v}$ are the electron number density and the current velocity, respectively, while $\mathbf{E}$ is the self-consistent electric field. In addition, m and e are the rest mass and the charge of the electron, respectively, ϵ_0 is the permittivity of free space and finally, $\overline{Z}$ and n_i are the

* Work supported by Extreme Light Infrastructure - Nuclear Physics (ELI-NP) Phase II, co-financed by the Romanian Government and the European Union through the European Regional Development Fund.
† stephan.tzenov@eli-np.ro

ISBN: 978-3-95450-197-7 doi:10.18429/JACoW-RUPAC2018-THXMH01

STATUS OF DEVELOPMENT OF SUPERCONDUCTING INSERTION DEVICES FOR GENERATION OF SYNCHROTRON RADIATION AT BUDKER INP

V. A. Shkaruba†, A.V.Bragin, S.V.Khrushchev, V.K.Lev, N.A.Mezentsev, V.M.Syrovatin, O.A.Tarasenko, V.M.Tsukanov, A.A.Volkov, A.V.Zorin, BINP, 630090, Novosibirsk, Russia

Abstract

The installation of superconducting insertion devices on storage ring gives an opportunity to increase the photon flux in the required range of synchrotron radiation spectrum and shift the photon spectrum to hard X-ray region. During more than 35 years BINP developed the superconducting insertion devices for generation of synchrotron radiation. More than 20 superconducting wigglers which were produced by BINP are used on many storage rings around the world. Each of them was optimized for the individual requirements of the experiments and taking into account the characteristics of the storage rings. However all the device can be conditionally divided into several groups with similar features: high field wigglers (up to 7.5 T) with long period (140 - 200 mm), middle field (2.5 - 4.2 T) with middle period (46 - 64 mm) and low field (2 - 2.5 T) with short period (30 - 34 mm). The superconducting wiggler cryostats which are developed in BINP are operated not only with zero liquid helium consumption but even with a lower relative to the atmosphere pressure despite of additional heat load from the electron beam and from the current of ~1000 A for supplying of superconducting magnet. This allows not only to avoid a helium loss but also to increase the level of the magnetic field due to the shifting of the critical parameters of superconducting wire. The features of magnetic and cryogenics systems of the superconducting wigglers produced in BINP are presented in this report.

INTRODUCTION

The superconducting insertion devices (ID) being installed on storage ring gives an opportunity to increase the photon flux of synchrotron radiation (SR) spectrum in the required range and shift the photon spectrum to hard X-ray region. Budker INP develops superconducting insertion devices technology during more than 35 years. The world's first superconducting 20-pole wiggler with magnetic field of 3.5 T and the period of 90 mm was created in BINP and installed on the 2 GeV VEPP-3 storage ring in 1979 [1]. Since 1995 Budker INP has created more than 20 superconducting insertion devices which operate on many SR sources. The features of magnetic and cryogenics systems of the superconducting insertion devices produced in BINP are presented in this report.

WAVELENGTH SHIFTERS

The insertion device is installed in a free straight section and is not an element of main magnetic lattice of storage ring. Therefore the main requirement for ID being installed on a storage ring is not to reduce the reliability of the machine. Such effect as tune shifts, beam dynamic reduction etc. should be compensated with use of external magnetic elements. One of the main demands for ID field distributions is not to disturb of beam orbit in any place except of the straight section. The condition for closed orbit is zeroing of first and second field integrals along of beam trajectory inside of the inserting device.

The simplest ID with magnetic structure that satisfies these conditions is a three-pole Wave Length Shifters (WLS) which consists of one main dipole with high magnetic field for generation of SR and two side poles with low field for compensation of orbit deviation [2]. The main parameters of high field superconducting WLS with the maximum field from 7 T to 10 T produced in BINP are presented in Table 1.

Table 1: The Main Parameters of Three-Pole High Field SC WLS Produced in BINP

SR source, year	B_{max}/B, T	Pole gap, /beam gap, mm	SR power, kW (E,GeV; I,A)
PLS, Korea, ’95	7.68/ 7.5	48/26	3.6 (2; 0.1)
LSU-CAMD, USA, ’98	7.55/7.0	51/32	5.3 (1.5; 0.3)
SPring-8, Japan, ’00	10.3/10.0	40/20	100 (8; 0.1)
BESSY-II, Germany, ’00	7.5/7.0	52/32	13 (1.9; 0.5)
BESSY-II, Germany, ’01	7.5/7.0	52/32	13 (1.9; 0.5)

The field in the side dipoles should be minimized to reduce the contribution of radiation of the so-called “second source” from the side poles to the spectral flux of photons of the main pole. Three-pole WLS has a disadvantage in a shift of the radiation point in horizontal plane due to the displacement of the beam orbit for different field values in the main dipole. To fix the radiation point in the center of the shifter at any field level on the main pole two additional steering magnets can be used as presented in Fig.1.

† V.A.Shkaruba@inp.nsk.su

ISBN: 978-3-95450-197-7 doi:10.18429/JACoW-RUPAC2018-THCBMH02

EVALUATIONS OF PARAMETERS STABILITY FOR S-BAND RF GUN CAVITY DUE TO EFFECTS OF PULSED RF HEATING

V. Paramonov*, A. Skasyrskaya, INR of the RAS, 117312, Moscow, Russia
B.L. Militsyn, UKRI STFC/ASTeC, Daresbury, Warrington, Cheshire, UK

Abstract

Requirements to high stability of electron beam arrival time in modern FEL facilities transform to requirements of high stability of amplitude and phase of electric fied in RF photocathode gun which is used as electron injector. To provide high quality of bunches, gun cavities with high electric and hence magnetic RF fields. Effects, related to pulse RF heating, result in change of the cavity frequency and quality factor during even few μs RF pulse. Cavity deformations due to pulse heating are considered and corresponding cavity detuning are evaluated. Resulting deviations of the phase and amplitude of the RF field in the gun cavity as a function of RF pulse duration are estimated.

INTRODUCTION

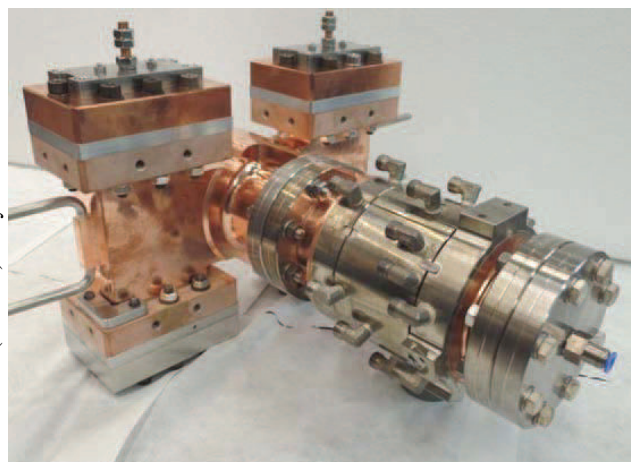

Figure 1: S band HRRG RF cavity for the CLARA project.

Photocathode RF guns are now widely used for generation of short and bright electron beams in modern Free Electron Laser (FEL) facilities. For low repetition rate FEL the guns are usually based on S-band normal conducting RF cavities. Despite of specific requirements to different facilities and details of technical decisions used, design and operating mode of the gun cavities have common, typical patterns. As a typical modern example Fig. 1 illustrates High Repetition Rate Gun (HRRG) photocathode gun designed for the CLARA project, [1]. HRRG 1.5 cell cavity has a coaxial input RF coupler with symmetric feed.

To provide electron bunches with small transverse emittance the gun operate in pulsed mode with a high, of up to $\sim 120\ \frac{MV}{m}$ electric field E_c at the cathode surface. With a need it results in a high, of $\sim 250\ \frac{kA}{m}$ magnetic field at the surface H_m and the high density of the pulsed RF losses P_s of up to $\sim 4.5 \cdot 10^8 \frac{W}{m^2}$. Effects of the pulsed RF heating take place during RF pulse $\tau \sim (3 \div 6)\ \mu s$ then the temperature at some parts of the cavity surface T_s rises up to $(19 \div 30)\ C^o$.

One of the critical requirements to the linear accelerator based FEL facilities with laser seeding is high arrival time stability of the electron bunches. Essential impact on the arrival time gives the amplitude and phase of the pulsed RF field in the gun cavity, [2]. Temperature rise of the cavity during RF pulse leads to thermal deformations and change of the cavity parameters. It directly lead to deviations in the amplitude and the phase of the RF field in the cavity.

PROCESS DESCRIPTION

Process of thermal elastic deformations is described by the coupled equations for temperature $T(\vec{r},t)$ and displacements $\vec{u}(\vec{r},t)$ distributions, [3]:

$$\begin{aligned} div(gradT(\vec{r},t)) - \frac{\rho_m C_p}{k_c}\frac{\partial T(\vec{r},t)}{\partial t} - \\ - \frac{\alpha_t E_Y T_0}{3k_c(1-2\nu)}\frac{\partial div\vec{u}}{dt} = 0, \\ \frac{3(1-\nu)}{(1+\nu)} grad(div\vec{u}) - \frac{3(1-2\nu)}{2(1+\nu)} rotrot\vec{u} - \\ - \alpha_t gradT(\vec{r},t) - \frac{3(1-2\nu)\rho_m}{E_y}\frac{\partial^2\vec{u}}{\partial t^2} = 0, \end{aligned} \quad (1)$$

where $\rho_m, C_p, k_c, \alpha_t, E_Y$ and ν are the density, the specific heat, the heat conductivity, the coefficient of linear thermal expansion, the Young's modulus and the Poisson ratio, respectively. The first equation in Eq. 1 describes the heat diffusion from the heated surface into the cavity body. This process is well studied and explained in [4] and related references. The pulsed temperature rise T_s of the surface over the average steady-state value and the heat penetration depth into body D_d can be estimated as:

$$T_s = \frac{2P_s\sqrt{\tau}}{\sqrt{\pi k_c \rho_m C_p}}, \quad \alpha_d = \frac{k_c \tau}{\rho_m C_p}, \quad D_d = \sqrt{\alpha_d \tau}, \quad (2)$$

where $\alpha_d \approx 10^{-4}\ \frac{m^2}{s}$ is the thermal diffusivity for copper. For the RF pulse duration $\tau = 1\ \mu s,\ 3\ \mu s,\ 6\ \mu s$ and $10\ \mu s$ the heat penetrates to the depth $D_d = 10.7\ \mu m,\ 18.5\ \mu m,\ 26.2\ \mu m$ and $33.8\ \mu m$ respectively.

The second equation in Eq. 1 is a typical wave equation for displacements $\vec{u}$ with source $\alpha_T gradT(\vec{r},t)$. Equation describes propagation of longitudinal elastic waves of compression from the source with velocity $V_l =$

* paramono@inr.ru

ISBN: 978-3-95450-197-7 doi:10.18429/JACoW-RUPAC2018-THCDMH01

MAGNETIC FIELD OF THE 40–80 MEV H^- CYCLOTRON C-80: EXPERIMENTS AND CALCULATIONS

S.A. Artamonov, E.M. Ivanov, G.A. Riabov,
NRC KI - PNPI, Gatchina, Leningrad district, 188300, Russia

Abstract

The paper concerns to the final parameters of the magnetic field distribution of the new H-minus isochronous cyclotron C-80 and results of 3D computer calculations and experimental measurements before the installation of the vacuum chamber into the cyclotron gap. The cyclotron C-80 with variably energy 40 - 80 MeV and current up to 100 μA is planned to be used as for applied physics program – for production of medicine isotopes, for therapy of eye melanoma and surface forms of cancer, for radiation resistance tests of electronic components – as well as for fundamental research in nuclear physics, solid state physics and biology.

GENERAL DESCRIPTION

The magnet and the magnetic system are the most important part of the cyclotron, and a considerable attention was paid to their design. The magnetic field of the cyclotron C-80 should meet several requirements. The magnetic field rigidity at the final orbit must reach Br = 13.2 kGs·m, which corresponds to 80 MeV energy of the proton beam. For insuring the isochronism, the magnetic field averaged over the azimuth when going from the centre of the magnet to the final orbit should increase by ~8.5%. The azimuthal variation of the magnetic field should provide the vertical and horizontal transversal focusing. Some room should be left for a high frequency system: the gap between the shims should be wider than 160 mm. In distinction from a standard cyclotron, there is an additional and essential requirement for an H^- machine – to keep H-minus losses due to dissociation less than some percent. Acceleration of H^- ions has obvious advantages: a possibility for 100 % extraction of the beam with high intensity and variable energy. On the other hand, it requires a special source of H^- ions, high vacuum, and what is most important, the magnetic field strength in the magnet sector should not exceed in our case 16.8 kGs to prevent H^- electromagnetic dissociation.

2D CALCULATION AND OPTIMIZATION

A few years ago, as a first approximation, the magnetic structure of the cyclotron was designed on the basis of 2D calculations by using the POISSON program and measurements on two small models [1-3]. The geometry and the key parameters of the magnetic system for the cyclotron were selected:

The major unit of the cyclotron, its electromagnet, was designed using the model of the magnet of the PNPI SC-1000 synchrocyclotron (SP-72). This electromagnet has been a traditional design with an E-shaped magnet yoke and a pole of 1.5 m in diameter with gap 289 mm. The calculations have showed that simple increasing of the pole radius from 0.75 m to 1.025 m causes not only the increasing of the magnetic flow up to more than1.6 of previous value but and the saturation the iron in the pole end. Therefore the cross section of the yoke has been increased by 16% and the height of the side pillar decreased by 0.5 m. These procedures allowed decrease the maximum field in the magnet yoke down to 23.5 kGs, decrease the excitation current down to 800 A and reduce the power consumption down to 120 kW.

Also the hill and valley gaps were chosen by the method of the filling factors [4] that was adapted to cyclotron. It was supposed that the initial height of each of the sectors would be equal to 90 mm, and during further optimization it was not changed. For obtaining the required isochronism, the height of the correction sector shims was varied. The initial heights of these shims were chosen equal to 20 mm. They were then optimized by 3D calculations to obtain an isochronous field. Besides, in the course of the optimization, special constrained conditions were imposed. It was required that the amplitude of the main 4-th field harmonic should not exceed ~3000 Gs, and the field near the extraction radius $r \approx 90$ cm should be $B \leq 16800$ Gs. To reduce H-minus dissociation losses, a magnetic structure of C-80 with high spiral angles was proposed [2]. Under these conditions, the H-minus dissociation should be below 5% [5]. For these purposes, additional valley shims were introduced into the magnetic system, and their geometrical parameters were also varied.

3D CALCULATION AND OPTIMIZATION

At the second stage, the main parameters of the cyclotron magnetic system were refined and optimized by computer simulations with the 3D MERMAID code [6,7], and the dynamics simulations were performed with the code in [8]. The main peculiarities and modifications of the preliminary design can be formulated as follows [9]:

The detailed 3D geometry of the magnet yoke, of the sectors (4 pairs), sector shims (17 correction shims in each sector), and the valley shims, the coils, and the external boundaries was introduced in the computer model. Because of a big angular extension of the spiral sectors in C-80, it was necessary to use in the calculations a half of the magnet with the corresponding symmetry boundary conditions. The external boundary of the area where the calculations were performed was chosen rather far to get rid of its influence on the magnetic field in the working region and to determine correctly the fringe field. The fringe field was taken into account for correct calculations of the extraction beam optics. Thus, for the

ISBN: 978-3-95450-197-7 doi:10.18429/JACoW-RUPAC2018-THCDMH02

POWER SUPPLY SYSTEMS OF HIGH-VOLTAGE KICKERS ON THE BASIS OF TPI- AND TDI- THYRATRONS

V.D. Bochkov, D.V. Bochkov, V.M. Dyagilev, V.G. Ushich, Pulsed Technologies Ltd., 5, Yablochkova str., 390023, Ryazan, Russia
O.V.Anchugov, D.A.Shvedov, G.I. Budker Nuclear Physics Institute SB RAS, 630090, Novosibirsk, Russia
A.A.Fateev, Joint Institute for Nuclear Research, Joliot-Curie str. 6, 141980 Dubna, Moscow Region, Russian Federation
V.A.Sytchev, M.P.Ovsienko, NRC "Kurchatov Institute"- IHEP, 142281 Moscow Region, Protvino, Russian Federation

Abstract

This report is a survey of lifetime tests with cold-cathode TPI-thyratrons, or pseudospark switches (PSS) in kickers of various accelerators. Descriptions of design and electrical circuits of power kickers as well as lifetime, test results of devices utilizing 25 and 75 kV TDI- and TPI-thyratrons in injection and extraction kickers of the FEL (the Duke University, USA), NIKA installations (JINR) and accelerator U70 in Kurchatov's Institute – IPHE are presented.

INTRODUCTION

High-voltage kicker power supplies, both existing and under construction in new MegaProjects, are subject to the most stringent requirements. As for operation of the kickers high current (about 10s of kiloamperes) at load impedance of several Ohm are required, the operating voltage should be as high as 100 kV, pulse duration of 0.2-5 μs, rate of current rise higher than 100 kA/μs, timing instability (jitter) less than 10 ns. The time interval between pulses depending upon the quantity of injected bursts for every switch can be from tens of microseconds up to several seconds. The switches should be able to operate both positive and negative voltages.

Normally high-power thyratrons and spark gaps have been used as the switching components. In particular, for CERN-made accelerators in NRC "Kurchatov Institute"-IHEP working gas pumped spark gaps were utilized. In the recent time there have been many reports on application of solid state-switches in kicker [1-3]. However gas-discharge thyratrons are still in demand. For example it is known that in the international project – FAIR accelerator (Facility for Antiproton and Ion Research) Helmholtzzentrum für Schwerionenforschung in Darmstadt, Germany) classical thyratrons will be used to drive kicker magnets. The company TeleDyn-e2v reported the fact that it won contract to supply 30 thermionic cathode, deuterium hollow anode thyratrons CX2593X, featuring 4 high-voltage gaps, operating voltage up to 100 kV (https://www.e2v.com/news/e2v-thyratrons-to-drive-kicker-magnets-at-fair-accelerator/).

Application of thyratrons to deliver average current 5-10 A at the expense of heating power up to several hundreds of watts [4, 5], like CX2593X and CX1925, is not quite reasonable, especially in kicker drivers, operating at frequency up to 60 Hz. The toughest competition with solid state switches makes the thyratron designers to elaborate solutions without shortcomings inherent in classic thyratrons as power heater circuits, insufficient reliability and lifetime, high costs. Cold cathode thyratrons have been designed in Germany, USA, France, Russia and other countries [6]. To date TDI- and TPI-type pseudospark switches operating at voltages up to 150 kV, used in various pulsed power application, including free electron lasers, accelerators [5, 7, 8]. In kicker drivers TPI-switches are capable of operating at either polarity of driving voltages, feature record low recovery time, small outline dimensions and relatively low cost.

TDI-type thyratrons are used as crowbars, providing a unipolar impulse and protection of the unit elements [9], eliminating dangerous overvoltages.

CIRCUIT AND TEST OF TPI-THYRATRONS DRIVEN KICKERS

System of High-Voltage Nanosecond Generators for Injection-Extraction Kickers for FEL Complex of the Duke University

A 1.2 Gev booster-synchrotron was created in order to increase the electron beam current in the main ring of the free electron laser SR FEL [7]. This works considers a system of nanosecond generators of beam kick pulses on the injection and extraction kickers of the FEL booster as well as a kicker system to inject the beam into the main ring of the SR FEL. In the nanosecond generators, energy is switched to the load with the use of the Pseudo-Spark Switch (PSS, thyratrons with a cold cathode) of the TPI-family (see Tables 1, 2 and 3).

Table 1: System Specifications of Injection Generator with TPI1-1k/20

Pulse duration, ns	106
Maximal amplitude, kV	15
Pulse front time (level of 0.1-0.9), ns	8
Pulse decay time at the level of (0.1-0.9), ns	8

ISBN: 978-3-95450-197-7 doi:10.18429/JACoW-RUPAC2018-THCDMH03

CHALLENGES OF OBTAINING OF ULTRA-HIGH VACUUM IN NICA PROJECT

A.V. Smirnov#, A.R. Galimov, A.N. Svidetelev, JINR, Dubna, 141980 Russia

Abstract

NICA is the new accelerator collider complex under construction at the Joint Institute for Nuclear Research in Dubna [1]. Operating pressure in the beam pipes of booster and collider is not more than 2×10^{-9} Pa. Operating temperature of the beam chambers 85% surfaces from 4.2K to 80 K. These parts cannot be baked. Maximum temperature of bake out is 80 C. The beam pipes have a high length and a low conductance. The paper describes problems and paths of decision of achievement ultra-high vacuum in the beam pipes of the NICA complex. For this purpose, in collaboration with Vakuum Praha [2], a test bench for the most effective pumping of the accelerator chamber of the superconducting fast cycling synchrotron has designed and built.

The article provides the simulation results of vacuum distribution in superconducting accelerators with "warm" chamber parts at room temperature. The specialized programming code was developed for this purpose. The simulation has revealed a necessity of installation additional pumping equipment along the booster perimeter. To solve this problem, development of original design of titanium sublimation pump operating at cryogenic temperatures has started in collaboration with the Budker Institute of Nuclear Physics [3].

KEY POINTS TO OBTAINING OF ULTRA-HIGH VACUUM

An achievement of ultra-high vacuum conditions in particle accelerators is very complicate task, which needs to solve different technical tasks during design, production, assembling and service of the vacuum chambers. In the NICA project two accelerators will be operate under ultra-high vacuum conditions: booster synchrotron and collider rings [4].

Vacuum Chamber Design

The typical materials for ultra-high vacuum chambers are stainless steel, cooper, and ceramics. In the NICA project, usually the stainless steel 304 and 316L is used for the vacuum chamber under room temperature and 316LN under cryogenic temperatures.

All composite materials and metal alloys must have certificates for the using in the ultra-high vacuum system. The saturated vapor pressure of all materials must be less than the residual gas pressure. In case of failure to comply with these conditions, the chamber sections shall be provided with additional differential pumping. Some diagnostic systems cannot be baked to a temperature of 280 C and must be separated by gate valves and have its own pumping systems.

The cryogenic vacuum chambers inside superconducting magnets cannot be baked out before the cooling because the material of magnets is not designed for high temperature. In this case, the water cannot be effectively removed from the cryogenic chamber. The main part of the water will be frozen during cooling of the cryogenic chamber but the transitions between “cold” and “warm” parts are not baked and not cooled.

Beam Life Time and Pumping Systems

The pressure for booster and collider rings is estimated on the level of 10^{-9} Pa, which is defined by the beam life due to an interaction with the residual gas. The estimation of the beam dynamics instability shows that this effect is not significant for the design beam intensity. Only for the beam intensity for two order larger the dynamics vacuum instability can play role in the beam lifetime.

The standard solution to reach the vacuum condition up to 10^{-9} Pa is using the combination of the ion pump (IP) with different types of getter: titanium sublimation pump (TSP) and non-evaporated getters (NEG). In the collider and booster for the beam pipes under cryogenic temperature SIP was chosen with IP combination [5].

NEG pump can be used for the cryogenic chamber only when this pump can be separated from the beam pipe with the vacuum valve. During activation procedure, the NEG pump extracts a lot of hydrogen, which absorbs on the wall surface and needs the additional time to pump back to NEG. It means that the vacuum chamber cannot be cool down to the cryogenic temperature immediately after the NEG activation.

The design of the vacuum stand for “cold” chambers in superconducting arcs was elaborated in the collaboration with Vakuum Praha [2]. The vacuum stand includes the oil-free preliminary pumping system with fore vacuum and turbo pimps, ion pump with combination of the TSP pump. The vacuum test under the room temperature show good results. Finally, this vacuum stand will be tested with the real vacuum chamber under the cryogenic temperature.

Pressure Distribution in Booster

The simulation of the pressure distribution in the booster along the vacuum chamber shows that 22nd ion pumps with TSP is not enough to reach the necessary vacuum condition. One of solution is to install an additional TSP between each magnets in the booster [6].

The collaboration between JINR and BINP has started to investigate the possibility of the TSP operation under cryogenic temperatures. First experiments show that TSP can operate under cryogenic temperature and heat inflows during TSP heating up to 1000 C are not a problem for the booster cryogenic system. Next step is to test the full-size

#smirnov@jinr.ru

ISBN: 978-3-95450-197-7 doi:10.18429/JACoW-RUPAC2018-THCDMH05

NEW RF SYSTEM FOR VEPP-5 DAMPING RING

G.Ya. Kurkin, Yu.A. Biryuchevsky, E.K. Kenzhebulatov, A.A. Kondakov, A.Yu. Martynovsky, S.V. Motygin, V.N. Osipov, A.M. Pilan, E.A. Rotov, I.K. Sedlyarov, A .G. Tribendis,
Budker Institute of Nuclear Physics, 630090, Novosibirsk, Russia.

Abstract

The VEPP-5 injection complex serves to obtain high-intensity electron and positron bunches for injection into colliders of the Institute of Nuclear Physics SB RAS. The old RF System operated at 700 MHz - the 64 harmonic of the revolution frequency. Due to the large beam length from LINAC up to 70% of the particles were lost during injection.

Therefore, in 2015, the decision was made to install into the ring the new RF cavity operated at the first harmonic of the ring revolution frequency of 10.94MHz. To reduce the geometric dimensions, ferrites were used in the cavity. The RF cavity was manufactured, and RF power amplifier and a new RF control system were prepared. After testing the RF system at the stand, in August 2017 the RF cavity was installed instead of the former 700 MHz cavity. The new RF system is now in operation since September 2017. The paper presents main features of the cavity design and fabrication. RF power amplifier and operation of the control system are described.

INTRODUCTION

In the Damping Ring (DR) [1 - 3] of the VEPP-5 injection complex, bunches of particles with a duration of ~ 5 nsec are injected with a significant energy spread (See Table 1). The particles in the DR circulate and during the time of damping the energy spread decreases and it becomes possible to inject them into the colliders for experiments with colliding electron-positron beams.

The transition to a lower harmonic of the RF system increases the capture of particles injected into the DR. One can also consider the proposal to increase the pulse duration from the electron gun to increase the charge of particles injected in a single cycle.

Table 1. Damping Ring Designed Parameters

Parameter		Value
Revolution frequency		10.94 MHz
RF ratio		64
Particles energy		510 MeV
Particles number		$2 \cdot 10^{10}$
Energy loss per turn		5.9 keV
Orbit compaction factor		0.022
Injection repetition rate		50 Hz
Energy spread e+, e-		3%, 1%
Energy spread of damped particles		0.07 %
Damping time	H	11.3 msec
	V	17.5 msec
	L	11.9 msec

RF CAVITY

The available length of the gap in the ring for the cavity is 600 mm. To reduce the geometric dimensions, ferrites are used in the cavity. In Russia ferrite rings of two suitable standard sizes are manufactured at the factory of JSC ”FERROPRIBOR” in St. Petersburg: 250 x 180 x 25 and 180 x 110 x 20.

Using only one larger ring size is not desirable and does not pass. For required RF voltage amplitude of ~ 10kV at the frequency of 10.9 MHz, cooling of rings is difficult due to the large amplitude of RF magnetic field in the ring and, correspondingly, the large dissipated power density.

It was decided to use both ring sizes. At the request of the customer, the manufacturer reduced the outer diameter of the inner ring from 180 mm to 174 mm. At first, the modules were manufactured in which a smaller ring was inserted into a larger one and rings were glued to a copper disk (see Fig. 1). The disk has a tube with water soldered along the external perimeter of the disk. As an adhesive, the organosilicon compound PentElast-712 type A was used.

The inner ferrite rings are cut into two halves along their diameters and glued together with a gap of 1.3 mm to equalize the average RF magnetic field in the large and small rings. In the gap between the halves of the inner ring, part of the magnetic flux may be closed through the

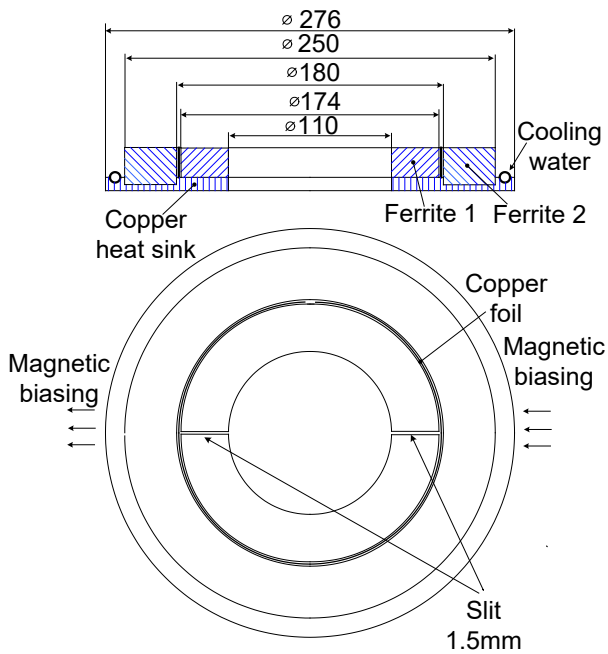

Figure 1: Ferrite module.

ISBN: 978-3-95450-197-7 doi:10.18429/JACoW-RUPAC2018-THCEMH01

TANGO ACTIVITIES IN BINP

A. Senchenko†, G. Fatkin, E. Kotov, S. Serednyakov, V. Sitnov
Budker Institute of Nuclear Physics, Novosibirsk, Russia
also at Novosibirsk State University, Novosibirsk, Russia

Abstract

Several years of experience using TANGO Control system are discussed in this paper.

Construction of Linear Induction Accelerator (LIA-20) was the driving force for introduction of TANGO in Budker Institute. In the frame of this project, significant number of TANGO Classes for different types of hardware were developed and basic program infrastructure was provided. This progress made it feasible to apply TANGO to other facilities. Therefore, it was used in some subsystems at VEPP-2000 and vacuum stand. This paper presents overview of construction of TANGO based control system. The problems, which arise during its introduction to existing control system, are discussed as well.

INTRODUCTION

In 2015, construction of Linear Induction Accelerator (LIA-20) was started. It will provide electron beam with energy 20 MeV, current up to 2kA and lateral size after focusing on the target less than 1 mm. Channels number and types presented in Table 1. For this project, it was decided to develop new hardware and new control system [1].

Table 1: Number of Channels

Type	Channel Number
Fast (<10 us)	594
Slow (> 10 us)	1485
Timing	1485
Interlock	1485
Technological control	1000
Total	6000

The expected lifetime of this facility is longer than 10 years, so it is necessary to pay attention to overall control system design and to selection of components. The experience gained during construction and operation of other facilities, such as VEPP-2000 and LIA-2, enable us to formulate general and technical requirement.

General requirements:

- Maintainability.
- Extensibility. Extension of system should not result in complete redesign of CS.
- Reusability. It should be possible to apply some solutions to other facilities.
- The use of outdated technologies should be avoided.

Technical requirement:

- It should be distributed control system.
- Ecosystem. Utilities, scripting, archive system and tools for rapid user interface (UI) development should be available.

TANGO satisfies these requirement. It is developed by consortium which consists of more that 10 scientific organization, such as ESRF, ALBA, MAX IV, SOLEIL, SKA, etc. Therefore, the risk of being abandoned in nearest future is significantly reduced. Moreover, large user community increases chance to find and to correct errors on early stages. It is worth to mention that TANGO was chosen at “Nuclotron-based Ion Collider fAcility” (NICA)[2].

TANGO has a rich ecosystem:

- Core libraries in C/C++, Python, Java
- Bunch of utilities for development and monitoring (Pogo, Jive, Astor)
- UI library: Taurus, ATK
- HDB++ archiving system

TANGO AT LIA-20

Creation of CS was started in the late 2015. Tight schedule of facility construction demanded to provide a test stand for accelerating modules and pulsed power supplies as soon as possible. So it was decided to divide development into two stages. At first stage, all hardware was provided with Tango Class and client program. These programs form minimum viable control system and serves as building blocks for software of the second stage. The second stage involves creation of high-level programs that operate in terms of entire facility.

The test stand was equipped with prototype of software at the end of first quarter of 2016. One year later, in first quarter of 2017, 5 MeV version of LIA-20 was put in operation. By that time, almost all VME [3] and CANBus devices were supported and the first stage accomplished.

The second stage was aimed at providing software that will facilitate operation of the facility. Work was started with Time Editor [4]. This program provides a way to define all delays and sequence of events as set of equations.

† a.i.senchenko@inp.nsk.su

ISBN: 978-3-95450-197-7 doi:10.18429/JACoW-RUPAC2018-THCEMH02

MODERN DIGITAL SYNCHRONIZATION SYSTEM FOR LARGE PARTILE ACCELERATORS

G. Fatkin*, A. Senchenko, M. Vasilyev, Ya. Macheret BINP and NSU, Novosibirsk, Russia
A. Selivanov BINP, Novosibirsk, Russia

Abstract

The review of modern approach to synchronizing large physical installations including accelerators is given in this paper. This approach is based on using digital modules connected by an optical link to transfer a mixed clock/data signal. A sub-nanosecond jitter and nanosecond resolution can be achieved this way as well as dynamic delay compensation and precision timing. Several modern synchronization systems based on this principle are discussed: White Rabbit, MRF, J-PARC and BINP developments.

INTRODUCTION

In recent years the approach to the synchronization of large physical installations has drastically changed. With new developments in digital electronics and optical technologies transferring a signal including carrying frequency and encoded data over a distance of several kilometers became possible. Using them a scheme was devised that allows to achive an unprecedented precision, flexibility and range for synchronisation of multitude control stations. This scheme allows to synchronize multitude of devices over the distance of multiple kilometers with jitter less than 100 fs.

A range of systems based on these principles were developed and are used in physical installations around the world. Most notable of them are: The White Rabbit Project (CERN) [1] which is planned for use in ESRF, SKA and several other installations; Micro-Research Finland (MRF) timing system [2] that is used in NSLS, Libera, ELI, and FRIB; J-Parc timing system [3] and Greenfield Technology timing system [4] used in Soleil, AWE, etc. This approaches were also recently used in synchronisation system of LIA-20 accelerator [5] in a system developed at BINP. Now let us describe the principles of their operation.

SYNCHRONISATION SCHEME

For the sake of simplicity let us let us consider two nodes, each of them functioning as a clock. By clock we mean a counter working on a specific stable frequency. The synchronization of two clocks then consists of several procedures:

- syntonisation – equalizing the frequencies;
- tuning of the phases;
- synchronizing the counter values;

In practice one of this clocks typically with a better frequency source such as a rubidium oscillator, or GPS-transmitted atomic clock frequency is considered a master-clock, and other one is a slave-clock.

* G.A.Fatkin@inp.nsk.su

Let us first consider the syntonization of these two clocks. The general idea between all of the modern synchronisation systems is shown on Fig. 1. In the master module the frequency from the master clock is mixed with data using an encoder. Then the produced clock/data signal from encoder is fed through an optical transmitter (TX) to an optical line. On a slave module the optical signal is converted to an electric one by a receiver (RX) and is fed to a clock data recovery scheme (CDR). Basically this scheme consists of a phase-locked loop that locks onto a frequency and provides it furhter to a module and a data recovery circuit. The data recovery circuit is more complicated and we will not discuss it in this article, but generally it performs a decoding operation based on the incoming clock/data signal and a frequency obtained by PLL.

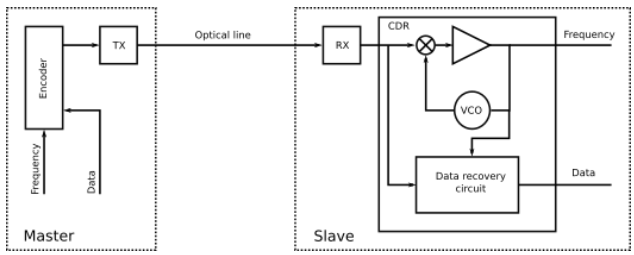

Figure 1: Synchronisation scheme.

The PLL is a central element in this scheme that determines the quality of the frequency traking. A received frequency from PLL is strictly locked to a transmitted master frequency, and with modern PLL's the accuracy in order of tens of picoseconds is attainable with ease. It should be noted also that the PLL can be used to create a frequency that is in a rational ratio to its input. This can be convenient in cyclic machines and is used to obtain an RF from master frequency source.

The ability to transmit data using this scheme is utilized to synchronously transfer the messages. This messages can contain delay and phase difference measurements as well as command sequences.

To measure the transmission delay between the following procedure is used: master module sends a special message to the slave module which sends back a reply immediately after receiving. Master module measures the time necessary for the transfer and thus gets a double transmission delay. There are some problems with this method if you want to achive an accuracy better than several nanoseconds, because in general the transmission line is assymethric, thus Master-Slave and Slave-Master delays can be different. To solve this problems an elaborate calibration schemes are used. After the Master-Slave delay is measured it can be transmitted to a slave module to be used

ISBN: 978-3-95450-197-7 doi:10.18429/JACoW-RUPAC2018-THCEMH03

EXPERIENCE ON THE APPLICATION OF AUTOMATED CONTROL SYSTEMS FOR CYCLOTRONS WITH DIFFERENT ENERGIES OF ACCELERATED PARTICLES

A. N. Kuzhlev,Y. N. Gavrish, P. A. Gnutov, A. S. Ivanenkov,
JSC «NIIEFA», 196641, St. Petersburg, Russia

Abstract

In the report are given the results on the development and application of automated control systems for a series of cyclotrons designed in the JSC "NIIEFA" with energies of accelerated hydrogen ions (H^-, D^-) from 1 up to 80 MeV.

INTRODUCTION

The JSC "NIIEFA" was a pioneer in the development of cyclotrons in our country. For more than seventy-year history, more than thirty five types of cyclotrons [1] have been designed. Development computer technologies set a task of creation of a system of automated control for cyclotrons.

THE FIRST EXPERIENCE ON THE DESIGNING OF AN AUTOMATED CONTROL SYSTEM FOR CYCLOTRONS OF THE CC SERIES

In 2006, the development of a new series of cyclotrons with acceleration of negative hydrogen ions (H-, D-) was started. The first two cyclotrons CC-18/9 of the new series were intended for the Hospital of the University of Turku, Finland and Russian Research Center for Radiology and Surgical Technologies, Pesochny, St. Petersburg, Russia.

The main element of the ACS for these cyclotrons was the powerful MELSEC System Q PLC from Mitsubishi Electric with expansion modules for connecting all types of signals used in the cyclotron ACS.To reduce the length of connecting cables, 2 passive stations on the basis of MelsecFX2N 32DP module intended for data remote acquisition were placed in the cyclotron hall. These stations are connected to the central PLC as slave Profibus-DP modules (see Fig. 1).

As the operator's console, a personal computer on which the Windows application is installed is used. The software of the central programmable logic controller totally controls all the systems of a cyclotron.

In 2006-2007, both cyclotrons were successfully delivered to customers and continue to work until now. However, in the process of adjusting the cyclotron equipment, the main drawback of the ACS with a single controller was revealed - if there is a need to make changes in the software, it is necessary to stop all cyclotron systems, which significantly slows down the adjustment procedure. Another drawback of this ACS was the use for measuring beam currents of standard ADCs intended for measuring slowly varying signals. The current measurement was not highly accurate. In addition, in the process of intensive operation of the cyclotron, part of the electronic equipment in the cyclotron hall has broken down over time, because of the high radiation level.

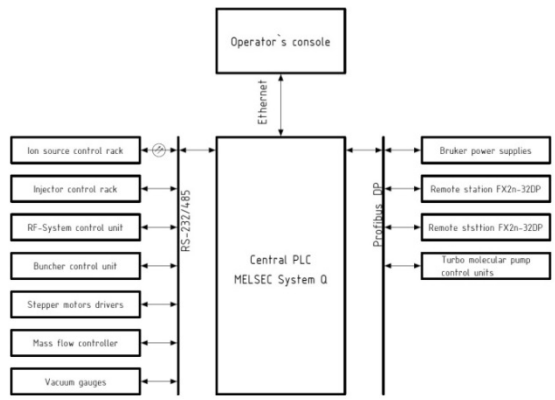

Figure 1: Block-diagram of the 1st ACS for cyclotrons of the CC series.

ACS OF THE 2-ND GENERATION

In 2007, the development of two cyclotrons was started: MCC-30/15 for delivery to the University of Juvaskula, Finland and CC-18/9 for FSUE "RFNC-VNIITF", Snezhinsk, Russia.

The following tasks were set during the development of ACS of these cyclotrons:

- Remove the drawback of ACS with one control controller and reduce the time of adjustment of equipment.
- Place electronic equipment in a radiation-safe place.
- Create a unified ACS suitable for cyclotrons of different types.
- Develop a high-quality system to measure the beam currents with a high-speed ADC and a possibility for the beam oscillogram display.
- Develop advanced RF-system control unit based on an industrial computer with digital synthesis and processing of signals built in an FPGA-based module.
- Provide the ability to connect several operator work-stations.

To solve these tasks, it was decided to create a control system with a distributed architecture (see Fig. 2).

The main element of the control system is the central computer, which is the server of the cyclotron modes database. It controls the data transfer between sub-systems and automatically starts sub-systems. Only

ISBN: 978-3-95450-197-7 doi:10.18429/JACoW-RUPAC2018-THCEMH04

CURRENT DEPENDENCE OF BUNCH DIMENSIONS IN VEPP-2000 COLLIDER*

Yu. A. Rogovsky†[1], E. A. Perevedentsev[1], D. B. Shwartz[1], M. V. Timoshenko, Yu. M. Zharinov,
Budker Institute of Nuclear Physics, 630090, Novosibirsk, Russia
[1]also at Novosibirsk State University, 630090, Novosibirsk, Russia

Abstract

The paper describes bunch dimension measurements in VEPP-2000 collider at energy 350 MeV. The three bunch dimensions (transverse sizes along with bunch length) was measured against bunch current to detect the energy spread growth. Emittance growth due to multiple intrabeam scattering was observed at bunch current below turbulence bunch lengthening threshold. The thresholds of these processes was used to estimate values of longitudinal impedance. Obtained values in a good agreement with predictions.

VEPP-2000 OVERVIEW

The VEPP-2000 is a small 24 m perimeter single-ring collider operating in the energy range below 1 GeV per beam [1] exploits the round beam concept (RBC) [2]. This approach, in addition to the geometrical factor gain, should yield the significant beam–beam limit enhancement.

Collider itself hosts two particle detectors [3], Spherical Neutral Detector (SND) and Cryogenic Magnetic Detector (CMD-3), placed into dispersion-free low-beta straights. The density of magnet system and detectors components is so high that it is impossible to arrange a beam separation in the arcs. As a result, only a one-by-one bunch collision mode is allowed. The layout of the VEPP-2000 collider is presented in Fig. 1.

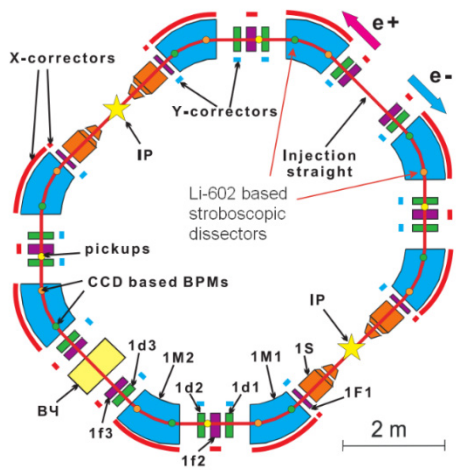

Figure 1: VEPP-2000 collider layout.

Beam Diagnostics

Diagnostics is based on 16 optical CCD cameras that register the visible part of synchrotron light from either end of the bending magnets and give full information about beam positions, intensities and profiles. In addition to optical beam position monitors (BPM) there are also four electrostatic pickups installed in the technical straight sections, two photomultipliers for beam current measurements via the synchrotron light intensity, and one beam current transformer as an absolute current monitor. Two phi-dissectors – stroboscopic image dissector [4] with electrostatic focusing and deflection that gives information about e+ /e− longitudinal distribution of particles and bunch length.

BUNCH DIMENSIONS

At the end of the luminosity-taking run (May 2018) a series of machine learning experiments was done – all thee bunch dimensions was carefully measured in wide range of bunch currents (1-100 mA) while RF cavity voltages changes around the values used in operations – U_{rf} = 18.5 / 49.5 / 38.5 / 9.3 / 4.7 / 4.6 / 18.6 / 68.5 kV (text colors corresponds to the line colors in pictures below). Measurements have been carried out for single bunch without collisions (i.e. 8 observation points for transverse sizes of electron bunch) which decays with time naturally.

The control system of the VEPP-2000 collider allow us to measure and even store (for offline analysis) almost all parameters of magnetic system, RF system, timings and measured beam parameters. The most of these parameters can be measured with effective frequency 1-5 Hz. The resolution of bunch current measurement is equal to 0.1 mA; bunch sizes – 5-10 um in transverse and 2-3 mm in longitudinal direction; RF cavity voltage – 0.2 kV.

The VEPP-2000 lattice was the same as for the data taking regimes at E=350 MeV and was carefully measured and corrected to be consisted with the machine model [5].

Horizontal bunch sizes shown for the places with significantly different dispersion function (see Fig. 2) and shows the growth with intensity variation.

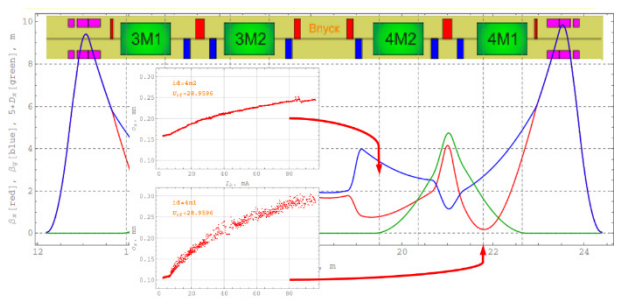

Figure 2: VEPP-2000 lattice functions for the luminosity-taking regime at E=350 MeV.

† rogovsky@inp.nsk.su

ISBN: 978-3-95450-197-7 doi:10.18429/JACoW-RUPAC2018-THZMH01

TOMOGRAPHIC RECONSTRUCTION OF THE LONGITUDINAL DISTRIBUTION FUNCTION OF IONS IN BUNCHES DURING ACCELERATION AT THE NUCLOTRON

V. M. Zhabitsky*, Joint Institute for Nuclear Research, Dubna, Russia

Abstract

Methods of processing a digital signal proportional to the longitudinal intensity of ions in bunches during their acceleration in synchrotrons are discussed. The method of computerized tomography is used for reconstruction a longitudinal two-dimensional distribution function of ions in the bunch from the data on its profiles depending on synchrotron motion of particles. Examples of tomographic studies of ion beams at the Nuclotron are presented.

INTRODUCTION

Methods of computerized tomography — mathematical algorithms for reconstruction of the internal structure of an object from the collection of projection data — are widely used in modern scientific research. Typically, projection data are obtained for a thin layer (cross-section of the object), the internal structure of which is described by a two-dimensional distribution function. A bunch of charged particles circulating along the orbit of the synchrotron and performing longitudinal (synchrotron) oscillations with respect to the synchronous particle [1] can be included to the class of tomographic objects. Indeed [2, 3], let $s_0(t)$ be the displacement of a synchronous particle with energy E_0 along the orbit relative to the accelerating section at time instant t. Then the longitudinal distribution function $f(E - E_0, s - s_0)$ of charged particles in the bunch occupying the position s and having energy E depends on deviations $E - E_0$ and $s - s_0$. The one-dimensional distribution function, which is a two-dimensional projection of the function $f(E - E_0, s - s_0)$ on the time axis coincides with the longitudinal intensity profile of the bunch $n(t)$ – the number of particles distributed in the bunch, as measured by the sensor of the pulse current. The analog signal $n(t)$ is usually converted into a sequence of digital samples $n[i]$ corresponding to the time instants $t_i = i \cdot T_{\rm clk}$ with a constant sampling period $T_{\rm clk}$.

The methods presented in [4] provide digital processing of the $n[i]$ signal generated by a proton bunch in the synchrotron CERN PSB in order to reconstruct the two-dimensional longitudinal distribution function of particles in the bunch. Methods of data recording and their subsequent processing in order to reconstruct the longitudinal two-dimensional ion distribution function in an accelerated bunch at the Nuclotron [5] are described followed.

BASIC PROCEDURE

It was demonstrated in [4] that the procedure of computerized tomography for bunches of charged particles in a synchrotron allows to reconstruct two-dimensional longitudinal distribution function of particles in the bunch, making synchrotron oscillations. The phase trajectories of particles with small deviations from the synchronous one are closed under the conditions of the phase stability principle and surround a stable equilibrium point $\phi = \phi_{\rm s}$. The impulse function $n(t)$ at each revolution is a projection of the bunch phase portrait on the time axis. To identify a set of digital sequences for bunch intensity profiles, a specialized digital device was used in [4] which allowed to synchronize the measurement process (see Fig. 1 and paper [3]) with accelerating voltage $\tilde{V}_{\rm rf}(t)$.

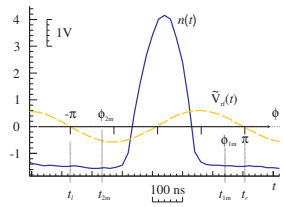

Figure 1: Graphs for $n(t)$ and accelerating voltage $\tilde{V}_{\rm rf}(t)$

As a result, a sequence of digital functions $f_j[i, j, k]$ was formed on each revolution of k for the bunch with the number j, which are a characteristic of the differential law of particle distribution by the slot i within the bunch with the number j on the turn k with the starting point $t_l = t_i(\phi_j[k] = -\pi)$. The set of these intensity profile data was used in the computational tomography procedure [4], where the **a**lgebraic **r**econstruction **t**echnique (ART) was used [6, 7]. Additional parameters of the computational algorithm in the given time of reconstruction of $t = t_{\rm init}$ for accelerating charged particles with rest mass m and charge q that circulates along the equilibrium orbit with average radius R_0 are the guide magnetic induction $B(t)$ and the speed of its changes in time $\dot{B}(t)$, the amplitude of the accelerating voltage on the gap $V(t)$ and speed of its change in time $\dot{V}(t)$, the rf harmonic number $h_{\rm rf}$, the transition gamma $\gamma_{\rm tr}$, the bending radius ρ.

The functional scheme of registration of data on the intensity of bunches for the purpose of tomographic studies at the Nuclotron was described in [3] and is shown in Fig. 2. Five equidistant bunches ($h_{\rm rf} = 5$) circulate along the orbit in the Nuclotron. The intensity of bunches is observed by the pick-up, the signal from which is available for users. The analog signal from the pick-up $n(t)$ goes to the two-channel digitizer ($T_{\rm clk} = 10$ ns). The second input of the digitizer is fed by the harmonic signal from accelerating section $\tilde{V}_{\rm rf}(t) = V_0 + V(t)\cos(\omega_{\rm rf}(t) + \varphi_0)$. The angular frequency $\omega_{\rm rf}(t)$ is determined in accordance with the law of change of the magnetic induction in dipoles $B(t)$. As a result,

* V.Zhabitsky@jinr.ru

ISBN: 978-3-95450-197-7 doi:10.18429/JACoW-RUPAC2018-FRXMH02

PRESENT STATUS OF BINP AMS

S.A. Rastigeev, A.R. Frolov, A.D. Goncharov, V.F. Klyuev, E.S. Konstantinov, V.V. Parkhomchuk, A.V. Petrozhitskii, BINP SB RAS, Novosibirsk, Russia

Abstract

The accelerator mass spectrometer (AMS) created at BINP is used for biomedical, archaeological and other applications. Current status and experimental results are described.

INTRODUCTION

The accelerator mass spectrometry is an ultra-sensitive method of isotopic analysis. The radiocarbon concentration in living organisms, plants and atmospheric air are about 10^{-12} in comparison with the main carbon isotope - ^{12}C. After death of the living organism, the radiocarbon concentration is reduced by 2 times for every 5730 years, according to the half-life of the radiocarbon. The radiocarbon concentration for 50 thousand years age objects is about $2*10^{-15}$. About 1 mg of carbon sample is required for radiocarbon analysis by AMS. So, the AMS is very demanded by users. So, it is possible to analysis of natural objects by using a small fraction. This allows obtain information about objects of cultural and historical value without destroying. And it is also possible to study the processes of natural deposits accumulation with a small spatial step. Similarly, the biomedical research can be conducted with a small number of radiocarbon labels introduced into living systems. In this case, the radiocarbon labels concentration can be detected in various organs of the living object under study without significant radiation exposure.

PRESENT STATUS

The BINP AMS is based on the folded type electrostatic tandem accelerator [1-3]. The AMS system consists of the ion source, low energy channel, tandem accelerator and high-energy channel. The low energy beam line is used for initial isotopes selection. The tandem accelerator is applied for rejection of the molecular ions. The high-energy beam line is used for the subsequent ions selection and for radioisotopes detection.

The most distinguishing feature of BINP AMS is the use of additional electrostatic separator of ion beam [4-6], located inside the terminal. In this configuration of the AMS, the ions background is significantly reduced by the energy filter in the high voltage terminal [7-8], because the energy of fragments is always less then the ion energy (at this moment). The next important distinguishing feature is magnesium vapours stripper [9] instead of the gas stripper. The gas flow into the accelerator tubes leads to big energy spread in the beam thus limiting the sensitivity and accuracy of spectrometer. The molecular destruction and ion recharging by magnesium are localized into the hot tube of the stripper. Moreover, time of flight and the time of the ion detection can be registered TOF detector [10,11] for filtering the background ions from electrical breakdowns.

Now the BINP AMS is a single Russian facility for radiocarbon analysis of samples by accelerator mass spectrometry. At the end of 2017, the facility was officially registered as a "unique scientific installation" called "BINP AMS SB RAS". Now every scientific organization can leave an online application on the site for the conduct of joint research with BINP using AMS. Over the past year, the about 1000 samples was analyzed at BINP AMS for 25 user organizations.

RADIOCARBON MEASUREMENTS

During the measurements of user samples, the injection energy of radiocarbon beam is about 25 keV. The terminal voltage of tandem accelerator is 1 MV. The 180° electrostatic bend is set to transmit the ions with charge state 3+.

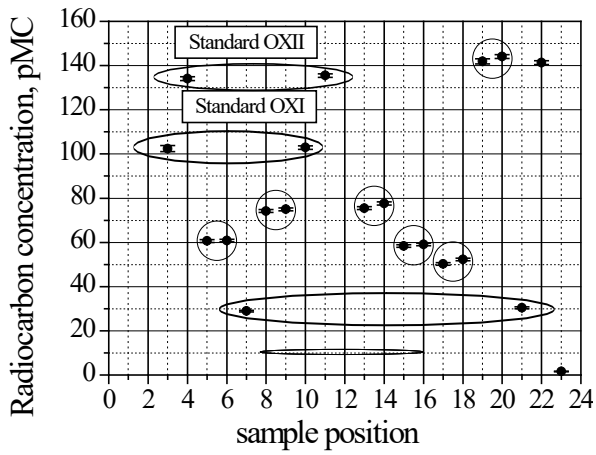

Figure 1: Example of AMS analysis of the sample wheel with user samples.

When measuring the concentration of radiocarbon in the samples, the switching algorithm is used. The isotope ^{14}C is detected by TOF telescope and ^{13}C currents are measured at the exit of AMS. For switching algorithm the high voltage of ion source and voltage on some electrostatic elements are changed. About 80% of the time is used on radiocarbon ions counting, the rest 20% of the time is used for isotope switching, the current ^{13}C measurements, and the sample wheel rotation.

The cycle of AMS-analysis of samples is represented as follows. For each sample, the ^{14}C ions are counted four times (10 seconds each) and twice the ^{13}C currents are measured for each 10 seconds counting. After that, the

ISBN: 978-3-95450-197-7 doi:10.18429/JACoW-RUPAC2018-FRXMH03

STATUS OF THE PROTON THERAPY COMPLEX PROMETHEUS

V.E. Balakin, V.A. Alexandrov, A.I. Bazhan, P.A. Lunev, A.A. Pryanichnikov, A.E. Shemyakov, A.I. Shestopalov, Yu.D. Valyaev, P.N. Lebedev Physical Institute of the Russian Academy of Sciences, Physical Technical Center (PhTC LPI RAS), Protvino, Russia

Abstract

The report overviews present status of the proton therapy complex Prometheus. The PTC Prometheus was developed and successfully implemented in the PhTC LPI RAS in conjunction with Protom Ltd. The complex is a Russian development and is fully produced within the territory of the Russian Federation.

At the moment, there are two such complexes are using for treatment in Russia - in the city hospital of Protvino and in the A. Tsyb Medical Radiological Research Centre (MRRC). PTC LPI RAS and Protom ltd. along with MRRC have accumulated almost three years of experience in the usage of the complex under clinical conditions. PTC Prometheus has proved to be efficient and reliable in two years of clinical use in the treatment of head and neck cancer. If there is a developed infrastructure, the capacity of the facility will able go up to 1000 people a year.

The low weight, low power consumption and compact dimensions of the complex allow it to be placed in ordinary hospitals, without constructing separate buildings.

In addition to that, PTC Prometheus was licensed to irradiate the entire human body in March 2017. The phase of preparation of a modified immobilization system for irradiating a recumbent patient was completed by summer 2018.

INTRODUCTION

Proton therapy (PT) is one of the most accurate and modern methods of radiotherapy and radiosurgery [1]. Protons can reduce the radiation load on surrounding tissues up to 30-50% in comparison with gamma rays. Therefore, in cases of tumors located near critical organs (for example head and neck cancer), proton therapy is the most advantageous of the available types of treatment for many patients. Given the advantages of this type of treatment over radiation therapy, using gamma radiation and electron beams, proton therapy is increasingly being used in the treatment of cancer. There is an increase of PT centres around the world [2].

In the world, active work is being carried out aimed at increasing the accuracy of dose delivery to the tumor, reducing the time that patients stay under the influence of radiation and increasing the availability of this method for a larger range of patients. New proton accelerators, as well as more cost-effective and accurate immobilization systems for patients are being developed for these purposes.

According to statistics, PT can be assigned to 50 thousand patients per year in Russia [3]. Unfortunately, in recent years, insufficient attention has been paid to this problem. Only four PT centres are working with patients in Russia now (except those mentioned above, there is Medico-Technical Complex JINR, which started its work in 1968 and annually irradiates several dozen people and MIBS in Saint-Petersburg that started treatment only this year). In addition to two proton therapy complexes Prometheus operating in the Russia, PhTC LPI RAS and Protom Ltd. successfully developed and produced two synchrotrons for the proton therapy complex “Radiance 330”. Two of these complexes have already been introduced in the Massachusetts General Hospital (Boston, MA, US) and McLaren Health Care Hospital (Flint, MI, US) and are preparing for irradiation of the first patients. Also one PTC Prometheus was delivered to Slovakia for radiobiological studies and possible applications in the future for therapeutic purposes.

THE PROTON THERAPY COMPLEX «PROMETHEUS»

The proton therapy complex “Prometheus” (PTC) (see Table 1) consists of an injection channel providing primary acceleration of protons, a synchrotron cyclically accelerating protons to the required energies, an extraction channel for slow extraction of the proton beam and a patient immobilization system.

Table 1: Main Characteristics of the Accelerator Complex

Characteristics	Values
The range of accelerated proton energies, MeV	30 - 330
Magnetic field at injection, mT	80.66
Maximum magnetic field, T	1.9
Outer diameter of the ring, m	5
Accelerator weight, tons	15

Injection Channel and Ion Source

The injection channel and the ion source were designed for the initial production of protons and their acceleration to the energy of approximately 1 MeV.

These modules consist of a pulsed arc source of ions with a pulsed hydrogen inlet, electrostatic lenses, a tandem high-voltage accelerator and a 630 kV voltage source. With the help of a pulse valve, hydrogen enters the ion source, an electric arc is ignited, which leads to the formation of plasma. The electrostatic lens draws negatively charged hydrogen ions and electrons from the plasma. Electrons are discarded by a separator. Hydride

ISBN: 978-3-95450-197-7 doi:10.18429/JACoW-RUPAC2018-FRCAMH01

THE CARBON ION BEAM EXTRACTION SCHEME FROM THE U-70 SYNCHROTRON FOR RADIOBIOLOGICAL RESEARCHES

A. V. Maximov, Y. M. Antipov, G.I. Britvich, S.V. Ivanov, V.A. Kalinin, O. P. Lebedev, E. A. Ludmirsky, A.P. Soldatov, G.V. Khitev, NRC «Kurchatov institute»-IHEP, Pronvino, Russia

Abstract

The carbon ion beam extraction scheme from the U-70 synchrotron of NRC «Kurchatov institute» - IHEP for radiobiological researches is presented. The double-step extraction scheme Piccioni-Wright is used. The beam extraction operates at magnetic field flat bottom of U-70 synchrotron with carbon ion energy 455 MeV/n. A technique to attain transversally uniform irradiation field and other results on operation are also presented.

THE ION BEAM EXTRACTION SCHEME DESCRIPTION

The table 1 shows some parameters at magnetic field flat bottom of U-70 synchrotron.

Table 1: The Parameters at Magnetic Field Flat Bottom of U-70 Synchrotron

Parameter	Value
Magnetic field (Hs)	355
Carbon ion energy (MeV/n)	455
Magnetic rigidity (Tl·m)	6.89
Betatron frequencies	9.86 / 9.80
Relativistic factors β / γ	0.74 / 1.49
Beam emittances Ex / Ey (mm·mrad)	25 / 15
Width of relative momentum distribution $\pm\delta_0$	$\pm 2\cdot 10^{-3}$

The double-step extraction scheme Piccioni-Wright is used [1]. In accordance to this scheme the internal target (T28) located in 28 straight section (+50 mm from beam closed orbit) and deflecting septum-magnet at 34 straight section (-62 mm from orbit) of U-70. In the extraction process the circulating beam dumped on the target and ion beam particles undergo ionization energy loss. The particles leaving the target make betatron oscillations with new orbit displaced inside the ring. After half the wavelength of the betatron oscillations further along the beam, the spatial separation between extracted part of beam and circulating beam is enough for thin septum of deflecting magnet layout. In this pace (beginning of 34 straight section) SM34 septum-magnet is located. The boundary horizontal trajectories of the extracted particles with momentums ($\pm\delta_0$ - Δ) and scattering angles $\pm 2\theta_{rms}$ are shown in Fig. 1.

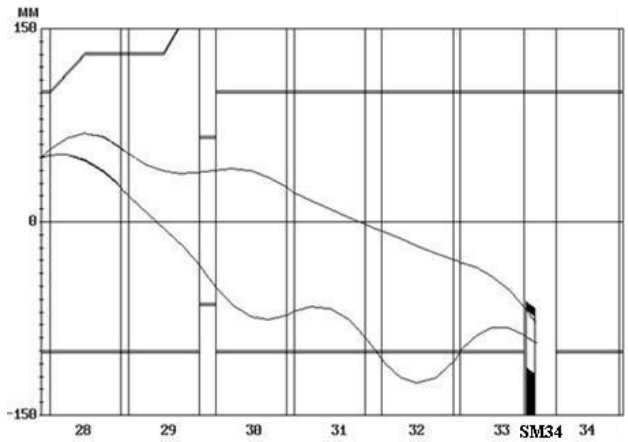

Figure 1: The boundary horizontal trajectories of the extracted particles.

The required value of the loss of the relative momentum of the particle on the target is given by the expression:

$$\Delta \geq 2\delta_0 + \frac{d_{sep} + \Delta R_{gap}}{D_{34} + D_{28}}$$

where d_{sep} –septum thickness, D_{28}, D_{34} – the values of the dispersion functions on the azimuths of the target and septum-magnet, ΔR_{gap} – the required value of the gap between the circulating beam and the coordinate of the septum magnet, $2\delta_0$ - width of relative momentum distribution.

The extracted beam size is estimated as follows:

$$\Delta X_n = 2\delta_0 (D_{34} + D_{28})$$

As the target material is used BE. Ionization loss of the carbon ions $^{12}C^{+6}$ with kinetic energy T ≈ 455 MeV/n in BE is equal 15.0 MeV / mm, so the required target thickness is equal ≈ 4 мм. The target height is chosen equal to 10 mm.

Dumping the beam at the target is carried out by transverse noise (stochastic) blow-up of horizontal betatron amplitudes of circulating beam [2]. The uniformity of the extracted intensity supported by feedback from beam loss monitor M28 located near the target T28 (see Fig. 2).

The calculated extraction efficiency of the ion beam is ≈ 75%. The practically achieved efficiency estimated as 50÷60%. The carbon ion beam injection intensity in U-70 is $(3\div 6)\times 10^9$ ions per cycle.

ISBN: 978-3-95450-197-7 doi:10.18429/JACoW-RUPAC2018-FRCAMH02

PROTON IRRADIATION FACILITY AT INR RAS LINAC

S. Gavrilov†[1], S. Bragin, A. Feschenko, V. Gaidash, O. Grekhov, Y. Kalinin, Y. Kiselev, S. Lebedev, A. Melnikov[1], V. Serov, A. Titov[1], O. Volodkevich, Institute for Nuclear Research of the Russian Academy of Sciences, Moscow, Russia
D. Arbuznikov, O.Podgornaya, E. Prokhorov, S. Razinkov, P. Tsedrik, S. Tsibryaev, RFNC, All-Russian Research Institute of Experimental Physics, Sarov, Russia
[1] also at Moscow Institute of Physics and Technology (State University), Moscow, Russia

Abstract

A new proton irradiation facility to study radiation effects in electronics and different materials was constructed at INR RAS linac. The beam intensity range is $10^7 \div 10^{12}$ protons per separate pulses up to 1 μA of average beam current. The energy is adjusted by switching on/off the fields in accelerating cavities and with energy degraders in the range 20÷210 MeV. Features of the facility development, in-air operation, diagnostics system, as well as experimental results of beam adjustment and test irradiation are presented.

INTRODUCTION

An accelerating complex based on a linear proton accelerator (linac) of Institute for Nuclear Research RAS is a multipurpose facility with a wide range of tasks for neutron research, radioactive isotope production and medical physics. In 2017 a new proton irradiation facility (PIF) was constructed to research proton irradiation induced effects in electronics, devices and materials.

A structural diagram of the linac is shown in Fig. 1. The main parts are: bending magnet with vacuum beam pipe, beam dump, target positioning system with energy degrader and beam diagnostic instrumentation. PIF is installed at the outlet of the linac in the 600 MeV beam energy area, where available bending magnet is used to deflect a beam from the linac axis by an angle of 7.5° for in air irradiation of targets.

PIF DESIGN AND MAIN PARAMETERS

Beam energy at the PIF is adjusted in the range 20÷210 MeV by a switching off/on of accelerating cavities, which provide discrete energy values with a full energy spread < 1%, for intermediate beam energy values an energy degrader should be used. However the presence of the degrader along with the outlet aluminium window with 1 mm thickness and 900 mm air gap leads to a significant increase of the energy spread, especially for low beam energies. Figure 2 shows an energy spectrum, calculated in TRIM [1], for a monoenergetic beam with 49 MeV initial energy after 4.6 mm aluminium degrader.

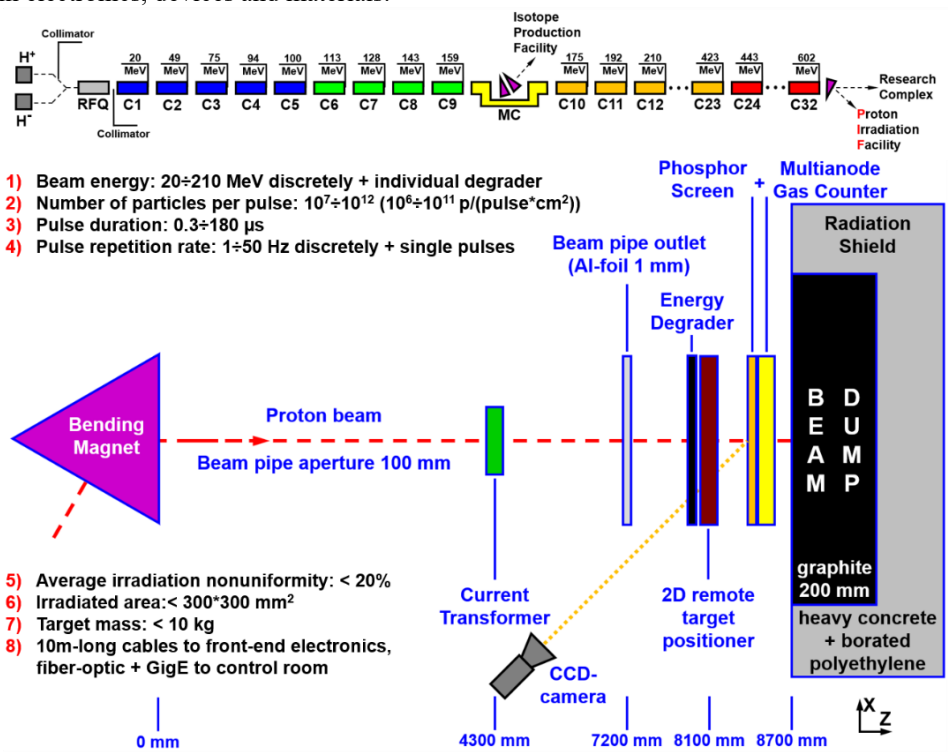

Figure 1: General layouts of the linac and proton irradiation facility at the outlet of the linac.

† s.gavrilov@gmail.com

ISBN: 978-3-95450-197-7 doi:10.18429/JACoW-RUPAC2018-FRCAMH03

RADIATION ONCOLOGY OPHTHALMIC CENTER BASED ON THE C-80 ACCELERATOR AT THE NRC "KURCHATOV INSTITUTE" – PNPI

A.N.Chernykh[1], V.S.Khoroshkov, G.I.Klenov, NRC "Kurchatov Institute" – ITEP, Moscow, Russia
D.Y.Minkin, National Research Center "Kurchatov Institute", Moscow, Russia
V.I.Maksimov, E.M.Ivanov, NRC "Kurchatov Institute" – PNPI, Gatchina, Russia
[1]also at NRC "Kurchatov Institute" – PNPI, Gatchina, Russia

Abstract

The greatest opportunities for the treatment of intraocular tumors are provided by proton radiation therapy. With such treatment, tumor resorption is achieved in 98% of cases, and the function of vision (to one degree or another) is preserved in 70% of patients.

The article gives an overview of the technological stages of proton radiation therapy for intraocular tumor and results of cooperation between NRC "Kurchatov Institute" - PNPI and NRC "Kurchatov Institute" - ITEP are used in the implementation of the technology to develop a PRT oncophtalmologic complex based on cyclotron C-80 NRC "Kurchatov Institute" - PNPI.

THE MAIN STAGES OF PROTON RADIATION THERAPY OF INTRAOCULAR TUMORS

Radiation therapy, especially proton radiation therapy, is a complex process that requires vast hardware, software and information resources at every stage of treatment:

- diagnosis;
- surgery to document tumor extension and placement of fiducial markers;
- simulation and radiographic measurements of markers;
- treatment planning;
- fabrication of individual collimators and bolus;
- positioning;
- radiotherapy (4-5 fractions);
- follow-up.

DIAGNOSIS

The primary symptom with which patients visit an ophthalmologist is a reduced/disturbed vision.

Intraocular tumors can be diagnosed by various methods. For the primary diagnosis, a fundus camera is used, and the images of the eye are examined (Fig. 1). Computed and magnetic resonance imaging are also used. The most accurate determination of the size of a malignant neoplasm is carried out by ultrasound.

SURGERY TO DOCUMENT TUMOR EXTENSION AND PLACEMENT OF FIDUCIAL MARKERS

Eye is sufficiently homogeneous medium and tomographic data is not enough to accurately differentiate the structures of the eye and tumor. Anatomical structure of the eye [1-5] requires special diagnostic and surgical preparation for irradiation. At the same time, conventional computed tomography is of little use because of the mobility of the eye, the small size of the irradiated structures and the increased requirements for the resolution of the equipment [6,7]. Usually, in case of uveal melanoma, the tumor grows to the center of the eye (pos. 6 Fig. 2), and the vitreous mass is inert and is not included in the tumor process.

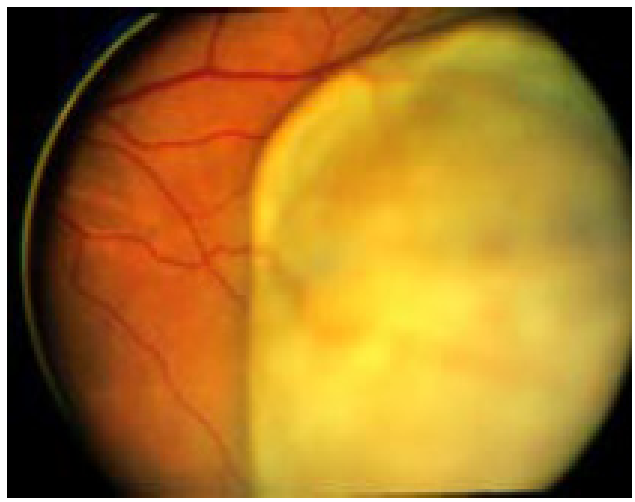

Figure 1: A snapshot of fundus chamber of the fundus with a intraocular tumor.

The main task of the stage is to define the boundaries of the base of the tumor and filing to the sclera of the eyeball, along the contour of the base of the tumor of the radiopaque clips (pos. 7 Fig. 2). To do this, a series of surgical manipulations with the eye. The eye is turned in the orbit to access the base of the tumor and illuminated so that the tumor casts a shadow on the sclera of the eyeball. And on the contour of the shadow, the surgeon hemmed tantalum clips. Based on the results of stapling the clips, the surgeon draws up a clinical protocol in which he enters data on the distance between the clips and their coordinates relative to the structures of the eye.

SIMULATION AND RADIOGRAPHIC MEASUREMENTS OF MARKERS

The main goal of the radiation simulation stage is to clarify the coordinates of the radiopaque clips and to check the mechanical properties of the eye for comfortable turning angles.

ISBN: 978-3-95450-197-7 doi:10.18429/JACoW-RUPAC2018-TUPSA02

CORRECTION OF THE MAGNETIC FIELD IN THE NICA COLLIDER

O. Kozlov, A. Butenko, S. Kostromin, I. Meshkov, A. Sidorin, E. Syresin, JINR, Dubna, Russia

Abstract

The magnetic field correction systems in the optimized lattice of the NICA collider are considered. The dipole, normal and skew quadrupoles, sextupole and octupole additional windings are placed in the corrector elements to compensate separately the alignment errors, betatron tune shifts, betatron coupling, chromaticity and non-linear fields. The overall correction effect should increase the dynamic aperture and provide the required beam and luminosity lifetime of the collider.

INTRODUCTION

The Nuclotron-based Ion Collider fAcility (NICA) [1] is a new accelerator complex being constructed at JINR. Two collider rings are designed and optimized to achieve the required luminosity at two interaction points (IP). The first IP is connected with Multipurpose detector (MPD) for the ion-ion (Au^{+79}) collider experiments in the energy range of 1÷4.5 GeV/u. The second IP is aimed for the polarized proton-proton (5÷12.6 GeV) and deuteron-deuteron (2÷5.8 GeV/u) collisions. The collider lattice is based on the technology of super-ferric magnets developed in VBLHE, JINR. The collider optics is optimized to obtain the required luminosity (Table 1) with the certain effects which set constraints on the lattice parameters: luminosity lifetime limitation by intrabeam scattering in a bunch (IBS), space charge tune shift, threshold of microwave instability, slippage factor optimization for efficient stochastic cooling, maximum required RF voltage amplitude. This paper considers the $^{197}Au^{+79}$ heavy ion mode of facility operation. The possible schemes of the correction of the linear and non-linear imperfections of the magnetic fields of the structural elements of the collider are supplied to the collider optics to increase the dynamic aperture.

LATTICE OF THE RINGS

Collider lattice was developed and optimized [2] with some constraints: ring circumference, a number of the dipole magnets in an arc, convenience of the beam injection into the ring. The rings are vertically separated (32 cm between axes) and use two-aperture superconducting magnets (dipoles and quadrupoles). Rings have the racetrack shape with the bending arcs and long straight section. The principal choice for the arc structure is the FODO optics with 12 periods. Circumference of the rings corresponds exactly to two Nuclotron circumferences. The project parameters of the collider ring are presented in Table 1.

Table 1: Project Parameters of the Collider Rings

Ring circumference, m	503.04		
Number of bunches	22		
Rms bunch length, m	0.6		
β-function in the IP, m	0.35		
Betatron tunes, Q_x/Q_y	9.44/9.44		
Chromaticity, $Q'_{x,0}/Q'_{y,0}$	-33/-28		
Acceptance π·mm·mrad	40		
Long. acceptance, Δp/p	±0.010		
Gamma-transition, γ_{tr}	7.088		
Ion energy, GeV/u	1.0	3.0	4.5
Ion number per bunch	$2.0\cdot10^8$	$2.4\cdot10^9$	$2.3\cdot10^9$
Rms Δp/p, 10^{-3}	0.55	1.15	1.50
Rms emittance, hor./vert. (unnorm.), π·mm·mrad	1.10/ 0.95	1.10/ 0.85	1.10/ 0.75
Luminosity, $cm^{-2}s^{-1}$	$0.6\cdot10^{25}$	$1.0\cdot10^{27}$	$1.0\cdot10^{27}$
IBS growth time, s	170	470	2000
Tune shift, $\Delta Q_{SC}+2\Delta Q_{bb}$	-0.050	-0.037	-0.011

Bending arc comprises 12 FODO cells with nominal betatron phase advances of 90^0 per cell. The cells with empty dipoles are used for horizontal dispersion suppression and convenient beam injection and extraction (dumping) schemes. Periodic FODO cell consists of four rectangular dipole magnets per cell (80 magnets per ring), two quadrupoles [3], multipole correctors and beam position monitors (BPM) (Fig. 1). The maximum field in 1.94 m dipole of 1.8 T and gradient in 0.47 m quadrupoles of 23 T/m. The long straight sections matched to the arcs contain the RF stations, electron and stochastic cooling devices, BPMs, superconducting quadrupole blocks. The optics in these sections produces the betatron tune variation, vertical beam separation in the rings and conditions for colliding beams in interaction points (IP). The schematic composition of the rings is given in Fig. 2. The Twiss-functions of the ring are shown in Fig. 3.

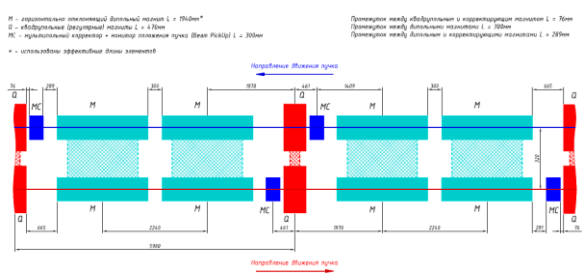

Figure 1: Periodic FODO cells for both rings.

ISBN: 978-3-95450-197-7 doi:10.18429/JACoW-RUPAC2018-TUPSA06

BEAM OPTICS OF OPERATING MODES FOR DAMPING RING OF INJECTION COMPLEX VEPP-5

K. V. Astrelina†, V. V. Balakin, F. A. Emanov, D. E. Berkaev, Budker Institute of Nuclear Physics Russian Academy of Sciences (BINP SB RAS), 630090 Novosibirsk, Russia

Abstract

Damping storage ring (DR) is the part of Injection Complex which provides electron and positron beams for BINP collider experiments since 2015. Basic lattice parameters of the ring (optical functions, dispersions, betatron frequencies, etc.) of the operating modes are presented in the article. Actual calculations of the ring aperture limitations and energy acceptance after RF-system reconstruction are given. Some instruments for the beam orbit control and magnet system adjustment were developed and can be applied to improve the productivity of beams generation.

INTRODUCTION

Injection Complex VEPP-5 (IC) has been built in BINP, launched in 2015 and produces the intense relativistic beams of electrons and positrons for the needs of BINP colliders VEPP-4M and VEPP-2000.

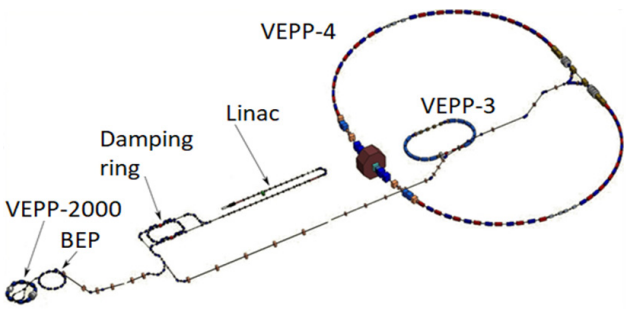

Figure 1: The system of BINP colliders.

Injection Complex includes Preinjector facility ("Linac" at Fig. 1) – the system of two linear accelerators and the conversion system for positron beams generation. Second machine as a part of IC is Damping ring - 27-meter synchrotron with quadrupole focusing. Preinjector and Damping ring are connected together with the couple of transport channels for electrons and positrons. Extraction channels system is used to deliver stored electron and positron beam to the colliders.

Damping Ring design is symmetric with two arcs with bending magnets and two straight sections between them (Figure 2). Electrons and positrons are injected to the ring at two different straight gaps and move in opposite directions. That allows to keep the ring magnet structure with unchanged magnet polarity and collect beams with different charge alternately.

Straight gaps are supposed to be non-dispersive to make it easier to match the injected beam parameters with the Damping ring acceptance.

† K.V.Astrelina@inp.nsk.su

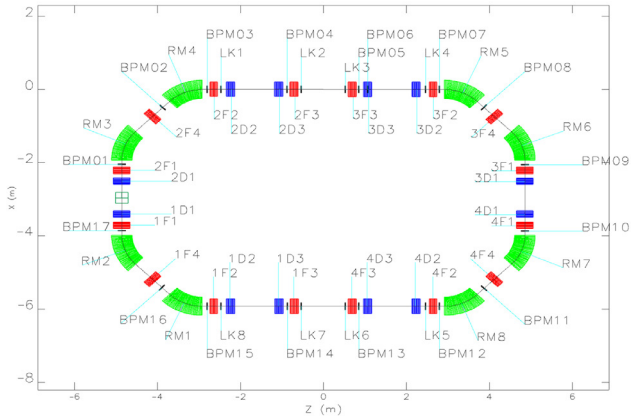

Figure 2: Damping Ring layout.

In order to inject new portions of particles to the stored beam in DR the following scheme is applied. The final parts of injection channels are in vertical plane. The final element of injection channel is vertical DC septum-magnet. It drives the newly injected beam to the horizontal trajectory which is parallel to the ring reference orbit. The stored beam is forekicked in horizontal plane closer to injected particles. When injected beam passes the septum, both bunches – stored and injected are kicked back to the ring orbit. Kickers are located in ¼ of betatron oscillation wavelength from the injection point to dump oscillations more effectively [1]. Residual transverse beam oscillations decay due to radiation damping.

DAMPING RING OPERATING PARAMETERS

Table 1: Damping Ring Parameters in 2017-2018

Beam Energy	395 MeV
Linac frequency	5 Hz
Electron storage rate	12.5 mA per cycle (6 shots) 7-10 mA/shot
Electron injection efficiency	30 %
Positron storage rate	12.5 mA per cycle (30 shots) 2.3 - 3 mA/sec
Positron injection efficiency	5.2 %
Betatron tunes positrons electrons	 ν_y=2.736, ν_x=4.645 ν_y=2.75, ν_x=4.635
Energy acceptance	+/- 0.025

ISBN: 978-3-95450-197-7 doi:10.18429/JACoW-RUPAC2018-TUPSA07

CALCULATION OF INJECTION EFFICIENCY TO DAMPING RING OF VEPP-5 INJECTION COMPLEX

K. V. Astrelina†, F. Emanov, N. Kremnev, Budker Institute of Nuclear Physics Russian Academy of Sciences (BINP SB RAS), 630090 Novosibirsk, Russia

Abstract

VEPP-5 Injection Complex (IC) is an electron and positron beam source for VEPP-4M and VEPP-2000 experimental facilities. IC consists of Preinjector - the system of two linear accelerators and conversion target, and Damping Ring where particle beams are collected before extraction to the users.

One of the factors that determine the performance of IC is the number of positrons which can be transported from Preinjector to Damping Ring and stored on the stable orbit. Estimations of the maximal efficiency of the beam generation include the beam loss calculations in the transport line between linear acceleraotrs and ring and analysis of the injected beam capture in the storage ring. Results of these calculations are presented in the report.

INTRODUCTION

Injection Complex VEPP-5 (IC) has been built in BINP, launched in 2015 and presently produces the intense relativistic beams of electrons and positrons for the needs of BINP colliders. Figure 1 demonstrates the main components of the complex.

Preinjector system (1 at Fig. 1) consists of two linear accelerators. At first the electron beam is generated, accelerated to 200 MeV and transported to the convertion system (2). If positrons are required to be stored, the electron beam is directed to the tantalum conversion target, positrons are collected from electromagnetic shower with the magnet flux concentrator [1] and transported along the second linear accelerator to the Damping Ring (Fig. 1, 3) and accelerated up to the ring operating energy (395 MeV in 2017-2018). In electron acceleration mode the electron beam bypasses the target and is also accelerated to the same operating energy value.

Damping Ring (DR) is 27-meter circular accelerator. DR can store both types of particles but not simultaneously. Most of the time Damping ring works with positrons since they are delivered to the machine in smaller quantities. When any type of particles is injected to the ring, new portions of particles are added to the circulated bunch until the required number of particles is stored. It is sufficient to store 3 pulses of electrons and 30 pulses for positrons at beam generation frequency 5 Hz. Synchrotron radiation losses are compensated by RF-cavity resonator that leads to a cooling down the transverse phase space of the beam.

Electrons and positrons are injected to the ring at two different straight gaps between arcs and move in opposite directions. Two different injection lines (4) connect Preinjector with the Ring. 3-degree vertical corrector located at the end of positron linear accelerator and drives positrons to the upper line and electrons to the lower one. Electron channel is straight in horizontal plane and contains the vertical chicane (so called "bridge") to pass by the arc of Damping Ring and inject beams to the non-dispersive straight gap. Opposite straight gap used for positron injection. The four-magnet horizontal achromatic parallel beam translation is used to drive positrons to the corresponding injection axis.

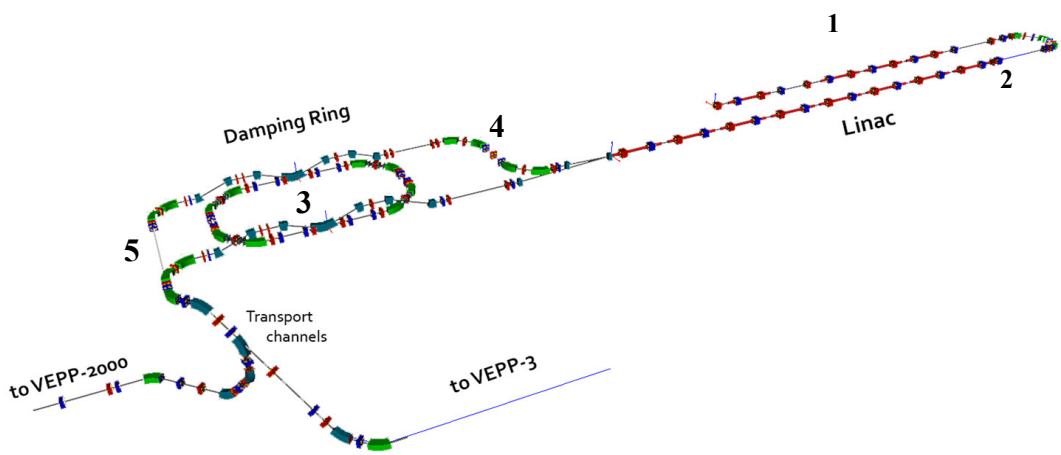

Figure 1: The layout of Injection Complex and extraction channels. 1 – Preinjector, 2 – conversion target, 3 – Damping Ring, 4 – injection channels, 5 – extraction channels.

† K.V.Astrelina@inp.nsk.su

ISBN: 978-3-95450-197-7 doi:10.18429/JACoW-RUPAC2018-TUPSA08

STABILITY OF CHARGED PARTICLE MOTION IN A STORAGE RING WITH FOCUSING BY LONGITUDINAL MAGNETIC DIELD.

S.A. Melnikov, I.N. Meshkov, Joint Institute for Nuclear Research (JINR), 141980, Moscow Region, Dubna, Russian Federation.

Abstract

Analytically calculated matrices of the optical conversion of the elements of the focusing system of the Low Energy Particle Toroidal Accumulator (LEPTA) and the longitudinal magnetic field perturbations appearing in the technical connections of the ring elements are presented. Based on the matrix data, a program was written in the Wolfram Mathematica environment, which allows simulating the multiturn dynamics of particles in a ring and investigating the stability of their motion.

THE LEPTA SET UP

The LEPTA (Low Energy Particle Toroidal Accumulator) setup (see Fig. 1) is a storage ring with a perimeter of 17.2 m with a circulating positron beam in the energy range 1-10 keV

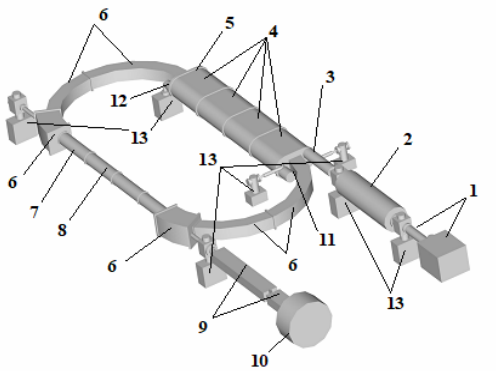

Figure 1: LEPTA set up diagram: 1 - injector; 2 - positron trap; 3 - section for injection of positrons; 4 - septum solenoids; 5 - kicker (located inside the septum solenoid); 6 - toroidal solenoids; 7 - solenoid and quadrupole coil; 8 - section of electron cooling, straight solenoid; 9-dipole analyzing magnet; 10 - coordinate-sensitive detector; 11 - electron gun; 12 - collector of electrons; 13 - the vacuum pump.

The LEPTA set up uses a section structure, which makes it possible to introduce additional straight sections where the injection and extraction sections of the beam and the diagnostic device are placed.

To maintain charged particle motion in the LEPTA, a longitudinal magnetic field is used that accompanies the particles from the source and along the entire orbit of the circulating beam. Thus, the particles in the LEPTA are "magnetized". The stability of the beam circulation is provided by introducing, in addition to the longitudinal magnetic field, the field of the helix quadrupole lens (further - quadrupole) in the section 7.

Between the individual focusing elements of the ring there are technical joints in which adiabatic perturbations of the magnetic field are formed (see Fig. 2). These gaps have a significant influence on the beam dynamics in the ring that also directly affects on the lifetime of circulating particles (see Fig. 3).

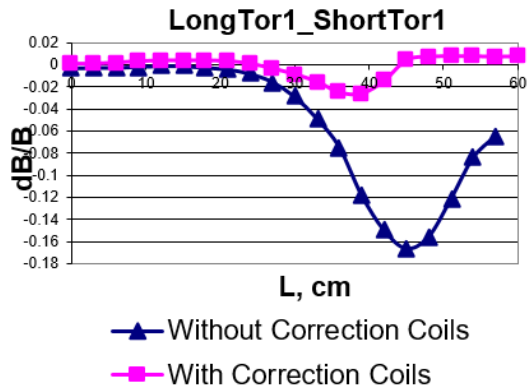

Figure 2: Experimentally measured perturbation of the longitudinal magnetic field before and after correction.

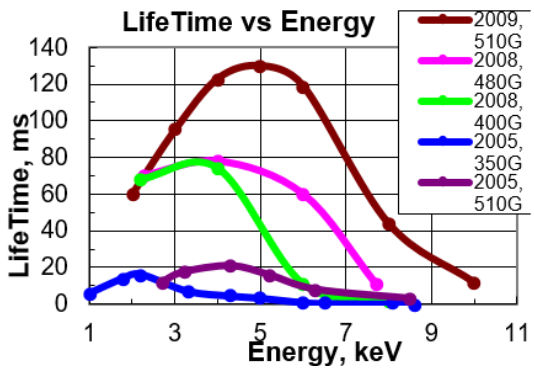

Figure 3: Experimentally measured dependences of the lifetime of a charged particle on their energy.

PARTICLE DYNAMICS IN THE LEPTA RING

The particle trajectory in an electromagnetic field is described by a differential equation [1]:

$$\frac{d\vec{p}}{dt} = e\vec{E} + \frac{e}{c} * \left[\vec{v} \times \vec{B}\right] \quad (1)$$

For a region with a quadrupole and straight solenoid, equation (1) has the form:

ISBN: 978-3-95450-197-7 doi:10.18429/JACoW-RUPAC2018-TUPSA09

DEGENERATE SELF-CONSISTENT DISTRIBUTIONS FOR CHARGED PARTICLE BEAM IN LINEAR TRANSVERSE FIELD

O.I. Drivotin, St.-Petersburg State University,
7/9 Universitetskaya nab., St. Petersburg, 199034 Russia *

Abstract

The present report is devoted to covariant description of the microcanonical distributions for a charged particle beam on the base of the covariant approach previously developed in the works of the author.

For microcanonical distribution, particles are distributed on some ellipsoid, representing three-dimensional surface in the four-dimensional phase space.

Goal of this work is to analyze how do particles are distributed on the surface of this ellipsoid It means that we concerned with particle density on that surface. Besides, we investigate evolution of the density in time to verify that spatial two-dimensional density in projection of the ellipsoid onto configuration space remains uniform.

Our approach is distinct from previously used common approach, according to which microcanonical distribution is described by the delta-function, and particle distribution on the ellipsoid is not considered.

INTRODUCTION

Microcanonical distribution for charged particle beam was firstly introduced in 1959 by Soviet physicists Kapchinsky and Vladimirsky [1] (see also [2]) and in our days is well known as Kapcinsky-Vladimirsky (KV) distribution.

Microcanonical distribution is widely applied in accelerator design as powerful tool for simulating of a charged particle beam of high intensity when particle interaction cannot be neglected.

Common desription of the microcanonical distribution is not quite correct from mathematical point of view because the mathematical expression for its phase density contains delta-function [2], which support is a point, while the support of the microcanonical distribution is three-dimensional surface of an ellipsoid in the four-dimensional phase space. In particular, such description does not allow to set initial distributions of particles for computer simulation of the beam.

Here we apply the covariant approach developed in the works [3, 4, 5, 6] for description of the microcanonical distribution. Covariant approach give us an opportunity to describe the distributions and to follow their evolution using various systems of coordinates in the phase space.

According to this approach, particle density is described by a differential form which degree is equal to dimension of support of the distribution.

* o.drivotin@spbu.ru

If particles distributed in some region in the phase space, then dimension of their support is equal to dimension of the phase space and density of such distribution is described by a differential form of top degree, containing product of differentials of all coordinates. If support of a distribution is a surface in the phase space, then degree of the density form is less than dimension of the phase space, and such form can be written as a term containing only product of differentials of coordinates introduced on this surface. Most degenerate case is the case when particles are situated in some points of the phase space. In this case we should use density of a point-like measure which is specified by a scalar function, i.e., differential form of zero degree.

From this point of view, it is clear that microcanonical distribution should be described by a density specified on 3-dimensional surface of the ellipsoid, and this density is a form of 3 degree.

INTEGRALS OF PARTICLE MOTION IN LINEAR TRANSVERSE FIELD

Consider stationary charged particle beam in transverse electric field which is linear in transverse cartesian coordinates x and y

$$E_x = k_x x, \quad E_y = k_y y. \tag{1}$$

Assume that particles of the beam move with the same longitudinal velocity, and that at initial cross-section of the beam particles fill a four-dimensional ellipsoid in phase space of transverse motion

$$X^T B_0 X = 1, \quad X^* = (x, \dot{x}, y, \dot{y}).$$

Consider most common case $B_0 = \|b^0_{ik}\|$, $b^0_{ik} = b^0_{ki}$. If $b^0_{xy} \neq 0$, one can take other cartesian coordinates related with the old ones with orthogonal transformation in which $b^0_{xy} = 0$ (new coordinates are also regarded here as x, and y. Let introduce an assumption that $b^0_{x\dot{y}} = 0$, $b^0_{\dot{x},y} = 0$, $b^0_{\dot{x},\dot{y}} = 0$. Therefore, further we will consider the matrix of the form

$$B_0 = \begin{pmatrix} b^0_{xx} & b^0_{x\dot{x}} & 0 & 0 \\ b^0_{\dot{x}x} & b^0_{\dot{x}\dot{x}} & 0 & 0 \\ 0 & 0 & b^0_{yy} & b^0_{y\dot{y}} \\ 0 & 0 & b^0_{y\dot{y}} & b^0_{\dot{y}\dot{y}} \end{pmatrix}. \tag{2}$$

Assume also that equations of the transverse motion are linear:

$$\frac{d^2x}{dt^2} = -Q_x x, \quad \frac{d^2y}{dt^2} = -Q_y y. \tag{3}$$

ISBN: 978-3-95450-197-7 doi:10.18429/JACoW-RUPAC2018-TUPSA10

CONTROL THEORY MODEL FOR RFQ CHANNEL OPTIMIZATION

O.I. Drivotin, St.-Petersburg State University,
7/9 Universitetskaya nab., St. Petersburg, 199034 Russia *

Abstract

The common approach for RFQ channel design [1] allows to find geometric parameters of sections of the channel including cell lengths, apertures and coefficients of modulation of electrodes forming the channel. According to that approach, the phase of so called synchronous particle changes slowly. Our previous computations [2] indicate that quality of beam in this channel can be better, if synchronous phase changes more quickly with some oscillations.

To find opportunity for improving the structure, we propose a control theory model for charged particle beam in the RFQ channel. The problem includes some model particle distribution, and dynamics equations depending on control functions. The synchronous phase is chosen as one of the control functions. Great attention is paid to choice of the quality functional.

A numerical solution of such problem can be achieved by an iterative method based on computation of the functional variations. In real problems, we can parametrize the control functions. Then functional variations can be approximated by derivatives of functional on control functions parameters.

INTRODUCTION

The present report is devoted to the simple control model, which allows to solve difficult problem of optimization of the accelerating channel with radio frequency quadrupoles (RFQ) [1]. This model is based on the general model for dynamical systems with two sets of dynamical variables: phase variables of longitudinal and transverse motion with assumption that the longitudinal motion does not depend of the transverse motion.

The control problem is formulated as problem of finding of three control functions which describe geometry of the channel: the accelerating efficiency, the modulation coefficient and derivative of the synchronous phase. Method of the numerical solution based on previously known methods is considered.

BEAM DYNAMICS CONTROL

Consider a beam describing by particle distribution density $\varrho(x)$ in the phase space Ω, $x \in \Omega$ [3, 4, 5, 6]. Let particle trajectories described by the differential equation

$$\frac{dx}{dt} = f(t, x, u),$$

where t is trajectory parameter, u — control function, $u(t) \in U \in R^r$. Assume that vector f is defined in a domain $[t_0, T] \times \Omega \times U$, and the solution of the Cauchy problem for this equation with initial condition $x(t_0) = x_0$ uniquely exists for any x_0 under consideration.

Let at the initial moment t_0 the particle distribution density is given on some $m-$ dimensional surface S $\varrho(t_0, x) = \varrho_{(0)}(x) = \varrho_{(0)\,1\ldots m}(x)\, dx^1 \wedge \ldots \wedge dx^m$, $m \le dim\Omega$, where x^i, $i = \overline{1, m}$, are coordinates on S which can be taken also as some of coordinates in the phase space. The phase density satisfy to the Liouville equation or the Vlasov equation [3, 4, 5, 6]

$$\varrho(t + \delta t, F_{f,\,\delta t}x) = F_{f,\,\delta t}\varrho(t, x),$$

Here $F_{f,\,\delta t}$ denotes Lie dragging along vector field f by parameter increment δt [7].

Let introduce functional charachterizing quality of the controlled process

$$\Phi(u) = \int\limits_{\Omega} g(x_T)\varrho(T, x_T).$$

The problem of minimizing of the functional on control function u from U will be called the terminal problem of beam control with account of particle distribution density.

BEAM MODEL

Consider RQF channel which is sequence of cells with quadrupole symmetric modulation of four electrodes. Let L is the cell length, which is slowly rises along the channel. Take approximate expression for cartesian components of electric field E in some cell

$$E_x = u_0(\frac{2\varkappa}{a^2}x + \frac{2k^2T}{\pi}x\sin\eta)\cos\omega t,$$

$$E_y = u_0(-\frac{2\varkappa}{a^2}y + \frac{2k^2T}{\pi}y\sin\eta)\cos\omega t,$$

$$E_z = u_0\frac{4kT}{\pi}\cos\eta\cos\omega t.$$

Here $2u_0$ is intervane voltage, ω is frequency of the field oscillations, a is aperture of the cell, $k = \pi/L$ η is the phase of electrode modulation, $\eta(z) = \int\limits_{z_0}^{z} k(z')\, dz'$, T is acceleration efficiency, m is modulation coefficient.

As longitudinal motion in this model does not depends of transverse motion, consider particle distribution in the phase space of longitudinal motion. As coordinates take

* o.drivotin@spbu.ru

ISBN: 978-3-95450-197-7 doi:10.18429/JACoW-RUPAC2018-TUPSA11

DEVELOPMENT OF A SOFTWARE COMPLEX FOR MODELING, ANALYZING AND OPTIMIZATION THE DYNAMICS OF CHARGED PARTICLE BEAMS IN SYNCHROTRONS AND TRANSPORT CHANNELS

V.V. Altsybeyev, V.A. Kozynchenko*, D.A. Ovsyannikov, Saint-Petersburg State University, Saint-Petersburg, 199034 Russia

Abstract

The paper considers a new version of the software complex developed for modeling, analyzing and optimization the transverse dynamics of charged particle beams in synchrotrons and transport channels. Considered code provides the calculation of transverse dynamics of the charged particle beam in synchrotrons and transport channels based on the linear model, as well as the calculation of the structural functions of synchrotrons and transport channels, the beam acceptance and emittance, beam dynamics optimization. In the new version of the software complex, the ability to carry out calculations on a remote computing cluster, the web user interface. To store the results of calculating the beam dynamics, a database is used.

INTRODUCTION

At present, the Nuclotron – a synchrotron for the acceleration of beams of multiply charged ions, protons and deuterons is successfully functioning at the Joint Institute for Nuclear Research (Dubna, Russia) [1], as well as the project NICA is being implemented to create a collider of protons and heavy ions. The NICA accelerator complex is assumed to produce the beams of high quality with sufficiently rigid characteristics.

In contrast to analogous foreign software packages, such as MAD-X (CERN) and OptiMX (FNAL), the DAISI focuses on solving the problems of restoring the errors in magnetic fields and errors in alignment of magnetic elements, as well as also on the optimization of the beam dynamics in synchrotrons and transport channels.

At present, a software complex for modeling and optimizing dynamics in synchrotrons and transport channels is under development on the basis of the DAISI program complex [2], which provides high-performance computing using remote computing resources. The development of such a software package has been stipulated by the need of using high-performance computing tools for solving both the multi-parametric optimization problems of beam dynamics in synchrotrons and the problems of restoring the actual synchrotron parameters.

The program complex involves a friendly web graphical user interface and various sets of tools, methods and algorithms for calculating the beam dynamics, orbit correction, and restoring the parameters of the accelerator complexes. The software complex in point was used for solving the problem of placing the dipole magnets in the Nuclotron booster being under development and now it is being improved further to solve various problems within the framework of the NICA project..

DESCRIPTION OF THE PROGRAM COMPLEX

The software complex consists of a control program, a database and calculation modules, and a web user interface. The control program provides the start of calculations by user commands, data extraction from the database and saving of information about the performed calculations in the database.

Calculation modules provide executing the distributed calculations on remote computing nodes. At present, it has been implemented the module for calculating the linear transverse dynamics of the center of gravity of the beam, the module for calculating the beam transverse dynamics, the module for providing the arrangement of dipole magnets in synchrotrons, as well as the module of correcting the orbits under various restrictions imposed on the value of the maximum orbit deviation from the synchrotron axis in the different sections of the synchrotron

MODULES

The Module for Calculating the Lateral Dynamics of the Center of Gravity of the Beam in the Synchrotrons Based on a Linear Model

The module for calculating a transverse beam dynamics in the synchrotrons and transport channels provides computing the lateral dynamics of the center of gravity of the beam at the synchrotrons that is based on a linear model and uses the transport matrices of structural elements of the synchrotrons and transport channels (dipole bending magnets, focusing and defocusing quadrupole lenses, drift gaps, and multipole magnetic correctors). When calculating the dynamics, the structural elements intended for the slowed-down beam extraction

* v.kozynchenko@spbu.ru

ISBN: 978-3-95450-197-7 doi:10.18429/JACoW-RUPAC2018-TUPSA12

DYNAMICS OF THE SPHERICAL CLOUD OF CHARGED PARTICLES

A.S. Chikhachev
Federal State Unitary Enterprise "RFYaTs VNIITF im. akad. E. I. Zababakhina", VEI-branch
Krasnokazarmennaya, 12, 111250, Moscow, Russia

Abstract

In work the behavior spherically of a symmetric dense cloud of the charged particles which are under the influence of own field is studied. The kinetic description based on "Meshchersky's integral" is used. The movements of particles from the center of symmetry and to the center of symmetry of system are studied.

INTRODUCTION

In this work the behavior spherically of a symmetric clot is considered. At the same time for the description of the radial movement Kapchinsky-Vladimirsky's integral as it is made in work [1] won't be used, and other approach connected with "Meshchersky's integral" will be offered (see [2,3]). Two types of the movement of particles - from the center of system and to the center of system of coordinates are considered.

THE MOVEMENT FROM THE CENTER OF SYSTEM

Hamilton-Jacobi's Equation with spherical symmetry has an appearance (see [4]):

$$\frac{\partial S}{\partial t}+\frac{1}{2m}\left(\frac{\partial S}{\partial r}\right)^2+\frac{1}{2mr^2}\left(\frac{\partial S}{\partial \theta}\right)^2+ \frac{1}{2mr^2\sin^2\theta}\left(\frac{\partial S}{\partial \phi}\right)^2+U(r,t)=0 \quad (1)$$

Here $r, \theta,\ phi$- coordinates in spherical system, S- Hamilton function. We will look for the decision (15) in a look:

$$S=\pm\int\sqrt{2m\left(H-U(r',t)-\frac{L}{2r'^2}\right)}dr' +\psi(t)+M_\phi\phi \pm\int_{\arcsin|\frac{M_\phi}{\sqrt{L}}}^{\theta}d\theta'\sqrt{L-\frac{M_\phi^2}{\sin^2\theta'}},$$

where M_ϕ - a moment projection to an axis of z, $L=\frac{M_\phi^2}{\sin^2\theta}+m^2(r^2\dot\theta)^2$ - a square of the full moment.

The integrals interfaced to energy H have an appearance:

$$J_H^{\pm}=\frac{\partial S}{\partial H}= \pm\int\frac{dr'}{\sqrt{\frac{2}{m}(H-U(r'))-\frac{L}{2m^2r'^2}}}-t$$

We will pass from H to an invariant of I, ("Meshchersky's integral") remaining at a certain dependence of potential function from $\vec r$ and t. In this case the Hamiltonian has an appearance:

$$H=\frac{p_r^2}{2m}+\frac{L}{2mr^2}+\frac{1}{\xi^2(t)}U\left(\frac{r}{\xi(t)}\right).$$

Here $p_r=m\dot r$. Using expression of a Hamiltonian, it is possible to receive expression for an invariant:

$$I=\frac{m}{2}(\dot r\xi-r\dot\xi)^2+U\left(\frac{r}{\xi(t)}\right) +\frac{\lambda m}{2}\frac{r^2}{\xi^2}+\frac{L}{2m}\frac{\xi^2}{r^2}, \quad (2)$$

Similar to integral of $J_H^{\pm}$ can construct integral of $J_I^{\pm}$, we will consider interfaced to I. In this section that there are only particles described by J_I^+ integral. Density of particles is expressed by integral in phase space:

$$n=\int d\vec q f(I,J_I^+,L). \quad (3)$$

We will present an element of phase space in the form:

$$d\vec q=dq_r dq_\theta dq_\phi,\quad dq_\phi=\frac{dM_\phi}{r\sin\theta},$$

$$dq_r=\frac{dI}{\xi\sqrt{\frac{2}{m}(I-U)-\lambda\frac{r^2}{\xi^2}-\frac{L\xi^2}{m^2r^2}}},$$

$$dq_\theta=\frac{dL}{2r\sqrt{L-\frac{M_\phi^2}{\sin^2\theta}}}.$$

Averaging on M_ϕ leads to expression:

$$n=\frac{\pi}{2r^2}\int\frac{dIdLf(I,L,J_I^+)}{\xi\sqrt{\frac{2}{m}(I-U)-\lambda\frac{r^2}{\xi^2}-\frac{L\xi^2}{m^2r^2}}}.$$

At the same time density of current of j_r has an appearance: ($\dot r$ can be expressed through I from (1.2)) $j_r=\frac{r\dot\xi}{\xi}n+\frac{\pi}{2r^2\xi^2}\int fdIdL$. We will make, further, replacement of variables: $r=\rho\xi, \tau=\int\frac{dt'}{\xi^2(t')}$. At the same time Poisson's equation takes a form:

$$\frac{1}{\xi^4(t)}\frac{1}{\rho^2}\frac{d}{d\rho}\rho^2\frac{dU}{d\rho}= -\frac{4\pi e^2}{\xi^3(t)\rho^2}\int\frac{dIdLf(I,L,J_I^+)}{\sqrt{\frac{2}{m}(I-U(\rho))-\lambda\rho^2-\frac{L}{m^2\rho^2}}}. \quad (4)$$

ISBN: 978-3-95450-197-7 doi:10.18429/JACoW-RUPAC2018-TUPSA13

ABOUT FOCUSING BY GRIDS

A.S.Chikhachev,
Federal State Unitary Enterprise " RFYaTs VNIITF im. akad. E. I. Zababakhina" -VEI-branch
Krasnokazarmennaya, 12, 111250, Moscow, Russia

Abstract

The possibility of steady acceleration of particles in the presence in a tube of drift of a foil which plane is parallel to an axis is studied. For calculation of the field the method of conformal transformations is used. Conditions of simultaneous acceleration with stability of the cross and longitudinal movement are found out.

INTRODUCTION

For focusing of bunches of heavy charged particles focusing by grids - the folga located along an axis which plane is parallel to an axis of the accelerating system is offered (see [1]). For studying of properties in the real work the simplest option of such system is considered - the foil settles down on a drift tube axis, and influence of a foil will be studied in flat geometry that gives the chance for calculation of the field to apply a method of conformal transformations.

THE FIELD IN A STRIP WITH A CUT

Method of conformal transformations. Let $z = x + iy, w = u + iv$. Transformation

$$w + ia = \frac{a}{\pi}\ln(1 - e^{\frac{\pi z}{a}}) \quad (1)$$

transfers a strip with a cut to z planes in a strip without cut in w plane. At this transformation

$$u = \frac{a}{2\pi}\ln\left(1 - 2e^{\frac{\pi x}{a}}\cos(\frac{\pi y}{a}) + e^{\frac{2\pi x}{a}}\right), \quad (2)$$

$$v = -\frac{a}{\pi}\arctan\frac{\sin\frac{\pi y}{a}}{e^{-\frac{\pi y}{a}} - \cos\frac{\pi y}{a}} - \frac{a}{\pi} \quad (3)$$

The straight line of $y = +a, -\infty < x < +\infty$ passes in half line $v = -a, 0 < u < +\infty$, top coast of drift $y = 0, x < 0$ meets to half line $v = -a, -\infty < u < 0$. Borders of the accelerating interval $[0, b]$ meets to $[\alpha, \beta]$ where $\alpha = \frac{a}{\pi}\ln 2, \beta = \frac{a}{\pi}\ln(1 + e^{\frac{\pi}{b}a})$. Particle moves along axes x in negative direction. Length of tube drift d are $d >> a$, where a-an aperture. Actual width of a foil as it will be visible from expression for the field on an axis, can be about a/π because of exponential decrease of the field. As boundary conditions we will put: $E_x(x, a) = f(x), \quad f = E_0\sigma x\sigma(b - x)$. Here $\sigma(x)$ - the Heaviside function. Components of the potential field $\vec{E}$ upon transition from w to z will be transformed by in a complaining way:

$$E_x = AE_u + BE_v, E_y = -BE_u + AE_v, \quad (4)$$

where

$$A = \frac{\partial u}{\partial x} = \frac{\partial v}{\partial y} = \frac{\exp(\frac{2\pi x}{a}) - \exp(\frac{\pi x}{a})\cos(\frac{\pi y}{a})}{1 - 2\exp(\frac{\pi x}{a})\cos(\frac{\pi x}{a}) + \exp(\frac{2\pi x}{a})} \quad (5)$$

$$B = -\frac{\partial u}{\partial y} = \frac{\partial v}{\partial x} = -\frac{\exp(\frac{\pi x}{a})\sin(\frac{\pi y}{a})}{1 - 2\exp(\frac{\pi x}{a})\cos(\frac{\pi x}{a}) + \exp(\frac{2\pi x}{a})} \quad (6)$$

We will pass, further, from boundary conditions for E_x to boundary conditions for E_u.. Using ratios 1.4-1.6 for $E_x(x, a)$ we will find :

$$E_u(u, a) = g(u) = \frac{E_0}{(1 - \exp(\frac{-\pi u}{2})}\sigma(u - \alpha)\sigma(\beta - u) \quad (7)$$

We will find, further, field components in w plane. From

$$E_u = \frac{1}{2\pi}\int\int dk du' g(u')\exp\{ik(u - u')\}\frac{\cosh(kv)}{\cosh(ka)}, \quad (8)$$

and for E_v we have:

$$E_v = \frac{1}{2\pi i}\int\int dk du' g(u')\exp\{ik(u - u')\}\frac{\sinh(kv)}{\cosh(ka)}, \quad (9)$$

Integrals in (1.8) and (1.9) can be expressed in elementary functions. Using (1.4) it is possible to calculate $E_x(x, 0)$ and $E_y(x, 0)$. $E_x(x, 0) \neq 0$ only at $x > 0$, whereas $E_y \neq 0$ only at $x < 0$. When transforming (1.1) this half shaft passes into $v = 0$. From (1.5) for definition of $E_x(x, 0)$ to know $E_u(u, 0)$. We will finally receive :

$$E_x(x, 0) = -\frac{1}{\pi}\Big[\frac{1}{\sqrt{e^{\frac{\pi x}{a}} - 1}}\ln\left(\frac{\sqrt{1 + e^{\frac{\pi b}{a}} - 1}}{\sqrt{1 + e^{\frac{\pi b}{a}} - 1}}\frac{\sqrt{2} + 1}{\sqrt{2} - 1}\right) + 2\left(\arctan\sqrt{\frac{1 + e^{\frac{\pi x}{a}}}{e^{\frac{\pi b}{a}} - 1}} - \arctan\sqrt{\frac{2}{e^{\frac{\pi x}{a}} - 1}}\right)\Big] \quad (10)$$

For definition of $E_y(x, 0)$ needs to find $E_v(u, -a)$. Can be received:

$$E_y(x, 0) = \frac{1}{\pi}\frac{1}{\sqrt{1 - e^{\frac{\pi x}{a}}}}\ln\left(\frac{\sqrt{1 + e^{\frac{\pi b}{a}} - 1}}{\sqrt{1 + e^{\frac{\pi b}{a}} - 1}}\frac{\sqrt{2} + 1}{\sqrt{2} - 1}\right) - \frac{1}{\pi}\ln\left(\frac{\sqrt{1 + e^{\frac{\pi b}{a}}} - \sqrt{1 - e^{\frac{\pi x}{a}}}}{\sqrt{1 + e^{\frac{\pi b}{a}}} + \sqrt{1 - e^{\frac{\pi x}{a}}}}\frac{\sqrt{2} + \sqrt{1 - e^{\frac{\pi x}{a}}}}{\sqrt{2} + \sqrt{1 - e^{\frac{\pi x}{a}}}}\right) \quad (11)$$

ISBN: 978-3-95450-197-7 doi:10.18429/JACoW-RUPAC2018-TUPSA14

NUMERICAL COMPUTATION OF DYNAMIC APERTURE FOR THE NICA BOOSTER

A.V. Butenko, O. Kazinova#, S.A. Kostromin, A.V. Tuzikov, V.A. Mikhaylov, JINR, Dubna, Russia

Abstract

Modern accelerators are made with high-field superconducting dipoles, quadrupoles and sextupoles that exhibit unintentional imperfections of the guiding field-shape due to construction tolerances, persistent currents and magnetic saturation. This deviation from linearity has a profound influence on the beam dynamics. In this work the research of nonlinear beam dynamics for the NICA booster was carried out. Sextupole and octupole fields for dipole and quadrupole magnets, according to ongoing magnetic measurements, were taken into account, as well as adjustment errors for magnets. Numerical simulation in MADX program has been used to evaluate the dynamic aperture for the booster. The results showed that dynamic aperture is exceeded its geometrical acceptance at least in three times.

INTRODUCTION

The sextupole field increases quadratically with x and while we compensate the chromaticities, these same sextupoles generate nonlinear, quadratic perturbations especially for particles with large betatron oscillation amplitudes. These perturbations are known as geometric aberrations. The art of accelerator design is then to correct the chromatic aberrations while keeping the geometric aberrations at a minimum. This can be achieved by distributing sextupoles along the orbit at properly selected locations. However, even with carefully distributing the sextupoles around the ring lattice, we still deal with a nonlinear problem and we cannot expect to get perfect compensation. There will always be a limit on the maximum stable betatron oscillation amplitude in the storage ring. This limit is called the dynamic aperture in contrast to the physical aperture defined by the vacuum chamber. There is no analytical solution for the dynamic aperture and it is determined by numerical particle tracking programs only [1].

NUMERICAL SIMULATION

The booster of the NICA project [2] is a heavy ion superconducting synchrotron [3]. Magnetic lattice of the booster consists of 4 quadrants, each of which includes 6 DFO-periods. Main parameters of the booster are shown at Table 1. The booster resonance diagram with marked operating point is shown at Fig.1. All simulation and modelling processes were made using MADX program [4]. Dynamic aperture was defined as stable motion region for particles after specified number of revolutions.

Despite the progress in explanation of nonlinear phenomena, there still is a gap between analytical, numerical prediction and reality. Especially, perturbation theory is limited near resonances. The resonant conditions can lead to continuously growing betatron amplitudes and rapidly, after at most a few thousand turns, particles will be lost on the booster vacuum chamber.

Table 1: Main Parameters of the Booster

Type	Value
Ions, max MeV/u	$_{197}Au^{31+}$, 578
Circumference, m	210.96
Maximum magnetic field, T	1.8
Maximum magnetic rigidity, T·m	25.2
Number of dipole magnets	40
Curvature radius for dipole magnets, m	14.09
Effective length of dipole magnets, m	2.2
Number of quadrupole magnets	48
Effective length of quadrupole magnets, m	0.47
Vacuum chamber, mm^2	129 x 68

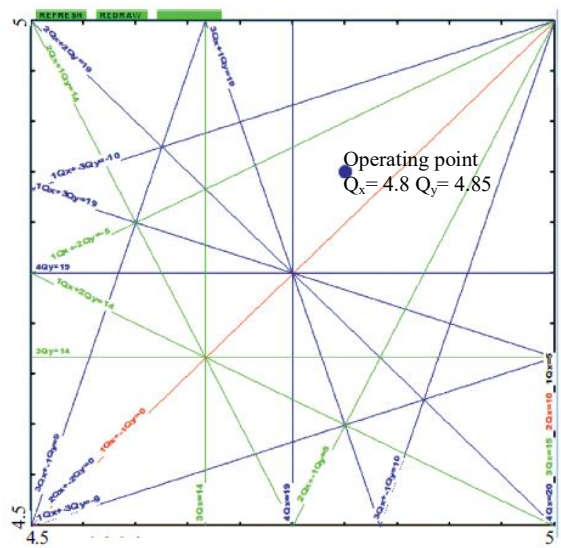

Figure 1: Resonance diagram for the booster with lines up to 4th order.

Resonances of 3rd Order

There are 2 the closest resonances near the operating point: $1Q_x - 2Q_y = -5$ and $3Q_x = 14$. Consider the first resonance with such betatron tunes: Q_x=4.8, Q_y=4.9. Dynamic aperture (see Fig.2) has no visible changes inside the vacuum chamber. The green line on the X-PX graph concerns to the wall of the vacuum chamber in X-

#kazinova.olga@gmail.com

ISBN: 978-3-95450-197-7 doi:10.18429/JACoW-RUPAC2018-TUPSA15

PARTICLE DYNAMICS SIMULATION IN NUCLOTRON OF THE NICA COMPLEX ACCOUNTING INFLUENCE OF THE LEAKAGE MAGNETIC FIELD

I. Avvakumova, A. Kovalenko, V. Mikhaylov, A. Tuzikov VBLHEP, JINR, Dubna, Russia

Abstract

The aim of the current work was to demonstrate main parameters of beam dynamics in the Nuclotron while functioning as a part of NICA. Thereby, processes of beam circulation and slow extraction were modelled. The influence of leakage fields of injection and extraction systems septa magnets (Lambertson magnets) was demonstrated. Calculations were carried out via MADX package.

INTRODUCTION

The Nuclotron, superconducting heavy ion synchrotron with iron shaped magnets, has been under operation since 1993. Physics experiments were carried out only in internal circulating beams before March, 2000. Preparation of the extraction system elements [1], their final bench tests and installation in the ring were performed in 1999. In 2000 the works were completed, and the equipment was installed into the ring and put into operation that made it possible to carry out further experiments at the extracted beams as well [2], [3]. Systems of fast beam extraction from Nuclotron into collider and beam injection from Booster into Nuclotron are under construction now. Both of them include Lambertson magnets as well as slow beam extraction system does [4].

NUCLOTRON COMPOSITION. LAMBERTSON MAGNETS LOCATION AND PURPOSE

Nuclotron consists of 8 superperiods, or octants. Regular superperiod is shown on Fig. 1. Lambertson magnets location is also shown there.

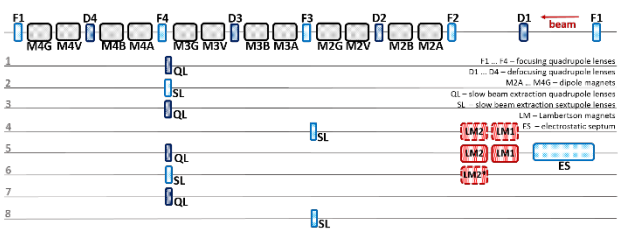

Figure 1: Composition of the Nuclotron elements.

One pair of Lambertson magnets in the fifth octant, LM1 and LM2, serve as a part of beam deflecting system during slow beam extraction process. Other three Lambertson magnets are being built now: one pair, which is absolutely the same as the existing one, would provide fast extraction from Nuclotron into collider and single Lambertson magnet is intended for injection system Booster-Nuclotron.

The aim of work is to demonstrate how leakage fields, which are produced by existing and additional Lambertson magnets, would affect beam dynamics in Nuclotron during beam circulation and slow extraction.

SIMULATION AND RESULTS

Firstly, circulating beam dynamics was observed for betatron tunes Q_x=7.40, Q_y=7.45 and at the value of guiding magnetic field about 0.45 T. This value corresponds to the energy of beam injection from Booster ring to Nuclotron. Single LM2* was expected to have significant effect on beam motion, in view of the fact that it will have it's own power supply and field value 1T.

On the figures below, results of calculations are shown. Three modes of beam circulation were considered: all Lambertson magnets are turned on and so all LM's leakage fields have effect on beam dynamics (see Fig. 2a, 2b), only couples of LM are turned on (see Fig. 2c, 2d) and all Lambertson magnets are turned on, but short-connected loops in all LM2 are turned off (see Fig. 2e, 2f).

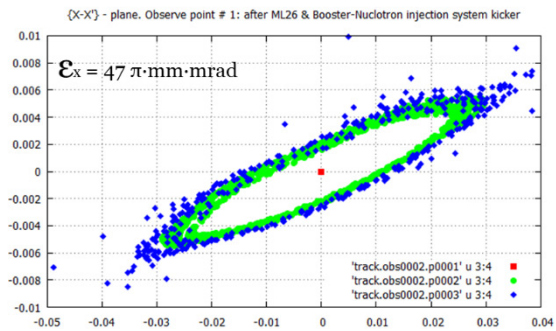

Figure 2a: XX' plane with all LM's leakage fields turned on (the first regime).

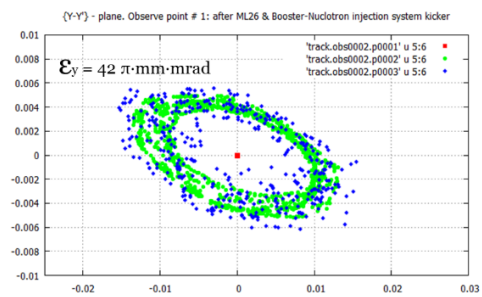

Figure 2b: YY' plane with all LM's leakage fields turned on (the first regime).

ISBN: 978-3-95450-197-7 doi:10.18429/JACoW-RUPAC2018-TUPSA16

COMPUTER CODES FOR CALCULATION OF ELECTROMAGNETIC RADIATION GENERATED IN MAGNETIC FIELDS

N. V. Smolyakov†, R. G. Chumakov, NRC KI, Moscow, Russia

Abstract

Software for simulation of different characteristic of spontaneous electromagnetic radiation, generated by a relativistic electron beam in external magnetic field, is presented. It consists of different computer codes, which are in consistent with each other. These codes calculate spatial distributions of electromagnetic radiation spectral densities, spatial distributions of radiation power, electron beam emittance effects. The set of input parameters allows including the real geometry of experiment into simulations. For example, the near-field effects are taken into account. The electron beam emittance is simulated by numerical convolution of the Gaussian electron distribution in a beam with the spatial distribution of the electromagnetic radiation, generated by one electron.

INTRODUCTION

It can be assumed that the undulator has a perfect sinusoidal magnetic field, such as the planar or helical [1], elliptical [2], two-harmonic [3] and figura-8 [4] undulators. In this case, the spectral-angular density of undulator radiation in the far-field region involves a series of Bessel functions. This method is used in the computer codes SMUT [5], URGENT [6], and US, which is incorporated into the software toolkit XOP [7]. This approach has a high speed of computation as their main advantage. At the same time, they cannot work with imperfect magnetic fields, near-field effects also cannot be taken into account.

Some computer codes are able to use a real magnetic field map and compute the Fourier transformation of the radiation field numerically. One of three ways can be used. The spectral integrals may be evaluated by the saddle point method [8]. This approach uses the formulae for standard synchrotron radiation and is applicable to insertion devices with strong magnetic fields [9, 10]. This method is used in the computer code RADID [9, 11].

The second method involves the calculation of the radiation field in the time domain followed by the Fourier analysis in order to find the radiation spectrum. Such method is used in the codes B2E [12], UR [13], YAUP [14], and SPECTRA [15] and is also integrated in the code RADID [9, 11, 16, 17]. It gives direct insight into the physics of radiation emitting process and enables the calculation of radiation spectra in a wide range simultaneously, while requiring huge amount of memory for angular distribution computation [14].

The Lienard-Wiechert retarded potentials can be integrated in the frequency domain. This method is used in the codes SpontLight [18], SRW [19], WAVE [20], SPUR [21] and in a number of others programs [12, 22-26]. The main problem of this approach comes from the fast oscillating factor in the integrand, requiring the use of extreme care in integration routines. Comparative studies of these algorithms can be found in [9, 27, 28].

Emittance effects are usually simulated by the Monte Carlo method or by using the off-axis approximation [5], also known as the shift-invariant property of the radiation pattern [23]. The Monte Carlo method, generally considered to be the most accurate, is employed in a number of computer codes, such as RADID [9, 11, 16, 17], UR [13], SpontLight [18], see also papers [22, 25]. The problem with this approach is that the large number of individual computations for single-electron radiation can sometimes be too time consuming and impractical [17, 22, 29].

The off-axis approximation method is based on the concept that spatial distributions of radiation from different electrons are identical in form and are related to each other by the angle shifts arising due to angular and spatial electrons spread. If this is so, there is no need to compute the radiation for each electron separately and the computational task is simplified considerably. As we know, this idea was first proposed in the paper [30]. Owing to computational speed, this method is widely used in a number of computer codes such as SMUT [5], URGENT [6], B2E [12], YAUP [14], US [7], SRW [19], SPECTRA [15], see also [23, 24, 26]. It was believed for a long time that the off-axis approximation is valid in the far-field region only [5, 23], since the equations controlling the pattern of radiation in the near-field region are rather cumbersome. It was rigorously proven in [31] that the electromagnetic radiation, generated by a relativistic electron in an external magnetic field, has the shift-scale invariance property. This proves the applicability of the off-axis approximation in the near-field region.

This paper describes the development of a set of computer codes for modeling of spontaneous electromagnetic radiation, generated by a relativistic electron beam in external three-dimensional magnetic field. It consists of three main computer programs. The first program computes the distributions of spontaneous radiation spectral density from one electron. The second program computes the distributions of spontaneous electromagnetic radiation power. The last program simulates the electron beam emittance effects.

ANALYTICAL EXPRESSIONS

For definitenesss, we will consider here the case of undulator magnetic field. It is assumed that the electron does not lose any kinetic energy due to emission of radiation in the magnetic field. Let the *X*-axis of the right-hand Cartesian coordinate system is directed horizontally, the *Y*-axis is directed upwards and the *Z*-axis is aligned with the undulator axis. The magnetic field is presumed to be

† smolyakovnv@mail.ru

ISBN: 978-3-95450-197-7 doi:10.18429/JACoW-RUPAC2018-TUPSA17

NOVEL APPROACH TO DESIGN OF THE COMPACT PROTON SYNCHROTRON MAGNETIC LATTICE

V. A. Vostrikov†[1], S. E. Karnaev, Yu. A. Pupkov,
Budker Institute of Nuclear Physics, 630090 Novosibirsk, Russia
[1]also at Novosibirsk State University, 630090 Novosibirsk, Russia

Abstract

A compact proton synchrotron for cancer therapy has been developed. The proposed magnetic lattice includes short dipole magnets with opposite direction of the field. The lattice optical functions are close to the usual for weak-focusing synchrotrons. At the same time, it allows achieve value of momentum compaction factor less than unity, and thereby avoid intensity limitations due to longitudinal instabilities. Multiturn injection and resonance extraction description finalizes the presented design of compact proton synchrotron.

INTRODUCTION

Every year new facilities for hadron therapy are commissioning worldwide. In the market, several companies supply turnkey solutions based on cyclotrons and synchrotrons. Various research groups develop new conceptions, and optimize traditional design.

Last years, an interest in the compact single room proton therapy systems has grown significantly in the cancer treatment community. It is the cost effective solution for small hospitals to be involved into the proton therapy. First single room proton therapy facility supplied by Mevion Medical Systems shown successful results of operation [1, 2]. Now most manufacturers propose single room modifications of supplied equipment. Two of them, HITACHI and PROTOM developed compact particle therapy systems based on synchrotrons [3, 4]. These accelerators have diverse conceptions and significantly different parameters.

The presented article describes the results of an attempt to find an optimal design of compact proton synchrotron. The main idea is that optimum should be between the systems mentioned above and should incorporate merits of both.

MAGNETIC LATTICE

Lattice with non-gradient bending magnets and edge focusing is the most compact. Such lattice was used in the facility developed in BINP [5]. An imperfection of the system was the low intensity of proton beam about of $5 \cdot 10^8$ particles per cycle. The intensity limitation was caused by longitudinal negative mass instability at injection energy and small vertical aperture [6]. The main reason of instability growth is the large value of momentum compaction factor $\alpha > 1$. Instability can be suppressed by beam energy spread but for intensity about of 10^{10} protons, the required energy spread is larger than achievable energy acceptance of synchrotron.

Installation of one quadrupole lens per cell moves optics to the normal regime. Maximal values of ß-functions are increased significantly, so vertical aperture shall be enlarged accordingly when transverse acceptance saving. Note that value of momentum compaction factor should be small enough to avoid transition crossing in the treatment energy range. It is the traditional lattice design, but disadvantages of this solution are high costs and energy consumption.

Further increasing of quadrupoles number can provide good enough optics. However, additional quadrupoles enhance free space problem and impede injection and extraction.

Application of field gradient bending magnets provides useful design, also. However, a limitation of field value leads to enlarging of synchrotron dimensions.

Therefore, the weak focusing lattice with non-gradient bending magnets is most simple and cost effective. The negative mass regime problem or in other words the problem of additional horizontal focusing shall be solved. Bending magnets edges determine vertical focusing and fix it. So, the bending angle is an operating parameter only. The bending angle is increased up to more than 360° for achieving of required values of horizontal tune, momentum compaction and transition energy. Finally, for closing reference orbit magnetic field in part of magnets shall be reversed. It is a simple solution which is used sometime in storage rings for high energy physics. After optimization the novel compact lattice for proton synchrotron was developed.

SYNCHROTRON DESIGN

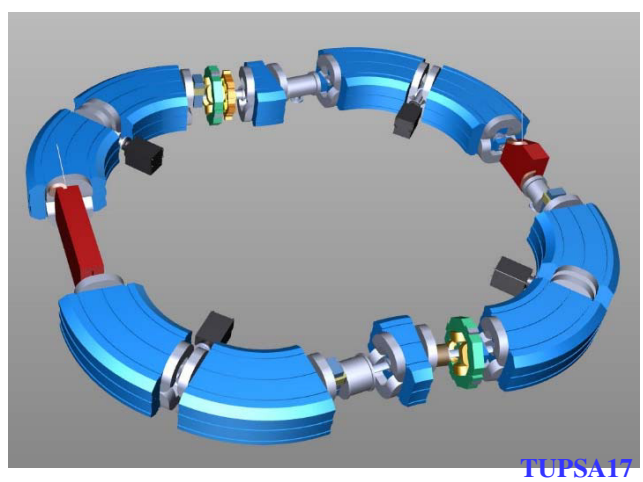

Figure 1: 3-D model of the synchrotron.

† V.A.Vostrikov@inp.nsk.su

ISBN: 978-3-95450-197-7 doi:10.18429/JACoW-RUPAC2018-TUPSA22

COMMISSIONING OF ELECTRON COOLING SYSTEM OF NICA BOOSTER

A.V.Smirnov, L.V.Zinovyev, A.S.Sergeev, S.V.Semenov#, A.G.Kobets, A.A.Sidorin, E.A.Kulikov, S.Yu.Kolesnikov, Yu.A.Tumanova, Joint Institute for Nuclear Research, Dubna, 141980 Russia
V.V.Parckhomchuk, M.I.Bryzgunov, A.V.Bubley, V.B.Reva,
Budker Institute of Nuclear Physics, Novosibirsk, 630090 Russia

Abstract

At the NICA project, two electron cooling systems were planned at the booster and collider. The booster cooler will be used for the multiturn injection procedure and for the formation of necessary beam parameters before injection from the booster to Nuclotron. This article presents the status of the commissioning of the electron cooling system at the NICA booster. The electron cooling system was produced in BINP (Novosibirsk) and delivered to JINR (Dubna) last year [1]. This year the commissioning of the cooler was done for parameter of the injection energy of ions 3.2 GeV/u. In the nearest future it will test for the intermediate ion energy 100 GeV/u. Finally, the cooler should operates at both energy during one injection cycle.

COOLER PARAMETERS

In order to achieve the required beam parameters in NICA booster, an electron cooling system (ECS) was designed, which was manufactured at INP (Institute of Nuclear Physics, Novosibirsk) [2]. In 2017 the system was shipped to JINR and its assembly and commissioning have been started. The distinctive feature of the present system is that for the first time ever an electronic cooling method with a magnetized e-beam will be applied to the superconducting synchrotron, which imposes some additional requirements for the construction and start of ECS, which itself is at room temperature (Fig. 1).

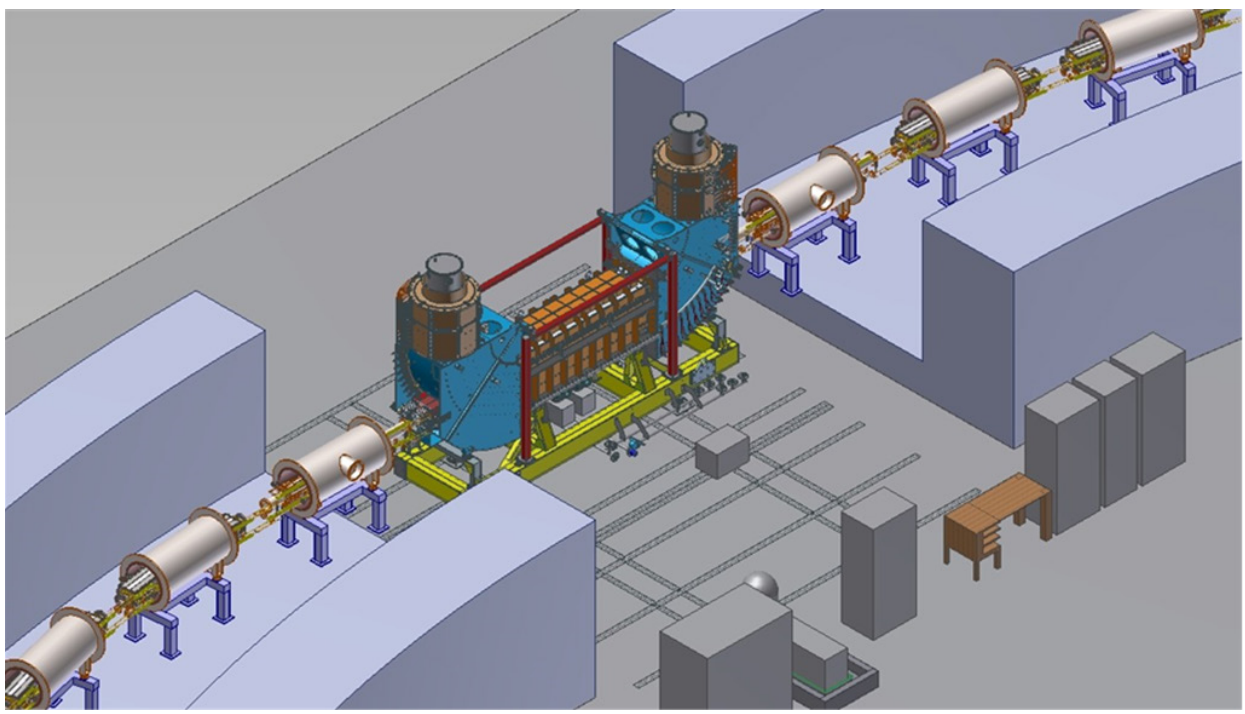

Figure 1: Electron cooling system in the booster.

The report describes the main steps of assembly and start of ECS directly in a straight booster section, which includes: MEP installation (water, electricity, air, oil system), geodetic works on putting the system on site. The measuring data of magnetic field uniformity of forward magnet unit (solenoid) are given (Table 1).

The vacuum and magnet systems assembly takes several steps because of ECS structural features. At the final stage of vacuum system assembly the vacuum chamber is baked up, bulk getters and cathode of electron gun are activated. On finishing the assembly and testing of the high voltage system, the e-beam is sent from the gun to the collector.

servsemenov@gmail.com

ISBN: 978-3-95450-197-7 doi:10.18429/JACoW-RUPAC2018-TUPSA23

TEST BENCH FOR THE NICA STOCHASTIC COOLING ELEMENTS

I. Gorelyshev*,[1], V. Filimonov, V. Khomutova, A. Sidorin[1], JINR, Dubna, Russia
[1]also at Saint Petersburg State University, Saint Petersburg, Russia

Abstract

Stochastic cooling is one of the crucial NICA (Nuclotron-based Ion Collider fAcility) subsystems. Cooling efficiency depends on quality of system elements. A new test bench has been created at JINR for incoming control of pickups, kickers and amplifiers, tuning and adjustment of the comb filter etc. The description of the test bench is given. Methodics of the measurements that should be done on the test bench are discussed. The results of the first measurements are given.

INTRODUCTION

Stochastic cooling system (SCS) for NICA collider is under development in JINR [1]. Main equipment for the NICA SCS consist of 6 pickups, 4 kickers and 64 power amplifiers. Supply of the equipment is in progress and to perform incoming quality tests a test bench has been created. A number of measurements should be done for pickups and kickers: shunt impedance dependence on the pickup structure length and azimuthal loop position, electrical centre behaviour as a function of frequency, influence of high-order mode suppressors and ceramic vacuum chamber, kicker standing wave ratios (SWR). Also measurements for the amplifiers are the following: gain dependence on frequency and input power, linearity of gain (intermodulation products) and phase frequency response, group delay deviations from a constant value and reproducibility of all the parameters mentioned above.

TEST BENCH

The test bench consists of of the ring slot coupler type pickup/kicker prototype [2,3] with mechanical support, comb filter, power meter, attenuators and vector network analyser (VNA). The typical measurement scheme is shown in Fig. 1.

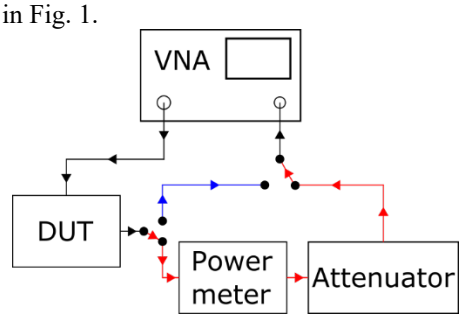

Figure 1: The measurement scheme for devices under test (DUT): red line for active devices, blue – for passive ones.

Passive devices (e.g. pickups/kickers, cables etc.) are measured by direct connection to the VNA. To prevent VNA ports from damage caused by high power from active devices (e.g. amplifiers) the power meter and attenuator are added to the scheme between the output port of the DUT and the input port of the VNA.

All measurements for the test bench are listed in Table 1. Measurements except the influence of intermodulation distortion (IMD) are performed by the scheme presented in Fig. 1. The measurement of IMD is discussed in details in section below.

Table 1: List of Measurements

Pickup/Kicker	***Amplifiers***
Impedance dependence on the azimuthal loop position	Gain vs frequency
Impedance dependence on the longitudinal loop position	Gain vs input power
Electrical center position as a function of frequency	Gain linearity of frequency and power
Influence of High Order Mode suppressors	Phase linearity
Influence of ceramic vacuum chamber	Group delay
Kicker SWR	IMD
Reproducibility	

POWER AMPLIFIER MEASUREMENTS

General Measurements

The total output power of one NICA SCS kicker is estimated to be 500 W. Every kicker will consist of four sections, each of them can dissipate power of 125 W. Every section will be driven by 30 W amplifier units distributed by 4 directions as shown in Fig. 2. This scheme requires precise reproducibility of amplifier performance. The amplifier response should be close to constant gain and linear phase.

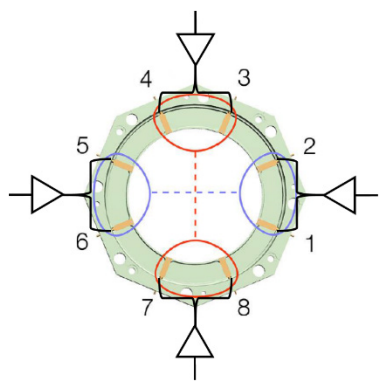

Figure 2: Feed scheme of one kicker section.

The combination of this requirements is unavailable in commercial amplifiers, therefore, research and

* ivan_v_gorelyshev@mail.ru

ISBN: 978-3-95450-197-7 doi:10.18429/JACoW-RUPAC2018-TUPSA24

TEST BENCH MEASUREMENTS FOR THE NICA STOCHASTIC COOLING PICKUP AND KICKER*

V. Khomutova*, V. Filimonov, I. Gorelyshev, A. Sidorin, VBLHEP, JINR, Dubna, Russia

Abstract

A new test bench for measurements of Nuclotron-based Ion Collider fAcility (NICA) stochastic cooling elements has been created at Joint Institute for Nuclear Research (JINR). The following measurements for NICA stochastic cooling pickups/kickers based on Ring-slot coupler structure has been provided: impedance dependence on azimuthal and longitudinal loop positions, electrical center position behavior as a function of frequency and standing wave ratio (SWR) of the kicker. The results of the listed measurements are given.

INTRODUCTION

Stochastic cooling system (SCS) for NICA collider is under development in JINR. It is required for beam accumulation and luminosity preservation of the collider. Stochastic cooling system it is a microwave broadband system with feedback via the beam that leads to a decrease in the amplitudes of the betatron oscillations and the energy spread of the beam particles. This system consists of pickup and kicker, amplifiers, electrical delay elements and other optional characteristic elements.

Since JINR had no experience with the stochastic cooling, in 2008 it was decided to develop a test channel at Nuclotron before the implementation at NICA. Test channel has bandwidth 2-4 GHz and 60W output power. Pickup and kicker for the test channel were manufactured in FZJ (Juelich, Germany) on the basis of design proposed for HESR of the FAIR project [1]. During experiments at the Nuclotron performed in close cooperation with FZJ personnel the kicker was tested at the design power and the beam cooling was demonstrated for coasting and bunched beams [2]. However the initial design does not satisfy exactly to the NICA requirements. First of all it does not guarantee obtaining of residual gas pressure at the level of 10^{-11} Torr necessary for the collider operation. A few important characteristics of the structures were not measured during the first experiments. In the last run of the Nuclotron operation (spring 2018) the structures were tested with low intensive heavy ion beams. Measurements of the beam transfer functions (BTF, see Fig. 1-2) demonstrated excellent sensitivity of the structure (stable signal of sufficient amplitude was measured at intensity down to 10^5 of the circulating particles). However the maximum of the amplitude response is displaced from the middle of the band (3 GHz) to about 2 GHz (see Fig. 2).

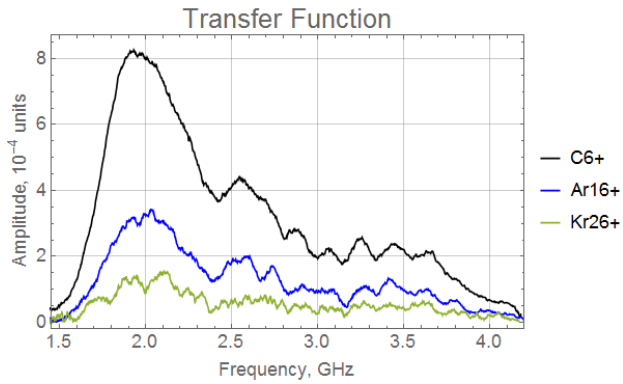

Figure 1: Plot of BTF amplitude. The intensity of carbon beam is $3 \cdot 10^8$ elem. charges, argon – $1.5 \cdot 10^7$, krypton – $2 \cdot 10^6$.

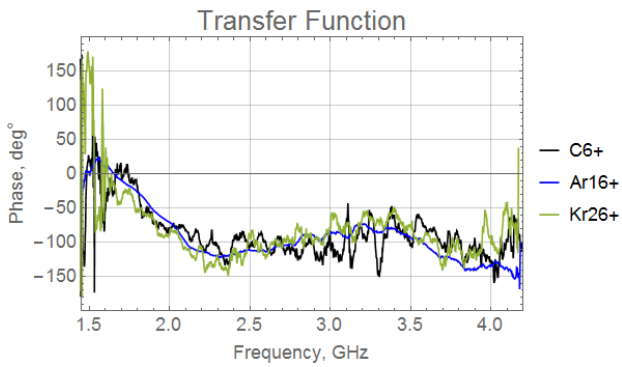

Figure 2: Plot of BTF phase for the same intensities of corresponding particles.

To avoid the mentioned disadvantages modifications of the initial design were proposed and for test of an improved structure specialized test bench has been constructed at JINR.

PICKUP AND KICKER DESIGN

The HESR type design of the pickup and kicker is based on Ring slot couplers proposed by R.Stassen (see Fig. 3). 8 loops distributed uniformly along the azimuth are used to measure or apply a signal.

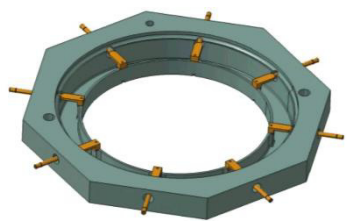

Figure 3: Ring-slot coupler design.

* valeriya2309@gmail.com

ISBN: 978-3-95450-197-7 doi:10.18429/JACoW-RUPAC2018-TUPSA25

CONSTRUCTION AND RF TEST OF THE DEBUNCHER FOR NICA LIGHT ION INJECTOR BEAM LINE

D. A. Zavadtsev, J. Z. Kalinin, L. V. Kravchuk, V. V. Paramonov, D. V. Churanov, Institute for Nuclear Research of RAS, Moscow, Russia
A. A. Zavadtsev†, Nano Invest, LLC, Moscow, Russia
A. V. Butenko, A. V. Smirnov, E. M. Syresin, Joint Institute for Nuclear Research, Dubna, Russia

Abstract

Debuncher is to be installed in the present beam line after the LU-20 linac in the light ion injector of the NICA facility. The purpose of the debuncher is to reduce by a factor of up to ten the ion energy spread in the accelerated beam before injection into the Nuclotron. Relative ion speed is 0.1. Split-ring cavity driven from solid state RF amplifier at 145.25 MHz, should provide effective RF voltage up to 200 kV at 4 kW peak RF power. The RF controller allows adjust effective RF voltage for different ions: 58 kV for Z/A=1, 121 kV for Z/A=0.5 and 190 kV for Z/A=0.3. The debuncher cavity is provided with the stepper-motor driven capacitance tuner with 2 MHz tuning range.

INTRODUCTION

The debuncher has been developed [1] as a prototype for the new light ion injector for the Nuclotron based Ion Collider fAcility and Multi Purpose Detector (NICA/MPD) [2]. The debuncher is intended to reduce the width of the energy spectrum of the accelerated ion beam after the linear accelerator LU-20 and 6 m drift space by a factor up to ten.

The debuncher consists of the cavity, the RF amplifier, the RF controller and the vacuum system.

The present report describes the construction and low power RF test of the debuncher cavity. The high power RF test will be performed some later, when the vacuum system will be ready.

MAIN PARAMETERS

After consideration and simulation of several different cavity types the split-ring has been chosen as an accelerating cavity.

The main specified parameters of the debuncher are

- operating frequency f=145.25 MHz,
- effective accelerating voltage UT=0-200 kV,
- range of the tuning Δf=±250 kHz,
- coupling coefficient of the feeding line and the cavity β=1,
- input power P_m=20-30 dBm,
- pulse length τ=100-300 μsec,
- rise/fall length τ_R=200 μsec,
- repetition rate $F\leq$0.5.

The calculated parameters of the optimized shape of the split-ring cavity are

- shunt impedance $R_{sh.eff}=(UT)^2/P$=11.68 MOhm,
- unloaded Q-factor Q_0=9516,
- effective voltage UT=200 kV,
- power loss P=3.4 kW,
- max electric field E_{max}=8.0 MV/m,
- relative max electric field E_{max}/E_k=0.62.
- multipacting not found.

CAVITY CONSTRUCTION

The debuncher cavity includes following parts: split-ring, case with flanges, input coupler, pick-up antenna, tuner and directional coupler. The design is shown in Fig. 1.

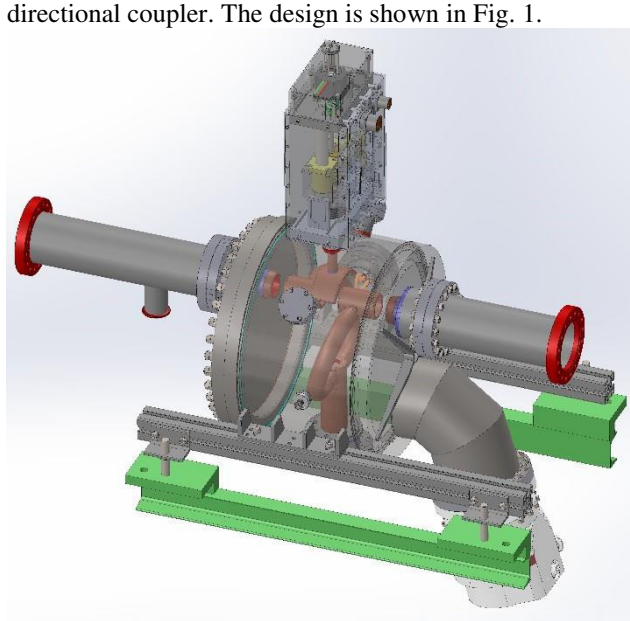

Figure 1: Debuncher cavity design.

Split-ring

The split-ring is a half wave-length vibrator with drift tubes at the ends and cylindrical rod support (Fig. 2). The split-ring is manufactured of Oxygen-free copper and brazed with 72%Ag-28%Cu brazing alloy in special fixture, guaranteed precise designed shape after brazing.

The split-ring is fixed on the special platform in the cavity case. The right position of the split-ring in the cavity is provided by following way. The split-ring was fixed on the platform with the bolt and the pins. Then the half-drift tubes were installed in the case with the bolts and the pins. Then assembled split-ring and platform were installed in the case using special fixture. This special fixture provides precise coaxial position of the split-ring drift tubes and the half-drift tubes of the case. Also the fixture provides precise position of the split-ring drift tubes along the beam line

† azavadtsev@yandex.ru

ISBN: 978-3-95450-197-7 doi:10.18429/JACoW-RUPAC2018-TUPSA26

ELECTRODYNAMICS OF WEAKLY COUPLED RF CAVITIES

V.G.Kurakin, Lebedev Physical Istitute, Moscow, Russia

Abstract

The configuration formed by a pair of coupled identical rf cavities may manifest unexpected electromagnetic properties concerning its interaction with external rf sources and charged particle beams. Coupling splits resonance frequency of such a system into two different frequencies corresponding to different modes – 0 and π. If cavity walls losses take place, that is cavities Q-values are finite for both modes, composite cavity resonance curves may overlap. This means that both cavity modes are excited effectively by external rf generator or by an intensity modulated charged particles beam traversing cavities. Thus, mixed mode excitation takes place, and resonance properties of such mixed mode as well as beam current loading effect differ qualitatively and quantitatively from those for real cavity eigen modes.

In this paper, field approach is used to describe two coupled cavities system behavior. The expression for any cavity mode amplitude allows obtaining frequency dependence of cavity mixed mode amplitude for both cavities of the system under consideration. Appropriate formulae are supplemented by plots and vector diagrams.

INTRODUCTION

Let us consider rf circuit consisting of two coupled identical rf cavities Here and in following analysis only the main TM mode of each cavity having the lowest eigen frequency is taken into account (TM_{010} in the case of pill box cavities). This unit has two resonance frequencies corresponding to the different composite cavity modes – 0 and π. In the first case, the field phases in both cavities are the same, while in other one components of rf fields are opposite in neighboring cells. The following frequency dependence for field amplitude A_i and field phase φ_i takes phase for this composite cavity excited by external rf generator

$$A_i(\omega) = \frac{a_i}{\sqrt{1+\left(2Q\frac{\omega-\omega_i}{\omega_i}\right)^2}};$$

$$\tan\varphi_i(\omega) = 2Q\frac{\omega-\omega_i}{\omega_i} \quad i=1,2 \qquad (1)$$

Q_i and ω being quality factor and frequency respectively, while a_i stands for field amplitude at resonance for each mode.

Let us assume that Q-value as well as a_i are the same for both modes and the cavity is excited at the frequency ω_r satisfying the conditions

$$\tan\varphi_i(\omega) = 2Q\frac{\omega_r-\omega_i}{\omega_i} = \pm 1 \qquad (2)$$

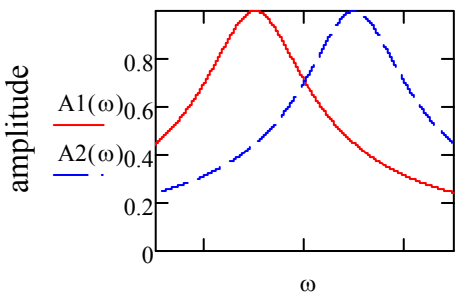

Figure 1: Zero and π modes two coupled cavities.

In this particular case resonance curves for both modes overlap as it is shown on Fig. 1. Appropriate vector diagram on complex plane is shown on Fig. 2 for both coupled cavities. One might say that united cavity operates at $\pi/2$ mode since as it is seen from diagram the appropriate phase shift between both cavities is equal to this value but is not the case. Resonance conditions take place at the frequency ω_r, but frequency mentioned is not the cavity eigen frequency.

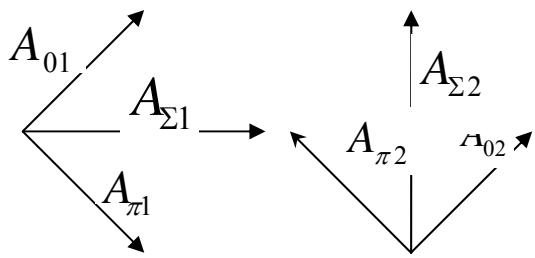

Figure 2: Vector diagrams of voltages in weakly coupled cavities.

Assuming the cavity 1 being excited by an external rf generator over feeder or by modulated charged particles beam let us consider charged beam loading properties of both cavities, beam being accelerated in the cavity 2. We consider that pill box cavities are coupled over an aperture in cylinder part of cavities walls (so called parallel coupling). Induced by accelerated beam rf voltage (or any field component) in cavity 2 is determined by first term of equation (1), while $\varphi_i = \frac{\pi}{4}+\pi$, $i=1,2$ (We consider that charged particles are accelerated on the crests of rf voltage excited in cavity 2 by external rf

ISBN: 978-3-95450-197-7 doi:10.18429/JACoW-RUPAC2018-TUPSA27

INJECTION REGION PROBING BY BEAM AT VEPP-2000 STORAGE RING

D. Shwartz†[1], I. Koop[1], E. Perevedentsev[1], Yu. Rogovsky[1], M. Timoshenko,
Budker Institute of Nuclear Physics, Novosibirsk, 630090, Russia
[1]also at Novosibirsk State University, Novosibirsk, 630090, Russia

Abstract

VEPP-2000 electron-positron collider for multiple injection and stacking uses traditional scheme with pre-kicker, kicker and pulsed thin septum magnet. It was found earlier that despite the shielding septum stray field disturbs the circulating beam and sweeps its betatron tune long after the magnet pulse. This work presents the beam-based measurements of mechanical aperture at the interaction region and discusses stray field mapping technique.

INTRODUCTION

During VEPP-2000 commissioning phase the observation was done that circulating beams are disturbed by weak leakage fields of pulsed septum magnet ME5. The typical pickup signal from the beam disturbed by septum stray field is shown in Fig. 1. The time of full-sine magnet driving pulse corresponds to 280 μs/ 82 ns = 3400 turns (shown with green zone). One can see that stray field has much longer decay time.

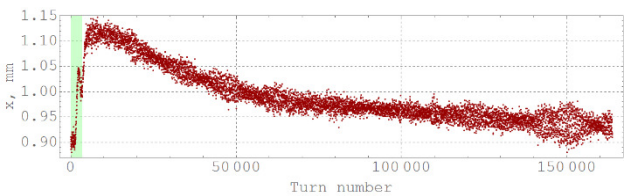

Figure 1: Beam closed orbit distortion observed by pickup.

Finally, it was proposed to make beam-based measurements of septa stray fields.

VEPP-2000 OVERVIEW

VEPP-2000 storage ring description and basic parameters can be found elsewhere [1-6]. It is a small 24 m perimeter single-ring electron-positron collider with energy range of 150-1000 MeV per beam. It operates with round beams and uses solenoids for final focusing [7].

The injection scheme [8] is dictated by very tight room. Although the additional powerful pulsed magnet (ME4/MP4, see Fig. 2) is introduced to relax the septum magnet ME5/MP5, the latter should produce field over 20 kGs for injection at collider top energy of 1 GeV.

VEPP-2000 BPM system is based on 16 CCD matrices reading beam profiles via synchrotron radiation (SR) outputs from each edge of dipoles (see blue and red dots in Fig. 2) [9].

For pulsed closed orbit (CO) distortions only the fast pickup BPMs are useful. VEPP-2000 storage ring is equipped with only 4 pickups [10]. Each pickup works either in slow CO measurement regime or in external trigger regime when electronics captures the set of turn-by-turn data.

The schematic layout of the VEPP-2000 collider is presented in Fig. 2. The points of SR output for electron and positron beams are shown with blue and red. Green marks show the arrangement of pickups.

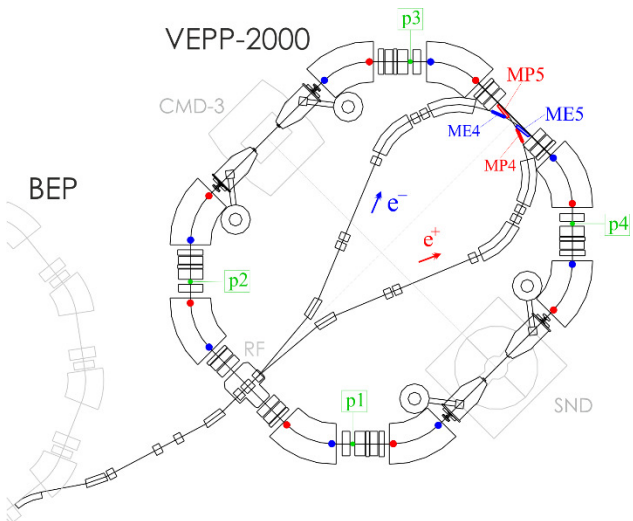

Figure 2: VEPP-2000 storage ring layout.

Septum Magnet Design

The septum magnet is an eddy-current type magnet with full-sine driving current pulse (see Fig. 3). The pulse rising time is T/4 = 70 μs, the current amplitude is up to 40 kA. The septum knife thickness is 2.5 mm and it includes 0.5 mm ferromagnetic shield introduced to suppress leakage field in circulating beam vacuum chamber.

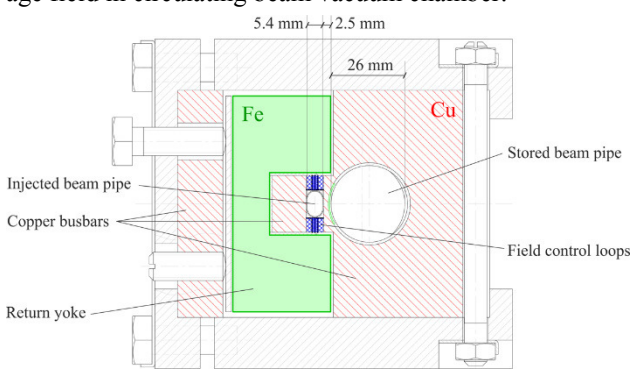

Figure 3: Septum magnet cross section. Red hatched area corresponds to copper components: bus bars and knife. With green are shown iron return yoke and shielding.

† d.b.shwartz@inp.nsk.su

ISBN: 978-3-95450-197-7 doi:10.18429/JACoW-RUPAC2018-TUPSA29

EMITTANCE MEASUREMENT ON KRION-6T ION SOURCE BY PEPPER-POT METHOD

S. Barabin†, A. Kozlov, T. Kulevoy, D. Liakin, A. Lukashin, D. Selesnev, Institute for Theoretical and Experimental Physics of NRC Kurchatov Institute, Moscow, Russia
E. D. Donets, E. E. Donets, Joint Institute for Nuclear Research, Dubna, Moscow Region, Russia

Abstract

The Krion-6T ion source is an electron string ion source (ESIS) of multicharged ions. It will be used as an ion source for the heavy ion linac at the NICA project, but has been tested on an existing injection facility - Alvarez-type linac LU-20 with new RFQ type fore-injector. The transverse emittance measurements were carried out on the initial part of channel (IPC) of the low energy beam transport (LEBT) channel, between the ion source and RFQ fore-injector by pepper-pot method. Beams of multicharged Argon and Xenon ions are observed. Measurements of the profile and emittance were performed over several energies for each type of ions. The results of the measurement are presented, and some points of emittance calculations are considered.

INTRODUCTION

The Nuclotron-based Ion Collider fAcility (NICA) project at JINR (Dubna) has a goal to set up experimental studies of both hot and dense strongly interacting baryonic matter and spin physics. The experiments will be performed in collider mode and at fixed target [1]. The first part of the project program requires heavy ion collisions generation of $^{179}Au^{79+}$ nuclei. The beams at required parameters will be delivered by two superconducting synchrotrons: the Booster and the Nuclotron. The injector for the designed Booster ring is the new heavy ion linear accelerators HILAc (Heavy Ion Linear Accelerator) for the $^{179}Au^{31+}$beams with new ESIS type ion source Krion-6T [2] (for high charge state heavy ions). The source was optimized for production of ions with charge to mass ratio of $q/A \geq 1/3$ in order to provide complex test of all its systems at operation on existing injection facility. The source was installed at High-Voltage (HV) platform of the LU-20 fore-injector. Beam of Ar^{16+} was accelerated and extracted for users.

Low Energy Beam Transport Channel

The ion source is situated on high-voltage platform (up to 150 kV). The LEBT channel [3] (Fig. 1) begins from electrode with potential U0, after which a DN 250 vacuum valve is installed. In initial part of channel (IPC) the focusing electrodes with potentials U1 and U2 are located. IPC ends the tube with potential, falling off from U3 up to 0. Two solenoids, placed after initial part, form beam at the input of RFQ.

The emittance of the KRION-6T source was estimated in [4], and for a beam pulse duration of 8 μs, the 4 rms emittance value from the source should be 0.6 mm mrad. On the other hand, for $q/A \geq 1/3$ RFQ cavity require 1.5 π mm mrad input beam emittance [1]. To test KRION-LEBT-RFQ compatibility and check KRION-LEBT channel quality, emittances before the RFQ input should be measured.

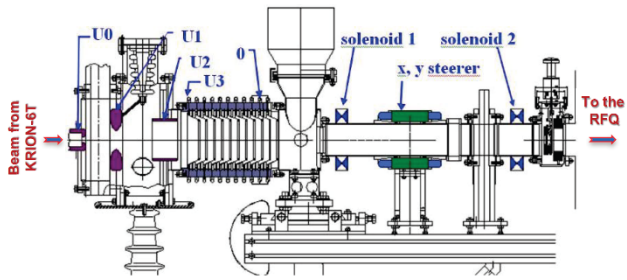

Figure 1: The LEBT Channel.

EXPERIMENTAL SETUP

The beam emittance before entering RFQ was measured at the IPC LEBT exit, since this is the only place where the emittance meter can be installed without moving both the KRION-6T source and RFQ cavity. To mounting the emittance meter, a final part of the LEBT channel was disassembled, and the emittance meter was installed after the IPC of LEBT (Fig. 2).

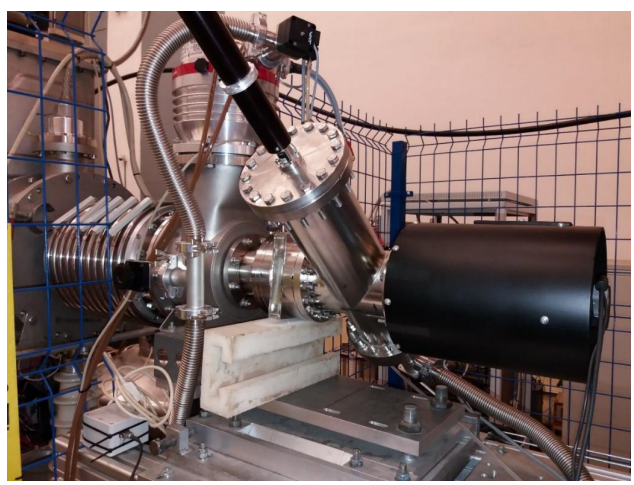

Figure 2: Emittance Meter.

† barabin@itep.ru

ISBN: 978-3-95450-197-7 doi:10.18429/JACoW-RUPAC2018-TUPSA30

THE RESEARCH OF PLASMA LENS WITH DISCHARGE INITIATION BY THE ELECTRON BEAM

A. Drozdovsky, A. Bogdanov, S. Drozdovsky, R. Gavrilin, A.Kantsyrev[1], V. Panyushkin, I. Roudskoy, S.Savin, V. Yanenko[1], NRC «Kurchatov Institute» - Institute of theoretical and experimental physics, Moscow, Russia
P. Sasorov, Keldysh Institute of Applied Mathematics, Moscow, Russia
[1] also at National Research Nuclear University MEPhI, Moscow, Russia

Abstract

Currently, works are actively underway to create laser accelerators with focusing of the obtained beams by plasma lenses. Our studies have shown that the density distribution in a plasma discharge initiated by an electron beam is more uniform than in a discharge with its usual formation. Moreover, the homogeneity region lasts 0.5 μs, including the maximum discharge current. These discharges are more suitable for focusing beams.

INTRODUCTION

Since the plasma lens with a large focusing force has small dimensions, it is used in the creation of new compact laser accelerators [1]. The focusing properties of the plasma lens are determined by the distribution of the discharge current density. The distribution is generally heterogeneous and varies to a considerable extent with time. The beam at different moments of the discharge pulse [2, 3] can be focused to a point, to a ring or something else. In the existent plasma lenses, the discharge process begins with a breakdown on the surface of the tube. In our case, when a high voltage pulse is applied to the discharge tube, an injected electron beam creates a plasma channel. That causes the breakdown throughout the tube cross section, but not only at its periphery. For this type of discharging, the estimated calculations in the MHD approximation were carried out [4]. They showed a smoother discharge and a relatively lower level of pinching and a lower plasma temperature.

EXPERIMENTAL FACILITY

The installation (Fig. 1) consists of the electron gun with magnetic lenses, the experimental chamber with the scintillators located in it and the chamber of Z-pinch formation [5]. The amplitude of beam current is 100 A, the electrons energy is 250 kV and the duration of the beam at the peak is 60 ns.

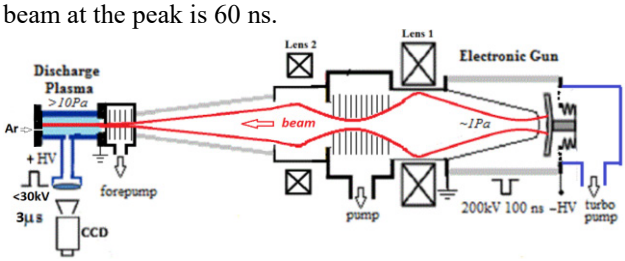

Figure 1: Installation for the research of plasma lens.

* Work supported by the Russian Foundation for Basic Research (grant 18-02-01187/18)

Studies are expected to be performed in a wide range of pressures, from 0.1 to 10 mbar. The problem is that the pressure in the electron gun should not exceed 0.02 mbar. The easiest way to solve it consists in installation of the decouple mylar film. Thereto a volume separation device with movable mylar tape was developed. To prevent a significant increase of the beam phase volume, the film thickness should be about 1 μm, which complicates the operation of the device and slows down the experiments. For studies in the field of low pressures, up to 0.5 mbar, it is possible to manage without the film due to the pressure gradient created by the used differential pumping system: packages of diaphragms are set near the crossover of electron beam. Vacuum pumping at the outlet and inlet of the electron gun is performed by turbomolecular pumps, and in front of the discharge chamber – by two forvacuum pumps. As a result, the ratio of pressure in the discharge tube and in the gun was reached up to 10.

Figure 2 shows a horizontal section of dynamic system of volume separation using a mylar tape with elements of plasma radiation detection. The plasma punches a hole in the tape in each the discharge pulse, but to the next pulse the tape is pulled to the next position. The discharge chamber is used in two versions:

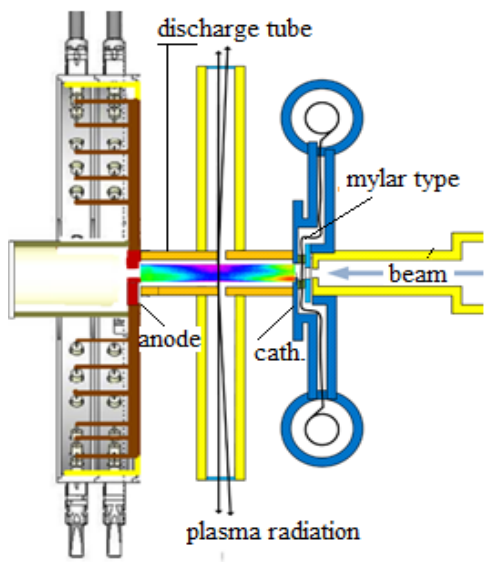

Figure 2: The horizontal slit of the discharge chamber.

- ceramic tube (Fig. 2): length is 16 cm, internal diameter is 3 cm, wall thickness is 5 mm;

ISBN: 978-3-95450-197-7 doi:10.18429/JACoW-RUPAC2018-TUPSA31

CALIBRATION OF MEASUREMENT OF ABSOLUTE DEE VOLTAGE FOR U-400M ISOCHRONOUS CYCLOTRON AT FLNR JINR

A.T. Issatov[1], R.K. Kabytayeva[1], I.A. Ivanenko, I.V. Kalagin, S.V. Mitrofanov, Yu.G. Teterev,
Flerov Laboratory of Nuclear Reactions, Joint Institute for Nuclear Research, Dubna, Russia.
[1] also at L.N.Gumilyov Eurasian National University, Astana, Kazakhstan.

Abstract

Results of measurement of absolute dee voltage of the isochronous cyclotron U-400M at FLNR JINR are presented. X-ray technique was applied for measurements. Measurements were made at the following frequencies of the resonance system: 12.8, 13.317, 15.012, 15.1 and 17.5 MHz. To accurately determine the maximum energy of X-ray spectrum, a modeling of X-ray spectrum was carried out by the software package FLUKA. An influence of the absolute dee voltage on the capture factor was estimated by the program Center.

INTRODUCTION

The direct measurement of dee voltage on cyclotrons by the method of adding additional measuring circuits to the resonant circuit is convenient for operational work, but it does not give reliable results for the all frequency range of RF-system of cyclotrons. To adjust a cyclotron to the ion acceleration mode with minimal losses in the central region (the maximum capture factor of the beam acceleration) and to ensure the centering of the accelerated beam, the amplitude of the RF voltage on dees must correspond to the calculated value. The measuring circuits must be calibrated to determine the actual dee voltage. For calibration, a technique for measuring the spectrum of bremsstrahlung X-rays can be used.

Electrons escaping from the surface of DEE and liner are accelerated in the RF field and emit a bremsstrahlung spectrum when hitting a metal surface. The endpoint energy of the spectrum is a measure of peak DEE voltage [1].

THE CONTROL OF DEE VOLTAGE BY PICK-UP ELECTRODES

Measurements were carried out on an isochronous cyclotron U-400M FLNR, JINR. The frequency range of U-400M: f_a = 11.5÷24 MHz, the calculated value of the dee voltage is Ud = 130 kV. The operational control of the dee voltage on the U-400M is made by 8 pick-up electrodes on each dee, located 4 on the top and 4 on the bottom (Fig. 1). The electrical scheme of dee voltage controlling by using pick-up electrodes is shown in Fig.2. The purpose of this work was to measure the actual voltage on dees and calibrate the voltage control circuit with pickup electrodes.

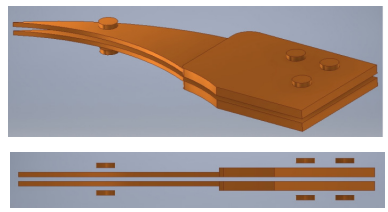

Figure 1: The sketch of dee and pick-up electrodes for measuring of dee voltage.

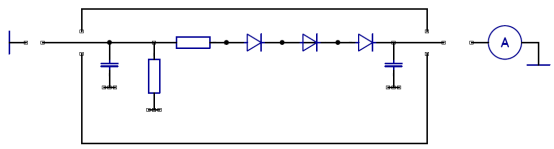

Figure 2: The electrical scheme of dee voltage controlling by using pick-up electrodes.

X-RAY SPECTRUM MEASURING

The XR-100CdTe detector was used to measure X-ray from dees of U-400M. The digital pulse processor PX5 was used to data acquisition (Fig. 3).

The XR-100CdTe is a high performance x-ray and gamma ray detector, preamplifier, and cooler system using 5 x 5 x 1 mm Cadmium Telluride (CdTe) diode detector mounted on a two-stage thermoelectric cooler. The XR-100-CdTe is capable of detecting energies from a few keV to several hundreds of keV, with an efficiency that peaks from 10 to 100 keV [2].

The PX5 includes Digital pulse shaping amplifier , Integrated multichannel analyzer and Power supplies.

The XR-100CdTe was calibrated with radioactive isotope of ^{180}Ta (Fig. 4). The energy resolution is 1.1 keV for 103.6 keV.

Figure 3: Photo of XR-100CdTe detector and PX5.

ISBN: 978-3-95450-197-7 doi:10.18429/JACoW-RUPAC2018-TUPSA32

PULSE SCANNING SYSTEM OF THE MEDICAL BEAM AND THE SYSTEM OF RECORDING THE POSITION OF THE BEAM AND THE DISTRIBUTION OF AN IRRADIATION DOSE OF THE OBJECT

I. Yudin, A. Makankin, V. Panacik, S. Tyutyunnikov, S. Vasilev, A. Vishnevskiy,
Joint Institute for Nuclear Research, Dubna, Russia
K. Laktionov, D. Yudin, N.N. Blokhin National Medical Research Center of Oncology,
Moscow, Russia

Abstract

This work describes the pulse scanning system of the medical beam and the system of recording the position of the beam and the distribution of the irradiation dose of the object. Our report deals with the construction of the carbon beam transport line for biomedical research at the NICA accelerator complex, JINR, Dubna.

We are discussed the compilation and realization of the plan of treating a tumor located at a depth up to 30 cm. The hardware realization of the beam scanning is shown.

We describe the wire chamber and read out electronics which were developed for on-line monitoring of the "intensive" extracted beams of relativistic nuclei. The system has been tested in several acceleration runs with deuteron beams with the intensity up to 10^{10} 1/s and carbon ion beams. The system allows one to make multiple measurements of the two-dimensional beam intensity distribution and beam position during the beam spill.

THE CHANNEL FOR BIOMEDICAL RESEARCH

One direction in the development of the JINR accelerator complex NICA [1] is the design of a test bench for biomedical research based on the JINR Nuclotron. While designing the test bench, the general technique for manufacturing the hadronic therapy complex is tested..

This channel is intended for the transportation of the $^{12}C^{+6}$ carbon ions with an intensity of ~2×10^{9} and an energy of 100–550 MeV/nucleon. The channel starts near the F3 focus of the primary channel [2].

Setup Restrictions

The following optical elements are used in the channel: dipole and deflecting magnets (SP-94) and a magnetic lens (ML-17).

The length of the transport channel is 12 m. The designed channel starts from a dipole magnet mounted in the primary transport channel at a distance of 5.25 m in front of the F3 focus of the primary channel. Optical elements (quadrupole lenses) are located over the channel. There is a beam trap at the end of the channel, the test bench in F_k (focus C, see [2]) is right before the trap, and the beam scanning system is before the test bench. The scanning system consists of two similar deflecting magnets rotating at an angle of 90° around the axis relative each other.

One natural restriction of beam transportation is that the diameter of the vacuum pipeline is equal to 0.25 m, which passes through all the quadrupole elements of the system. A magnet aperture of 0.3×0.13 m is a restriction at the final stage of the scanning system. The mutual position of the scan region and the system of scanning magnets is fixed.

The maximum current is limited for each quadrupole lens; this results in a limitation of the coefficient K <1.5 m^{-2} used for calculating the phase incursion on the lens at a preset energy range of 100–550 MeV/nucleon.

The beam cross section in the F3 focus of the primary transport channel is a circle 0.04 m in diameter, which makes it possible to define the initial conditions of beam propagation.

Results Obtained

For a preset aperture and the magnet arrangement, we have [2]: 1) a minimum focus diameter of 2.8 mm for an emittance of 25π mm mrad; 2) a minimum focus diameter of 5.6 mm for an emittance of 50π mm mrad. The region of target scanning is restricted by an aperture of two successive magnets in a plane normal to the beam. The magnet aperture is 0.3×0.13 m for a specific channel; this agrees with the planned scan region of 0.1×0.1 m. Solutions have been found for emittances of 25π mm mrad and 50π mm mrad based on the above specified restrictions. The beam cross section in the focus C (see [2]) is close to the minimum for the given scanning system geometry: 1) 3.0×3.0 mm for an emittance of 25π mm mrad; 2) 5.6×6.0 mm for an emittance of 50π mm mrad.

We suggest the following equipment for the additional channel: 1) magnetic lenses ML-17; 2) scanning and dipole magnets SP-94; 3) the pixel chamber and the wire chamber and readout electronics.

MONITORING CHAMBER SYSTEM

Functional test samples of detectors and electronics for them designed for monitoring the Nuclotron ion beam were constructed at LHEP department no. 5: 1) a wire chamber with front-end electronics and detection electronics installed in a data acquisition crate located far from the beam channel and 2) a pixel ionization chamber built with the use of electronics designed at JINR.

This system is designed to perform the following functions: 1) conduct multiple measurements of the ex-

ISBN: 978-3-95450-197-7 doi:10.18429/JACoW-RUPAC2018-TUPSA34

NUMERICAL MODELING AND DEVELOPMENT OF THE PROTOTYPE OF THE BRAGG PEAK POSITION DETECTOR WORKING IN REAL TIME MODE FOR HADRON THERAPY FACILITIES PROMETHEUS

A.A. Pryanichnikov, M.A. Belikhin, A.S. Simakov, P.N. Lebedev Physical Institute of the Russian Academy of Sciences, Physical Technical Center (PhTC LPI RAS), Protvino, Russia
I.I. Degtyarev, F.N. Novoskoltsev, E.V. Altukhova, Yu. V. Altukhov, R. Yu. Sinyukov, Institute for High Energy Physics of the National Research Centre "Kurchatov Institute" (NRC KI – IHEP), Protvino, Russia

Abstract

The purpose of this research was precision statistical simulation of multi-particle radiation transport using a realistic 3D model of clinical setup prototype and the systems of slot-hole collimators for on-line monitoring of Bragg-peak position at a proton therapy complex "Prometheus" to define of an available detecting accuracy and the choice of its optimum parameters. Numerical simulation of the experiments was carried out based on the RTS&T [1,2] high-precision radiation transport software package using files of evaluated nuclear data from ENDF/B VIII.0 library [5].

INTRODUCTION

Hadron therapy using the pencil beam scanning technique is the most accurate kind of remote radiation therapy. High accuracy is due to the fundamental physical property of protons and ions - to stop in the tissue at a certain depth, the so-called Bragg peak. This is why hadron therapy is used to treat critical organs, in particular the brain. However, accuracy in proton delivery is limited by uncertainty surrounding the hadron beam range. The detector considered in this paper is able to determine the hadron ranges by prompt gamma radiation [3] in real time mode. Basically this detector is planed to use with the proton therapy complex "Prometheus" [4].

NUMERICAL SIMULATION

Figure 1 illustrates the linear energy deposition and production of prompt γ-rays in inelastic nuclear interactions of primary protons in the water phantom. Definition of Bragg-peak position Zp comes down to a problem of longitudinal (along a beam direction) coordinates definition for a spatial point Zγ in which density of prompt γ-rays production decreases practically to zero:

Zp = Zγ - ΔZ, where ΔZ - calculated coefficient.

The elementary diagram for basic elements of calculated system (the water phantom, collimator system, plate of scintillation detectors) is shown on fig. 2.

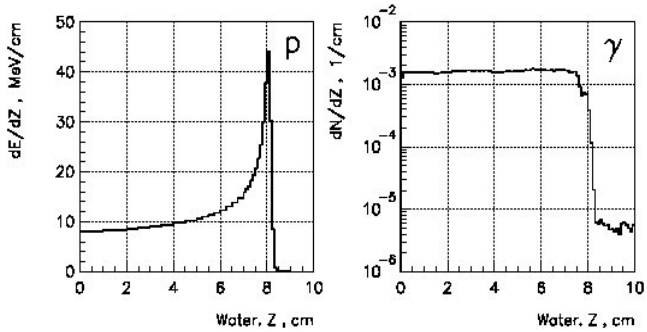

Figure 1: The deep distribution of energy deposition and the density of prompt γ-rays production from the primary proton beam with an energy of 100 MeV in the water phantom.

The prompt γ-rays flux is formed by the system of the slot-hole collimators made of heavy alloys of the residence permit brands (tungsten-nickel-iron, WNiFe). The water phantom is cylinder of 20 cm long and with a radius of 10 cm in which center the proton beam with energy of 100 MeV is dumped. The distance along a beam from a front edge of the collimator to the phantom is 19.2 cm.

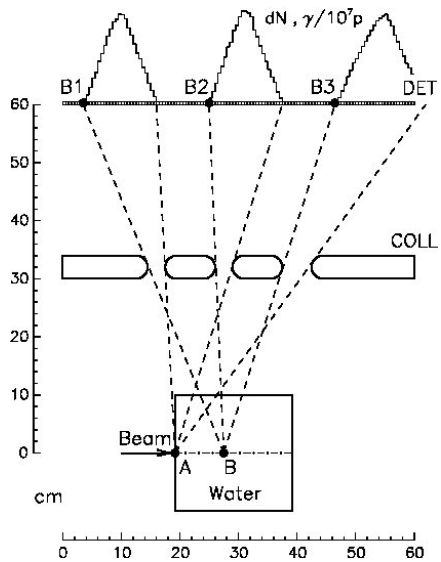

Figure 2: The design scheme of the clinical setup (side view).

ISBN: 978-3-95450-197-7 doi:10.18429/JACoW-RUPAC2018-TUPSA35

PROTON THERAPY: RIDGE FILTER IMPROVEMENTS FOR SAKE OF THE DOSE CONFORMITY

I. A. Yakovlev, S. V. Akulinichev, Yu. K. Gavrilov, INR RAS, Moscow, Russia

Abstract

The method of passive scattering in proton beam therapy has some benefits and drawbacks. One of the drawbacks is the formation of hot lesions in the proximal region beyond the borders of the target volume. It leads to the rise of the integral dose of irradiation and lowers the irradiation conformity.

To date, a solution to this problem has been proposed by some other authors in the form of a multi-layer energy filter. Such a filter has a different amount of material and provides different energy modulation at different impact parameters. Nevertheless, the design of that device leads to an increase in the dose within the planned target volume, which may be critical in some cases. We propose a different design of the depth dose formation device – a composite ridge filter. Our solution allows changing the Bragg peak modulation width by eliminating the selected elements of the energy modulating ridge, while further changing the radiation intensity in the given target region due to the beam absorption. In our previous study, we have performed a Monte-Carlo simulation and obtained a spherical contour of 95% isodoses. Now we have developed a method for more accurate selection of device geometry, thereby reducing the controlled level of isodoses to 90% and lower. We continue our calculations to improve the conformity of irradiation and prepare experimental tests with proton beams of INR linac.

DOSE FORMATION METHODS OF PROTON THERAPY

Proton therapy is a progressive method of radiotherapy. The main benefit of this technology is a form of its depth dose distribution involves the increase of energy deposition with depth and a sharp fall-off after a specific region called Bragg peak [1]. The depth of the peak depends on the initial beam energy so it allows irradiating a deep-seated target while sparing surrounding healthy tissues.

In proton therapy, there are two essential methods of dose formation. The first way is to deflect a narrow beam by the magnetic fields to irradiate the target point by point. This technique is called a « pencil beam scanning method » and is known as the most accurate way to irradiate the target conformally. However, this method does not allow to irradiate the whole target simultaneously. It may lead to the heterogeneity of dose distribution and a local overdose of several parts caused by uncontrolled tissue movement. The second technology involves the installation of various objects on the beamline. These tools wide the beam by scattering and spread out the Bragg peak (SOBP) by changing the energy spectrum. This method is called « passive scattering », one of a possible formation system is shown in Fig. 1. This method is cheaper in comparison with the first one and allows to irradiate the whole area with a single field. Nevertheless, it struggles from the stray neutron radiation caused by the interaction with the beam delivery system. Also the «passive scattering» method leads to the emergence of overdosed region beyond the borders of the target volume (shown as red lines in Fig. 1). These problems reduce the quality of proton therapy treatment with passive scattering.

POSSIBLE SOLUTION

One of the possible solutions to rule the proximal edge of dose distribution is a construction of Multi-layer ridge filter [2]. The idea is to control the width of SOBP in local regions by increasing the number of layers of thin ridge filters as shown in Fig. 2. This method copes with the given goal of changing the radiation field form but leads to an increase in the dose in the narrowing regions of SOBP (Fig. 2). Thus, to decrease unnecessary influence the lateral beam profile has to be changed.

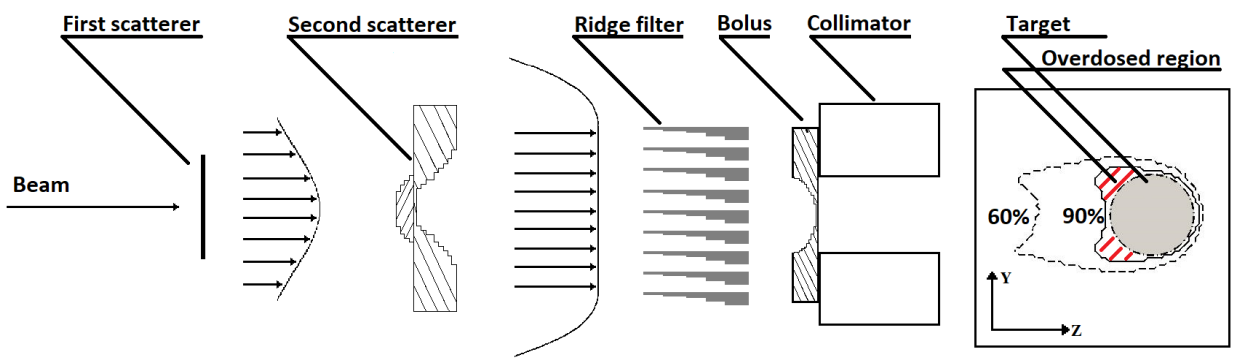

Figure 1: Passive scattering dose delivery system.

ISBN: 978-3-95450-197-7 doi:10.18429/JACoW-RUPAC2018-TUPSA38

NEUTRON MONITORS FOR HIGH ENERGY ACCELERATORS

I.L. Azhgirey, I.S. Bayshev, I.A. Kurochkin, V.A. Pikalov, O.V. Sumaneev and V.S. Lukanin
NRC "Kurchatov Institute" - Institute for High Energy Physics, 142281 Protvino, Russia

Abstract

Thermal neutron counters inside moderating shell are used widely at high energy accelerators. Response of these detectors to neutrons of different energy depends on material, size and shape of moderator. Radiators and absorbers can also modify this response significantly. The main application of counters in moderators is neutron dosimetry. Some dedicated sets of these detectors (Bonner spheres) are even used sometimes to estimate neutron spectra. Monitoring of fast neutrons at modern accelerator and experimental facilities is very important to keep radiation damage of electronic components under control.

One more step towards fast neutron measurements with thermal neutron counters in moderators is reported here. A set of neutron transport simulations is done to optimize moderator/radiator/absorber assemblies for higher sensitivity to neutrons with energies above 100 keV along with much lower sensitivity at lower energies. The resulting pair of the main and complementary monitors is designed.

INTRODUCTION

Early neutron detectors based on thermal neutron counters surrounded by moderators and radiators can be found in physics of cosmic rays [1]. Further a lot of attention was paid to the energy response of these detectors and therefore to the moderator shape and size. The famous neutron spectrometer [2] consisted of a set of spherical moderators with different diameters providing a set of different energy response functions. Adjusting the energy response of a single detector to the energy dependence of the dose equivalent let to use this detector as a neutron dosemeter [3]. Since that time many tens of developments and improvements of the Bonner spectrometer and the Andersson-Braun dosemeter have been published. This type of neutron dosemeters is used at high energy accelerators worldwide.

Enclosures of modern accelerator facilities contain a very large amount of complicated and expensive electronic equipment. Radiation monitoring is necessary there to evaluate performance degradation of electronics under irradiation [4].

Neutron component of radiation fields in these enclosures dominates in most cases. Neutron energy spectra stretch from the thermal region to high energies of a few GeV. Fast neutrons with energy above 100 keV are known to be responsible for the radiation damage of electronic components. Measurement of fast neutron fluences can add significantly to the existing radiation monitoring. Neutron counters in moderators with the specially adjusted energy response functions can be used for this goal.

Such a monitor must not be too large (say the overall dimension less than 30 cm) or too heavy (say the weight below 20 kg). Along with that its response curve must be significantly lower at energies below 100 keV than at higher energies. Figure 1 from [5] gives a detailed view of the response functions in a wide range of moderator sizes. The response curves of the type we need are observed for the 8 inch and larger spheres. In other words the moderator thickness must be greater than 7 cm.

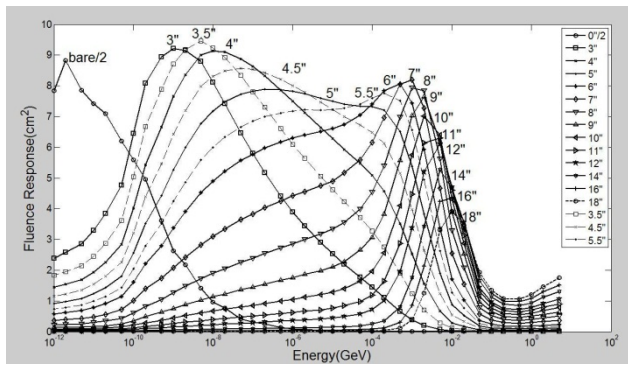

Figure 1: Borrowed from [5]: Energy response functions of Bonner spheres with different diameters. The bare counter diameter is equal to 2 inches.

DETECTOR CONFIGURATION

The thermal neutron counter SNM-14 combines a relatively high sensitivity with reasonable dimensions. Mechanically it is a 154 mm high thin-walled tube with the 18.5 mm outer diameter. These dimensions suggest the shape of the detector as an assembly of cylindrical layers of moderator, absorber and radiator around the counter.

A set of preliminary simulations of the response function was done varying the layers thickness. The materials of the moderator, radiator and absorber were polypropylene (CH_2), lead (Pb) and cadmium (Cd) respectively. The well-known code systems MARS [6] and FLUKA [7] were used for the simulations. More or less acceptable configuration of the detector has been found but the sensitivity to low energy neutrons remained non-negligible.

Most likely a single detector of the reasonable size and weight cannot solve the problem of the low energy tail considerably. A pair of detectors can be more efficient provided the response curve of the second (complementary) detector will be close to the response curve of the main detector below 100 keV and much lower at higher energies. Another set of simulations allowed finding the

ISBN: 978-3-95450-197-7 doi:10.18429/JACoW-RUPAC2018-TUPSA39

THE PROTON RADIOGRAPHY FACILITY AT THE U-70 SYNCHROTRON

A. V. Maximov, O. V. Zyatkov, N. E. Tyurin, Y. S. Fedotov,
NRC "Kurchatov institute" – IHEP, 142281 Protvino, Russia,
A. L. Mikhailov, K. L. Mikhailyukov, O. V. Oreshkov, I. A. Tkachenko, M. V. Tatsenko,
RFNC–VNIIEF, 607190 Sarov, Russia

Abstract

The results on operation and development of proton radiography facility (PRGC-100) at the U-70 synchrotron are presented. PRGC-100 is designed to look inside the objects with mass thickness from 10^{-1} g/cm^2 up to 450 g/cm^2 and the field-of-view up to 220 mm at proton beam energy 50÷70 GeV. The measured spatial resolution is 90 μm for thin objects and less than 500 μm for the objects of 350 g/cm^2 thickness. The development of the beam extraction systems for PRGC-100 as well as the first results on testing the proton microscope mode is presented.

FACILITY DESCRIPTION

The proton radiography facility PRGC-100 was created with partial use of the existing infrastructure - injection tunnel (IT) of accelerator storage complex UNK [1].

The extraction of the accelerated proton beam in IT is performed by the fast extraction system which includes the kicker magnet KM-16 and the two septum magnets EM-62 and EM-64 [2]. The single-turn extraction mode provides up to 29 proton bunches with intervals between bunches 165 ns and extraction duration up to 5 μs. The bunch intensity is (2÷4) ×10^{11} proton. The width of beam relative momentum distribution on the basis of ±2σ is ±0.8×10^{-3} and corresponds the bunch duration about 20 ns.

The magnetic structure of the PRGC-100 includes a beam transport line from the proton synchrotron U-70 and the optics of PRGC-100 itself, consisting of three quartets of quadrupole lenses. Each quartet is constructed of four pairs of quadrupole lenses 30Q180-6,7 (Fig. 1) [3] and provides image transmission coefficient –1.

The facility has rich diagnostic equipment for beam monitoring consisting of 12 profile detectors and 7 television stations.

At the beginning of the first quartet, a subsystem for initial beam image registration is established. The objects are installed before the second quartet. A proton beam passing through an object is formed by the second and third quartets for registration and obtaining the image of the object under study.

The length of each quartet is 65.2 m.

Figure 1: Section of PRGC-100 with quadrupole lenses and radiation protection blocks.

The beam collimators are located in the middle of the second and third quartets (the focus points). The quartet structure of PRGC-100 is schematically shown in Fig. 2.

PRACTICAL RESULTS

The facility was commissioned in 2014. At present the capabilities to provide the required beam parameters are significantly expanded.

The facility allows to study inside of various static and dynamic objects with thickness from 10^{-1} g/cm^2 to 450 g/cm^2 with field of view up to 220 mm at proton beam energy 50-70 GeV [4].

The magnetic system of the beam transport line allows controlling the diameter of the proton beam from 30 mm to 240 mm depending on the size of the object under study and the required proton flux density.

There were created wide-aperture multi-frame image recording systems and quality monitoring of each proton bunch [4].

The total exposure time for dynamic radiography was increased in several times due to the use of "portional" fast resonant extraction (FRE) with pauses between the extracted bunches. In this mode, the beam is ejected by a kicker magnet KM-16 beyond the separatrix of the betatron motion on the third order resonance 3×Qr=29

ISBN: 978-3-95450-197-7 doi:10.18429/JACoW-RUPAC2018-TUPSA41

EFFECT OF TIN ION IMPLANTATION ON THE PROPERTIES OF AMORPHOUS $Ge_2Sb_2Te_5$ THIN FILMS

D.N. Seleznev, A.L. Sitnikov, A.V. Kozlov, P.A. Fedin, T.V. Kulevoy,
NRC "Kurchatov Institute" - ITEP, Moscow, Russia
S.A. Kozyukhin, Kurnakov Institute of General and Inorganic Chemistry of the RAS, Moscow, Russia
P.I. Lazarenko, A.A. Sherchenkov, A.O. Yakubov, D.A. Dronova, National Research University of Electronic Technology, Zelenograd, Moscow, Russia

Abstract

Alloys along the quasi-binary line between Sb_2Te_3 and GeTe with compositions $(GeTe)_m(Sb_2Te_3)_n$, in particular $Ge_2Sb_2Te_5$, have been intensely studied and are used in the state-of-the-art PCM devices. However, properties of this thin film materials are not optimal and should be improved. In this work, we investigated the effect of tin ion implantation on the properties of amorphous $Ge_2Sb_2Te_5$ thin films. The Sn ion implantation was done on Multipurpose Test Bench (MTB) [1] at NRC "Kurchatov Institute"-ITEP. The MTB consists of MEVVA type ion source, electrostatic focusing system, the system of current and beam profile measurements. The charge spectrum of the Sn beam was measured by the time-of-flight method, the beam profile as well as beam current were also measured. The beam`s accelerating voltage was calculated by SRIM code in order to implant ions on the required film`s depth. Tin ions were implanted into GST films at 40 kV accelerating voltage. Effect of Sn ion implantation (1 at. %) on the electrical properties of magnetron GST thin films was investigated.

INTRODUCTION

Alloys along the quasi-binary line between Sb_2Te_3 and GeTe with compositions $(GeTe)_m(Sb_2Te_3)_n$ (GST) have been intensely studied and are used in the state-of-the-art PCM devices. Doping is the effective method for purposeful change of the properties of GST [2, 3]. In particular, the introduction of tin dopant has a significant impact on the electrical and thermal properties of the bulk Ge-Sb-Te and thin films on their basis [4]. Ion implantation is a doping method, which is very often used for changing the electrical properties of thin films. By choosing appropriate implantation parameters and film thickness uniform Sn distribution along the film thickness and homogeneous properties can be provided. However, implantation process of Sn ion in the GST thin films is not investigated yet. So, the aim of this work is to study the effect of Sn ion implantation (1 at. %) on the electrical properties of magnetron GST thin films.

SAMPLES PREPARING

Thin films of the GST composition were prepared by DC magnetron sputtering at room temperature. The pressure of Ar during the process was $5 \cdot 10^{-3}$ Torr, the sputtering power was 100 W. The amorphous thin films were deposited on the silicon wafers and substrates of thermally oxidized silicon with planar electrodes (TiN/W/TiN). The thicknesses of thin films were controlled by the atomic force microscopy (NT-MDT Solver Pro) and were ~40 nm.

TOF DIAGNOSTICS OF Sn ION BEAM

In order to avoid the surface effects the Sn ions were implanted on the middle of the film thickness. The implantation depth was determined by acceleration voltage as well as by charge state beam. The Time-of-Flight method was used to determine the beam charge state of MEVVA ion source with Sn cathode [5]. The 5 peaks were observed at the output of TOF channel: T1 – 48 μs, T2 – 33 μs, T3 – 22.5 μs, T4 – 17 μs, T5 – 14 μs. The peaks T1 and T2 corresponds to Sn^+ and Sn^{2+}, while T3-T5 to residual gas and hydrocarbons. The total amount of Sn ions consists of 43% Sn^+ ions and 57% Sn^{2+}.

THE ACCELERATING VOLTAGE OF Sn ION BEAM

In order to make Sn ions Bragg peak position at the GST225 film required depth the accelerating voltage was determined by SRIM code. The simulation has shown that Sn ions Bragg peak is located at 20-25 nm depth at 40 kV accelerating voltage (see Fig. 1).

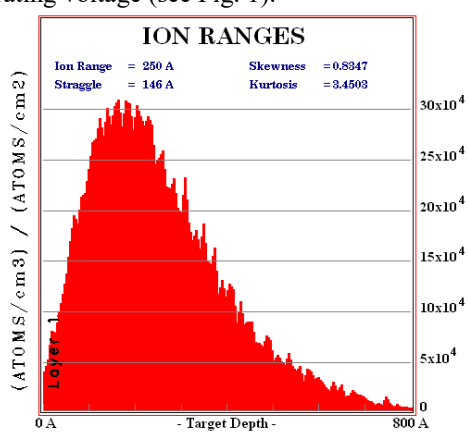

Figure 1: The Bragg peak of Sn ions (Sn^+ and Sn^{2+}) in the GST225 film at 40 kV accelerating voltage.

ISBN: 978-3-95450-197-7 doi:10.18429/JACoW-RUPAC2018-TUPSA43

CYCLOTRON SYSTEM FOR THAILAND INSTITUTE OF NUCLEAR TECHNOLOGY

Yu.K. Osina, Z.A. Andreeva, A.V. Galchuck, Yu.N. Gavrish, S.V. Grigorenko, V.I. Grigoriev, M.L. Klopenkov, R.M. Klopenkov, L.E. Korolev, K.A. Kravchuck, A.N. Kuzhlev, I.I. Mezhov, A.G. Miroshnichenko, V.G. Mudrolyubov, G.V. Muraviov, V.I. Ponomarenko, K.E. Smirnov, S.S. Tsygankov, M.V. Usanova, A.V. Vanin, O.L. Veresov, Yu.V. Zuev
JSC «NIIEFA», 196641, St. Petersburg, Russia

Abstract

In 2020, the CC-30/15 cyclotron complex is planned to be commissioned at the Institute for Nuclear Technologyes of the Kingdom of Thailand. The main task of the project is the development of nuclear medicine in Thailand.

The complex is created on the basis of the cyclotron of negative hydrogen and deuterium ions with finite energy in the ranges 15-30/9-15 MeV and the current of the extracted beam of 200/50 μA, respectively. A beam transport system ensures the formation and delivery of beams to five ports. Two of them are target devices designed for large-scale production of radionuclides of zirconium-89, copper-64, thallium-201 and gallium-67. A pneumatic system for the installation, discharge and delivery of targets to radiochemical laboratories is provided. The remaining ports will be used in the program of scientific research in the field of neutron physics and radiation technologies.

The main equipment of the complex was developed; production and factory testing should be completed in the third quarter of 2019.

In September 2017, a project was launched to create a modern nuclear physical center at the Institute of Nuclear Technology of the Kingdom of Thailand (TINT). The center is intended for large-scale production of radionuclides and the implementation of a program of scientific research in the field of neutron physics and radiation technologies. The Center is based on the cyclotron system CC-30/15 of JSC "NIIEFA". The system includes the CC-30/15 cyclotron, the branched beam transport system, the target complex, the system for transporting irradiated targets to protective boxes of radiochemical laboratories, the sample irradiation system and support systems. The main parameters and characteristics of the cyclotron system are presented in Table 1.

Table 1: The Main Parameters and Characteristics of the Cyclotron System

Parameter name, characteristics	**Parameter value**
Type of ions: • accelerated • issued	 H- / D- H+ / D+
Accelerated ion energy, MeV • protons • deuterons Energy regulation in steps of not more than 1 MeV	 15...30 9…15
Number of beam output devices for simultaneous operation	2
Total current of the output beam, μA • protons • deuterons Current control from 0 to maximum value The stability of the current is not worse than ± 5% when operating in continuous mode at the maximum energy for 12 hours	 200 50
Power consumption, no more, kW • in standby mode • in the operating mode	 30 200
Number of beam lines	3
Number of ports for setting targets or other end devices, not less than	5
Target complex with solid targets	availability
Automated system for transporting irradiated targets to protective boxes	availability
Sample irradiation system	availability

ISBN: 978-3-95450-197-7 doi:10.18429/JACoW-RUPAC2018-TUPSA45

PROVISION OF DOSE HOMOGENEITY IN EXPERIMENTS FOR DEVELOPING METHODS OF FOOD IRRADIATION

P. A. Bystrov, IPCE RAS, 199071 Moscow, Russia
V. P. Filippovich, [142703] Vidnoe, Moscow region, Russia
A. V. Prokopenko, MEPhI, 115409 Moscow, Russia
N. E. Rozanov, S. N. Puchkov, MRTI RAS, 117519 Moscow, Russia

Abstract

At present, interest is growing in the use of an electron beam irradiation for preserving food. Presented the study of using electron beam irradiation on food products, having a density, comparable to the density of water. The study uses computer code "BEAM SCANNING" for calculation the dose distribution in products. One-sided and two-sided irradiation of objects under different ways of laying is considered.

INTRODUCTION

At present, there is a significant increase in interest in technology of radiation food processing in Russia. This is due to beginning of the normative documents development in 2014 for use of radiation technologies in agriculture and food industry [1]. In April 2015, a fundamental document was published - State Standard ISO 14470-2014 [2].

The development of irradiation technologies led to increase in number of irradiation centers, based on electron beam accelerators. In comparison with both conventional canning methods and ɣ-irradiation, the electron beam irradiation technology is most effective and safe. It allows replacing or dramatically reducing the use of food preservatives, fumigants and other chemicals [1]. When irradiating products with an electron beam, it is easy to control the average absorbed dose; the products are disinfected in a sealed package, which is the advantage of the method.

Using an electron beam to irradiate products, one should be very careful, since food products have strict limitations on the minimum and maximum allowable dose. Inhomogeneous irradiation can lead to low efficiency of the process if some product areas are less irradiated, or deterioration of the quality in case of local overexposure. This entails the most stringent requirements for the development and verification of irradiation techniques.

This technology has long been applied to the disinfection of dry products having a low density. When processing objects, having a density comparable to that of water, an inhomogeneous radiation dose profile may arise due to the insufficient penetrating power of the electron beam. This problem makes impossible irradiating of large nomenclature of products. In experimental work this problem can lead to errors when performing studies on irradiation.

Another problem with electron beam technology is the possible reduction of radiation dose in separately irradiated small objects which have sizes, comparable to depth of beam penetration. In this case the effectiveness of irradiation can be dramatically decreased.

When irradiating objects, which have characteristic sizes of less than 5 centimeters, density greater than that of water with electron beam of electron energy less than 10 MeV, one can't be sure of the uniformity of the dose distribution. The dose profile in this case can hardly be predicted.

In order to find the distribution profile of doses in the objects of the study, the irradiation process is simulated using a specially modified computer code "BEAM SCANNING" [3-7]. Special modification made possible the calculation of dose profiles in the objects having more complicated shapes rather than a box.

MATERIALS AND METHODS

This installation "Raduga", presented on Fig. 1 is based on a linear accelerator. The characteristic parameters of the accelerated beam: average energy is about 5 MeV, pulse beam current is up to 250 mA, pulse duration is 4-6 μs, repetition frequency is 300 Hz, average beam power is 1.5-1.7 kW. The installation is provided with local radiation shielding and automated conveyer.

Figure 1: Radiation installation "Raduga".

ISBN: 978-3-95450-197-7 doi:10.18429/JACoW-RUPAC2018-TUPSA46

EFFECT OF OZONE IN EXPERIMENTS ON THE DEVELOPMENT OF FOOD IRRADIATION METHODS

P. A. Bystrov, Yu. S. Pavlov, O. V. Souvorova, IPCE RAS, 199071 Moscow, Russia
V. P. Filippovich, N. V. Ilyhina, RRICT, 142703 Vidnoe, Moscow region, Russia

Abstract

Presented are the preliminary experimental results to evaluate the role of ozone in process of radiation sterilization comparing to ionizing irradiation. Computer modeling for the problem is provided.

INTRODUCTION

During sterilization by electron beam, ozone is formed in the air, which increases the efficiency of microorganism suppression. When studying the processes of radiation sterilization, it is necessary to estimate the contribution of the chemical factor of ozone formation. To make an accurate studies, one should evaluate the degree of influence of the ozone formation factor in air radiolysis.

The experiments on the irradiation of several cultures of microorganisms were performed, which make possible to find out the effect of ozone factor. Experiments were performed with different microorganisms.

To ease the calculation, the computer program "BEAM SCANNING" was used to model the experiments and to evaluate the factor of ozone creation.

MATERIALS AND METHODS

Irradiation center at IPCE RAS is based on radiation-technological installation with electron accelerator UELV-10-10-S-70 which is mounted in radiation-safe bunker and designed to perform irradiation by electron beam with electron energy up to 8 MeV, beam power up to 10 kW.

Figure 1: Radiation installation at IPCE RAS centre.

Radiation-technological installation consists of accelerator with beam scanning system attached to it and circular conveyer, which moves objects before the output window of accelerator, one meter far from output window. The conveyer with boxes and accelerator with beam scanning system of this installation are presented on Fig. 1.

Installation is used in different research, technological and commercial applications. Nominally, installation provides irradiation on conveyer at a dose rate near 3 kGy per second. This installation also makes possible to use a 5-6 MeV beam with low dose rate near 300 Gy/min. [1]. Installation is used for scientific research and applied studies of radiation-chemical transformations of materials and development of radiation technologies. One of the areas of research being held is the study of food irradiation.

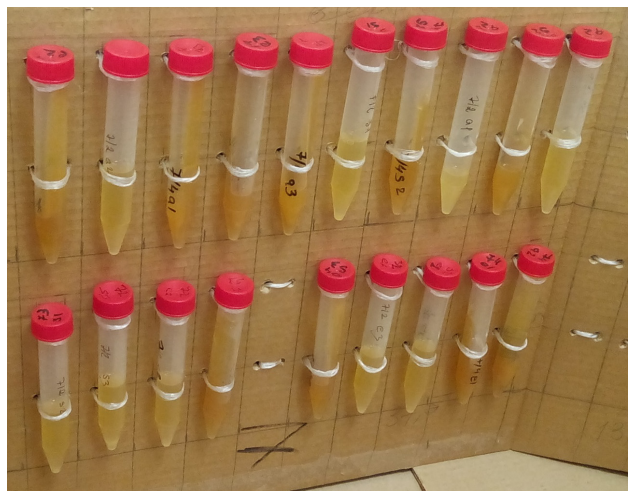

Figure 2: Test tubes with solutions.

In experiments carried out, irradiated closed test-tubes with model solutions of microorganisms, which have diameter of 15 mm and a height of 140 mm, as shown on Fig. 2. The study used Gram-negative E. coli bacterium with dimensions of 1.1-1.5 × 2.0-6.0 μm and gamma-positive coca Staphylococcus aureus, having spherical form with a diameter of 0.5-1.5 microns. The study used daily cultures of these microorganisms dissolved in meat-peptone broth. Single irradiation of microorganisms was carried out by electron beam with doses 3, 5, 7, 10 kGy in two positions of processed test-tubes: horizontal and vertical. Tubes were attached to the conveyor wall using copper wire thickness of 1 mm.

Three experiments were used in each case. Microbiological examination of irradiated and control samples were performed on the day after irradiation. Control ampoules were stored under the same conditions as irradiat-

ISBN: 978-3-95450-197-7 doi:10.18429/JACoW-RUPAC2018-TUPSA47

REGULARITIES OF INHIBITION OF CONDITIONALLY PATHOGENIC MICROFLORA UNDER THE INFLUENCE OF ACCELERATED ELECTRON BEAMS

V P Filippovich, A Y Kolokolova, N V Iluhina†, Russian Research Institute of Canning Technology, 142703, Vidnoye, Russia
A. V. Prokopenko, National Research Nuclear University - Moscow Engineering Physics Institute, 115409, Moscow, Russia
A. V. Gordeev, State research center Burnasyan federal medical biophysical center, 123098, Moscow, Russia
Y S Pavlov, A.N. Frumkin Institute of Physical Chemistry and Electrochemistry of Russian Academy of Sciences, 119071, Moscow, Russia

Abstract

Article is devoted to the study of the irradiation efficiency of model systems containing conditionally pathogenic microorganism by electron beams with energy of 7 and 10 MeV. The research on the effectiveness of inhibition of the initial degree of inoculation of the microorganisms E. coli and Salmonella were carried out. Irradiation doses up to 10 kGy performed at radiation-technological installations the A.N. Frumkin Institute of Physical Chemistry and Electrochemistry RAS and State Research Center Burnasyan Federal Medical Biophysical Center. The results of the effective inhibition of initial contamination degree for the two samples, which model liquid and solid nutrient media, were obtained. It is shown that it is necessary to take into account not only the effectiveness of microorganism inhibition on specific products, but also the installation efficiency for a particular sample.

INTRODUCTION

According to the international Commission of FAO (Food and Agriculture Organization) UN world food losses at all stages of production reach 30%. Especially significant losses of fruits and vegetables. Recently, Russia has revived its interest in radiation technologies as a basis for the development of an innovative economy. Radiation treatment of food products leads to delayed germination, disinsection (destruction of insects), slowing down the maturation process, lengthening the shelf life and suppression of pathogenic microorganisms.

The use of radiation technologies in agriculture and food industry is a global trend [1]. According to IAEA statistics, there are more than 1,500 electron accelerators in the world, mainly used for food processing, medical device sterilization and radiation chemistry. The largest number of accelerators installed in the United States (more than 500 units) and Japan (more than 300). Also, accelerators are numerically predominant in the BRICS countries [2].

The advantages of radiation technologies are food processing, with a high degree of efficiency and productivity, accuracy of radiation dosing, the possibility of irradiation of packaged products, the lack of high heating of the product, low operating costs and compliance with accepted environmental standards [3, 4]. The low sterilization temperature allows the sterilization of thermolabile objects.

The intensity of irradiation of food products can vary from a number of characteristics:

- product contamination before and after irradiation. (Knowing the value of the initial contamination of the product, you can calculate the dose, after irradiation of which the number of living cells will reach the normalized level.)
- spectrum of microorganisms [5]. (Resistance to ionizing radiation varies among microorganisms. The most sensitive to irradiation among bacteria are gram-negative, especially *Ps. aeruginosa*, *E. coli*. Somewhat more resistant gram-positive bacteria. Weak resistance to radiation differ psychrophilic bacteria. Very resistant to ionizing radiation were some micrococci and spores of the genera *Bacillus* and *Clostridium*.
- physical and chemical properties of the product (aggregate state). [6,7].

Thus, the study of the effect of ionizing radiation on food products and agricultural raw materials should be approached by a comprehensive solution of problems based on the characteristics of the studied products.

Despite numerous studies in this area, existing teaching methods need to be optimized to allow exposure to all types of fruit and vegetable products. The main problem is the possibility of minimizing the impact of ionizing radiation. The solution to this problem is possible in two ways: by reducing the intensity of irradiation or by using installations with different electron beam characteristics.

In this paper, a comparative analysis of the irradiation efficiency of the same object on two radiation installations with different beam characteristics was carried out. The used electronic accelerators have differences in beam energy, beam power, scattered beam formation system and transportation of the processed object. Various parameters of the units should be taken into account when irradiating food products with electron beams, especially at low doses from 1 to 5 kGy. Studies were carried out using model systems that allow to standardize irradiation conditions to obtain reproducible results. The efficiency of inhibition of the microorganism coli and Salmonella

ISBN: 978-3-95450-197-7 doi:10.18429/JACoW-RUPAC2018-TUPSA48

THE STUDY OF ELECTRON BEAM IRRADIATION EFFECT ON MULTILAYER POLYMER MATERIALS

V. Tarasyuk†, Russian Research Institute of Canning Technology, 142703, Vidnoye, Russia
A. V. Prokopenko, National Research Nuclear University - Moscow Engineering Physics Institute, 115409, Moscow, Russia
N. R. Kil'deeva, N. A. Sazhnev, A.N.Kosygin Russian State University, 117997, Moscow, Russia
A. V. Gordeev, State research center Burnasyan federal medical biophysical center, 123098, Moscow, Russia
N. E. Strokova, M.V. Lomonosov Moscow State University (MSU), 119991, Moscow, Russia

Abstract

The work is devoted to the investigation of a multilayer polyamide/polyethylene film material 80 μm thick after its processing with an electron beam with an energy of 10 MeV and doses of 3 to 18 kGy in the Burnasyan Federal Medical Biophysical Center of the federal medical biological agency. Infrared spectroscopy was used to study the structure of a polymer material before and after irradiation of each layer. Atomic emission microscope was used to study the surface of a film. Evolution of the film surface characteristics can lead to a change in the barrier properties of film material used for packaging in the food industry. Investigation of polymer film treated with fast electrons showed stable results on dispersion at doses up to 18 kGy.

INTRODUCTION

Radiation technologies of food processing and food packing is accurate radiation dosing of radiation, the possibility of exposure of packaged products, a high degree of efficiency and performance, and low operating costs [1]. High-energy electrons beam treatment reduces level of pathogenic bacteria and viruses. The applied dose is relatively different from 0.05 – 0.15 kGy to inhibit sprouting of potatoes and onions to 2.0 – 10 kGy to improve technological properties of food products and to 30 - 50 kGy for sterilizing meat products.

In the industry to maintain sterilization effects and increase the shelf life of foods often radiation sterilization is carried out in the package. Basically multilayer film materials of different composition are used. By combining multiple layers of different polymers, the manufacturer is able to create film materials with desired properties for each type of agricultural products, taking into account the respiratory processes.

During radiation sterilization by electron beam in polymeric materials can simultaneously undergo the process of crosslinking and degradation, followed by oxidation process and the appearance of such functional groups as: –C=O, –OH, –O–O–H, –C–O–O–C– [2-5].

The structure of the polymer material surface under the action of irradiation changes and forms a variety of reliefs in the form of ripples, irregularities of granular type and through holes. This phenomenon is used for the manufacture of polymeric microporous membranes [6-9].

The aim of this work is to identify the dependence of surface structure of the polymer material with the change of functional groups in the IR spectra before and after fast electrons irradiation.

RESEARCH METHODS

When storing fresh agricultural produce best results showed the multilayer film materials composition of polyamide/polyethylene in a percentage ratio of 20:80 (PA/PE) [10-11].

PA/PE samples were irradiated by 10 MeV electrons at accelerator UELR-10-10-40 at doses from 3 to 18 kGy. Approximate (desirable) doses of irradiation of samples and real doses of irradiation of packs with samples according to indications of detectors in control points are presented in Table 1. The results are shown in Table 1.

Table 1: Absorbed Doses of Fast Electrons

Established dose, kGy	**Irradiation on installations**	
	UELR-10-10-40	
	Beam output dose, kGy	***D*, absorbed dose, kGy**
3	3.0 ± 0.3	3.2 ± 0.3
6	5.8 ± 0.5	6.2 ± 0.6
9	8.3 ± 1.1	8.3 ± 0.7
12	11.5 ± 1.2	11.5 ± 1.1
15	14.1 ± 2.6	14.1 ± 1.3
18	16.7 ± 1.4	17.3 ± 1.4

The infrared spectrum from 400 to 4500 cm^{-1} are characteristic basic intense absorption bands to the PE-layer related to the stretching (2820-2980 cm^{-1}) and the deformation (1480 cm^{-1}, 725-740 cm^{-1}) fluctuations -CH_2- groups. Absorption bands related to deformation vibrations of -CH_3 groups are observed in the region 1380-1370 cm^{-1}. Characteristic absorption band for the PA-layer: the deformation vibration of the N-H in the region of 3040 cm^{-1}, 1550 - 1570 cm^{-1} and the carbonyl group bending vibrations in the 1620-1680 cm^{-1}. The most characteristic absorption of functional groups in the test sample is presented at Table 2.

ISBN: 978-3-95450-197-7 doi:10.18429/JACoW-RUPAC2018-TUPSA49

INSTALLATION FOR IRRADIATION OF THIN FOILS BY HALO PROTON BEAM ON IHEP ACCELERATOR

Ya.N.Rascvetalov†, A.A. Aseev, V.N. Klyushnikov, G.I. Krupny, M.A .Maslov, V.N. Peleshko,
Institute for High Energy Physics of the National Research Centre "Kurchatov Institute"
(NRC KI - IHEP), Protvino, Moscow Region, Russia

Abstract

The halo of proton beam arises due to proton elastic and coulomb scattering on the internal target. On 70 GeV IHEP accelerator (U-70) halo contains up to several percent of proton beam.

It was shown by Monte Carlo method [1-3] that on thin target (0.05-1 g/cm^2 foils) each halo proton crosses the foil specimen up to 10^3 – 10^5 times before it will be lost during U-70 cycle. The radiation damage level in foil specimens at 10^{20} crossings was estimated at about 0,17 dpa (displacement per atom).

Accumulation of hydrogen and helium atoms during exposure was calculated for iron, nickel and chromium specimens.

Some factors limiting the rate of accumulation of radiation damage and ways for its solutions are discussed.

Simple installation with various material foils as targets is described together with the first proton exposure results of copper foils.

It is important, that foils irradiation by beam halo may be provided independently out of the main U-70 physical program.

As concluded, radiation damage level compared with results got during one year research nuclear reactors can be accumulated during one U-70 run (one month).

INTRODUCTION

The materials radiation damage studies are caring up as usual on research nuclear reactors.

The given paper is devoted to study of possibilities and conditions for creation of high levels of radiation damage in samples of metals at circulating proton beam of 70 GeV IHEP accelerator. The choose range (0.05-1 g/cm^2 foils) of testing materials as a thin targets ensure multiple intersection of sample by each proton during one accelerator circle. It corresponds to multiple growth of proton fluence, that incident on thin internal target and, consequently, an increase in the dose on the sample. The high radiation levels in local specimen area may be created even at low intensity of circulating proton beam.

SIMULATION OF PROTONS CIRCULATION INSIDE VACUUM CHAMBER

The length of the main accelerator ring is 1480 m. Accelerated to the final energy, the proton makes n ~ $4\cdot10^5$ revolutions during one cycle of the accelerator during the duration of the maximum of the magnetic field (2 s). When internal target (specimen) is in the beam the number of revolutions are decreased by nuclear interactions and coulomb and elastic scattering to large angles.

However, for a thin target, the number of passes through the target can be still significant n ~ 10^3 and higher.

Simulation results of this process by Monte Carlo method for various materials are given in table 1.

Table 1. The Number of Passes – n vs. Target Materials and Their Thickness

Target	$\lambda_{nuclear}$, cm	Target thickness, microns		
		10	50	100
		n. the number of passes		
		$\times10^4$	$\times10^3$	$\times10^3$
Al	35	3,45	7,00	3,50
Fe	17	1,70	3,40	1,70
Cu	15	1,50	3,00	1,50
Ti	21	2,10	4,20	2,10
V	20	2,00	4,00	2,00
Cr	19	1,90	3,80	1,90
Ni	16	1,60	3,20	1,60
Zr	13	1,30	2,60	1,30

Theoretically, all the protons of the beam (~ $5\cdot10^{13}$ proton/circle) can go through the target many times. For example, the number of passes through the copper target with a thickness of 50 microns is $1.5\cdot10^{17}$ proton/circle or $4\cdot10^{22}$ proton/month. The main limit of this value is radiation heating.

INSTANTANEOUS RADIATION HEATING OF THIN TARGET

In our estimation we assume that the value of instantaneous radiation heating should not exceed $0.3\cdot T_{melt}$.

For this aid the maximal limitations on the proton beam intensity were calculated and are given in the table 2.

Table 2. Proton Beam Intensity That Corresponds Target Heating up to $0.3\cdot T_{melt.}$

element	$0.3\cdot T_{melt.}$, ^{0}C	Maximal intensity, proton/circle vs. target thickness		
		10 micron	50 micron	100 micron
Al	198	$2,5\cdot10^{11}$	$1,3\cdot10^{12}$	$2,5\cdot10^{12}$
Fe	460	$6,3\cdot10^{11}$	$3,2\cdot10^{12}$	$6,3\cdot10^{12}$
Cu	325	$4,6\cdot10^{11}$	$2,3\cdot10^{12}$	$4,6\cdot10^{12}$
Ti	540	$7,2\cdot10^{11}$	$3,6\cdot10^{12}$	$7,2\cdot10^{12}$
V	516	$7,0\cdot10^{11}$	$3,5\cdot10^{12}$	$7,0\cdot10^{12}$
Cr	549	$6,9\cdot10^{11}$	$3,5\cdot10^{12}$	$6,9\cdot10^{12}$
Ni	436	$6,1\cdot10^{11}$	$3,0\cdot10^{12}$	$6,1\cdot10^{12}$
Zr	570	$8,3\cdot10^{11}$	$4,2\cdot10^{12}$	$8,3\cdot10^{12}$

† Jaroslav.Rascvetalov@ihep.ru

ISBN: 978-3-95450-197-7 doi:10.18429/JACoW-RUPAC2018-TUPSA50

EXPERIMENTAL FACILITY "RADIOBIOLOGICAL TEST SETUP ON ACCELERATOR U-70" AS CENTERS FOR COLLECTIVE USE (CCU)

V.A. Pikalov, Y.M. Antipov, Institute for High Energy Physics named by A. A. Logunov of National Research Centre «Kurchatov Institute» (NRC «Kurchatov Institute» - IHEP), Protvino, Russia
S.I. Zaichkina, S.S. Sorokina, O.M. Rozanova, E.N. Smirnova, S.P. Romanchenko, O.R. Dyukina, Institute of Theoretical and Experimental Biohpysics of Russian Academy of Sciences (ITEB RAS), Puschino Moscow Region, Russia
E.E. Beketov, E.V. Icaeva, M.V. Troshina, A.A. Lychagin, A.N. Solovev, S.N. Koryakin, S.E. Ulyanenko, A. Tsyb Medical Radiological Research Center – branch of the National Medical Research Radiological Center of the Ministry of Health of the Russian Federation (A. Tsyb MRRC), Moscow, Russia

Abstract

The experimental facility "Radiobiological test setup on accelerator U-70" was created on NRC "Kurchatov Institute" - IHEP, Protvino to carry out radiobiological and physical experiments on the extracted beam of carbon nuclei with an energy up to 450 MeV / nucleon. This test setup is designed as a center for collective use. Specialists from 5 Russian institutes participate in radiobiological research of the cell structures and laboratory animals, and in experiments on nuclear physics and dosimetry. The study of the biological effectiveness of carbon nuclei for the purposes of hadron therapy, as well as to evaluate the effect of high-energy ion irradiation on human cognitive functions are the main goals of these radiobiological experiments. The experiments performed on the radiobiological test setup at U-70 was briefly reported.

INTRODUCTION

The experimental facility "Radiobiological test setup on accelerator U-70" was created on NRC "Kurchatov Institute" - IHEP. The facility is designed to carry out radiobiological and physical experiments on a deduced beam of carbon nuclei. Radiobiological test setup has all the necessary equipment for conducting experiments. On the basis of the facility in 2017, the Center for Collective Use "Radiobiological Test Setup on Accelerator U-70".

The parameters of the carbon beam on the facility RBS:

- energy 450 MeV / nucleon;
- period 8 s;
- intensity - 1.5 - $2.0 \cdot 10^9$ nucleons per cycle;
- • Output mode - slow output - 0.6 sec.;
- the size of the uniform radiation field (± 2.5%) - Ø 60mm [1].

Equipment for carrying out radiobiological experiments:

- a water phantom;
- 3D moving system;
- ionization chambers for monitoring of radiation;
- TLD radiation dosimeters;
- radiochromic films Gafchromic EBT3.

Specialists from 3 institutes conduct radiobiological experiments at the "Radiobiological Test Setup on Accelerator U-70"

- Tsyb Medical Radiological Research Center – branch of the National Medical Research Radiological Center of the Ministry of Health of the Russian Federation (A. Tsyb MRRC).
- Institute of Theoretical and Experimental Biohpysics of Russian Academy of Sciences (ITEB RAS).
- State Scientific Center of Russian Federatiot - Institute of Biomedical Problems (SSC RF – IMBP RAS).

The experiments performed on the radiobiological test setup was briefly reported.

A. TSYB MRRC

Comparison of the biological efficiency of accelerated carbon ions and heavy recoil nuclei on chinese hamster cells [2].

Studies were carried out to determine the biological effectiveness of accelerated carbon ions upon irradiation of cell cultures on the plateau and at the peak of the Bragg curve, as well as heavy recoil nuclei (C, N, O) induced by 14.1 MeV neutrons in the monolayer of cells upon irradiation in the absence balance of secondary charged particles. The studies were performed on normal (V-79 and CHO-K1 lines) and tumor (B14-150) chinese hamster cells.

The experiments used transplant cultures of chinese hamster cells of three lines: CHO-K1 (ovarian cells, clone of CHO line), V-79 (lung fibroblasts), B14-150 (fibrosarcoma) obtained from the Cell Culture Bank at the Cell Culture Department of the Institute of Cytology RAS officially for laboratory experiments.

The results for the V-79 line are shown in Figs. 1 and 2.

ISBN: 978-3-95450-197-7 doi:10.18429/JACoW-RUPAC2018-TUPSA52

NEW EXPERIMENTAL CHANNALS AT NUCLOTRON

M.M. Kats*, T.V. Kulevoy,
"Kurchatov Institute" – ITEP, Moscow

Abstract

In framework of NICA project two new experimental channels are under development. At first channel the biological experiments under ion beam irradiation are planned. At second one the radiation resistance of electronics and its' components under heavy ion irradiation will be tested. The structure of channels includes several dipoles, focusing quadrupoles and active scanning systems. The results of the channel simulation providing lossless transportation for different ions (from C to Au) with energy per nucleon from 0.25 GeV to 0.8 GeV are presented and discussed.

INTRODUCTION

Significant project NICA in JINR (Dubna) is devoted mainly to problems of experimental physics of high energy. It consist of ion sources, linacs, buster, Nuclotron and collider with its experimental equipments. In addition a few experiments on extracted beams with fixed targets both in physics, and for testing influence of different ion beams on biological and electronics objects are planned. For those aims extracted from Nuclotron beam must be transported to two new targets. According to requirements for biological experiments the beam with sizes less 10x10 cm^2 and with minimal background are needed. Meanwhile to test elements of new electronics, the beam with sizes from 2x2 cm^2 up to 20x20 cm^2 is needed. Experimental targets must be irradiated with uniformity better than ±10%.

The place for new channels location is shown on Fig.1. The dimension of stands with additional place for beam collimators and supported devices are about 3m*3m in plan. For stands service the comfortable pass with 1 m width must be provided.

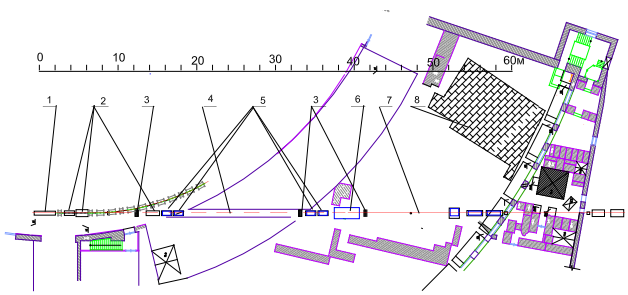

Figure 1: The place for new channels location . 1 – septum magnet, 2 – magnets for bend extracted ion beam in vertical plane to the top, 3 – devices of JNIR PIK for measurement shape of the beam, 4 –beamline with angle 0.105 to the top, 5 – exsisting quadrupoles, 6 – magnet SP12, 7 – beamlines in horizontal direction, 8 – concrete walls.

*markmkats@gmail.com

Behind each stand the beam stop with dimension in plan of 4m*4m must be placed at distance at least 3m. The maximal magnetic field for new magnets must be limited by B < 1.6 T.

After extraction from Nuclotron ion beam is bended up by 3 dipoles in vertical plane with angle near 0.105 rad. At the ground flow another dipole SP12 putthe beam horizontally. Four existing quadruples in front of the last dipole provide the beam focusing.

The beam properties depend on the mode of Nuclotron and extraction system operation as well as on the experiment request. The beam extraction time can be from 0.1 to 10 sec. Stability of extracted beam intensity can be near ±5%.

At the exit of Nuclotron the extracted beams can be different both by ions (from C to Au) and by ions energy (0.25 < t < 0.8 GeV, t kinetic energy per nuclon) and by phase volumes in both planes and by its impulses spread dP/P [%]. Intensity of extracted beams can be from 10^4 to 10^9 per sec. The P(max)/z и P(min)/z for extracted ions can be calculated using equations:

$$P/z = (T^2+2TM)^{0.5}$$
$$T=A*t,$$
$$M=A*0.936\ GeV$$

where T is a total kinetic energy of ion, A – an atomic mass, t – kinetic energy per nuclon, 0.936 is a mass of one nuclon, z is charge of ion. As result t(max)=0.8 GeV, t(min)=0.25 GeV.

For output channel development we have used

$$P(max)/z\ (Au^{+79})=3.6\ GeV/c.$$

Parameters of extracted beams were received from Nuclotron team (see Fig.2):

X*X'=3mm*mrad, Y*Y'=8mm*mrad, dP/P=0.1%.

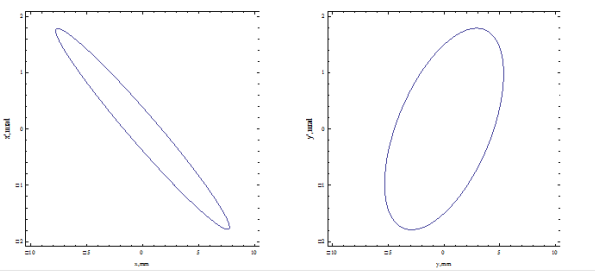

Figure 2: Phase volumes of extracted beams at level 2*sigma.

GENERAL APPROACH

The most restriction of the project is the requirements of homogeneous irradiation for targets with different dimensions. The increase of total beam spot at the target to provide the required homogeneity leads to loss of the high part of beam intensity. The "active scanning" as it

ISBN: 978-3-95450-197-7 doi:10.18429/JACoW-RUPAC2018-TUPSA54

BELA INJECTION COMPLEX FOR SIMULATION EXPERIMENTS

A. Ziiatdinova, P. Fedin[1], A. Nikitin[1], S. Rogozhkin[1], T. Kulevoy[1], NRC Kurchatov institute – ITEP, 117218 Moscow, Russia
[1]also at National Research Nuclear University MEPhI, 115409 Moscow, Russia

Abstract

BELA (Based on ECR ion source Linear Accelerator) project is under design in NRC «Kurchatov Institute» – ITEP. Injection complex of the accelerator based on two ion sources is intended for different tasks and has multi-channel transport system. One of the tasks is double beam irradiation for reactor materials radiation resistance analysis. Heavy and light ion beams from ion sources will irradiate a target at the same chamber simultaneously. Simulations were carried out for Fe^{10+} at 3.2 MeV ions. The paper includes description of injection complex layout and results of the ion transport in the target material.

INTRODUCTION

Creation of new high-tech power plants, like fusion reactors, and improving the efficiency and safety of existing nuclear power plants includes the development of new materials that can withstand the extreme radiation, temperature and mechanical loads during operation. For the certification of new materials, a set of appropriate damaging doses is required in conditions close to real operating conditions. Certification of new materials for radiation resistance requires the use of reactor radiation. This takes long time, and, in addition, reactor irradiation leads to high induced radioactivity of the materials, which significantly complicates subsequent studies of the samples. For this reason, methods for express analysis of the radiation resistance of structural materials, such as simulation experiments on the irradiation of materials with accelerated heavy ion beams, are required to conduct pre-certification studies. It is known that heavy ions irradiation initiates a cascade production of structural defects similar to that occurring during reactor irradiation. This method allows to save material and time resources at early stages of material development, and to reject samples with obviously weak characteristics. Currently, simulation experiments are conducted at the HIPr-1 [1] and SIRMAT [2] in the NRC "Kurchatov Institute" – ITEP. Now simulation experiments are carried out with pulsed beams with controlled heating of the target to create conditions as close as possible to real operation conditions of nuclear reactors [3, 4]. Reactor irradiation simulation requires simultaneously damage production and H/He injection. Implanted H/He amount has to be in certain ratio to damage value [5]. In this regard, there is need to create a new facility for simulation experiments based on an ion source which able to generate continuous beams. Multifunctional injection complex of BELA is under development in NRC "Kurchatov institute" - ITEP (Fig. 1). The injection complex based on two ion sources is intended for different tasks and has multichannel transport system. One of the tasks is double irradiation simulation experiments for reactor materials.

In addition, for more realistic reproduction of reactor conditions, helium and hydrogen ions will be implanted into damaged region by the heavy ion beam. This process simulates the accumulation of gas products of nuclear reactions, as well as the introduction of hydrogen isotopes from plasma in fusion reactors. In order to avoid distortion of the simulated radiation damage processes in the experiments with ion beams, it is necessary to minimize the surface effects. Therefore, studies are carried out in the intermediate region between the surface of the irradiated sample and the maximum of the implantation ions profile. Simulation experiments analysis makes on defined depth interval. Upper depth dependences on concentration of implanted ions. Down depth is defined by surface effects. This interval decreases with irradiation dose and the experimental temperature increasing [6].

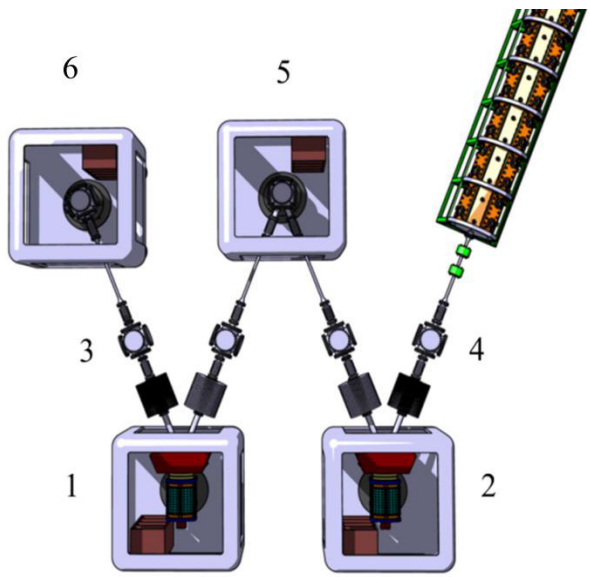

Figure 1: Scheme of the BELA injection complex: 1 – heavy ion source, 2 – light ion source, 3 – transport system, 4 – matching line with RFQ, 5 – double irradiation target chamber, 6 – single irradiation target chamber.

DOUBLE BEAM IRRADIATION

Double beam irradiation scheme is shown on Fig.2. Main beam is Fe^{10+} from ion source (1) line directly irradiates the target and produces lattice damage. H^+/He^+ ions are implanted at specific angle to the surface from the gas ion source (2).

In order to determine the implantation region, ion transport in target material was made using SRIM / TRIM software package.

ISBN: 978-3-95450-197-7 doi:10.18429/JACoW-RUPAC2018-TUPSA55

ELV ACCELERATORS ARE A TOOL FOR INNOVATION

N. K. Kuksanov, S. N. Fadeev, Y. I. Golubenko, D. A. Kogut, A. I. Korchagin, A. V. Lavrukhin, P. I. Nemytov, R. A. Salimov, E. V. Domarov, A. V. Semenov, D. C. Vorbyev, V. G .Cherpkov, I.K. Chakin, The Budker Institute of Nuclear Physics (BINP), Novosibirsk, 630090, Russia

Abstract

BINP SB RAS produces industrial electron ELV accelerators for radiation technologies. The main innovative applications are cross-linking of the insulation of wires and cables, production of heat shrinkable tubes and films, production of foamed polyethylene, and radiation modification of rubber blanks for tires.

Model range of ELV accelerators covers the range of electron energies from 0.3 MeV to 2.5 MeV, beam power up to 100 kW, and beam current to 100 mA. All models have similar concept but differ in overall dimensions, length of accelerator tube, and the number of high-voltage rectifying sections. This makes it easy to adapt accelerators to the requirements of technology. The system of automated control of accelerators and communication with technological lines is constantly developing.

ELV accelerator with an energy of 0.3-0.5 MeV and beam current up to 130 mA was developed and tested. The accelerator is compact in size and installed in local steel shielding. Electron beam is extracted through a two-windows extraction system with one titanium foil 180 mm wide.

ELV ACCELERATORS

By now over 170 ELV accelerators were delivered inside Russia and abroad [1]. Due to compactness and high performance properties, ELV accelerators proved to be competitive both in the Russian and in the world markets. Thus, in China they make about 1/3 of the total amount of powerful industrial accelerators, and in Republic of Korea – almost 2/3.

The main features of ELV accelerators:

- High electron beam power in wide energy range;
- High efficiency of electron beam from the main (70-80%);
- High stability of accelerator parameters. Energy and beam current instabilities do not exceed ±2.5%;
- Simple procedure of accelerator control for operator;
- Accelerator has simple design and high reliability;

ELV accelerator common view is presented in Fig. 1.

Parameters of the main models of ELV accelerators are given in Table 1.

ELV-4 accelerator installed at JSC "Belaruskabel" (formerly "Mozyrkabel") in 2016 is shown Fig. 2.

Models of accelerators differ in overall dimensions, length of accelerator tube, and the number of high-voltage rectifying sections.

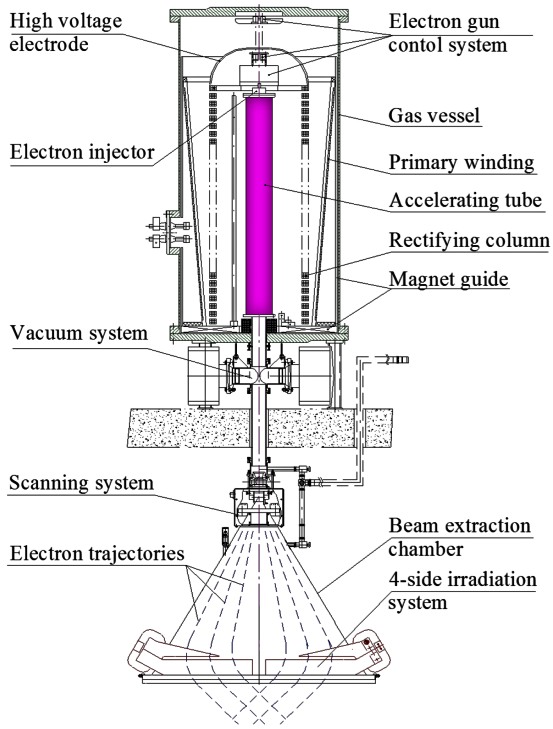

Figure 1: ELV accelerator common view.

Figure 2: ELV-4 accelerator JSC "Belaruskabel" ("Mozyrkabel").

ISBN: 978-3-95450-197-7 doi:10.18429/JACoW-RUPAC2018-TUPSA56

A COMPACT HIGH-VOLTAGE SOURCE ON THE BASIS OF ELV ACCELERATOR

V.G. Cherepkov, J.I. Golubenko, S.N. Fadeev, D.A. Kogut, A.I. Korchagin, N.K. Kuksanov, R.A. Salimov, A.V. Semenov, A.B. Sorokin, D.S. Vorobyev,.Budker Institute of Nuclear Physics SB RAS, 11, Academic Lavrentiev ave., Novosibirsk, 630090, Russia.

Abstract

Electron accelerators of ELV type are widely used in industrial and research organizations. The high-voltage rectifier of ELV accelerator is used as a high-voltage source of the tandem accelerator for boron neutron capture therapy (BNCT) at the Institute of Nuclear Physics SB RAS. As a source of high voltage, a more adequate source has been developed for subsequent ELV-based machines. Its parameters are: voltage - 1200 kV, load current - 20 mA, voltage polarity - positive. New specific requirements are put forward for this rectifier; therefore, its design has a number of differences in comparison to the ELV design. In particular, high voltage is transmitted to the accelerator-tandem over a sectioned feeder that lies within the rectifier column of the source. In order to reduce the overall dimensions of the source in its rectifier sections, a rectification circuit with four times voltage magnification is used. The operating frequency of the primary supply voltage is 1400 Hz. At present, the source has been manufactured, undergoes bench tests and is being prepared for use in the BNCT complex.

PROBLEM

Accelerators of ELVs have found wide application both in industry and for scientific research. One of the latest applications is the use of ELV as a source of accelerating voltage U_0 tandem for boron-neutron capture therapy [1]. In an installation operating for more than 10 years, the standard rectifier of ELV accelerator is connected to the sectioned high-voltage feeder of the tandem accelerator [2]. The potential distribution over the electrodes of the feeder and the tandem accelerator is provided by a special high-resistance divider Rd. However, when the beam current of accelerated ions is spilled onto the tandem electrodes, the uniformity of the voltage distribution across the electrodes is violated, which leads to breakdowns of the vacuum isolation of the tandem.

Since maintaining the uniformity of the voltage between the electrodes by reducing the resistance Rd became impossible, it was decided to connect the tandem electrodes directly to the rectifier sections of ELV type, as shown in Fig. 1.

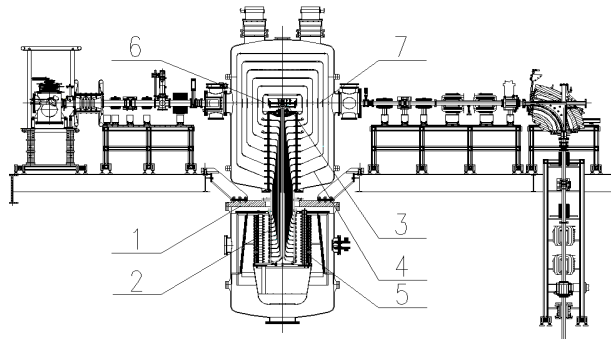

Figure 1: Tandem accelerator circuit: (*1*) high-voltage source; (*2*) sectional high-voltage feeder; (*3*) gas charge – exchange; (*4*) target electrode of the tandem; (*5*) rectifier sections; (*6*) beam H(-); (*7*) beam H(+).

THE DESIGN OF THE RECTIFIER

To solve this problem, a new source of accelerating voltage was developed, manufactured and tested without load at INP SB RAS (see Fig. 2).

In comparison with ELV, the following changes were made to its construction:

1. The rectifier is rotated by 180^0 vertically ("upside down").
2. The primary winding (item 3) has an enlarged diameter. It is fixed in the shell of the vessel (item 1) on three supports (item 4).
3. The primary voltage is supplied to the primary winding by special terminals (item 19). The frequency of the supply voltage of the primary winding f = 1400 Hz.
4. A column of 18 rectifying sections (item. 9) is mounted on a textolite base (item 10).
5. The base and the column with three rods (item 13) are fastened to the single block of the rectifying column with nuts (item 8).
6. The rectifier column unit is located inside the primary winding (see Fig. 2).
7. The photo of the rectifier section (item 9) is shown on (Fig. 3).
8. The diagram of the rectifier section with quadruple alternating voltage is shown in Fig. 4. Maximum rectified section voltage Us = + 80 kV, load current I0 = 20 mA.
9. The coil of the rectifying section has 2000 turns.

ISBN: 978-3-95450-197-7 doi:10.18429/JACoW-RUPAC2018-TUPSA58

A METHOD FOR MEASURING THE POSITRON LIFETIME IN SOLID MATTER WITH A CONTINUOUS POSITRON BEAM

A. A. Sidorin†, P. Horodek[1], V. I. Hilinov, A. G. Kobets[2], V. V. Kobets, I. N. Meshkov[3], O.S. Orlov, K. Siemek[1], Joint Institut for Nuclear Research, 141980 Dubna, Russia
M. K. Eseev, Northern (Arctic) Federal University named after M.V. Lomonosov, 163002 Arkhangelsk, Russia
[1]also at Institute of Nuclear Physics of PAS, 31342 Krakow, Poland
[2]also at Institute Institute of Electrophysics and Radiation Technology of NAS of Ukraine 61002 Kharkov, Ukraine
[3]also at St.Petersburg State University 199034 St.Petersburg, Russia

Abstract

The report proposes the scheme and design of the setup for formation a continuous monochromatic positron flux with controlled time of arrival at the target, independent of the injection time in a limited time interval. The setup is designed to perform experiments to measure the positron lifetime with the positron annihilation spectroscopy method (Positron Annihilation Lifetime Spectroscopy – PALS). PALS method allows to distinguish defect types in the materials. It is possible to vary the positron energy in the present version of the setup that allows us to analyze the distribution of defects along the depth of the sample. The scheme of periodic RF voltage generation of a given form and measurement of the positron lifetime, is discussed.

PALS METHOD

In positron annihilation spectroscopy the most informative and hence the most attractive for applications is a method based on the measurement of the positron lifetime in the sample (Positron Annihilation Lifetime Spectroscopy — PALS) [1]. In the simplest case of PALS positron-active isotope ^{22}Na most commonly used, decays emitting the positron, and, with a delay of about 3 ps, a gamma quantum. The last one is used as a start signal; a stop sign is a pair of gamma-quanta, which appear at annihilation of a positron with an electron of the atom of the target (test sample). Significantly, the lifetime of positrons in vacancies increases several times.

Flow of monochromatic positrons is efficient to use in the PALS method. The flux is generated by the sources with ^{22}Na isotope and moderator — monochromatizator. The yield of slow positrons, about 1% of the total decays, is achieved by using as the moderator solid neon, which is freeze from the gaseous phase on the foil of the closed radioactive source that is cooled to a temperature of 7-8 K. So the Cryogenic Source of Slow Monochromatic Positrons (CSSMP) is developed and being used at the Joint Institute for Nuclear Research. [2]. The method of formation of an ordered positron flux (OPF) and measurement of positron lifetime in the sample with a precision of about 30 ps is proposed. The proposed method is a development of the well-known scheme of bunching the flux of slow positrons.

† sidorinalexsey@gmail.com

ORDERED POSITRON FLUX FORMATION

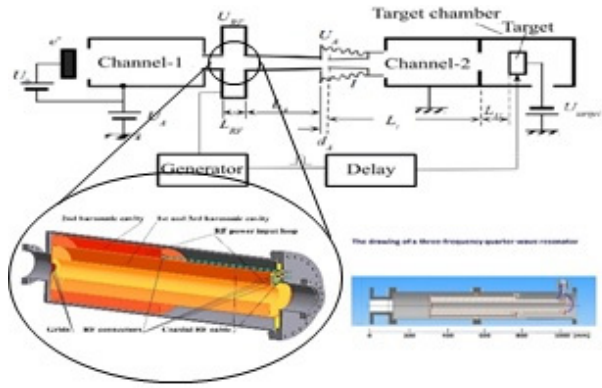

Figure 1: The scheme of installation for generation of an ordered flux of positrons: e^+ - cryogenic source of slow positrons based on the ^{22}Na isotope, Channel-1, 2 — the positron transfer channels, $U_0 > 0$ is the potential between the source and the Channel-1, $U_A > 0$ — potential difference between Channels 1 and 2, L_{RF} — RF voltage system with U_{RF} of special form, L_A — 1-st drift section of the PAS channel, d_A — accelerating gap with the static electric field U_A, I — vacuum insulator, L_t — 2nd drift section of the PAS channel, L_U — the gap between the entrance to the test chamber and the target with the sample to be studied, U_{target} — negative potential of the target.

Generation of an OPF (see Fig. 1) is performed by using a RF-voltage $U_{RF}(t)$ of the special form (see Fig. 2 and 3). Positrons from CSSMP come to the entrance of the RF gap from channel 1 at some random time tinj (injection). When crossing the gap with RF ordering voltage the positron accelerates depending of time arrival to the entrance of the RF gap. Then positrons reach the target strictly periodically, independently of time when they came to the RF gap. The positron transfer channel is equipped with an

ISBN: 978-3-95450-197-7 doi:10.18429/JACoW-RUPAC2018-TUPSA59

SETUP FOR SECONDARY ELECTRON-ELECTRON EMISSION COEFFICIENT STUDY

O.S. Orlov†, A.G. Kobets[1], I.N. Meshkov[1], A.A. Sidorin, V.I. Hilinov,
Joint Institute for Nuclear Research, 141980, Dubna, Russia
[1] also at IERT, 61002, Kharkov, Ukraine

Abstract

Setup for measurement of secondary electron yield from metal surfaces and other materials is developed. This work is related to the well known problem of electron cloud formation in the synchrotron vacuum chamber during the beam passage. It is planned to measure the dependence of the second electron yield (SEY) on the chamber material type and the structure of the surface of the chamber wall. The constructed setup allows us to register the spectrum of secondary electrons.

ELECTRON CLOUDS

Electron clouds are clusters of secondary emitted electrons generated in the accelerator chamber due to acceleration of ionizing electrons of residual gas in electric field of the beam of particles in the accelerator and their resonance multiplication because of secondary electron emission from walls of the vacuum chamber of the accelerator. The character of this phenomenon is similar to the known effect of the multipactor – develop of discharge in cavities of RF devices. The density of electron clouds depends on the coefficient of secondary electron emission (K_{SEE}) of a material of the vacuum chamber.

Electron clouds that are present in accelerators and colliders with a high intensity beam form a positive feedback, which excites the instability of the beams. Generation of electron clouds also brings about an increase in pressure in the vacuum chamber, up to entire loss of the beam, because the formation of electron clouds is accompanied by desorption of gas molecules absorbed in walls of the chamber. In addition, the heat load on cryogenic surfaces of the vacuum chamber increases. An increase in pressure in the vacuum chamber also causes a rise in emittance of the beam due to scattering of the beam particles on the residual gas. In addition, the work of the beam testing instrument is defective because of electromagnetic disturbances initiated by secondary electrons.

Preliminary calculations of K_{SEE} for the vacuum chamber of the NICA Collider have shown that, for the material of a wall with K_{SEE} below 1.3, the effect is insignificant [1].

MESUREMENTS OF COEFFICIENT OF YIELD OF SECONDARY ELECTRON EMISSION

Measuring of the SEY coefficient was performed preliminarly at the setup [2] during irradiation of the studied sample by an electron beam with energy in the range of from 100 to 3000 eV. The principle scheme of the K_{SEE} measurement is shown in Fig. 1. The accelerated initial electron beam (I_1, E_1) hits the studied sample and knocks out secondary electrons from it (E_2, I_2). A negative potential is applied to the sample, and its value is chosen in the range of from –3000 to 0 V, depending of the chosen value of energy of incident electrons.

$$E_e = e(U_{cathode} - U_{anode}). \quad (1)$$

The primary and second electrons drift in the crossed electric **E** and magnetic **B** fields in the same direction transverse to the vector **B**. The values of **E**, **B** field are tuned in such a way that primary electrons come to the sample under studying and secondary electrons come to the collector. The collector is suspended under potential U_{coll} of the collector is measured. The K_{SEE} is determined from the values of primary beam current I_1 and secondary electron current I_2, which are equal to the current of the voltage source connected to the tested sample I_{sample} (Fig. 2). Full balance of the currents is described by the system of two equations:

$$\begin{cases} I_{sample} = I_1 - I_2 \\ I_{coll} = I_2 - I_3 \end{cases}. \quad (2)$$

Here I_3 is the current of the secondary electrons from the collector.

That gives the value of secondary electron emission coefficient:

$$SEY = \frac{I_1 - I_{sample}}{I_1}. \quad (3)$$

The dependence of K_{SEE} on the energy of the initial electron beam and on charge density imposed by the initial beam on the surface of the sample is measured in the experiments. Measurements will be performed without and with cleaning of the sample by sample heating that remove molecules of absorbed residual gas from the surface of the sample. Sample heater is based on electric bulb.

The first results of the stand work (see Fig. 3) showed that the stand works properly and the following results were obtained for a sample of steel at a vacuum of 10^{-7} tor: I_{gun} = 20 uA, I_{col} = 26 uA, I_{sample} = -7,5 uA, SEY=1,375.

Further vacuum condition improving, finalizing the sample holder, comparing the results with other installations is necessary.

ISBN: 978-3-95450-197-7 doi:10.18429/JACoW-RUPAC2018-TUPSA60

BEAM LINES FOR GAS FILLED SEPARATOR EXPERIMENTS AT DC280 CYCLOTRON

V.I. Lisov†, G.G. Gulbekyan, V.V. Bashevoy, A.V. Eremin, G.N. Ivanov, I.V.Kalagin, V.I. Kazacha, N.Yu. Kazarinov, N.F. Osipov, V.K. Utenkov, Joint Institute for Nuclear Research, FLNR, Dubna, Moscow region, Russia

Abstract

The design of two beam lines for ion transportation from the cyclotron DC280 to the Gas Filled Separators (GSF) is presented. The beam lines include commutating magnet with variable magnetic field induction up to 1.5 T that gives the possibility to bend ion beams in five directions providing ion transportation through the beam lines to five experimental setups. The beam focusing in the beam lines is provided by set of quadrupole lenses having the gradients up to 7.7 T/m. The beam lines are intended for the efficient ion transportation of elements from Helium to Uranium with the atomic mass to charge ratio in the range of 4-7.5 at the energies from 4 up to 8 MeV/amu. The ion beam power will reach the value about 3 kW. The water cooled current limiting aperture diaphragms will be installed into all beam lines to prevent the tube damage. The beam diagnostics consists of the Faraday caps (FC), slit collimators, sector aperture diaphragms and ionization beam profile monitors. A new structure of the beam line #3 and calculation results for $^{48}Ca^{9+}$ and $^{48}Ca^{7+}$ ion beam transportation from the extraction point to the new gas-filled separator GFS2 are listed. In addition, a new structure of the beam line #4 and calculation results for $^{48}Ca^{8+}$, $^{50}Ti^{8+}$, and $^{54}Cr^{9+}$ ion beam transportation from the extraction point to the new GFS3 are presented.

INTRODUCTION

DC-280 cyclotron designed at the Flerov Laboratory of Nuclear Reaction (JINR, Dubna) is intended for carrying out fundamental and applied investigations with ions from He to U (masses A from 2 up to 238) produced by a ECR ion source. One may vary the energy of the ions extracted from the cyclotron from 4 up to 8 MeV/amu.

Utilization efficiency of the accelerator is determined in many respects by quality of the transportation system for the extracted ions. Widely branched system of the beam lines allows one to carry out numerous investigations. Description of the bending magnet and all five beam lines was given in [1].

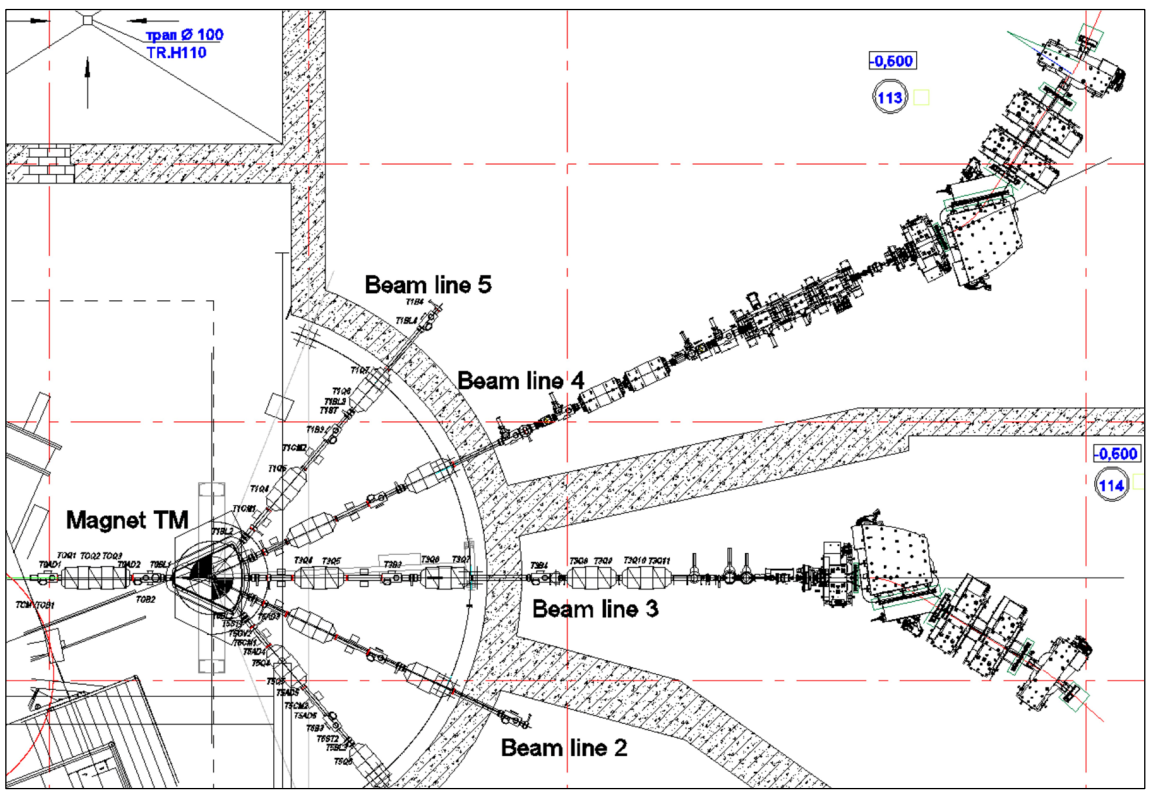

Figure 1: Layout of the beam lines #3 and #4 for heavy ion transportation.

†lisov@jinr.ru

ISBN: 978-3-95450-197-7 doi:10.18429/JACoW-RUPAC2018-TUPSA61

DEVELOPMENT OF THE ION BEAMS HIPR-1 TRANSPORT CHANNEL FOR ION ENERGY LOSSES MEASUREMENT IN PLASMA TARGET*

E.Khabibullina†, R.Gavrilin, P.Fedin, S.Visotski, A.Kantsyrev, A.Golubev, T.Kulevoy,
Institute for Theoretical and Experimental Physics NRC "Kurchatov Institute", Moscow, Russia

Abstract

The research of the processes occurring during the interaction of heavy ions with plasma is carried out on the Heavy Ion RFQ HIPr-1 (Heavy Ion Prototype) in the ITEP. The HIPr-1 is a heavy ion RFQ linac that accelerates ion beams generated by either a MEVVA ion source or a duoplasmatron. It provides accelerated beam of ions from C^{+} to U^{4+} with energy of 101 keV/u and up to 3 mA of current. Gas-discharge plasma target, which was produced in ITEP, is used for the measurement of ion energy losses in the ionized matter. The diaphragms at the entrance and the exit of the plasma target provide the necessary vacuum into the transport channel (which is 10^{-6} mbar), while the gas pressure in the target equals to 1-10 mbar. The design of the beam transport channel for performing experiments to determine the energy losses in plasma was developed based on the beam dynamics simulation. According to the obtained results the first successful tests on the HIPr-1 were held.

INTRODUCTION

Investigation of ion stopping in an ionized matter is important for obtaining new knowledge in high energy density in matter and plasma physics. Especially interesting is the investigation of the interaction of heavy ions with low energy range from 40 to 500 keV/u with strongly ionized low temperature hydrogen plasma [1,2]. Work on the determining of the ions energy losses in a plasma is carried out into heavy ion RFQ linac Heavy Ion Prototype (HIPr-1) [3] at ITEP. HIPr-1 accelerates heavy ion beams in the pulsed mode with pulse length of 450 μs and repetition rate up to one pulse for four seconds. HIPr-1 layout is shown in Fig. 1. A metal ion beam is generated using the metal vapor vacuum arc ion source (MEVVA). To generate a gas ion beam the duoplasmatron ion source is used [4]. In RFQ structure the beam is accelerated up to 101 keV per nucleon total energy (5.6 MeV for Fe). The RFQ structure was produced for accelerating of heavy ions with the mass to charge ratio ~60 [5].

Transport channel includes three magnetic quadrupole lenses and two observation chambers.

Below are the results of the development of the transportation channel and the launch of an experimental bench based on HIPr-1.

PLASMA TARGET

Plasma target (PT) was developed at ITEP [6], plasma inside PT ignited by electrical discharge in two coaxial quartz tubes (see Fig. 2). The capacitor bank with charging voltage range from 2 to 5 kV produces the discharge of hydrogen with maximal current up to 3 kA. As laser interferometry measurement [7] shows the linear free electron density of plasma is in the range from $3.3*10^{17}$ to $1.3*10^{18}$ cm^{-2}. For the plasma temperature measurement will be applied spectrometric method.

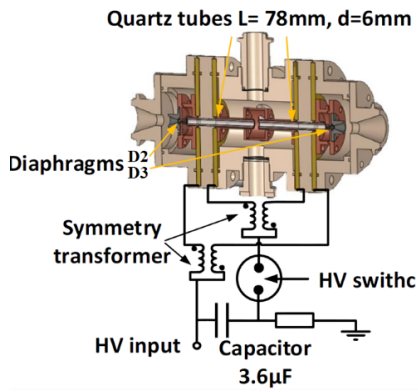

Figure 2: Plasma target.

The plasma target was installed between the third quadrupole lens and the observation chamber.

For plasma generation the initial hydrogen pressure should be from 1 to 10 mbar in PT. In order to guarantee required vacuum magnitude 10^{-6} mbar in the transport channel in front and back of the plasma target a set of four diaphragms was used. In Fig. 3 the diaphragms locations, the vacuum system and the beam diagnostic system are shown.

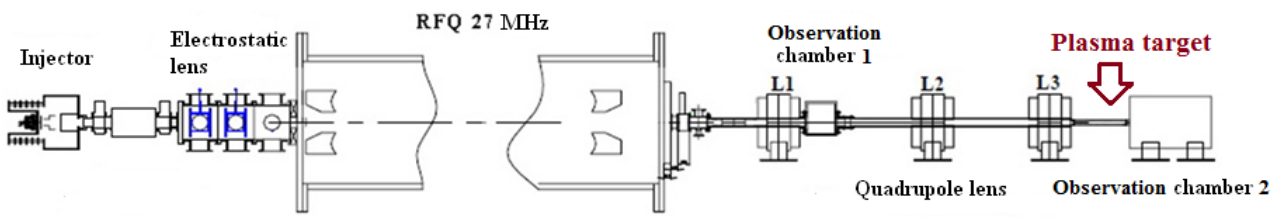

Figure 1: Layout of the HIPr-1.

* Work supported by RFBR grand №18-02-00967
† email address: Ekaterina.Khabibullina@itep.ru.

ISBN: 978-3-95450-197-7 doi:10.18429/JACoW-RUPAC2018-WEPSB02

FEATURES OF THE FORMATION OF AN ELECTRON BEAM IN A LINEAR ACCELERATOR ON PARALLEL-COUPLED STRUCTURE

Yu. D. Chernousov†, I.M. Ikryanov, I.V. Shebolaev,
Voevodsky Institute of Chemical Kinetics and Combustion SB RAS, Novosibirsk, Russia

Abstract

The highest possible, close to 100%, rate of electron capture into acceleration mode has been achieved in an electron linear accelerator based on a parallel-coupled accelerating structure (PCS). High capture rate has been achieved by using an electron gun with high-frequency beam current control, entrance PCS resonators focusing the beam, and in-built into the PCS magnetic periodic focusing system of the solenoidal type based on permanent magnets (MPFS). This study investigates beam dynamics in the developed gun and PCS. The electron gun forms a cylindrical weakly-converging beam in the first resonator of the PCS as a sequence of short pulses with the accelerating frequency, the first and following resonators of the PCS focus, group and accelerate the beam and MPFS focuses and transports electrons to the PCS exit.

INTRODUCTION

Reaching high efficiency of capturing electrons into the acceleration mode is an important problem in the development of a low-energy electron accelerator. The capturing efficiency is usually 30-40% [1, 2]. By forming a sequence of electron bunches at the frequency of the following acceleration from a continuous beam using velocity pre-modulation and grouping, the capturing efficiency can be raised to 70% [2]. The capturing can be further improved by the effects of ultrahigh frequency (RF) focusing as a low-energy beam is flying through the accelerating cavities [1, p. 201]. To focus and transport the beam, an external magnetic field is used, which is generated by solenoids placed over the accelerating structures.

In order to achieve high capturing efficiency, the designed accelerator uses all the mentioned beam formation and focusing techniques on its parallel-coupled structure (PCS). A three-electrode electron gun with RF current control injects the beam into the PCS as a sequence of short pulse bunches at the frequency of the following acceleration, which are shorter than the half-period of the accelerating field. The electron gun optics forms a cylindrical, weakly convergent beam with a diameter close to that of the input port of the first cavity. This form is optimal for the efficient focusing of the electrons by the RF fields of the input and further cavities of the PCS. The PCS has an integrated permanent magnet-based magnetic periodic focusing system (MPFS) [3], which further focuses the accelerated beam and transports it to the PCS outlet.

Due to the techniques and devices used in the PCS accelerator, an extremely high, nearly 100%, efficiency of capturing into the acceleration mode was achieved [4].

† chern@catalysis.ru

Below, the dynamics and details of the beam formation in the electron gun, the first cavities, and the accelerator as a whole are discussed.

FORMING THE BEAM IN THE GUN

Grid-controlled electron guns have been proposed for and used in microwave generators, or klystrods, and they are used in the injection systems of electron accelerators [5-8]. This kind of a gun forms a beam which contains a sequence of electron pulse bunches at the frequency of the following acceleration with beam duration within half of the accelerating field period. The pulse current is formed by a cathode grid cavity with a concentrated grid-cathode capacitance. A microware power applied to the cavity generates a microwave voltage at the grid-cathode gap, and current pulses with duration close to the microwave half-period are injected in the grid-cathode gap under a negative cathode potential relative to the grid (π-injection). The microwave power is applied to the cathode grid cavity by two antennas, one grounded and the other under the injection voltage [5, 6].

Under microwave control, the current varies across the entire range from zero to the maximum within a short generated pulse; therefore, electron beam shape must be made weakly dependent from current. This quality of the beam can be achieved by a focusing electrode with an optimal aperture angle of 135°, while the anode electrode should be flat. Then, the electron beam in the gap between the electrodes will have a parallel cylindrical shape, diverging in a relatively small angle beyond the anode in a wide current range [8, p. 150].

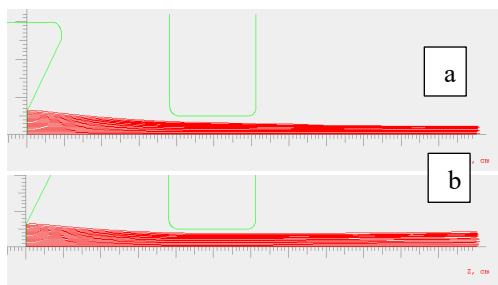

Figure 1: Shape of gun electrodes and beam trajectories. a - beam current ~0.6 A, b - beam current ~1 A.

A similar shape of the electrodes is used in this work. To adjust the beam divergence beyond the anode port, the aperture angle of the focusing electrode was chosen equal to 128°. A cathode grid assembly of the GS-34 lamp is used, which has emitting surface diameter 13 mm and transit ports diameter in the accelerating cavities 10 mm, therefore the diameter of the flat anode electrode port was made

ISBN: 978-3-95450-197-7 doi:10.18429/JACoW-RUPAC2018-WEPSB04

THERMODYNAMICS SIMULATION FOR THE CW RADIO-FREQUENCY QUADRUPOLE ACCELERATOR

S. M. Polozov, Y. Y. Lozeev, National Research Nuclear University "MEPhI",
115409, Moscow, Russia

Abstract

Design and construction of CW high intensity linacs are important issues of worldwide accelerator technology development. RFQ linacs are useful for large scale research facilities such as SNS, ADS and FRIB. RFQ are necessary to use for low-energy nuclear and radioactive ion physics (e.g., DERICA - Dubna Electron – Radioactive Ion Collider fAcility project, Dubna, Russia) [1]. Some solutions are applied for RFQ to operate in CW mode. The decrease of the accelerating field and of the RF field overvoltage is one of such solutions. The maximal field for CW RFQ traditionally limit by 1.3-1.5 of the Kilpatrick criterion value comparatively with 1.8-2.0 for the pulse mode. But the thermostabilization of the RFQ cavity is very important problem. Accelerating structure undergoes high thermal loads for operating a CW mode, therefore water cooling system is needed. In this report, a selection of an optimal resonator shape and water cooling system configuration was done and thermodynamics simulation results are also presented.

INTRODUCTION

Today CW RFQ ion linacs are used as an initial part for large scale accelerator facilities mainly in accelerator driven subcritical reactors (China Accelerator Driven Sub-critical System, [2]) or compact neutron sources (FRANZ, Frankfurt Neutron Source, [3]) or rare isotope accelerators (FRIB, [4]).

Current results of thermodynamics simulations of CW-RFQ cavity are presented in this paper. Accelerating structure is segmented-vane cavity (SV-RFQ) operating on 162 MHz. Main parameters of CW RFQ are presented in Table 1. Results of the beam dynamics study and previous design of the SV-RFQ cavity were presented in [5-8].

Table 1: Main Parameters of the CW RFQ

Parameter	Value
Ions	protons
Input energy, keV	46
Output energy, MeV	2
Frequency, MHz	162
Voltage, kV	90
Length, cm	345
Average radius, cm	0.530
Vanes half-width, cm	0.412
Modulation	1….2.25
Synchronous phase	−90°….−33°
Max. input beam current, mA	10
Max. input emittance, cm·mrad	6
Particle transmission, %	> 99

COMPARISON OF THERMODYNAMICS SIMULATION FOR TWO MODELS OF THE SV-RFQ CAVITY

CW operation mode of accelerating structures implies high thermal loads which can lead to operating mode frequency shift. As it was shown by simulations, power losses for 162 MHz CW-RFQ are about 100 kW (or ~35 kW per meter) for the maximum E-field at the electrode surface 15.8 MV/m. Such values of the dissipated power increase equilibrium cavity temperature up to 430 K, so water cooling is critical for the cavity. A number of water coolant channels usually are fabricated inside the cavity electrodes in order to provide its thermal stabilization under CW mode.

Water coolant channels can be drilled around magnetic coupled windows as the main points undergoing strong thermal loads are nearby their edges. Current distribution varies depending on the coupled window shape. Semi-elliptical and rectangular windows were chosen for comparison. Models with semi-elliptical and rectangular windows with their coolant system are presented in Fig. 1 and 2 respectively. Main parameters of coolant system are presented in Table 2.

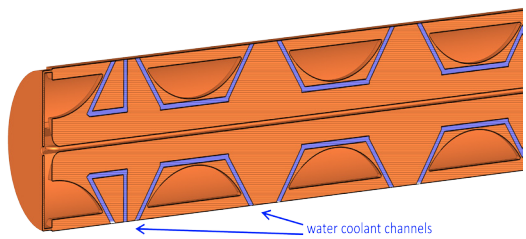

Figure 1: Water coolant system layout for model with semi-elliptical windows.

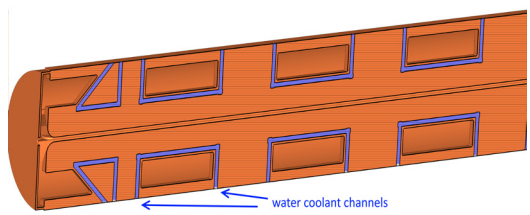

Figure 2: Water coolant system layout for model with rectangular windows.

ISBN: 978-3-95450-197-7 doi:10.18429/JACoW-RUPAC2018-WEPSB05

BEAM DYNAMICS SIMULATION RESULTS IN THE 6 GEV TOP-UP INJECTION LINAC OF THE 4TH GENERATION LIGHT SOURCE USSR

S.M. Polozov, I.A. Ashanin, Yu.D. Kliuchevskaia, M.V. Lalayan, A.I. Pronikov, V.I. Rashchikov
National Research Nuclear University - Moscow Engineering Physics Institute, Moscow, Russia
also at NRC "Kurchatov Institute", Moscow, Russia

Abstract

The new project of 4th generation synchrotron light source USSR (Ultimate Source of Synchrotron Radiation, early known as Specialized Synchrotron Radiation Source, SSRS-4) is under development today. It was proposed that USSR will include both storage ring and soft FEL and one linac will used for injection in synchrotron and as a bunch driver for FEL. The general concept of the top-up linac is proposed and the beam dynamics was simulated. It is suggested to use two RF-guns in this linac similar to Super-KEKB, MAX-IV and CERN FCC. One of the RF-guns should be classical with thermionic cathode and will be used for injection into storage ring. The second one having photogun will use to generate a bunch train for FEL. Current results of the top-up linac general scheme development and first results of the beam dynamics simulation will present in paper.

INTRODUCTION

Starting 2017 the new project of 4th generation synchrotron light source called Specialized Synchrotron Radiation Source (SSRS4) is under development in Russia. Current version of SSRS4 general layout includes 6 GeV main storage ring and top-up injection linac. Free-electron laser will also include in SSRS and top-up linac will used both for injection in the storage ring and for generation of the drive beam for FEL. Such layout leads to two linacs operation modes: 6 GeV beams for injection and 6-7 GeV high-brilliance bunches for FEL. It leads to the same for-injection scheme as it was used for SuperKEK-B and MAX-IV and is proposed for FCC-ee [1-2]: two RF-guns with photocathode and thermionic cathode and one main linac with large number of identical regular sections (see Fig. 1).

The conceptual design of new linac is now under development. The top-up injection scheme into SSRS4 main storage synchrotron is preferable. Thus it is proposed to use the same linac with two RF-guns. First of them will photogun and can be used to generate the drive beam for FEL. The second one will RF-gun with thermionic cathode can be used for injection in to storage ring. Both injectors will work with the same regular part of the linac which consists of 80-90 identical sections.

The possible layouts of SSRS4 injection linac are shown in Fig. 1. Let us present results of the beam dynamics simulation for photogun, RF gun with thermionic cathode and for the regular part also. The RF power requirements for linac will be also briefly discussed.

The planning storage beam current for the main ring will be close to 200 mA and the single bunch injection scheme is discussed as the main propose. But for FEL we need to generate a train of bunches to realize the effective generation, in SASE mode for an example. This demand leads to the one specific need for the linac section – the beam loading should be not sufficiently influences to the output beam energy in the bunch train. This effect will limit the bunch charge generated on the photocathode. For example, the train can consists of 10-12 bunches with the charge of 200-250 pC or of 20-300 bunches with the charge of 100 pc, but in not consists of 10 bunches with 1 nC charge. The operating frequency was chosen equal to 2856 MHz.

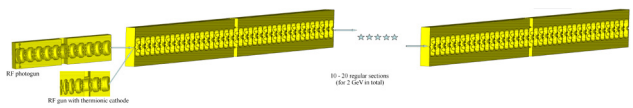

Figure 1: Possible scheme of the linac layout (RF gun with thermionic cathode is an option for high intensity drive bunches production for e^-/e^+ conversion).

BEAM DYNAMICS IN PHOTOGUNS

The beam dynamics simulation was done both for RF-guns and regular section using the BEAMDULAC-BL code [3-5]. This code was developed at MEPhI for beam dynamics simulations in RF linacs and transport channels. It has modular structure and a number of routines to solve different tasks: initial particles distribution (uniform, Gauss, KV, waterbag, etc.), motion equation integration (4th order Runge-Kutta method), beam emittance and other output beam parameters calculation, post processing and other. The code package has versions that take into account own space charge effects: both Coulomb part and RF part (beam irradiation and beam loading) self-consistently. The BEAMDULAC-BL code version was designed to study the beam dynamics in high-intensity electron linacs, it is discussed in detail in [5] and it was tested for a number of e-linac designs [6-9].

The beam dynamics simulation in the RF-photogun shows that 250 pC and 10 ps bunch can be easily accelerated by 5.5-cell accelerating structure with comparatively low accelerating gradient of 600 kV/cm. The current transmission coefficient is close to 100 % here and RF field amplitude of 600 kV/cm is quite enough to have 10.5 MeV after photogun. The bunch energy spread FWHM is about ±1 % (or ±300 keV). The optimization of the ptotogun structure was also done and

ISBN: 978-3-95450-197-7 doi:10.18429/JACoW-RUPAC2018-WEPSB06

EXPERIMENTAL RESEARCHES OF HIGH-POWER ELECTRON BEAM CHARACTERISTICS PERFORMED ON A RESONANCE ACCELERATOR OF CONTINUOUS OPERATION

A.M. Opekunov, N.V. Zavyalov, A.N. Belyaev, Ya.V. Bodryashkin, I.V. Zhukov, I.A. Konyshev, V.V. Kuznetsov, N.N. Kurapov, I.A. Mashin, L.E. Polyakov, G.P. Pospelov, S.A. Putevskoj, M.L. Smetanin, A.V. Telnov, A.N. Shein, I.V. Shorikov, RFNC-VNIIEF, Sarov, Russia

Abstract

A resonance accelerator [1] is being created in RFNC-VNIIEF to generate a beam with electron energy from 1.5 to 7.5 MeV and average beam power up to 300 kW. The accelerator basis is half-wavelength coaxial cavity. Electrons gain required energy after multiple passes through accelerating cavity.

The present paper gives the results of electron dynamics computer simulation in terms of space charge effect. Electrons injection parameters into the accelerating cavity, which allows beam production with sufficient electron energy, were defined.

Novel experiments on the facility were carried out at the RF power level up to 180 kW. The measured electron energy after the first pass of acceleration is 1.5 MeV. Then the beam turns back to the accelerating cavity with the aid of the beam recirculation system. The measured electron energy after the second pass is 3 MeV. Energy spectrum of electrons in a bunch also was determined and the average beam current was measured on each acceleration stage.

INTRODUCTION

The produced accelerator is designed to operate both in pulse-periodic and continuous mode of radiation production. The design and principle of such accelerator operation are minutely described in paper [1].

At present the accelerator complex (Fig. 1) involves a coaxial accelerating cavity (100 MHz), RF injector (100 keV, 40 mA), RF generator (180 kW), RF power input unit, vacuum system, cooling system, automated control system as well as some elements of beam transport, delivery and extraction systems.

Acceleration process is based on multiple passes of electron beam through the accelerating gaps of coaxial half-wavelength cavity (type of oscillations T_1) on the level of median plane where the magnetic component of RF field is entirely absent

Electric field distribution in accelerating gaps arised in the cavity at RF power of ~ 165 kW is sufficient for electron energy gain up to 1.5 MeV per one pass in the accelerating phase of RF field.

BEAM DYNAMICS CALCULATION

The calculation of electron beam dynamics was performed using program ASTRA [2]. The basic task at this stage is to define the criteria of electron beam injection to the accelerating cavity at which the sufficient conditions for electron energy gain by 1.5 MeV per one pass with minimum current losses at all sections are realized.

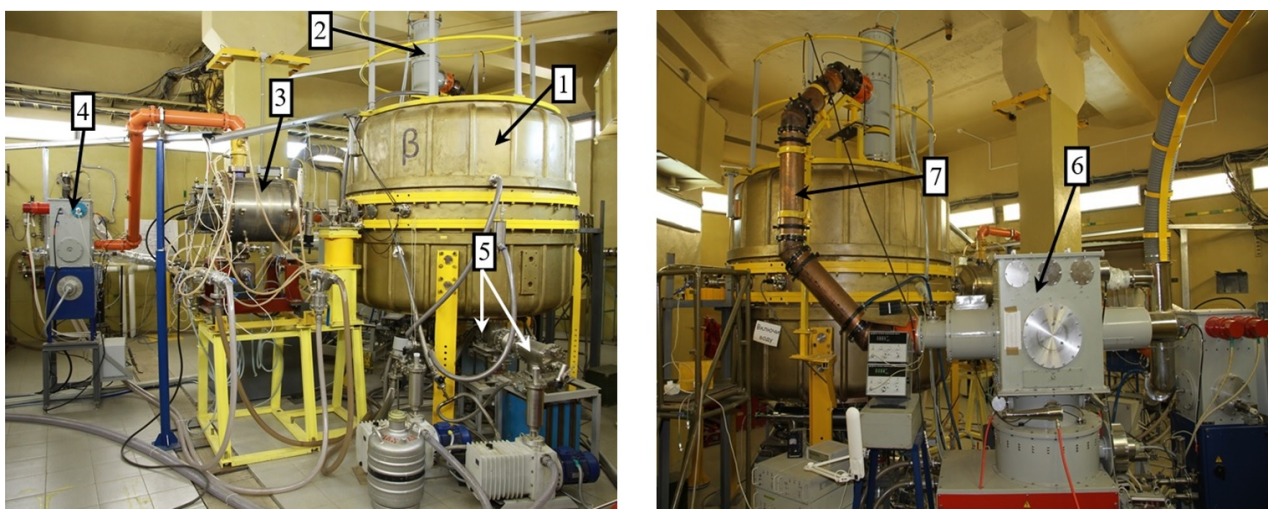

Figure 1: Accelerator external view: 1 – accelerating cavity; 2 – RF power input unit; 3 – RF injector; 4 – generator of RF injector 16 kW; 5 – vacuum pumps; 6 – RF generator 180 kW; 7 – coaxial feeder.

Opekunov@expd.vniief.ru

ISBN: 978-3-95450-197-7 doi:10.18429/JACoW-RUPAC2018-WEPSB07

INJECTION SYSTEM OF CONTINUOUSLY WORKING RESONANCE ACCELERATOR WITH HIGH POWER OF ELECTRON BEAM

L.E. Polyakov#, A.N. Belyaev, I.V. Zhukov, V.V. Kuznetsov, N.N. Kurapov, A.M. Opekunov, G.P. Pospelov, S.M. Treskov, A.N. Shein, I.V. Shorikov, RFNC-VNIIEF, Sarov, Russia

Abstract

The paper presents a modified variant of injection channel for electron accelerator augmented by diagnostic equipment and additional magnetic optical elements.

To optimize operation modes of a new injection channel elements a computer simulation of electron dynamics was performed.

An experimental bench with a capability for electron beam diagnostics was developed on the basis of conducted calculations. Composition and geometry of the upgraded injection channel are fully reproduced on the experimental bench.

By the results of calculation and experimental studies an optimal variant of the injection channel is proposed. Such modified channel is supposed to be introduced into the acceleration complex.

INTRODUCTION

Designed resonance accelerator is intended for the electron beam production with discrete values of energy 1.5, 4.5 and 7.5 MeV and average power up to 300 kW [1]. The accelerator is based on the coaxial cavity, operating at the frequency 100 MHz.

Parameters of beam injection into the accelerating cavity possess a vital importance in approaching design characteristics of the output electron beam. Therefore, it is necessary to efficiently control the electron beam characteristics on the injection stage during accelerator operation. As of today there is lack of beam diagnostic devices in the existing injection channel. The presented paper proposes a variant of channel modification by diagnostic equipment and additional beam-focusing elements. The implemented equipment was tested on the experimental bench. Performed tests will also allow to optimize working parameters of RF injector and focusing elements.

ACCELERATOR INJECTION CHANNEL

The accelerator's electron injector is a grid-controlled hot-cathode gun based on the RF quarter-wavelength coaxial cavity (100 keV, 40 mA, 100 MHz) [2]. An advantage of such injector is a capability for longitudinal beam bunching by emission phase variation.

The external view of the active injection channel is shown in Fig. 1. A list of magnetic optical elements involves two focusing solenoids (2) and (4) and a magnetic quadrupole lens (5), required for compensating various effects of transverse components of electric field along of the beam trajectory in accelerating cavity [1].

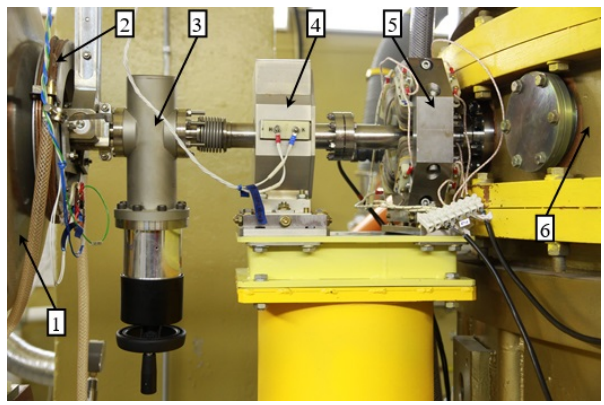

Figure 1: External view of injection channel: 1 – RF injector; 2 – focusing solenoid №1; 3 – high vacuum valve; 4 – focusing solenoid №2; 5 – magnetic quadrupole lens; 6 – accelerating cavity.

DIAGNOSTIC EQUIPMENT

Two space-divided resistive current pickups are planned to use in electron energy, pulse current and bunch length measurement (Fig. 2).

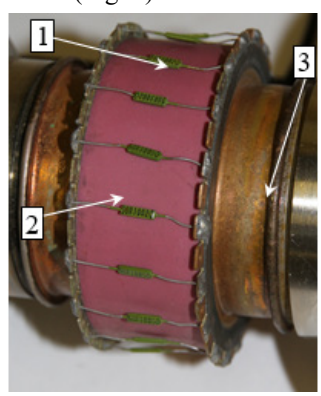

Figure 2: External view of resistive pickup: 1 – resistor 50 Ohm; 2 – ceramic insulator; 3 – beam transporting channel.

Diagnostic system based on the beam position monitor (BPM) and electromagnetic beam corrector (EBC) was developed to control a transverse beam position in the injection channel. BPM is a cylindrical chamber and four capacitive pickups in the form of disks, mounted

LEPolyakov@vniief.ru

ISBN: 978-3-95450-197-7 doi:10.18429/JACoW-RUPAC2018-WEPSB08

PROSPECTS OF CREATING A MODERN RESONANCE ELECTRON ACCELERATOR

A.N. Shein#, A.V. Telnov, I.V. Shorikov, RFNC-VNIIEF, Sarov, Russia

Abstract

The paper reports a brief description of a linear electron accelerator LU-10-20 and the necessity for its upgrading. A review of existing native and foreign RF power sources, meeting the assigned requirements for the RF power supply system of the upgraded accelerator, is presented. A design of the travelling wave accelerating structure based on disk-loaded waveguide is presented.

Preliminary electro-dynamic calculations of the accelerating section fed by the selected RF power source are presented as a paper result.

INTRODUCTION

A linear resonance electron accelerator LU-10-20 [1] aimed at carrying out radiation processing of materials and researching radiation processes has been functioning in RFNC VNIIEF since 1994. The average energy of accelerated electrons is up to 10 MeV, the average electron beam power – up to 12 kW. This accelerator has demonstrated that it is highly useful for performing radiation researches and tests.

Currently the major part of accelerator systems, such as RF power supply system and accelerating structure, have lost its original characteristics during a long-term performance and possess an obsolete material and component base. That is why the design and development of a modern accelerator complex with the similar output parameters of electron beam, high reliability and large period of undisturbed operation is highly promising. Such a linear accelerator should replace LU-10-20 in future.

RF POWER SOURCES

The base for development of a modern accelerator complex based on linear resonance electron accelerator is a RF power supply system. Magnetrons and klystrons are mostly spread as RF power sources. They possess by rather a high efficiency, high reliability and a large lifetime.

Magnetrons and klystrons should correspond to the following requirements to supply the required electron beam parameters: the output average power – about 20 kW, output pulse power – approximately 10 MW, operating frequency – up to 3 GHz.

These requirements are met by RF power sources, meant for employment in linear electron accelerators, produced by a number of native and foreign manufacturers of microwave-devices. Table 1 reports parameters of some RF power sources of the given manufacturers.

Table 1: Magnetrons and Klystrons Parameters

Name	$f_{oper.}$, MHz	$P_{pulse.}$, MW	$P_{aver.}$, kW	Manufacturer
Magnetron MI-328	1818	6,5	22	«Toriy» (Moscow)
Klystron KIU-15	1818	20	18	«Istok» (Fryazino)
Magnetron MI-435	1886	10	22	«Toriy» (Moscow)
Magnetron MI-470	1886	10	30;50	«Toriy» (Moscow)
Klystron KIU-53	2797	12	18	«Kontakt» (Saratov)
Klystron KIU-147A	2856	6	25	«Toriy» (Moscow)
Klystron VKS-8262F	2856	5	36	CPI, USA
Klystron TH 2128 A	2856	45	20	Thales, France
Klystron TH 2128 E	2856	30	24	Thales, France
Klystron TH 2100 C	2998	45	20	Thales, France

All above-mentioned RF power sources have output power pulse duration from 4 up to 16 μs.

To modernize LU-10-20 linear accelerator most suitable are magnetrons MI-328, MI-435 and MI-470 produced by «Toriy», as well as klystron KIU-15 manufactured by «Istok». These microwave-devices allow provision of required average electron beam power not less than 10 kW and average accelerated electron energy up to 10 MeV. Additional factor in favor of selection of Russian manufacturer of microwave-devices is more profitable delivery conditions, as compared to the foreign analogs.

TYPE OF ACCELERATING STRUCTURE

The accelerating structure for linear resonance electron accelerator, meant to replace LU-10-20, should provide an output average power of an electron beam more than 10 kW with average energy of electrons up to 10 MeV.

Linear resonance electron accelerators have two types of accelerating structures: standing wave and travelling wave structures. Standing wave structures have a high efficiency of the use RF power from microwave-device for electron acceleration and can provide forming and further acceleration of the electron bunches without use of a focusing solenoid. Travelling wave structures allow possibility to vary the energy of accelerated electrons within some limits by a change of electron beam current. These structures possess less strict requirements for

ANShein@vniief.ru

ISBN: 978-3-95450-197-7 doi:10.18429/JACoW-RUPAC2018-WEPSB09

DISTINCTIONS OF RF PARAMETERS TUNING FOR ACCELERATION PERIOD OF STRUCTURE WITH SPATIALLY PERIODIC RFQ FOCUSING

O.K. Belyaev, Yu.A. Budanov I.A. Zvonarev,
NRC "Kurchatov Institute" – IHEP, Protvino, Moscow region, Russia

Abstract

Distinctions of RF-tuning for accelerating structure with spatially periodic RFQ focusing are considered. Capacitor's method for tune of resonance frequency with minimum accelerating fields distortions presented. Experimental and theoretical results are shown.

The resonance of an intermediate electrode holder in accelerating structure with spatially periodic RFQ focusing is described. The different designs of the holder to escape the influence of this resonance on acceleration are considered. The variant of water cooling design of the holder for low relative pulse duration accelerator is offered.

INTRODUCTION

The accelerating structure with spatially periodic radio frequency quadrupole (RFQ) focusing is used for acceleration of hydrogen ions. In IHEP considerable experience of design and tuning of these structures is accumulated. There are two RFQ drift tube proton linacs, named the LU-30 and LU-30M, in the IHEP Protvino, that are presently in operation. Both accelerators are the unique machines employing high-frequency quadrupole focusing up to 30 MeV at exit. Since 1985 till now, LU-30 routinely operates as an injector to booster proton synchrotron, thus feeding the entire accelerator complex of IHEP. The LU-30M is now run in a stand-alone test operation mode.

Period of this structure consist of an axial gap (accelerating), and a quadrupole gap (focusing). These gaps are separated by intermediate electrode. Gap's electrodes and an intermediate electrode holder are installed in resonator with longitudinal magnetic field [1], [2], [3].

Work is currently under way on advancing of tuning techniques for spatially periodic RFQ focusing accelerators with attraction of modern numerical methods.

Opportunity for tuning of working frequency with minimum accelerating field distortions is shown by experimental and numerical methods. The resonance of an intermediate electrode holder also is described.

CAPACITOR TUNING OF FREQUENCY

Frequency tuning of resonators for LU-30 and LU-30M has been realized by turn of copper rings in a resonator magnetic field in vacuum. Turn of one ring changes frequency approximately on 8÷25 kHz, depending of the resonator Q-factor and the size of a ring. The method offered now allows expanding a range of tuning frequency essentially with minimum accelerating field distortions.

Offered capacitor tuning of frequency has significant feature. Tuning elements in the form of the metal flat disks located at holders are settled down in the field of low amplitude electric field of the resonator.

On Fig. 1 placing of tuning elements on an internal surface of the container of the H-resonator is shown and parameters of tuning elements - an angle of an inclination **fi** and the distance to surface of resonator **dd** are shown.

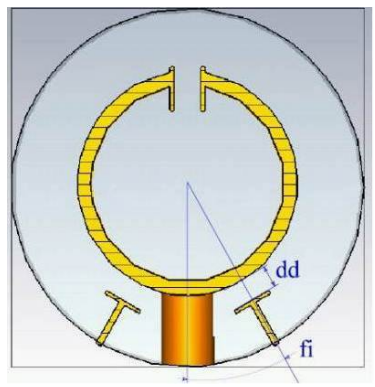

Figure 1: Cross section of H-resonator with tuning elements and dummy load.

On fig. 2 the curve of change of resonant frequency for the H-resonator for position of electrodes with the angle to a vertical fi=30 ° is shown, this frequency is a function of distance from a flat part of tuning electrodes to an external surface of the H-resonator dd.

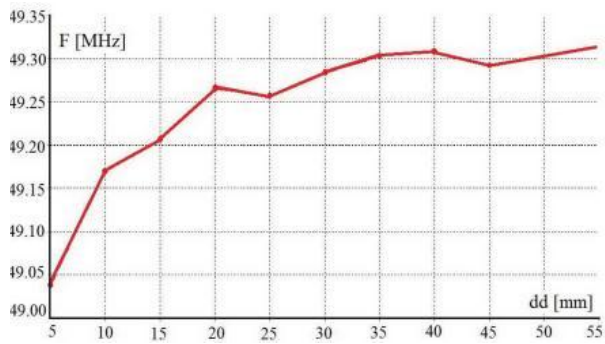

Figure 2: Frequency as a function of space dd.

From the analysis of the function represented on Fig. 2 follows, that effective tuning of frequency is possible at change dd in the range from 5 mm to 35 mm. The further increase of an interval dd not essentially influences frequency of the resonator, but too small size dd can lead to breakdown.

ISBN: 978-3-95450-197-7 doi:10.18429/JACoW-RUPAC2018-WEPSB10

STUDY OF THE NON-UNIFORM COUPLED SYSTEM MODEL OF CDS SECTION AND WAVEGUIDE SEGMENT BASED ON MULTIMODE APPROXIMATION

I.V. Rybakov†, V.V. Paramonov, Institute for Nuclear Research of the RAS, Moscow, Russia

Abstract

With the development of the new CDS cavity for the first four-section cavity of the main part of INR RAS linac replacement application of the bridge devices, similar to existing rectangular waveguide segments-based devices, is supposed. Numerical simulation of a complete cavity coupled with bridge devices requires unattainable computing resources. For this reason, the analytical representation for the coupled non-uniform system based on multimode approximation is considered. The analytical model for a system consisting of a short CDS section coupled with a rectangular waveguide segment is presented. The model is calibrated by direct numerical simulation. A generalization allowing parameters selection for the new CDS cavity sections and bridge devices coupling based on the presented model is proposed.

INTRODUCTION

The first cavity of the main part of INR linac works for proton acceleration in the range β=0.4313 – 0.4489 with acceleration gradient $E_0 T\cos\varphi_s$ = 2.5 MV/m and the synchronous phase φ_s=-33°. The cavity has the aperture radius r_a= 17 mm, operating frequency f_a=991.0 MHz and the required operating regime is with RF pulse length τ=200 μs and Repetition Rate (RR) up to 100 Hz. The cavity consists of four DAW sections connected by three rectangular-cross bridge devices through slots [1]. The input of RF power is implemented through the bridge between sections 2 and 3. Each section of the cavity consists of 18 – 21 periods of the structure.

The new CDS structure was proposed for the first cavity replacement [2]. The bridge devices for the new cavity are proposed to be similar with existing system. A simplified schematic of the connection between two CDS sections is shown at Fig. 1.

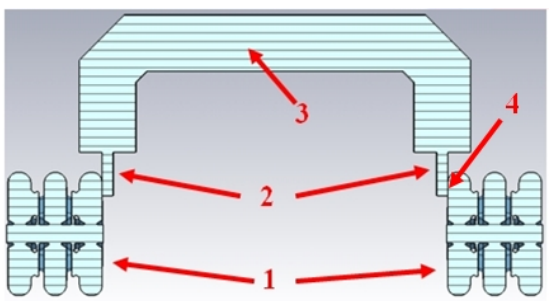

Figure 1: Schematic sketch of two CDS sections with a bridge device, 1 – cavity sections, 2 – transition waveguide, 3 – bridge device, 4 – coupling slot.

In case of RF input through the bridge device the full cavity with bridge devices should be tuned as complete system [3]. In this case numerical simulations of the cavity with bridge devices require unattainable computing resources. Therefore the analytical model based on multimode approximation is considered [3].

ANALYTICAL MODEL

We consider the non-uniform system consisting of bi-periodic structure cavity coupled with a segment of rectangular-cross waveguide (bridge) through the slot. The field distribution in the cavity could be represented as a sum of eigenmodes with frequencies $\omega^c{}_n$ [4]:

$$\overline{H}^c = \sum_n h_n^c \overline{H}_n^c, \mu_0 \int_{V_c} \overline{H}_n^c \overline{H}_n^{c*} dV = 2W_0 , \quad (1)$$

where V_c is the cavity volume, W_0 is stored energy. The magnetic field in the waveguide segment could be presented similarly:

$$\overline{H}^b = \sum_k h_k^b \overline{H}_k^b, \mu_0 \int_{V_b} \overline{H}_k^b \overline{H}_k^{b*} dV = 2W_0 , \quad (2)$$

$h_n{}^b$ and $h_n{}^c$ are the amplitude coefficients. The magnetic field in the bridge and cavity is excitated by the tangential electric field of the slot:

$$h_n^c = \frac{j\omega \int_{S^s} \left[\overline{E}^s \overline{H}_n^{c*}\right] d\overline{S}}{2W_0(\omega^2 - \omega_n^{c\,2})}, \quad h_k^b = \frac{j\omega \int_{S^s} \left[\overline{E}^s \overline{H}_k^{b*}\right] d\overline{S}}{2W_0(\omega^2 - \omega_k^{b\,2})} , \quad (3)$$

where E^s is the slot field, dS is normal to the slot area S^s. Herewith the magnetic field on the slot radius r_s in the cavity and the bridge can be presented as:

† irybakov@inr.ru

ISBN: 978-3-95450-197-7 doi:10.18429/JACoW-RUPAC2018-WEPSB11

FEATURES OF ACCELERATION AND FOCUSING OF CLUSTER ION BEAM IN RESONANT LINAC STRUCTURES

S.V. Plotnikov, V.I. Turchin, NRC KI – ITEP, Moscow, Russian Federation

Abstract

The prospective opportunity for high-temperature plasma generation by opposing collision of accelerated to 10-20 keV/amu cluster ion beams of hydrogen isotopes within the rectilinear section of magnetic trap was considered earlier in ITEP. It showed the aggregate deuteron (or tritium) atom per charge unit in accelerated cluster ions may consider a possibility to create the thermonuclear fuel mass up to values when the mutual retardation of all the nucleons in colliding beams. In the present work some examples of earlier created RF accelerating systems for heavy ion linac may be considered as prototypes for study of features and some off-beatings of heavy cluster ions of hydrogen isotopes for plasma generation are discussed. Some features of basic possibility for creation such kind accelerator systems for ion with mass-to-charge ratio of 10^3-10^4 are considered.

INTRODUCTION

Currently NRC KI ITEP is working on the study of processes occurring under the influence of an intense accelerated heavy ion beam on a substance in various states including extreme thermodynamic ones. One of the approaches is related to the effective transformation of the energy of accelerated super-heavy (cluster) hydrogen ions into the energy of thermal motion of nuclei as a result of turbulent relaxation of plasmoids in mutual collisions of accelerated cluster ions. These studies in particular are a consequence of the fact that traditional fusion schemes based on the initiation of a thermonuclear reaction by heating and compressing the fuel-containing target with powerful beams of accelerated heavy ions lead to create very complicated bulky and expensive complexes.

An original method of high-temperature plasma generation by counter-collision of hydrogen cluster ions accelerated to the energy of 10-20 keV per deuteron inside a magnetic trap was proposed in ITEF about 30 years ago by V.V. Okorokov et al.[1]. The bottom line is that due to the large number of deuterium atoms per charge unit in clusters it is possible to bring the density of particles in accelerated beams to values that provide mutual inhibition of all deuterons of colliding clusters. Thus, clusters allow accelerating the mass of matter necessary for initiating a thermonuclear reaction due to reducing the space charge effect by 3-4 orders.

The method has no fundamental limitations for the production of thermonuclear plasma with a temperature of not only 10 keV (DT-synthesis), but also 100 keV (DD-synthesis) and even 200-500 keV (p-Li, p-B and D-He^3 – the so-called "neutron-free" fusion. To obtain a temperature of 10 keV the energy of each cluster at $N=10^3$ must be at least 20 MeV.

LINAC FOR CLUSTER IONS

The term "cluster" is used to show that the beam particles are combined into atomic clusters connected by van der Waals forces. The size of these clusters span a wide range from dimer to micro-crystals or micro-droplets containing millions of atoms.

Let us estimate the possibility of creating an accelerating-focusing system with the mass of accelerated single-charge ions of $N=10^2$-10^6 with no going into details of the physical implementation of this approach just taking into account the features of cluster ion acceleration. Note that cluster charge is usually equal to z= +1 since even at z= +2 the cluster is broken by the Coulomb field of these charges.

In Fig. 1 the example of cluster ion source is shown. Gas clusters are composed of atoms of a substance that is in a gaseous state under normal conditions. To obtain gas clusters it is necessary to use cooling. This is usually achieved by use the cooling effect of the gas expanding in the supersonic nozzle. Depending on the nozzle parameters clusters of any size can be generated.

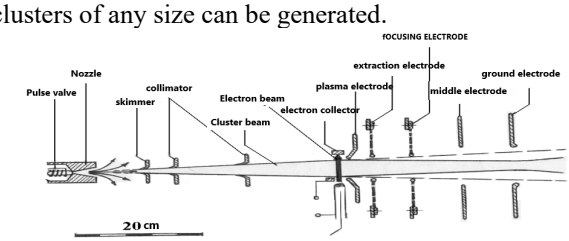

Figure 1: Scheme example of cluster ion source.

In Fig. 2 the mass spectrum coming from the cluster ion source [2] is shown. Due to wide mass spectrum it is required to capture the maximum part of this spectrum in the acceleration mode. The most natural seems to be the cluster acceleration in RFQ linac. The calculations show in the acceleration mode can be captured ~50% of the continuous mass spectrum obtained from this type source.

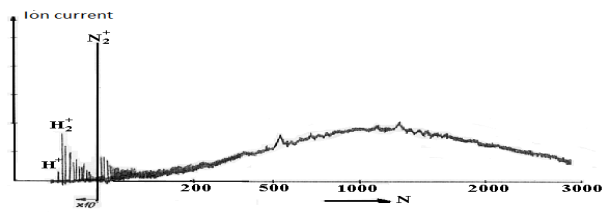

Figure 2: Typical spectrum of hydrogen cluster beam.

The 2.5 MeV 6 MHz RFQ linac designed for heavy ion acceleration with mass-to-charge ratio of ~100 was earlier created in ITEP (Fig.3) [3]. The linac structure with such a low frequency of the accelerating field required the solution of number of some technological problems. The spiral supports are made in three-rayed star form to provide acceptable mechanical stiffness. Acceleration of heavy

ISBN: 978-3-95450-197-7 doi:10.18429/JACoW-RUPAC2018-WEPSB12

ACCELERATION OF THE MULTICHARGED IONS WITH DIFFERENT A/Z RATIOS IN SINGLE RFQ CHANNEL WITHOUT MAGNETIC FIELD FOCUSING

D. Ovsyannikov, Saint-Petersburg State University, St. Petersburg,
Yu. Svistunov, Saint-Petersburg State University and JSC "NIIEFA", St. Petersburg, Russia
V. Altsybeyev*, A. Durkin, Saint-Petersburg State University

Abstract

There are considered acceleration of few types multicharged ions with different A/Z ratio in single accelerating RFQ channel without outer focusing magnetic field. RFQ may be independent accelerator or as part of injection system into DTL of high energy. There are considered compact RFQ with high operating frequency (for example frequencis of P-diapason). So magnetic focusing is absent mathematical methods of control theory are used for optimization of RFQ vane geometry to obtain exit beam parameters suitable for further acceleration. It is possible separate acceleration a few type of ions in single RFQ channel or simultaneous acceleration if (case of heavy ions) ion currents are very small.

INTRODUCTION

The purpose of this paper is to study the possibility to use a radio-frequency quadrupole (RFQ) with high operating frequency for acceleration of somewhat ion types with different A/Z in single RFQ accelerating channel without outer focusing magnetic field. Forces if space charge are considered under modelling.

At present multicharged ions are used for different applications purposes such as implantation, medical radiation therapy, filter manufacturing and researches of nuclear structure. In this last case contemporary heavy ion injectors are complex systems which can include many different elements, for example [1]: an ECR source, an extracting system, magnetic and electrostatic lenses, an accelerating column, single and multi–harmonic bunchers, a RFQ, superconducting resonators. In the papers [2, 3] it has been shown that the use of RFQ after low-energy beam transport(LEBT) improves emittance, capture ratio and current value ot the ion beams.

Resonators for multicharged ion injector that could accelerate the ions in diapason from hydrogen to uranium and from carbon to uranium were considered in papers [4] and [5] respectively. Naturally, the operating frequencies of these resonators are low (85 and 5 MHz accordingly), and they need a strong additional focusing magnetic field to provide good particle dynamics.

Separate acceleration of two or more ions types in single accelerating channel of RFQ withouth magnetic field focusing is considered in this paper. RFQ may be independent accelerator or first part of accelerating tract.

* v.altsybeev@spbu.ru

The successful acceleration of the different types of ions separately in single RFQ channel depends on the fulfillment of a few conditions.

1. Initially RFQ channel is designed to accelerate an ion beam with the greatest A/Z ratio. It is the main particle.
2. Velocities of the ions of different types injected into the RFQ channel must be equal to the RFQ input.
3. To obtain better conditions for the acceleration of other ions (not main) the matching section geometry needs to be optimized (see [6]) and there should be a possibility to change the intervane voltage depending on the ion type in the determined limits.

The examples of ion dynamics modelling in such RFQ and description of the used codes are given below. The initial data for modeling can be found in [2, 3, 7, 8]. In general case formation of the beam for injection into RFQ can require optimization of the LEBT parameters. Possible procedure of particle dynamics optimization is presented in [9].

RFQ OPTIMIZATION AND BEAM DYNAMICS MODELING

Software package DAISI was used for RFQ designing. For dynamics modeling the DAISI uses the standart model with standing-wave approximation [10].

$$\frac{d^2z}{d\tau^2} = Q_z,\ \frac{dS_{11}^{x,y}}{d\tau} = S_{21}^{x,y},$$
$$\frac{dS_{21}^{x,y}}{d\tau} = Q_{x,y}S_{11}^{x,y} + S_{22}^{x,y},\ \frac{dS_{22}^{x,y}}{d\tau} = 2Q_{x,y}S_{12}^{x,y}.$$

Here $\tau = ct$; Q_z, Q_x, Q_y is RF field and space charge forces; $S_{11}^{x,y}, S_{21}^{x,y}, S_{22}^{x,y}$ — elements of $G^{x,y} = \begin{pmatrix} S_{11}^{x,y} & S_{21}^{x,y} \\ S_{21}^{x,y} & S_{22}^{x,y} \end{pmatrix}$, which describe the dynamics of the initial transversal distribution ellipses $G_0^{x,y}$ in phase planes $(y, dy/dt)$ and $(x, dx/dt)$. In this mode longitudinal motion dont depend on transversal one. Space charge forces may be included on optimization stage. Calculations by code LIDOS are used on this stage also for find correction of results. Two of methods of numerical optimization dynamics are used in DAISI: particle swarm method(PSM) and gradient descend paradigm for evaluation of synchronous phase sequence and acceleration efficiency. In PSM multivariable function optimization may

ISBN: 978-3-95450-197-7 doi:10.18429/JACoW-RUPAC2018-WEPSB13

FURTHER DEVELOPMENT OF SC CW-LINAC AT GSI

S. Yaramyshev[*,3], W. Barth[1,3], C. Burandt[1], M. Heilmann,
GSI Helmholtzzentrum fuer Schwerionenforschung, Darmstadt, Germany
K. Aulenbacher[2], F. Dziuba, V. Gettmann, T. Kuerzeder, M. Miski-Oglu,
HIM, Helmholtz Institute Mainz, Mainz, Germany
M. Basten, M. Busch, H. Podlech, M. Schwarz,
IAP, Goethe-University Frankfurt, Frankfurt am Main, Germany
[1]also HIM, Helmholtz Institut Mainz, Germany
[2]also IKP, Johannes Gutenberg-University, Mainz, Germany
[3]also National Research Nuclear University MEPhI, Moscow, Russia

Abstract

Recently the first section of a standalone superconducting continuous wave heavy ion linac HELIAC (HElmholtz LInear ACcelerator) as a demonstration of the capability of 217 MHz multi gap Crossbar H-mode structures has been commissioned and extensively tested with beam at GSI. The demonstrator set up reached acceleration of heavy ions up to the design beam energy and beyond. The required acceleration gain of 0.5 MeV/u was achieved with heavy ion beams even above the design mass to charge ratio at maximum available beam intensity and full beam transmission. This contribution presents further development and optimization of the HELIAC machine at HIM/GSI.

INTRODUCTION

During the last decades the Mendeleyev periodic table of elements was significantly extended up to the nuclei Oganessyan (Og) with the charge number Z = 118 and the mass number A = 294. Fusion-evaporation reactions of the accelerated medium and heavy ions with the heavy-element targets are recently the most successful methods for the laboratory synthesis of Super Heavy Elements (SHE) [1]. Due to the very low crossections of such reactions, the events are extremely rare, what requires weeks of beamtime. Obviously, an increased projectile intensity, in the best case in continuous wave (CW) mode, should improve the SHE yield [2,3].

For this purpose heavy ion superconducting (SC) CW HELIAC is developed at GSI Helmholtzzentrum für Schwerionenforschung (GSI, Darmstadt, Germany) and Helmholtz Institut Mainz (HIM, Mainz, Germany) [4-6] under key support of Goethe-University Frankfurt (IAP, Frankfurt-am-Main, Germany) [7,8] and in collaboration with Moscow Engineering Physics Institute (MEPhI, Moscow, Russia) and Institute for Theoretical and Experimental Physics (ITEP, Moscow, Russia) [9,10].

The Superconducting RF technology, being one of the main features of the HELIAC project, allows for the extremely high accelerating gradient of about 7 MV/m. Therefore it provides for the compact and efficient machine (Fig.1), which is foreseen to be integrated into GSI accelerator complex.

Due to its advanced characteristics, the HELIAC stays well in line with other modern CW and SC linac projects at the leading accelerator centers [11]. The design, construction and operation of CW proton and ion linacs are crucial goal of accelerator development worldwide. A large scale facility [12-14], such as accelerator driven system or spallation neutron source, implements a high energy CW linac as an essential part. A medium energy SC CW linac could be used for a number of applications [15], as high productivity isotope generation, material science and boron-neutron capture therapy [16-18]. Therefore further elaboration of superconducting technology [19] and development of SC CW linacs is of high relevance for the accelerator community.

From other side, the HELIAC, being an unique machine, certainly takes its place among a number of modern accelerator activities at GSI, namely the high current heavy ion UNILAC (UNIversal Linear ACcelerator) [20-23], recently upgraded for FAIR (Facility for Antiproton and Ion Research at Darmstadt) [24,25], the proton linac for FAIR [26,27] and proton beams from the UNILAC [28,29], the heavy ion linear decelerator HITRAP (Heavy Ion TRAP) [30,31] and the advanced project LIGHT (Laser Ion Generation, Handling and Transport) for laser acceleration of protons and heavy ions [32,33].

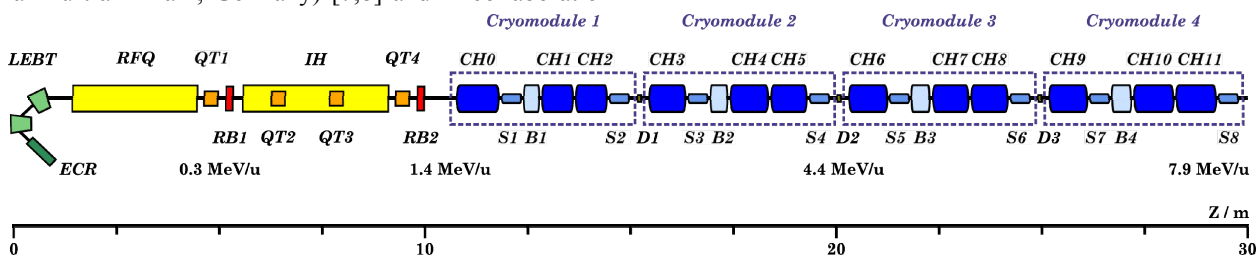

Figure 1: Conceptual layout of the heavy ion SC CW HELIAC with warm injector.

* s.yaramyshev@gsi.de

ISBN: 978-3-95450-197-7 doi:10.18429/JACoW-RUPAC2018-WEPSB16

CALCULATION AND MEASUREMENTS OF THE MAGNETIC FIELD OF IM90 BENDING MAGNET OF CYCLOTRON DC280 AXIAL INJECTION SYSTEM

V.I. Lisov†, I.A. Ivanenko, V.I. Mironov, FLNR, JINR, Dubna, 141980, Russia

Abstract

Nowadays a project of a high-intensity cyclotron of heavy ions DC-280, is realized in Flerov Laboratory of Nuclear Reactions of Joint Institute for Nuclear Research. The cyclotron must provide a middle-mass ion beam intensity (A-50) up to 10 μA/particle for solvation of super-heavy elements synthesis. In a channel of axial injection of the cyclotron, the IM90 magnet is used for beam separation with required ratio of mass to charge A/Z.

The results of calculations of electromagnetic field of IM90 magnet are presented at this paper. 3-D model of the electromagnetic field was created and the corresponding calculations were realized. A calculation of the effective length of the magnet and it comparison with the data of magnet measurements were carried out.

INTRODUCTION

The swivel magnet IM90 is used for the analysis of the beam spectrum in the high axial injection system (Figure 1).

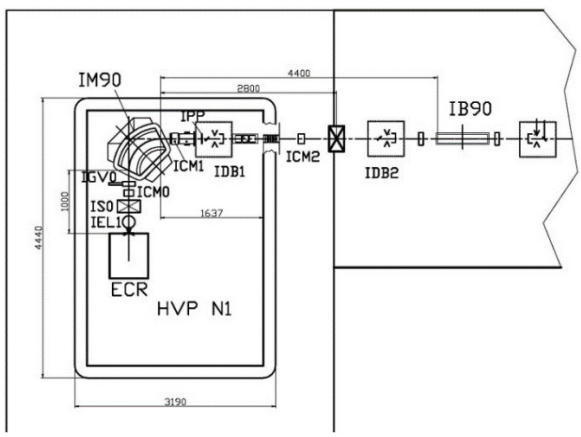

Figure 1: The scheme of the axial injection channel (view from above). Where: ECR- the ion sources; IM90 is the analysing magnet; IB90 is the bender; IS0, IS1, IS2, IS3 are the focusing solenoids; IEL1, IEL2 are the Einzel lenses; IAT is the accelerating tube; ICM0÷ICM3 are the steering magnets; IPP is the pepper-pot; ICP is the beam chopper; IDB1÷IDB3 are the diagnostic boxes; IBN is the polyharmonic buncher [1,2].

The ion beam will be extracted from ECR with the energy of 25 keV/Z. After extraction the ion beam will be focused by the IEL1 Einzel lens and by the IS0 solenoid to the IM90 analysing magnet input. The ion charge spectrum will be analyzed by means of magnetic field variation in the IM90 and by the IS0 with measuring the ion current by Faraday cup (FC) in the IDB1 diagnostic box.

The manufactured IM90 magnet is structurally differ from the computer model and the Technical Tasks 2012-2013. (Figure 2).

In according to the terminology of the technical specification, the magnet is made as a "closed" screen, but with expanded beams and magnet stands up to the screens. At the same time, the outer overall dimensions did not change, because they were determined by the location of screens. Screens are necessary to reduce the extent of the magnetic field of the magnet. The maximum calculated induction of the magnetic field is 0.14 T in the gap. It provides the analysis of the charge spectrum for all types of accelerated ions. The requirement to the analyzing magnet IM90, which is located on the high-voltage platform, is minimum possible energy consumption. As a result, the magnet is designed with excitation coils, which have indirect water cooling and work at medium current density of not more than 2.5 A / mm^2. The main characteristics of the magnet are shown in Table 1.

The resolution of the magnet allows to analyze all types of beams accelerating in the cyclotron DC-280.

Table 1: Main Parameters of IM90 Magnet

Magnetic field induction, T	0,14±1%
Gap, mm	110
Active pole length, mm	785,4
Inhomogeneity of magnetic induction in the zone ±65 mm	$\pm 1 \times 10^{-4}$
Operating voltage of coil, V	76,8±2,5%
Cooling of coil - water	Distilled water
Water pressure difference, kG/cm^2	4,0±5%
Total cooling water flow , l/min	3
Nominal power supply, kW	1,41±2,5%
Total weight of magnet, kg	2326

†lisov@jinr.ru

ISBN: 978-3-95450-197-7 doi:10.18429/JACoW-RUPAC2018-WEPSB17

NEW QUADRUPOLES INSTALLED AT VEPP-2000 FOR HIGH ENERGY OPERATION WITHOUT FINAL FOCUS

D. Shwartz†[1], I. Koop[1], N. Nefedov, V. Prosvetov, P. Shatunov, Yu. Shatunov[1], A. Utkin,
Budker Institute of Nuclear Physics, Novosibirsk, 630090, Russia
[1]also at Novosibirsk State University, Novosibirsk, 630090, Russia

Abstract

The family of four weak quadrupoles was replaced at VEPP-2000 electron-positron collider with new one. New quads with increased bore diameter made with higher field quality and equipped with fiducial points are excited by water-cooled coils fed with new 300 A power supplies. That allowed to double integrated gradient and to implement so called "warm" operation mode (with switched-off final focus solenoids) above 500 MeV energy level. Presented in the paper "warm" modes are used for beam scrubbing and for resonance depolarization technique of Compton backscattering beam energy measurement system cross-calibration.

INTRODUCTION

VEPP-2000 is a small, 24 m perimeter, single-ring electron-positron collider with energy range of 150-1000 MeV per beam [1-6]. It operates with round beams and uses solenoids for final focusing [7]. The layout of the VEPP-2000 collider is presented in Fig. 1.

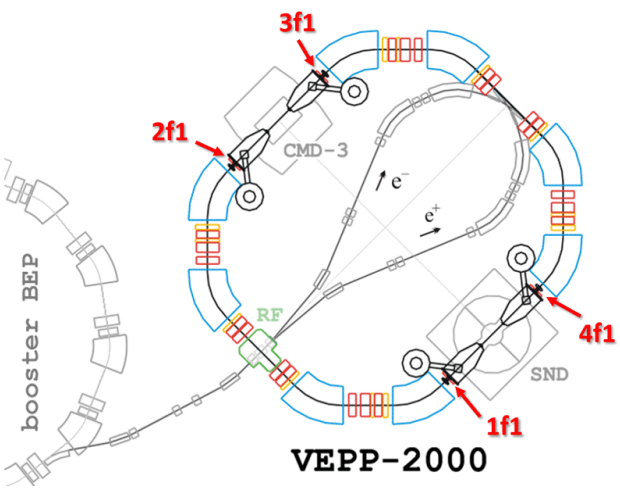

Figure 1: VEPP-2000 storage ring layout.

For the beam scrubbing after long shutdowns and resonance depolarization energy calibration technique [8] the special "warm" regime was proposed with final focus (FF) solenoids switched off. In this mode the family of weak quads (f1, see Fig. 1) is significantly stronger than in regular lattice that did not allow to use this regime above 500 MeV.

Compton Backscattering System

Beam energy at VEPP-2000 is measured online by the Compton backscattering (CBS) system [9]. In Fig. 2, one can find the typical edge of the spectrum of scattered photons. The oscillations in the left part are produced by interference of the MeV-scale scattered photons due to interaction of electrons with laser radiation along the curved path inside the dipole.

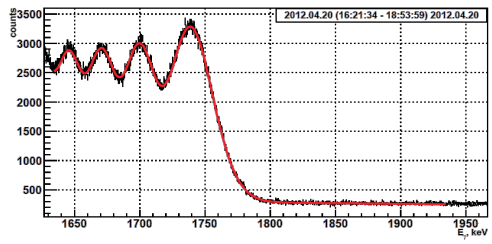

Figure 2: Compton backscattering measurements.

For cross-check of CBS system the resonance depolarization (RD) technique is used [10]. In Fig. 3 an example of three depolarizations is shown with different speed and direction of depolarizer frequency scan.

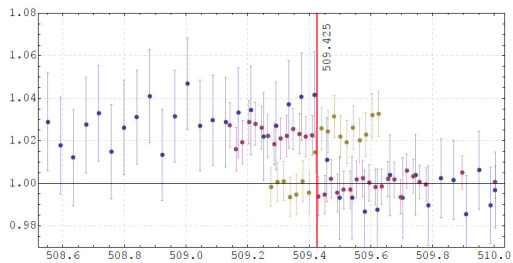

Figure 3: Resonance depolarization at VEPP-2000.

Unfortunately, it was found that RD can't be used for precise energy calibration in regular operation regime of VEPP-2000 due to residual closed orbit distortions inside FF solenoids. Nevertheless, in special "warm" mode the cross-check of all three energy control methods is carried out (see Fig. 4). Third method is based on precise magnetic field control by NMR probes in all dipoles. It is usually used for fast online control of relative energy variation.

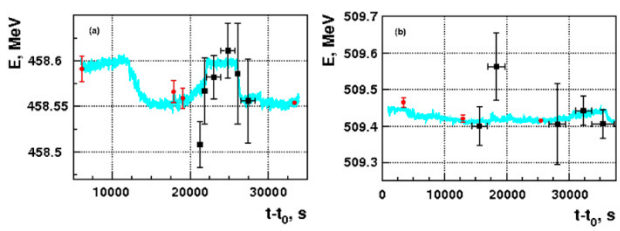

Figure 4: Beam energy control by CBS (black), RD (red) and NMR (blue) systems.

† d.b.shwartz@inp.nsk.su

ISBN: 978-3-95450-197-7 doi:10.18429/JACoW-RUPAC2018-WEPSB18

CONSTANT MAGNETIC FIELD MEASURING SYSTEM IN THE U-70 SYNCHROTRON

S. Sytov, N. Ignashin, V. Serebryakov,
NRC "Kurchatov Institute" IHEP (Institute for High Energy Physics),
Protvino, Moscow Region, 142281, Russia

Abstract

The mode of operation of the synchrotron for the circulation and retardation of carbon ions, using an independent programmable power supply of the ring electromagnet, required the creation of a system for measuring the constant magnetic field. This special power supply program forms the synchrotron "Magnet Cycle". It has the main plane part for beam injection and circulation and the medium plane for beam ejection stage. The medium plane magnetic field value defines the beam output energy. The measured values of the magnetic field on both the main and the medium plates of the cycle provide information important for the synchrotron operation.

MEASURING SYSTEM

The measuring system includes: magnetic field permalloy probe, the head electronic module, RS – 485 Interface, CPU, main U – 70 Control System.

The permalloy probe [1] is a specially designed permalloy wire core placed into a small diameter glass tube with two outer coils – signal coil and current one. The probe is placed on a moving plate, connected to a mechanical actuator and located in the measuring electromagnet pharynx (see Fig. 1). The measuring electromagnet is connected in parallel with the ring electromagnet. When the magnetic field vertical component (across the core axis) crosses the zero value, the signal coil generates a short pulse (see Fig. 2).

Figure 1: Permalloy Probe on the Actuator Plate.

The Block diagram of the measuring setup is shown in Fig. 3. The "StartIn" pulse from synchronization system comes to the digital measuring part to generate the strobe pulse (12 ms) to start the electron integrator. The ramp function current flows to the current coil of the probe (0 – 2A range maximum) after the integrator output signal amplification (PWR AMP). When the current coil magnetic field value becomes equal to the measured electromagnetic field, a pulse appears on the signal coil. Calculating the quantity of periods of the known frequency (20 MHz@50 ns) from "StartIn" to "MeasIn" pulses, one can obtain a value proportional to electromagnetic field.

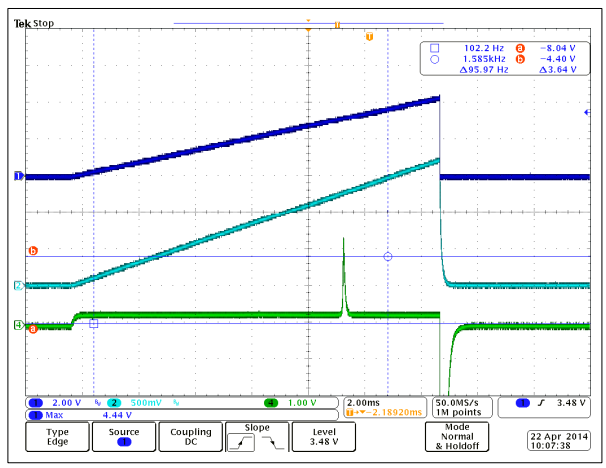

Figure 2: Measuring the Pulse from the Probe Signal Coil (4-th trace).

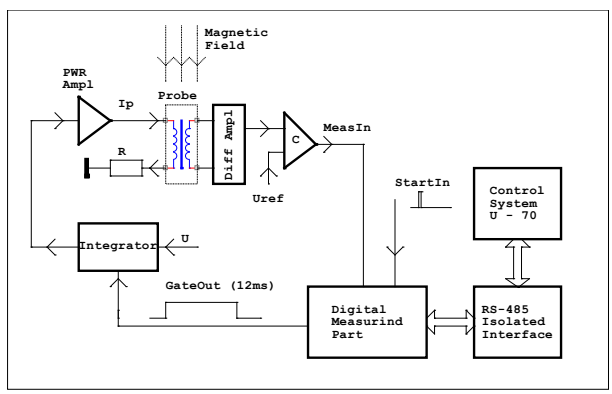

Figure 3: Measuring Setup Block Diagram.

To carry out accurate measurements, it is necessary to detect the midpoint of the "MeasIn" pulse. This is the main difficulty in making measurements, because its shape depends on the derivative of the magnetic field (for different values of the different pulse widths). In addition, at the beginning of the current build-up in the coil, a series of false impulses appear at the sensor output, which it is necessary to dispose of. This difficulty can easily be overcome with the proposed algorithm of digital signal processing. Its essence is shown in Fig. 4.

ISBN: 978-3-95450-197-7 doi:10.18429/JACoW-RUPAC2018-WEPSB19

A PROTOTYPE OF PULSED SEPTUM MAGNET FOR NICA COLLIDER INJECTION

E.V. Muravieva, A. S. Petukhov, A. V. Tuzikov, A. A. Fateev,
Joint Institute for Nuclear Research, Dubna, 141980, Russia

Abstract

The development and creation of the ion collider NICA continues at the Joint Institute for nuclear research. A scheme of beam injection into the NICA Collider using a pulsed septum magnet is presented. The duration of the pulse magnetic field is about 10 μsec, the amplitude of the field is about 0.5 Tesla. The conceptual design of the septum prototype and the power supply scheme are given. The power supply provides a current of about 50 kA in a current loop with an inductance of 1 μH.

MAIN CHARACTERISTICS OF SEPTUM MAGNET

To provide the injection of the ion beam in the collider NICA [1] there are two septum magnets (one piece for each ring).Main requirements for the parameters of septum magnet are shown in Table 1.

Table 1Septum Magnet Parameters

Effective length , mm	2500
Aperture, mm × mm	35×35
Pulse duration, nsec	>200
Pulse flat top duration , nsec	≥200
Field , T	0,5
Spatial inhomogeneity of the magnetic field in the beam area,%	<5
Deviation of the field through the bunch length,%	<5

Figure 1 shows the arrangement of the main elements at the injection site.

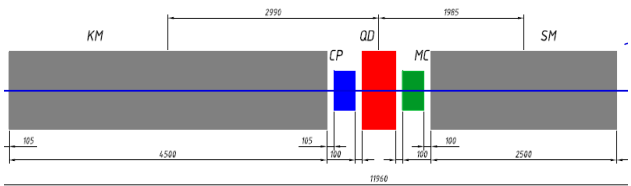

Figure 1: The arrangement of the main elements at the injection site. KM-kiker magnet, SM-septum magnet, QD- quadrupole lens

PROJECT OF SEPTUM MAGNET

When choosing the type of septum magnet we took into account the large duty cycle of procedure. Therefore, preference was given to a pulsed magnetic septum.

Several different types of magnets have been considered. The “iron-free" version of the septum was chosen [2].

The conceptual design of the" iron-free " septum magnet is shown in Fig. 2.

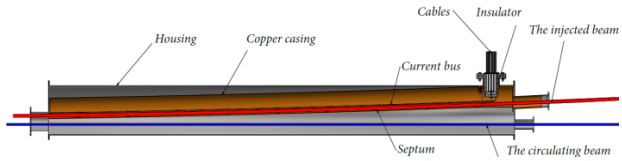

Figure 2: The conceptual design of the "iron-free" septum magnet.

In this design, the deflecting magnetic field is formed in the space between the current-carrying strip bus and a wide septum partition, which is both a reverse current conductor and a part of the common conducting screen, inside which all magnetic fields are concentrated – both working and scattered.

OPTIONS FOR TECHNICAL IMPLEMENTATION

The NICA Collider consists of a large number of superconducting elements. Groups of such elements are connected in series by current and cryogenic lines. Groups of such elements are connected in series by current and cryogenic lines.

Therefore, three variants of the technical implementation of the septum magnet are considered: “warm” (with bypass lines), “cold” (septum is inside the cryogenic volume) and “mixed” (septum magnet and bypass lines are inside general vacuum box).

PULSED POWER SUPPLY SYSTEM

Pulsed power supply is based on a capacity aperiodic discharge with the inductive load. This scheme (Fig. 3) allows forming a bell-shaped pulse.

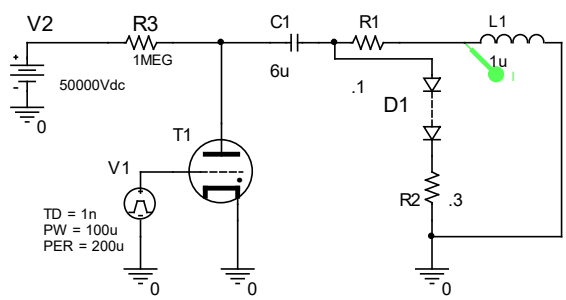

Figure 3: Scheme of pulsed power of the septum. L1 is the total equivalent inductance of the circuit, C1 is the storage capacitance and R1 is the equivalent resistance of ohmic and dielectric losses.

The D1-R2 circuit allows energy to be dissipated, what may be important for the cryogenic option. For switching it is assumed to use the hydrogen thyratron of the type of

ISBN: 978-3-95450-197-7 doi:10.18429/JACoW-RUPAC2018-WEPSB20

THYRATRON OPERATING PRESSURE MONITORING SYSTEMS

V.D.Bochkov, D.V.Bochkov, V.M.Dyagilev, I.V.Vasiliev, I.A.Salynov, V.G.Ushich
Pulsed Technologies Ltd., 5, Yablochkova str., 390023, Ryazan, Russia

Abstract

The known statistics data amassed for power thyratrons in accelerators show remarkable potential of the plasma switches in terms of lifetime covering the range from several thousand up to 120 thousand hours total [1 - 3]. The gap in the lifetime can be reduced both by measures of improvements in technology and implementation of thyratron parameters monitoring systems. It is known that the thyratron lifetime mainly depends on continuity of gas pressure and cathode emission. In this paper the initial research on some effective means of gas pressure monitoring automation is described. The pressure monitoring in thyratrons TGI-, TPI- and TDI-types is possible in absence of anode voltage either by registration of triggering parameters in a new igniter design or by a special built-in high-temperature pressure gauge.

INTRODUCTION

The main objective of the presented research is to sustain competitive position of thyratrons in respect to semiconductor switches. It takes improvements in lifetime and operation stability, easier maintenance, shorter readiness time at reasonable dimensions and cost.

The lifetime of thyratrons mainly depends on stable gas pressure and cathode emission. One the of standard maintenance operations during thyratron use is the so-called “ranging” – rather complicated procedure used to adjust optimum pressure in the tube during modulator maintenance. According to SLAC (Stanford Linear Accelerator Center) it is necessary to make the ranging at least every 500 hours, according to other sources depending on operation mode it is must be made at least once in 3 months.

There are not too much known means to facilitate the procedure.

In US patent № 3822086 [4] an apparatus for recharging and maintenance of operating pressure in a transmitter-receiver tube is claimed, comprising an electrical bridge circuit having electrical resistance dependent pressure sensor (e.g. thermistor), as one of the arms of the bridge, which reacts to the thermo conductivity when the pressure is changed (alike Pirani gauge). The reduction of the pressure below the pre-set value (with a variable resistor in the opposite arm) leads to increasing resistance of the thermistor. The resulting imbalance of the bridge circuit turns on a heater of the reservoir and H_2-permeable palladium membrane. At this the hydrogen passes by diffusion through the membrane into the volume of the tube. When the operating pressure is achieved the thermistor resistance is decreased and the subsequent balancing of the bridge circuit turns out the heater and the membrane.

The lack of information on commercial application of this clear and logical way in real devices since the moment of publication in 1974 most likely can be explained by no economical effect at that time and problems with reliability of the circuit components under conditions of severe electromagnetic disturbances and extensive high-temperature baking of the tube during outgassing procedure.

This is why English thyratron manufacturer E2V recommends to entrust the automatic monitoring to a simple temperature-depended solution with a barreter, located in the tube base [5]. However this way is based on the reaction to the variations in the environmental temperature operated without any connection to the gas pressure inside the thyratron and does not provide sufficiently effective adjustment of the pressure during lifetime.

INVESTIGATION OF THE INFLUENCE OF PRESSURE ON IGNITION PARAMETERS

We describe more effective way of automatic ranging with pressure monitoring by direct measurements of trigger pulse parameters.

We intend to carry on the research in several directions with respect to the following parameters to be investigated:

1) Anode delay time and trigger parameters (amplitude and pulse duration of current between ignitor and cathode) as the function of the pressure.
2) Working gas pressure stability in thyratron tubes.

Pulse voltage is measured by oscilloscopes Tektronix 2022, Tektronix TBS1152 и Rigol DS1104 with high-voltage probes Tektronix P6015A (1000:1) and pulse current by Rogowski coil 3-01 (Stangenes Industries).

It is shown that for standard TDI4-100k/45H thyratrons with a single pin of the igniter (Trig 2 in Fig. 2) and another lead of the igniter connected to the cathode inside the tube, trigger current of the thyratron in the system of trigger electrodes does not depend on working gas pressure (Fig. 1) in the reservoir heater pressure range from 0 up to 7 V. The trigger current delay time in respect to trigger voltage is constant ~ 100 ns.

In new design of thyratron TDI3-100k/45H trigger part (Fig. 2) with separate trigger pins (Trig 1 and Trig 2), disconnected from cathode, when one of the pins is connected short to cathode (e.g. Trig 1, when R_{ad} = 0 Ohm) the waveforms of trigger current remain the same as in Fig. 1. In case when to the pin Trig 1 in the igniter-cathode circuit the additional resistor R_{ad} was hooked up (Fig. 2) the waveforms obviously change and trigger cur-

ISBN: 978-3-95450-197-7 doi:10.18429/JACoW-RUPAC2018-WEPSB21

THE POWER SUPPLY OF PULSE MAGNETS WITH OUTPUT CURRENT UP TO 10 kA

V. Dokutovich†, D. Senkov, D. Pureskin, A. Chernyakin
Budker Institute of Nuclear phisics SB RAS, Novosibirsk, Russia

Abstract

At the present stage of development of accelerating technology, it is important to create beam input and output systems for newly created and modernized cyclic accelerators. At the same time, high requirements associated with high energy beams of charged particles and a substantial length of channels are imposed both on the magnetic system of the transport channels and on power supplies. Within the framework of the construction of the NIKA (JINR)[1] accelerator complex, a channel for the transportation of the Buster-Nuclotron beam is created in BINP. A powerful precision source with an output current of up to 10 kA and an energy in the pulse of up to 23 kJ is designed to power impulse dipole lenses and septum magnets in channel.

The presented article describes a pulsed source for magnetic lenses with a maximum output voltage of up to 2 kV and a maximum output current of up to 10 kA. The stability of the current amplitude in the pulse is ensured at a level better than 10-3. In this case, the stability of the magnetic field in the lenses can be improved to a value of 100 ppm by introducing an additional feedback on the field of the magnet using the integrating ADC VsDC produced by BINP.

The developed source meets both the requirements for stability of output parameters and automation requirements for integration into modern accelerator systems.

INTRODUCTION

At the moment, the program for the construction of the Buster-Nuclotron bypass channel is being implemented within the framework of the NIKA project (Dubna) [2]. The BINP plays a significant role in the construction of the channel.

The structural scheme of the bypass channel is shown in Fig. 1. The channel consists of magnetic correctors and a septum of magnets.

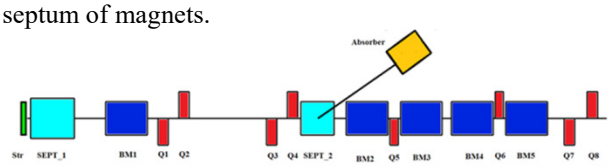

Figure 1: Magnetic system of the Buster-Nuklotron channel.

A high-voltage power supply is required to power the impulse dipole lenses (BM1-BM5) and the septum magnets (SEPT1, SEPT2, SEPT3), which would satisfy the following parameters in Table 1.

Table 1. Parameters Load

Parameter	dipole	septum 1	septum 2,3
Maximum current , kA	2	3	8
Pulse width , ms	30	0.1	1
Frequency, Hz	0,25	0,25	0,25
Maximum voltage, kV	2.1	1.6	1.6
maximum voltage, kV	10	16	60
Coil Resistance, mΩ	120	18	20
Storage capacity, μF	10	60	1600

Sources are built according to the scheme with a capacitive energy storage device, with its switching to the load and recuperation. In this regard, it has an increased efficiency. As management and diagnostics, a single-board computer is used that is responsible both for remote management and for manual and performing monitoring and protection functions.

STRUCTURE OF POWER SUPPLY

The structural diagram of the power supply is shown in Fig. 2. The operation of the power supply is based on the relatively long charging of the capacitor bank to the voltage of the required level through the "power inverter" and subsequent short-term discharge through the switch to the load. During the discharge process, a current pulse passes through the load, resembling a half-sinusoidal shape, and in amplitude it is many times larger than the charging current.

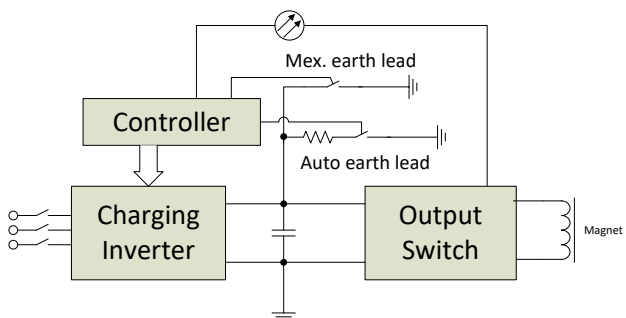

Figure 2: Structure of the power supply.

In the proposed sources, the amplitude value of the discharge current reaches 2 kA with the supply of a dipole

ISBN: 978-3-95450-197-7 doi:10.18429/JACoW-RUPAC2018-WEPSB22

THE CONTROLLER FOR THE POWER SUPPLY OF PULSE MAGNETS WITH OUTPUT CURRENT UP TO 10 KA

V. Dokutovich†, D. Senkov
Budker Institute of Nuclear phisics SB RAS, Novosibirsk, Russia

Abstract

As part of the construction of the NIKA project [1], implemented at JINR (Dubna), the Budker-Nuclotron transport channel is facing the Budker Institute of Nuclear Physics. For him, BINP, in particular, develops, manufactures and supplies a number of high-voltage power supplies of dipole and septum magnets.

As the development of accelerator technology, the issue of automation of scientific complexes and industrial accelerators is becoming ever more acute. With increasing beam energy, the necessary accuracy of maintaining the parameters of the accelerator grows. All this imposes new demands on the automation system of the accelerator complex. In addition, for power supplies with powerful drives for high energy, the issue of safe operation was always acute. It is necessary not only to monitor the load parameters, but also to ensure safety during routine maintenance and service operations.

The presented article contains a description of the controller for switching power supplies. A distinctive feature of the controller is the combination in one device, several, logically connected with each other. Realization within the controller of the fast protection device allowed to realize a qualitative analysis of the behavior of the power system by changing the voltage and current of the load, which is very important for determining future possible problems and not regular situations. The control is carried out via Ethernet, as well as manual control by means of a touch screen located on the front panel of the power supply. As the core, a digital signal processor is used, which makes it possible to implement the execution of local work scenarios by maintaining part of the autonomous functions.

This article describes the controller itself, its properties and the main application.

INTRODUCTION

As part of the construction of the NIKA project, implemented at JINR (Dubna), INP designs, manufactures and supplies a number of high-voltage power supplies for dipole and septum magnets of the Buster-Nuclotron transport channel [2]. The work of magnets is carried out in a pulsed mode. The source is made according to the scheme of a powerful capacitive energy storage device that is switched at the right time to the magnet windings. For the correct operation of the bypass channel, it is required to maintain the accuracy of the current in the winding when the beam passes no worse than 10^{-3} and the possibility of realizing the accuracy of the magnetic field by external feedback is no worse than 10^{-4}. Due to the fact that the power source contains an energy storage device with a stored energy of the order of 10 MJ, it is necessary to implement all safety measures when working with a high-energy installation in order to exclude the occurrence of a situation of a non-standard discharge of energy accumulated in the capacity when operating the sources.

To solve these problems, the described controller was developed, which combines both the functions of the interface and control unit and the functionality of the fast protection unit.

CONTROLLER

As already mentioned, the controller carries out a full set of control, measurement and lock communication functions. The controller controls the charging source by specifying the required voltage on the capacitance, and the output thyristors bridge is controlled via the fiber. As the main protective function, a powerful mechanized discharge key is controlled. At the end of the operation of the source, in the event of an abnormal situation associated with the danger of unauthorized discharging of the storage tank, or if a source of suspected malfunctioning of the power components of the source is suspected, the drive is first discharged with a powerful discharge resistor and then tightly closed with an electric key. If the drive is malfunctioning, the capacitance is shortened by means of a backup high-power discharge resistance.

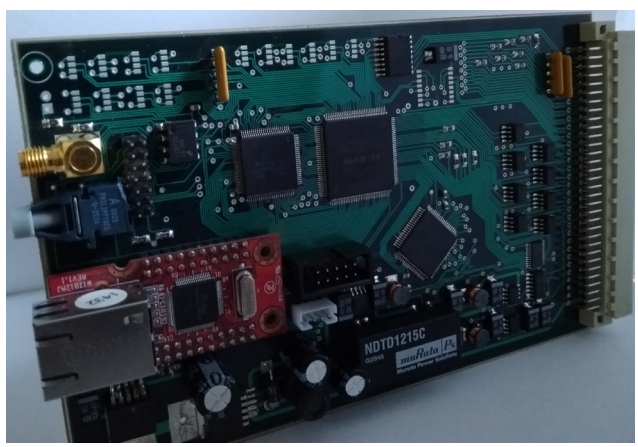

Figure 1: Controller.

As a consequence, it requires both a precision DAC interface and an ADC, as well as many binary I / O channels, to interrogate locks and control external devices. At the same time, a modular approach to device development was used, which allowed us to design a controller as a universal module (Fig. 1), which can be used in various applications.

ISBN: 978-3-95450-197-7 doi:10.18429/JACoW-RUPAC2018-WEPSB26

UPGRADING OF THE POWER SUPPLY FOR MAGNET U70 SYNCHROTRON

An. Markin, V. Kalinin, O. Lebedev, D. Hmaruk
Institute for High Energy Physics (IHEP) of NRC "Kurchatov Institute"
Protvino, Moscow Region, 142281, Russia

Abstract

At the accelerator complex U70 NRC "KI" - IHEP, there is work to expand the range of the working beam energy for physical experiments. We are talking about medium energies for protons (350 ÷ 1300) MeV/u, as well as carbon ions (250 ÷ 455) MeV/u. The presence of extracted beams of medium energies opens up new possibilities for proton radiography, radiobiological studies, etc.

Analysis of the options for obtaining beams of medium energies in the accelerator complex has shown that the creation of a deceleration regime for particles in the U70 is optimal. Firstly, we do not change the standard setting of the injection complex with the beam transport channels in the cascade of the LU30–U1.5, I100–U1.5 accelerators, and secondly for this regime we have a well-developed arsenal of technical means in the U70. The missing link is a regulated power supply for the U70 electromagnet with the following characteristics: power ≈ 30 kW; the maximum current is 150 A with accuracy not worse than $\pm 1 \cdot 10^{-4}$; the maximum voltage on the plugs ±450 V with accuracy not worse than $\pm 1 \cdot 10^{-3}$.

The ring electromagnet (REM) U70 is designed with combined functions that ensure the circulation of particles in the equilibrium orbit and simultaneously their focusing. The main characteristics and design features of the synchrotron electromagnet IHEP were published in [1]. REM in its simplest form can be represented as a C-shaped transformer with an air gap. The primary winding is the main winding of the REM, which creates a leading magnetic field, the secondary windings are the corrective windings of the magnetic field U70.

The report describes the upgrade of the source with pulse-width modulation (PWM) voltage for our purpose.

The existing commercial source was not satisfied due to electromagnetic incompatibility due to the transformer coupling of the windings creating a magnetic field in the U70. The problem was to suppress 100% of the output voltage ripple by approximately 1000 times (- 60 dB).

RESEARCH SOURCE WITH PWM + REM

Test №1

The power supply was connected to the U70 electromagnet. To obtain the energies indicated above, the law of current was established to form the magnetic cycle of slowing down the light ion beam (130 ÷ 80) A. The output characteristics of the current and voltage were measured. The following instruments were used: oscilloscope Tektronix 4000 series; Differential Probe DP-25, calibration ± 1 V ⇒ ± 200 V; current sensor LEM IT 200-S, calibration ± 10 V ⇒ ± 164 A. The signals were taken from the output of the power supply busbar. In Fig. 1 the results of tests a commercial power supply are given.

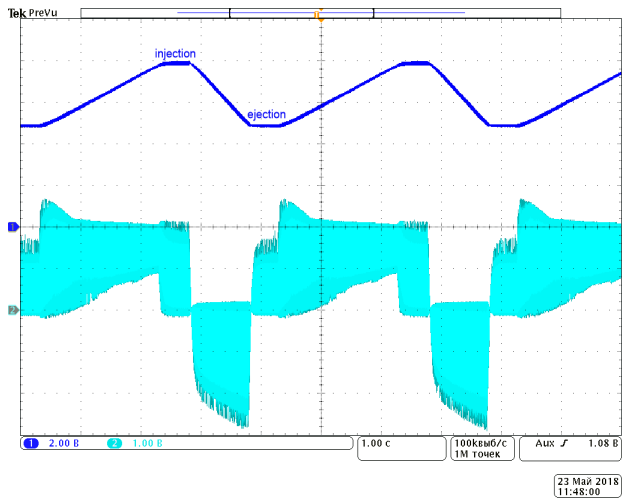

Figure 1: Current law, for the formation of the magnetic cycle of slowing down the beam of light ions in the U70, (130 ÷ 80) A. The upper trace – current, the lower trace – voltage with 100% ripple (Peak to peak) – 1000 V, frequency PWM ~20 kHz.

Low-pass filter (LPF)

To suppress pulsations, the required type of LPF was chosen. The calculation of filter elements is carried out in PSpice codes for the equivalent circuit shown in Fig. 2. An iterative, numerical method with optimization of the element values according to the established criteria was used [2-5]. The cutoff frequency of the LPF is 300 Hz. The suppression of pulsations at the fundamental generation frequency of 20 kHz reaches - 60 dB (refer Fig. 3).

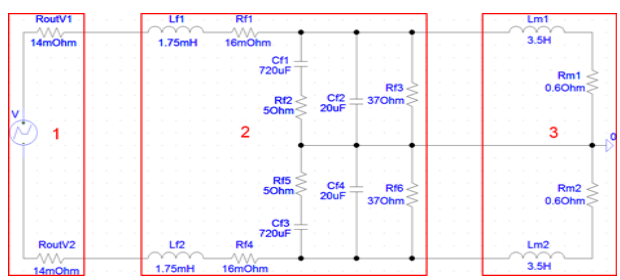

Figure 2: Equivalent simulation scheme. Blocks highlight the main parts: 1 – commercial power supply, 2 – LPF, 3 – load (REM U70).

ISBN: 978-3-95450-197-7 doi:10.18429/JACoW-RUPAC2018-WEPSB27

THE INFLUENCE OF THE UNCLOSED SUPERCONDUCTING MAGNETIC SHIELD ON THE DYNAMICS OF THE CHARGED PARTICLES BEAM

G.L. Dorofeev*[1], E.E. Donets, V.M. Drobin, JINR, Dubna, Russia
[1] also at NRC "Kurchatov Institute", Moscow, Russia

Abstract

The development of high-temperature superconducting (HTS) materials, especially HTS tapes of the second generation (2G HTS tapes) give us new opportunities to use superconductivity in high-energy physics devices and, in particular, in charged particle accelerators. The influence of the unclosed magnetic shield made of 2G HTS tape on the dynamics of a charged particles beam is studied in this paper. Within the framework of the simplest model of the interaction of the magnetic field of a charged particles beam with a superconducting shield, estimates of this influence are made. The superconducting shield shifts of a charged particles beam to its axis. In particular, the beam of ions $^{197}Au^{79+}$ energy of 4 GeV per nucleon and a current of 5 A passing at a distance of 5 - 10 mm from the axis of the superconducting screen with a radius of 50 mm and a length of 5 meter is shifted to the axis of the screen at a speed of about 130 m/sec. That is, the beam itself can be centered for a lot less than 1 second. The possibilities of using an unclosed superconducting shield to compress a charged particles beam are discussed, as well as the possibilities of controlling the shield.

INTRODUCTION

Magnetic fields are used in various areas of science and technology, in medicine, in industry, in devices of high energy physics, etc. Important for specific applications are the magnitude and quality (stability, uniformity,...) of magnetic fields. To improve the quality of magnetic fields, it is possible to use soft magnetic materials with high magnetic permeability (permalloy, μ - tapes of different composition, etc.) or superconductors. The difference between these materials is easy to demonstrate by the example of the behavior of hollow cylinders in a magnetic field, as shown in Fig. 1. Weakening of the magnetic field inside the cylinder made of soft magnetic material is due to the high magnetic permeability μ of the cylinder wall. That is, the shunting of the magnetic flux by a material with high magnetic permeability is used. The weakening of the field inside the cylinder can be radical with a noticeable (large) wall thickness and high permeability μ, which in some materials can reach 10^4. But to achieve zero magnetic fields inside the cylinder is in principle impossible. If the cylinder is not monolithic, and is a roll of μ - tape, its behavior in a magnetic field is no different from the monolithic, when the loss of energy at an alternating current in the system do not matter. It should also be noted that the need for high magnetic permeability leads to the limitation of the range of performance of such materials by magnetic fields of the order of tens of Gauss. In particular μ-tape can be used for shielding the magnetic field of the Earth.

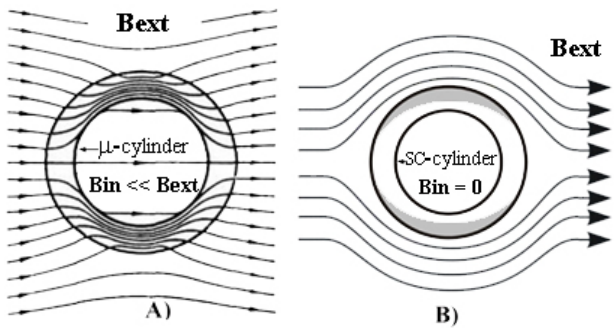

Figure 1: μ–cylinder -A) and the superconducting cylinder -B) in a perpendicular external field. Grey's are the flow region of the shielding currents in SP cylinder.

In the case of a superconducting material, the change in the external field induces shielding currents near its surface. As a result, the magnetic field does not penetrate inside the monolithic superconductor until the shielding currents reach a critical value. If the superconducting cylinder is a roll of thin superconducting tape (the simplest unclosed shield), the external magnetic field parallel to the axis of the cylinder is practically not shielded (the magnetic fields of the shielding current are small, since they are proportional to the thickness of the superconducting tape, and not to the size of the cylinder). At the same time, in an external magnetic field perpendicular to its axis, it behaves like a cylinder with a solid monolithic wall. That is, a roll of superconducting tape passes parallel to its axis, but shields the perpendicular components of the external magnetic field. This circumstance was used in the 70-ies of the last century. Bychkova M. I. and others [1,2] successfully demonstrated the possibility to use an unclosed magnetic shield in the form of a roll of superconducting tape made of alloy NT50 to increase the uniformity of the magnetic field of the superconducting solenoid.

Figure 2 shows design of a modern high-temperature superconducting wire in the form of a ribbon from the manufacturer's website.

*e-mail: dorofeevgl@mail.ru

ISBN: 978-3-95450-197-7 doi:10.18429/JACoW-RUPAC2018-WEPSB28

EM FIELDS IN A METAL IN AN EXTERNAL MAGNETIC FIELD AT LOW TEMPERATURS

V.N. Korchuganov, V.I. Moiseev, NRC KI, Moscow, Russian Federation

Abstract

Radio waves do not penetrate deep into the metal due to the high density of charge carriers in the metal. In the shorter-wave part of the spectrum, metals can be "transparent" only starting from ultraviolet, since the plasma frequencies in metals lie in the ultraviolet range. However, for a metal cooled to a low temperature and placed in an external magnetic field, the situation may change. Under these conditions, cyclotron orbits can be formed, and the relaxation time can significantly exceed the period of cyclotron motion of the charge carriers. For an electromagnetic wave with polarization normal to the induction vector of an external magnetic field, the exchange of energy with charge carriers in the metal turns out to be suppressed. Such a wave can propagate in the metal for relatively large distances (in comparison with the skin layer). In this connection, in electron storage rings at the azimuths, for example, of superconducting strong-field wigglers, with the magnetic field rise, the effect in the surface impedance change of the wiggler vacuum chamber metal can be manifested. This report is a brief review of some of the results known in plasma and solid state physics applicable to these conditions and of interest to accelerator technology.

INTRODUCTION

The electromagnetic waves can propagate in some conducting media in external magnetic fields at the frequencies much lower the plasma frequencies. This phenomenon is widely studied and used in plasma physics.

In metals under low temperatures, the relaxation time can significantly exceed the periods of cyclotron motion in external magnetic field and the cyclotron orbits can be formed. Under these conditions, the radiofrequency electromagnetic waves can propagate in metal in external magnetic field.

In this report, two theoretical approaches are used for the numerical analysis. One of them is the theoretical model of wave propagation in plasma [1] and the other one is the theoretical model of wave propagation in metal [2], [3]. The practical object of this report is the beam dynamics investigation in storage ring Siberia – 2.

The electron storage ring Siberia - 2 is 124 m in length with electron beam energies from 75 Mev up to 2.5 Gev. Beam life time is about 20 -30 hours in regular mode at the electron beam currents above 100 mA. Siberia-2 storage ring is equipped with a superconducting wiggler with magnetic field up to 7.5 Tesla.

ELECTROMAGNETIC FIELDS IN A PLASMA IN AN EXTERNAL MAGNETIC FIELDS

To describe the behaviour of electrons in metal, the simplest approximation is the model of free valent electrons. The energy spectrum of these electrons is discrete because of their motion is finite in metal volume. At zero temperature, electrons occupy in sequence lower energy levels up to the highest level – Fermi energy.

Two-component cold gas plasma can successfully illustrate some of the features and quantitative parameters of electromagnetic wave propagation in metals.

In external magnetic field, for plasma plane wave with time dependence

$$e^{i\left(\left(\vec{k}\vec{r}\right)-\omega t\right)},$$

within the linear approximation on the wave amplitudes, the equation for wave current density $\vec{j}$ and electrical field $\vec{E}$ can be written as [1]

$$\omega\left(\omega+i\nu\right)\vec{j} = = i\frac{\omega_0^2\omega}{4\pi}\vec{E}+\omega_i\omega_e\left(\vec{j}-\vec{h}\left(\vec{j}\vec{h}\right)\right)-i\omega\omega_e^{-}\left[\vec{j}h\right] \qquad (1)$$

In these relations, $\vec{k}$ is the wave vector, ω is the field frequency, ω_i and ω_e are the cyclotron frequencies of the ions and of the electrons, respectively, in external magnetic field.

The external magnetic field is introduced in the equation (1) by the field direction unit vector $\vec{h}$ and by the ion and electron cyclotron frequencies ω_i and ω_e determining the magnitude of the external magnetic field.

The own plasma wave magnetic field is neglected in the equation (1) because of the production of the current density $\vec{j}$ on the own magnetic field is the value of the second order of smallness.

In equation (1), energy dissipation is taken into account by the scattering effective frequency - ν.

The equation (1) describes the dynamics of charge carriers in electromagnetic fields and therefore must be completed by the Maxwell's equation determining the field dependence on currents:

$$k^2\vec{E}-\vec{k}\left(\vec{k}\vec{E}\right)=\frac{\omega}{c^2}\vec{E}+i\omega\mu_0\vec{j} \qquad (2)$$

The complete set of equations (1) - (2) gives the self-consistent solution for the wave current density $\vec{j}$ and the wave electrical field $\vec{E}$.

ISBN: 978-3-95450-197-7 doi:10.18429/JACoW-RUPAC2018-WEPSB30

SOFTWARE DEVELOPMENT FOR AUTOMATION OF NICA MAGNETS TRAINING AND DYNAMIC HEAT RELEASES MESUREMENT

B. Kondratiev*, V.V. Borisov, A.V. Bychkov, H.G. Khodzhibagiyan, S.A. Kostromin, A.V. Kudashkin, D.N. Nikiforov, M.V. Petrov, A.V. Shemchuk
LHEP, JINR,141980, Dubna, Moscow Region, Russia

Abstract

Training and measurement of dynamic heat releases is assumed for each NICA SC magnet. The software for automation of these processes is described. The results of training and the results of measured dynamic heat releases in the NICA booster dipole and quadrupole magnets at series tests are presented.

INTRODUCTION

For performating SC magnets training and the measurements of dynamic heat releases the software for controlling the power supplies, the energy evacuation switch[1], DAC, ADC modules and signaling equipment is necessary. LabView from National Instruments was used as the development environment for this software.

MAGNETS TRAINING

After the manufacturing of a SC magnet the training of quench current must be performed. This process implies the feeding of SC magnet with gradual increase of current altitude. Quenches are detected by the quench detector [2]. Training of magnets continues until the moment when the quench current altitude reaches plateau or the target value. For booster SC magnets it corresponds to 12100 A that includes the altitude of booster operating cycle [3] that equals 9680 A with the 25% reserve.

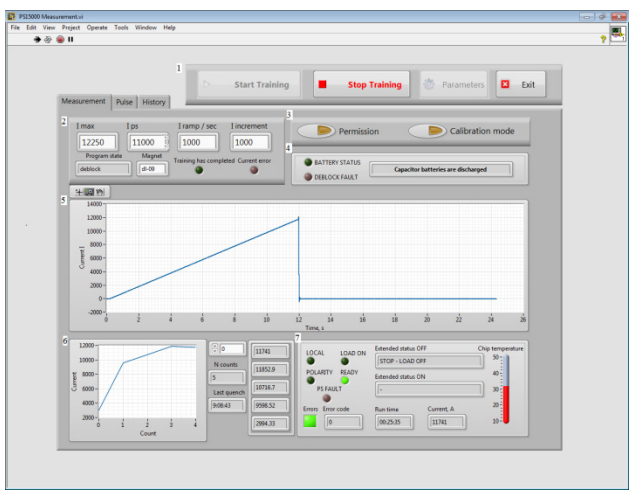

Figure 1: The main window of the training automation program:1 - Controlling buttons 2 - Training status bar, 3 - Buttons for permission of training resumption and for calibration of the detector, 4 - Status of energy evacuation switch, 5 - Current graph, 6 - Quenches quantity, 7 - Status of power supply.

Power supply PS15000 [4] is used for the training of dipole and quadrupole magnets. The maximum current altitude of this power supply is 15000A. The NI-PXIe4461 module is used as the ADC and DAC equipment for generating and measuring of current pulse signal. Commands for manipulating and for state monitoring of power supplies, energy evacuation key and signaling equipment are transmitted by the RS485/RS232 interface via the Moxa NPort 5650 converter.

Software for automation of magnets training (see Figure 1) includes processes of power supplies equipment manipulating, operating with DAC/ADC equipment, detecting of quench events, logging the data and events during SC magnets training. The training of SC magnets is performed by triangular current cycle. The standard current parameters of the training are listed in Table 1.

Table 1. The Standard Current Parameters of Training

Starting altitude, A	1000
Step current increment, A	1000
Final current altitude, A	12250
Current rate, A/s	1000
Time of pause, s	>3
Time of table, s	0
Time of transition areas, s	0.03

After the quench the program is waiting for the permission of training resumption. This permission comes to the program when the magnet achieves the required temperature.

THE RESULTS OF BOOSTER DIPOLE AND QUADRUPOLE MAGNETS TRAINING

Each SC magnet was trained before magnetic measurements and dynamic heat releases measurements. The resulting quantities of quenches are shown below. Some of quenches happened due to the false triggering of the quench detector.

Quenches quantity at the quadrupole doublets are presented in Figure 2.

ISBN: 978-3-95450-197-7 doi:10.18429/JACoW-RUPAC2018-WEPSB31

MAGNETIC MEASUREMENTS OF THE MULTIPOLE CORRECTORS OF THE NICA BOOSTER

T. Parfylo†, V. Borisov, S. Kostromin, H. Khodzhibagiyan, M. Shandov, I. Donguzov, O. Golubitsky, M. Kashunin, V. Mykhailenko, A. Shemchuk, D. Zolotykh, Joint Institute for Nuclear Research, 141980 Dubna, Russia

Abstract

The lattice of the NICA Booster includes eight superconducting multipole correctors for compensation of the main field errors of dipole and quadrupole magnets. The corrector includes four coils: quadrupole, two sextupoles and octupole. The magnetic field mapping at "warm" carry out by Hall sensor. High precision movement system for Hall sensor inside the magnet was developed and produced. The paper describes the design of the dedicated system, the results of the fist magnetic measurement and its comparison with calculations.

INTRODUCTION

NICA (Nuclotron-based Ion Collider fAcility) is the new accelerator complex being under design and construction at JINR since 2007 [1]. The accelerator complex includes two injector chains, a superconducting booster synchrotron Nuclotron and a collider consisting of two storage rings. The main goals of the Booster are the following: accumulation of $4 \cdot 10^9$ Au^{32+} ions; acceleration of the heavy ions up to energy required for effective stripping; forming of the required beam emittance with electron cooling system. According to specification [2], the lattice of the NICA Booster (see Fig. 1) includes eight superconducting multipole correctors for compensation of the main field errors of dipole and quadrupole magnets. The corrector includes four coils: quadrupole, normal and skew sextupole and octupole. Magnets produced at the Veksler and Baldin Laboratory of High Energy Physics (VBLHEP) at JINR.

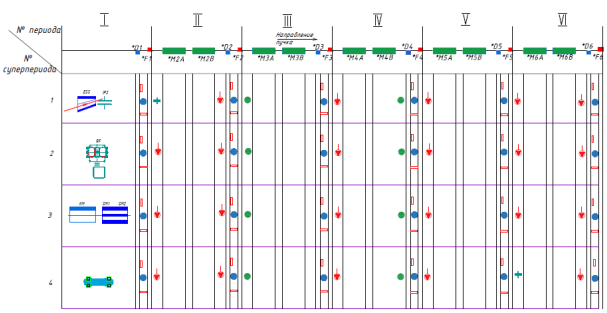

Figure 1: Green circles indicate multipole correctors.

MAGNET CIRCUIT DESIGN

Figure 2 shows the magnet front view. Magnet pole tip radius is 95 mm, outer diameter is 237 mm and leght 360 mm. Diameter of conductor with isolation 0.56 mm.

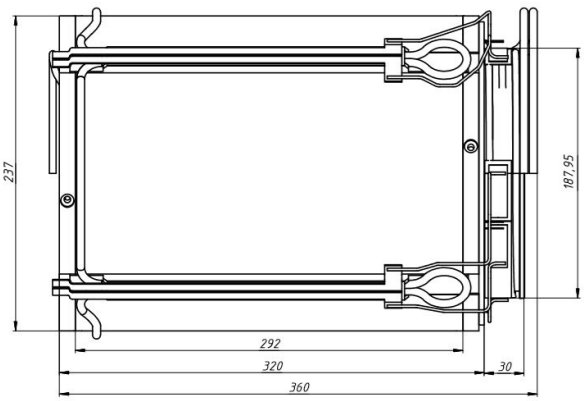

Figure 2: Main view of the multipole magnet.

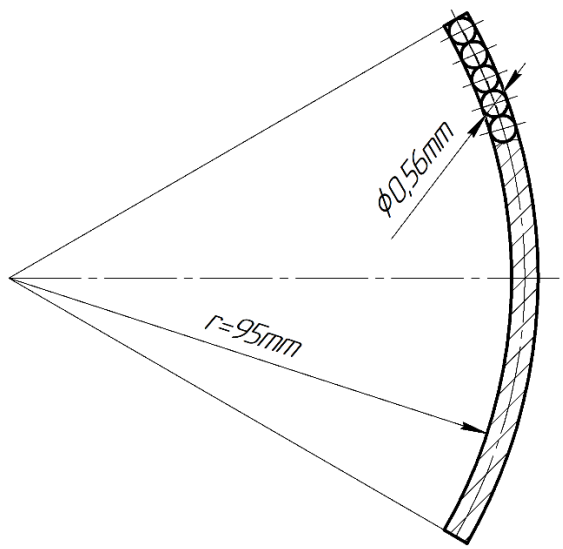

Figure 3: Coil cross-section.

The coils (Fig. 3) were exited using the same operating current. The different configurations of the coils that are related to different magnetic components of the magnet is shown in Fig. 4.

ISBN: 978-3-95450-197-7 doi:10.18429/JACoW-RUPAC2018-WEPSB32

THE PRESENT STATUS OF THE MAGNETIC MEASUREMENTS OF THE NICA COLLIDER TWIN-APERTURE DIPOLES

M. M. Shandov†, P. G. Akishin, V. V. Borisov, A. V. Bychkov, I. I. Donguzov, A. M. Donyagin, O. M. Golubitsky, M. A. Kashunin, H. G. Khodzhibagiyan, S. A. Kostromin, V. A. Mykhailenko, T. A. Parfylo, A. V. Shemchuk, D. A. Zolotykh, Joint Institute for Nuclear Research, 141980 Dubna, Russia

Abstract

The lattice of the NICA collider includes 80 twin-aperture superconducting dipole magnets. Serial production and testing of these magnets have been started at the Veksler and Baldin Laboratory of High Energy Physics of the Joint Institute for Nuclear Research (VBLHEP JINR) in Dubna, Russia. The measurement of the magnetic field parameters is needed to be conducted for both apertures of each collider magnet at the ambient and LHe temperature. Pre-series magnet with two different configurations of coils was successfully tested. This paper describes the present status and results of dipole magnets magnetic measurements and comparison of the results with calculations.

INTRODUCTION

The lattice of the NICA collider includes 80 twin-aperture superconducting (SC) dipole and 86 quadrupole magnets [1]. The collider operating modes are energies of 1.0, 3.0, and 4.5 GeV/u, which correspond to the constant operating fields of dipole magnets 0.4, 1.2 and 1.8 T. The Superconducting Magnets and Technologies (SCM&T) Department and the special technical complex [2] for assembly and testing of SC magnets for the NICA and FAIR projects were established at the Veksler and Baldin Laboratory of High Energy Physics JINR in Dubna, Russia. The measurement of the magnetic field parameters is needed to be conducted for both apertures of each collider magnet at the ambient and LHe temperatures. The design and main characteristics of magnets for the NICA collider are given in [3, 4]. Serial production and testing of these magnets have been started at JINR. Pre-series magnet with two different configurations of coils (pre-serial and serial) was successfully tested. According to the specification, the following parameters of collider dipole magnets have to be measured:

- main field component;
- effective magnetic length and relative standard deviation

$$L_{\text{eff}} = \frac{\int_{-\infty}^{\infty} B_y ds}{B_y(0)}; \; \delta L_{\text{eff}} = \frac{\Delta L_{\text{eff}}}{< L_{\text{eff}} >};$$

- magnetic field direction (dipole angle), angle between the magnetic and mechanical median plane:

$$\alpha_1 = -arctg\left(\frac{A_1^*}{B_1^*}\right),$$

$*$ – integrated harmonics;

- relative integrated harmonics up to the 7th.

PROCEDURE OF MAGNETIC MEASUREMENTS

The magnetic measurements (MM) procedure is based on the rotating coils method [5]. The magnetic measurement system (MMS) (see. Fig. 1) consists of three identical sections (1) that are mounted on the lodgment (2) which is installed inside the measuring shaft (3). Each section is resembled by sets of three measuring coils made as a printed-circuit board (PCB). Each coil is formed by 20 layers of the PCB - each layer contains 20 turns, in total – 400 turns.

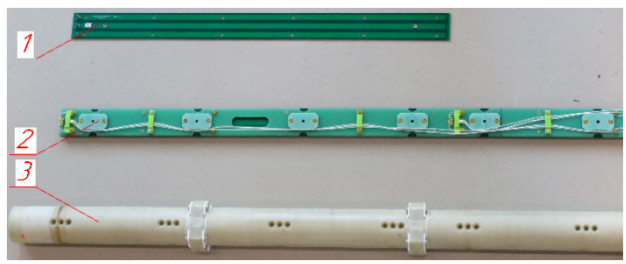

Figure 1: Main part of the MMS: 1. Section of three measuring coils (PCB); 2. Lodgment; 3. Measuring shaft.

The MMS construction is updated (see Fig. 2). In the centre of the magnet, the Hall probe (1) is installed on the central PCB for high resolution measurements of the magnetic field. Thermal contraction of the PCB is needed to be taken into account to compare results between magnets. For this task, special thermos-sensors PT100 (2) are mounted on the surface of each PCB. Special plates for inclinometer installation are included in the design of the serial MMS. The inclinometer with the system accuracy less than one arcsec [6] will be used to determine the frame of the measuring coil median planes relative to gravity.

MM are carried out at the ambient temperature with the operating current of 100 A ("warm" measurements) and at the temperature of 4.5 K with the maximum operating current of 10.8 kA ("cold" measurements). The step-by-step method of measurement with fast ramped magnetic field of 0.9 T/s (RC mode) and the constant velocity rotating method with the constant magnetic field (DC mode) were used. At least one full revolution has to be conducted for a

† shandov@jinr.ru

ISBN: 978-3-95450-197-7 doi:10.18429/JACoW-RUPAC2018-WEPSB33

SERIAL MAGNETIC MEASUREMENTS FOR THE NICA QUADRUPOLE MAGNETS OF THE NICA BOOSTER SYNCHROTRON

A. Shemchuk *, V. Borisov, A.Donyagin, S. Kostromin, O. Golubitsky, H.G. Khodzhibagiyan, M. Omelyanenko, A. Bychkov, T. Parfylo, I. Donguzov, M. Shandov, V. Mikhailenko, M. Kashunin, D. Zolotykh LHEP, JINR,141980, Dubna,Moscow Region, Russia

Abstract

NICA is a new accelerator collider complex under construction at JINR, Dubna. More than 250 superconducting magnets are needed for the NICA booster and collider. The NICA Booster magnetic system includes 48 quadrupole superconducting magnets. The rotating coils probe developed for series magnetic measurements of booster quadrupoles doublets, as well as measuring methods are described. Results of magnetic measurements in cryogenic conditions for 12 doublets are presented and discussed.

INTRODUCTION

At the Laboratory of High Energy Physics (LHEP), serial assembly and testing of NICA Booster magnets were started at end of 2016 at the special facility [1]. The program of testing of magnets includes «warm» and «cold» magnetic measurements. It is necessary to assemble and test 48 quadrupole magnets for the NICA booster synchrotron. According to the specification, a magnetic measurement system, which is able to measure the effective length, magnetic field harmonics and magnetic axis in cold magnet inside the cryostat, is needed.

QUADRUPLE MAGNET FOR THE NICA BOOSTER

Table 1: Main characteristics of the NICA Booster Quadrupole Magnets

Parameter	Unit	Value
Number of magnets		48
Field gradient (inj./max.)	T/m	1.3 /21.5
Effective magnetic length	m	0.47
Beam pipe aperture (h/v)	mm	128 /65
Operating current	kA	9.68
Ramp rate	T/(m·s)	14.3
Field error at R= 30 mm		$\leq 6\cdot10^{-4}$
Pole radius	mm	47.5

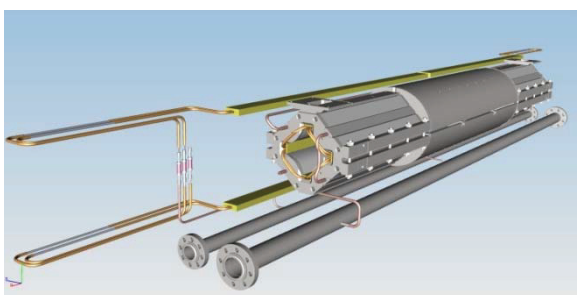

Figure 1: Booster doublet of quadrupole magnets.

The Nuclotron-type design [2], [3] based on a cold iron yoke and a saddle shaped SC coil have been chosen for booster quadrupole magnets. The doublet consists of a focusing and a defocusing lattice quadrupole magnets, which are connected with each other in a single rigid mechanical construction of about 1.8 m length (see Fig.1). The main parameters of the quadrupole magnets are presented in Table 1.

SPECIFICATION FOR MAGNETIC MEASUREMENTS

According to the specification, following parameters of a quadrupole magnet have to be measured with the required tolerances:

- Relative standard deviation of effective lengths

$$\delta L_{eff} = \frac{\Delta L_{eff}}{< L_{eff} >} \leq 5\cdot10^{-4}$$

$$L_{eff} = \frac{\int_{-\infty}^{\infty} B_2(s)\, ds}{B_2(0)}$$

- The magnetic axis with respect to magnets fiducials.
  $\sigma(\Delta x)$, $\sigma(\Delta y) \leq 0.1$ mm
- Relative integrated harmonics

b_2^*, a_2^*, a_3^*	$\leq 5\cdot10^{-4}$
b_3^*	$\leq 10^{-3}$
b_3^* at injection	$\leq 10^{-4}$
$b_n^*, a_n^*, n>3$	$\leq 10^{-4}$

MAGNETIC MEASUREMENT SYSTEM

The successful experience with prototype probe for quadrupole magnets [4], [5] based on fiberglass tube design allowed us to develop the new full-size probe for serial magnetic measurements of doublets. This probe as our probe for dipole magnets is based on radial harmonic coils arrays performed as a single multilayer PCB.

The Design of Probe

Mechanical Design. The probe design is based on long fiberglass tube as a rigid frame, which holds two PCBs with harmonic coils arrays in proper positions (see Fig. 2, 3, 4).The PCBs are not rigid and they require rigid holding plates. The plates design allows adjusting their positions in both transverse coordinates. After adjustment, plates are joined with the frame by 10 pins. Each of the PCBs covers measured magnetic field volumes of the quadrupole magnets "F" and "D". The

ISBN: 978-3-95450-197-7 doi:10.18429/JACoW-RUPAC2018-WEPSB40

METHODS AND APPARATUSES FOR STUDY OF CRITICAL CHARACTERISTICS OF HIGH-CURRENT SUPERCONDUCTORS

L.S.Shirshov
NRC "Kurchatov Institute" - IHEP, Protvino, Moscow region, 142281 Russia

Abstract

The complex of measuring devices has been created in IHEP to study the characteristics of low-temperature superconductors for currents up to 20 kA. The current-voltage characteristics of short superconducting (SC) cable samples, based on multifilament Nb-Ti alloy superconductors, were measured. The critical currents, depending on a temperature and a magnetic field up to 8 T, were measured,. The equipment was designed for measuring the minimum quenching energy (MQE) of SC sample in the normal state. It allows study the stability of the material to a short-term heat production on a separate piece of wire that is a part of the cable. The parameters of different designs of SC transformers for obtaining currents above 10 kA in the samples of partially stabilized SC cable coils of dipole and quadrupole magnets of accelerator storage complexes are given. The capabilities and limitations of different equipment options are compared.

INTRODUCTION

Superconducting magnets are widely used in a physical experiment, in particular, they are used in the magnetic structure of ultrahigh-energy accelerators [1]. For dipoles and quadrupoles of ring accelerators and colliders, the operating conditions of the current-carrying element of coils, based on the Nb-Ti alloy, is a current of 5-13 kA under the induction of the external magnetic field up to 8 T and at the temperature of 4.2 K or lower [2].

The main task in developing and optimizing the parameters of the SC cable is to obtain the maximum value of the operating current (and, correspondingly, the maximum permissible current density), while reducing the level of dynamic losses. For the dipole magnets of the SIS-300 accelerator, which is the last stage of the FAIR, the IHEP developed an SC-cable with a working current of 6 kA in the external magnetic field of 6 T and a temperature of 4.2 K, the ratio of copper/superconductor in the wires of the cable is 1.4 [3].

It is necessary to investigate the stability of the SC cable to thermal disturbances, arising in the magnet during its operation, in the SC cable with partial stabilization, along with the current-voltage characteristic I-V, $I_C(B, T)$. The criterion of stability is MQE.

When the current-carrying capacity of a 10 kA cable is reached, the conventional method of the introducing current from an external power supply becomes impractical because of arising a large heat in the low-temperature zone in the current leads. The induction method of current injection, using an SC transformer is used in the SC sample to reduce the losses of liquid helium and to achieve high current values. Further, options for the designs of transformers will be considered.

METHODS AND APPARATUSES FOR RESEARCH OF CRITICAL CURRENTS

The equipment, based on the SC-transformer, has been created, which makes it possible to carry out a measurement of the current-voltage characteristic of a short sample of a SC cable up to a current of 20 kA at the liquid-helium temperature (4.2 K). The coils of the transformer are extended in length and are produced in the shape of a racetrack, which allows one to insert a rod into the aperture with a diameter of 40 mm. A magnetic field up to the maximum of 8 T is produced by a SC solenoid [4].

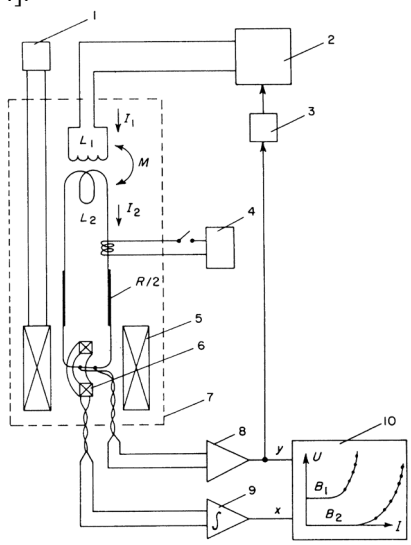

Figure 1: Scheme of the apparatus. 1 – solenoid power supply; 2- primary power supply; 3 – feed-back voltage level selection; 4 – heater power supply; 5 – solenoid; 6 – Rogowski coil; 7 – cryostat; 8 – sample voltage amplifier; - integrator; 10 – *x-y* plotter.

The automated system with a digital comparison scheme was developed by the criterion of the chosen voltage [5] for continuous measurement of the critical current dependence on the magnetic field $I_C(B)$ of SC wire samples. The use of this equipment in combination with the SC transformer allowed recording the I-V characteristic, starting from the level of 0.1 μV on the measuring section of the SC cable of various designs [6]. The scheme of the apparatus is presented in Fig. 1, general view of the device is presented in Fig. 2.

Such measurements were followed by a rapid input of current into the primary coil of the SC transformer until

ISBN: 978-3-95450-197-7 doi:10.18429/JACoW-RUPAC2018-WEPSB41

RESULTS OF MECHANICAL ANALYSIS OF WIDE-APERTURE QUADRUPOLE NODES FOR HED@FAIR EXPERIMENTS*

Y. Altukhov, I. Bogdanov, S. Kozub, E. Kashtanov, A. Olyunin, L. Tkachenko,
NRC "Kurchatov Institute" - IHEP, Protvino, Moscow region, 142281

Abstract

In the frame of collaboration with FAIR, the IHEP will develop and fabricate superconducting wide-aperture quadrupole magnets with the following parameters: the inner diameter of the coil is 260 mm; the integral field gradient is 66 T. The results of strength calculations of the most important components of these quadrupole magnets are presented in the article. Dependence of strains on the stresses of a superconducting cable for a quadrupole is presented. The stress-strain state of the collars is analyzed; the mechanical analysis of the helium vessel and the vacuum vessel of the superconducting quadrupole magnet is carried out.

INTRODUCTION

Novel studies on the fundamental properties of high-energy-density (HED) states in matter, generated by intense heavy ion beams, will be carried out by the HED@FAIR collaboration at the new accelerator Facility for Antiproton and Ion Research (FAIR) in Darmstadt, Germany [1-3]. In order to provide a strong transverse compression of energetic ion beams at the target, a special final focus system (FFS) will be used. This FFS has to provide a focal spot size of the order of 1 mm. Therefore, a large focal angle is required and consequently, wide-aperture high-gradient quadrupole magnets are employed in the FFS. This paper presented results of strength calculations of the most important components of these quadrupole magnets of the HED@FAIR FFS.

In the frame of collaboration with FAIR, the IHEP will develop and fabricate four superconducting wide-aperture quadrupole magnets with the following parameters: the inner diameter of the coil is 260 mm; the integral field gradient is 66 T. In accordance with these requirements, the design of the magnets, described below, has been developed and analyzed.

REQUIREMENTS TO THE QUADRUPOLE

The main requirements to the quadrupole magnet are: DC operating mode; the coil inner diameter is 260 mm; the minimal distance between quadrupole centers of two nearby magnets is 2.5 m; the integral of field gradient is 66 T. Additional requirements to the quadrupole magnet are: the radius of the good field quality is 110 mm; the field multipoles $|b_n|$, n = 6, 10, 14 are less than 2×10^{-4}; the integral multipole $|b_6^{int}|$ is less than 2×10^{-4}; the temperature margin is about 1 K.

*Work supported by the contract between FAIR and IHEP from 19.12.2016.

MATERIALS

It is possible to use the superconducting wire [4] for these magnets. The NbTi alloy multifilamentary composite superconducting wire consists of 8910 filaments of 6 μm diameter; the critical current density at 5 T, 4.2 K is 2.4 kA/mm^2.

The stainless steel Nitronic 40 is suitable for collars production. The collars is fastened with key, made of steel Nitronic 40. The mechanical properties of the Nitronic 40 steel, which will be used for collars and key, are presented in [5]. Particularly, yield strength is 450 MPa at 300 K and is 1390 MPa at 4.2 K.

It is proposed to use steel 1.4429 as material for the helium vessel, in which the yield strength is 280 MPa at 300 K [6]. The vacuum vessel will be produced with steel grade 1.4404, in which the yield strength is 220 MPa at 300 K [6].

GEOMETRY QUADRUPOLE

Figure 1 shows the cross section of the quadrupole.

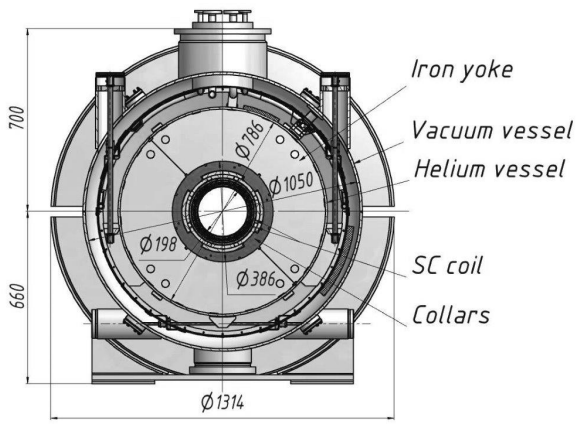

Figure 1: Cross section of the quadrupole.

The main part of the quadrupole is a superconducting coil, consisting of two layers. To ensure reliable and stable operation, it is squeezed by collars made of stainless steel, which have the necessary strength and rigidity to retain the magnetic forces that occur at current input. The coil together with the collars and the iron yoke, are placed inside the helium vessel. Through the helium vessel liquid helium is circulated, to support the coil in the superconducting state. The helium vessel is suspended on a special suspension system inside the vacuum vessel.

ISBN: 978-3-95450-197-7 doi:10.18429/JACoW-RUPAC2018-WEPSB43

AC LOSSES MEASUREMENTS IN HTS COILS

I. V. Bogdanov, E. M. Kashtanov, S. S. Kozub, V. A. Pokrovsky, L. M. Tkachenko,
P. A. Shcherbakov, L. S. Shirshov, V. I. Shuvalov, NRC "Kurchatov Institute" - IHEP,
142281 Protvino, Russia

Abstract

The possibility of production of the coils based on high-temperature superconductors (HTS) for accelerator applications is now under preliminary study in many accelerator centers and laboratories. The alternating magnetic field in these magnets causes energy dissipation (AC losses). The accurate measurement of AC losses is important for a comparison choice among different HTS conductors and for estimations of the total level of losses into final magnet too.

This article presents the measurement of transport AC losses (i.e. the losses in magnetic field which is generated by the alternating transport current) in HTS coils. Two model HTS coils with the racetrack geometry have been fabricated from 2nd generation HTS conductor supplied by two vendors. The measurement was performed by electrical method at the sinusoidal current with the amplitude up to 32 A and at the frequencies lain into interval from 5 up to 100 Hz. The measurement scheme and results are presented.

INTRODUCTION

Last years the possibility of use of high-temperature superconductor (HTS) coils for accelerator applications is under elaboration in many accelerator centers [1-4]. The unique properties of HTS can be utilized in magnets which produce very high fields (20 – 50 T) or magnets which operate at elevated temperatures (20 – 77 K). Also the fast cycling magnets have large interest. The alternating magnetic field in these magnets causes energy dissipation (AC losses). In practice about 0.1 - 0.01% of the energy saved in coil dissipates. The level of the AC losses becomes one of the main criteria at the development of superconducting magnets.

Two methods are usually applied for measurement of AC losses: calorimetric and electric [5]. The first method for racetrack HTS coils is described in [6]. It based on measurement of volume of the gas evaporated from liquid nitrogen due to dynamic losses. It is complicated and it demands the big expenses of time to attain the stationary condition, accounting of parasitic heat leakages and additional calibration.

The electric method is simpler and demands less time. Usually the inductive component of voltage on HTS coil is delivered from with the help of mutual inductance coil. Further the compensated signal was measured by the high-precision data acquisition system [6]. AC losses are obtained by integration of the product of voltage on a coil and current through a coil for one cycle. In the case of sinusoidal current the voltage on HTS coil is measured which is in phase to current. For this purpose the lock-in amplifier is used [7]. The power of AC losses is equal to the product of this measured voltage and current.

APPARATUS

The scheme of apparatus is presented in Fig. 1.

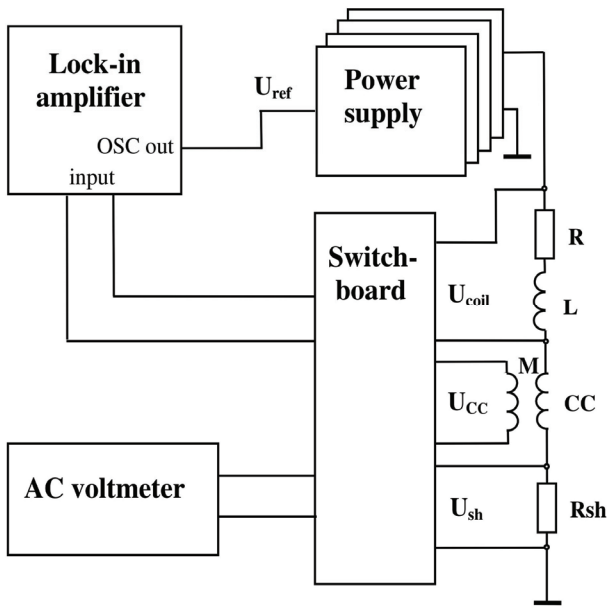

Figure 1: Electric scheme of apparatus for AC losses measurement in HTS coil.

The tested coil was powered by four operational power supplies (three KEPCO BOP 50-8M and one BOP 36-12M) connected in parallel and operated in the mode of current stabilization. For measurement of a current the AC voltmeter and 20A/75mv shunt are used. For obtaining the compensating voltage of the necessary value with a small shift of a phase and low noise the compensation coil CC has been manufactured. All its structural components were made of nonmagnetic materials. The frames of coils were made of glass-cloth-base laminate. The primary winding of the coil was made of the copper conductor with the cross section of 4.5 mm^2 in the glass tape insulation. It is wound in two layers on a frame with the outer diameter of 102 mm and has a length of 60 mm. The primary winding contains 39 turns. The secondary winding is wound by a copper wire with a diameter of 0.15 mm with enamel insulation on the frame with the diameter of 93 mm. It has the same length and contains 3024 turns. The secondary winding is inserted in primary winding and can move along axis with the help of a screw rod. The necessary value of coefficient of a mutual induction is tuned by mutual disposition of the coils and it can vary from 1.5 up to 7.8 mH.

ISBN: 978-3-95450-197-7 doi:10.18429/JACoW-RUPAC2018-WEPSB44

DEVELOPMENT OF TEST FACILITY FOR HED@FAIR QUADRUPOLES*

M. Stolyarov, A. Ageyev, R. Antonets, I. Bogdanov, V. Barmin, A. Kharchenko, E. Kashtanov, S. Kozub, A. Kalchuk, V. Luchentsov, A. Orlov, V. Pokrovskiy, E. Ptushkin, I. Terskiy, A. Vlasov, S. Zinchenko, NRC "Kurchatov Institute"–IHEP, Protvino, Moscow region, Russia

Abstract

Superconducting wide aperture high gradient quadrupoles for final focusing system of the HED@FAIR beamline are developed as a part of the collaboration contract between FAIR and NRC "Kurchatov Institute"–IHEP. Before the shipment to FAIR all manufactured quadrupoles are need to pass Factory Acceptance Tests (FAT) including cold tests to ensure that they are complied with contract specifications. Test facility for cold test of these quadrupoles is created at NRC "Kurchatov Institute"–IHEP. General description of test facility and information about its design and main characteristics are presented in the article.

TEST FACILITY

The HED@FAIR collaboration plans to generate high-energy-density states of matter using the intense heavy ion beams provided by the SIS 100 synchrotron of the FAIR facility [1]. For these experiments, it is necessary to deposit all the beam energy in the shortest possible time, i.e. to compress the ion bunch and to focus the ion beam down to a spot of one mm. Therefore, the final focusing system (FFS), containing the superconducting magnets is the most essential component of the HED@FAIR experimental installation. The proposed focusing system will have four superconducting wide aperture high gradient quadrupoles.

QUADRUPOLE MAIN REQUIREMENTS

The main characteristics of the quadrupole [2] are as follows: DC operating mode; the coil inner diameter is 260 mm; 2 m length 37.6 T/m central field gradient, 5.7 kA operating current, 5.9 T maximal field in the coil, 1079 kJ storage energy. Cold mass of quadrupole is about 6.5 tons. The cross section of the quadrupole is shown in Fig. 1.

PROGRAM OF QUADRUPOLE TEST

During the Facility acceptance test (FAT) [3], quadrupole must pass following procedures:

- Insulation Test – min. twice the operation voltage plus 500V during 2 min. between coil and vacuum vessel at room temperature.
- Vacuum tests on the cryostat at room temperature.
- Quadrupole cooling down.
- Vacuum tests on the cryostat after the quadrupole cooling down.
- RRR measurement of the coil during cooling down.
- Insulation Test – min. twice the operation voltage plus 500V during 2 min. between the coil and the vacuum vessel after cooling down to 4.5K
- Critical current measurement of the quadrupole at the ramp rate of 10A/s up to value by 10% higher than nominal current.

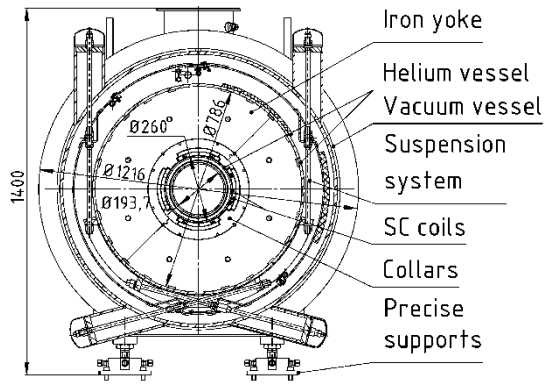

Figure 1: Cross section of the quadrupole.

- Magnetic measurements of central and integral multipoles at the nominal current.
- Measurements of the central gradient, constant of the magnet, the central integral field and the effective length of the quadrupole.
- Quadrupole operating at the nominal current for one hour.
- Quadrupole warming up.

TEST FACILITY DESCRIPTION

Test facility is needed to provide all these tests and ensure that quadrupole fulfils all criteria of FAT. It is also important to obtain all the necessary experimental data about the state of the quadrupole in real time, during the tests. General scheme of facility is shown in Fig. 2. Tested quadrupole is cooled by the satellite refrigerator [4]. Liquid helium for the satellite refrigerator is supplied by industry made cryogenic plant with liquefaction capacity up to 150 l/hr. Due to the large diameter of the quadrupole cold mass it is possible that intolerable stress could occur in the parts of the helium vessel during cooling down or warming up. To prevent it cooling down will be done in steps. Initially the inlet helium temperature will be 220 K. After all the cold mass is at 220 K, inlet helium temperature will be 60 K. Finally, the quadrupole will be cooled by liquid helium. In the same way will be arranged the warming up procedure. At the first step of warming up the inlet helium temperature is to

*Work supported by the contract between FAIR and IHEP from 19.12.2016.

ISBN: 978-3-95450-197-7 doi:10.18429/JACoW-RUPAC2018-WEPSB45

UPGRADE OF QUENCH RECORDING SYSTEM FOR MULTIPOLE SUPERCONDUCTING WIGGLERS AT BINP

M.Yu. Vasilyev†,[1], A.M. Batrakov, G.A. Fatkin[1], S.S. Serednyakov[1], A.A. Volkov,
Budker Institute of Nuclear Physics SB RAS, Novosibirsk, Russia
[1]also at Novosibirsk State University, Novosibirsk, Russia

Abstract

Magnetic poles of superconducting wigglers (SCWs) are passed through "training" phase during fabrication of SCWs at Budker INP. In "training" procedure magnetic field is increased until superconducting coils enter the resistive state. Quench Recording System (QRS) is used for registration of waveforms in each coils to determine fault initiator coil. The total number monitored coils reach 312. Outdated QRS is based on modules in CAMAC standard and requires modernization. The basis of the new system is VME64-BINP crate with multichannel digitizer ADCx32 and RIO-module for safe signal receiving in high-voltage common-mode environment. The structure and details of the new system, as well as the experience of using the old one are given in the report.

INTRODUCTION

Superconducting multipole wiggler (SCMW) is a series of magnets with sign-alternating polarity. SCMW creates lateral periodical deflection ('wiggle') of electron beam passing through. These deflections generate radiation with properties of Synchrotron Radiation (SR) depending on SCMW parameters: number of poles, period, magnetic field. The Budker Institute has manufactured wigglers, which are successfully used as insertion devices for such centres of synchrotron radiations as CLS (Canada), DLS (England), LNLS (Brazil), ELETTRA (Italy), BESSY (Germany), CAMD (USA), Siberia (Russia), ASHo (Australia), ALBA-CELLS (Spain), KIT (Germany) [1].

Each pole of the wiggler consists of a core of soft magnetic material, which is divided into two halves: lower half and upper one with four superconducting coils wound on each of them. All coils are connected in series in such a way that the magnetic field changes its sign from pole to pole.

"Training" is an important phase of SCMW manufacturing process. During the "training" procedure the magnetic field is increased until superconducting coils enter the resistive state. The voltage is monitored in each coil by Quench Recording System (QRS) to determine the fault initiator. Repeating this process several times helps to increase the acceptable magnetic field in coils until reaching the target value. The defective coils that are not able to withstand the necessary magnetic field can be also detected and replaced.

QRS based on modules in CAMAC standard has been used for this purpose over several decades. The first automated system for quench recording at BINP was created at 2001 for 49 poles wiggler for ELETTRA storage ring (Italy) [2]. Despite the high reliability of the existing system, its upgrade is required. CAMAC platform is becoming obsolete, and support of outdated modules, repair of the faulty ones or fabrication of the new batch, seems impossible due to the discontinuation of production of a significant part of used electronic components. In addition, the necessity of QRS expanding and increasing the number of channels is present.

CAMAC BASED QRS

Stand, which is currently in use for quench recording, is based on three pairs of modules in CAMAC standard: digitizer ADC–333 [3] and multiplexer MUX16->1x4. ADC-333 (Fig. 1) is a four-channel multiplexed digitizer with 12-bit resolution and 3 MSPS sampling rate. MUX16->1x4 (Fig. 2) is a carrier board with four embedded MUX-cards (Fig. 3), on each of which analog multiplexer 16 to 1 and 16-channel preamp are installed. The total number of measured coils reaches 192 channels (64 channels per modules pair). Pair of modules block diagram is shown in Fig. 4.

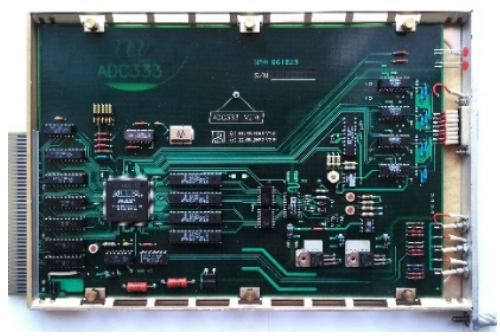

Figure 1: Digitizer ADC-333.

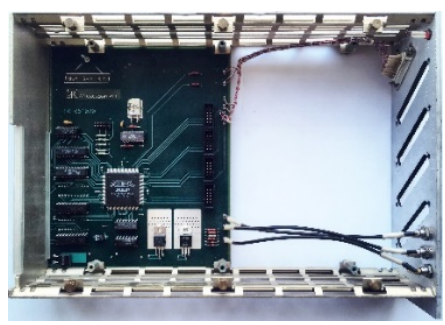

Figure 2: MUX16->1x4.

ISBN: 978-3-95450-197-7 doi:10.18429/JACoW-RUPAC2018-WEPSB47

COUPLER DESIGN FOR RISP SPOKE CAVITY*

V. Zvyagintsev †, R.L. Laxdal, Y. Ma, B. Matheson, Z. Yao, B. Waraich, TRIUMF, V6T 2A3, Vancouver, Canada

Abstract

The RISP project includes a heavy ion linac to accelerate ions up to 238U to 200 MeV/u with 400 kW of beam power. The same accelerator will also be capable of accelerating light ions with proton currents and final energy of 0.66 mA and 600 MeV. TRIUMF designed the superconducting single spoke resonator for the linac SSR1 at 325 MHz for beta=0.3. According to specifications the cavity will require the RF coupler to be capable for operation in CW regime close to full reflection with a forward power of 5 kW. This paper reports about the RF coupler specifications, simulations and design.

INTRODUCTION

The RISP multi-purpose accelerator facility has been proposed at the Institute for Basic Science (IBS), Korea, for research in atomic and nuclear physics, material science, bio and medical science, etc. It can provide various energy beams from protons to exotic rare isotopes up to uranium [1]. A prototype cavity of the β=0.3 single spoke resonator SSR1 has been designed and fabricated at TRIUMF under collaboration with IBS [2]. A coupler for the SSR1 spoke cavity operating at 2K was designed at TRIUMF.

COUPLER SPECIFICATIONS

The coupler specification is based on cavity and beam parameters, coupling and assembling considerations and cryogenic load for the cryomodule.

Cavity and Beam Parameters

The SSR1 main cavity parameters and nominal beam parameters are presented in Table 1. For nominal operation the coupler should transmit in the cavity an RF power of 1.64 kW for the beam and 5.4 W for the structure walls.

Table 1: Cavity and Beam Parameters

Parameter	Unit	Value
Frequency, f	MHz	352
Geometry beta, β_o		0.30
Shunt impedance, R/Q	Ohm	233
Quality factor, Q_o		5×10^9
Effective voltage, V_{eff}	MV	2.50
Cavity power, P_{cav}	W	5.4
Beam current, I_{beam}	μA	656
Beam power, P_{beam}	kW	1.64

Cavity Detuning and Forward Power

The forward power requirement is given by equation [3]

$$P_{for} = \frac{P_{cav}}{4\beta}\left[(1+\beta+b_o cos\varphi)^2 + \left(-2Q_o\frac{\Delta f_{tot}}{f_o} - bsin\varphi\right)^2\right] \quad (1)$$

where $b_o = \frac{P_{beam}}{P_{cav}}$, $\beta = \frac{Q_o}{Q_{ext}}$, $\Delta f_{tot} = \Delta f_s \pm \Delta f_d$ total detuning consists of static (controllable) detuning Δf_s=0 (we assume that it's compensated) and random dynamic (uncontrollable) detuning Δf_d. For estimation of power requirement we set the accelerating phase angle $\varphi = 0$ (for maximum beam power). Finally the equation (1) is reduced to

$$P_{for} = \frac{P_{cav}}{4\beta}\left[(1+\beta+b_o)^2 + \left(-2Q_o\frac{\Delta f_d}{f_o}\right)^2\right] \quad (2)$$

The cavity will operate at 2K in superfluid helium at a pressure of 31±0.3 mbar. The expected sensitivity to helium pressure fluctuations should be ≤ 10 Hz/mbar and results in detuning of ≤ ±3 Hz. These tend to be slow variations and easily compensated by the tuner.

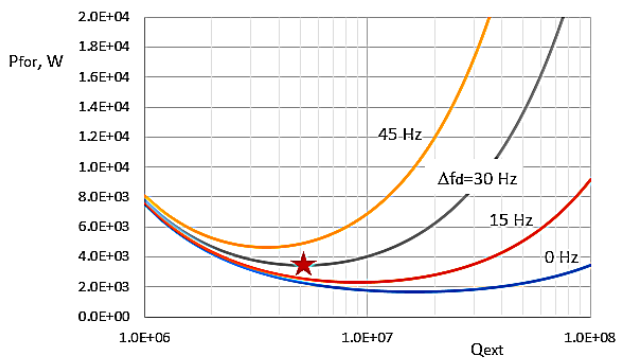

Figure 1: P_{for} vs. Q_{ext} for nominal accelerating regime at various Δf_d; optimum point P_{for}=3.4 kW at $Q_{ext}=5.2\cdot10^6$ for Δf_d=30 Hz is marked with red star.

The cavities will operate in CW regime so we do not consider Lorentz force detuning (LFD). This will only be an issue at turn on if the cavity is locked at low gradient and ramped up to higher gradient.

Microphonics is the main source of fast oscillation typically driven by the lowest mechanical mode. Previous measurements from other similar cavities (either SSR or

* Work supported by TRIUMF-RISP Collaboration
† zvyagint@triumf.ca

ISBN: 978-3-95450-197-7 doi:10.18429/JACoW-RUPAC2018-WEPSB48

INPUT POWER COUPLER FOR NICA INJECTOR COAXIAL HALF WAVE SC CAVITY

S. V. Matsievskiy*, M. V. Lalayan, M. G. Gusarova
National Research Nuclear University MEPhI , Moscow, Russia

Abstract

Nuclotron-based Ion Collider fAcility (NICA) is being built in Dubna, Russian Federation. Usage of the accelerator superconducting HWR cavities for the injector part of the accelerator is considered. According to technical requirements power coupler is able to withstand 13 kW of RF average transmitting power. Additionally, coupling tuning in small range should be possible. In this paper results of the 325 MHz HWR power coupler R&D are presented and discussed.

DESIGN OVERVIEW

New HWR cavities are being developed for the Nuclotron-based Ion Collider fAcility (NICA) injector. These cavities comprise the $\beta = 0.21$ accelerating section [1]. Accelerator will be operating in high duty pulsed mode, however power coupler simulations were done for CW mode due to ensure some safety margin.

Model of the HWR cavity is presented in Fig. 1.

Figure 1: HWR cavity model.

The current design is based on the resutls of thermal, mechanical and electrodynamic simulations discussed below. Coupler geometry was optimised to handle necessary RF power, match the cryogenic system requirements and assure certain operation reliability. RF power is coupled to cavity via port in cavity medial plane.

It was decided to base the design of the coupler on 50 Ohm coaxial transmitting line with outer diameter of

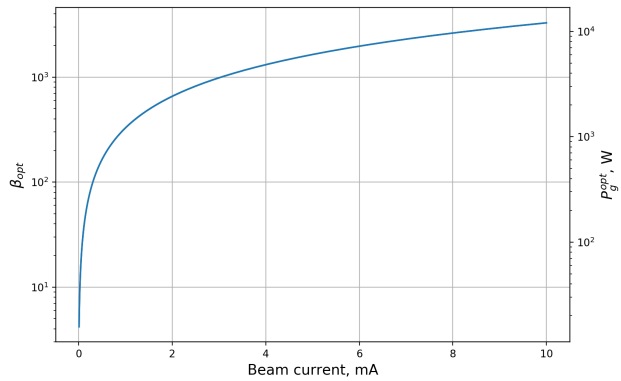

Figure 2: Power input coupling vs beam current.

47.5 mm. Conventional two RF window design was chosen. RF windows are pillbox-shaped cavities with flat ceramic disk (96 % Al_2O_3). Cold window will operate at 80 K, warm window will be at room temperatures.

For the coaxial inner conductor support rings PTFE was chosen.

According to the technical design specifications HWR power input must allow coupling tuning for operation at beam currents form 0 to 10 mA. Optimal cell coupling and RF power level for this range are shown in Fig. 2. Antenna movement in range ±7 mm will fulfill this requirement.

Bellows were introduced to the design. Cold bellows connect cavity with the cold RF window. Warm bellows mechanically decouple power coupler from the cryostat wall. Bellows metal thickness was chosen to be 0.4 mm. It is not to thin to bend significantly under its own weight yet still flexible enough to allow antenna movement in required range. To decrease temperature of the antenna and, therefore, radiation load on the 4 K line, antenna is also made out of copper.

The model of the coupler is shown in Fig. 3.

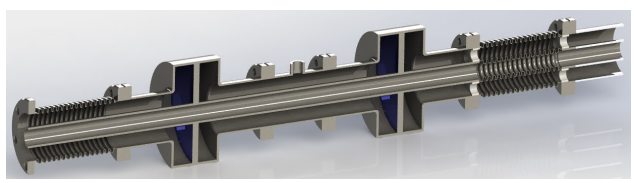

Figure 3: Two window coupler model.

HEAT LOADING

Copper coating of the conductors was considered [2, 3]. It drastically decreases the RF losses in the metal but also

* MatsievsliySV@gmail.com

ISBN: 978-3-95450-197-7 doi:10.18429/JACoW-RUPAC2018-WEPSB50

A STUDY ON IMPLEMENTATION OF MULTISTRIP CRYSTALS TO PROTECT THE SEPTUM-MAGNETS AND TO GENERATE THE GAMMA RADIATION ON THE U-70 ACCELERATOR

A.G. Afonin, E.V. Barnov, G.I. Britvich, Yu.A. Chesnokov, P.N. Chirkov, A.A. Durum, M.Yu. Kostin, I.S. Lobanov,V.A. Maisheev, I.V. Poluektov, S.F. Reshetnikov,Yu.E. Sandomirskiy, D.A.Savin, A.A.Yanovich, NRC "Kurchatov Institute" - Institute for High Energy Physics, 142281 Protvino, Russia

Abstract

Recently started studies on the application of volume reflection of particles in crystals for the steering beams (for extraction and collimation of a circulating beam in accelerators). Volume reflection is more efficient than channeling, but requires amplification of the deflection angle by applying multicrystals. The report discusses two new applications of multicrystals made like multistripe structures: 1. The property of effective deflection of particle beam was used to protect the septum-magnets of the U-70 in the process of extraction of the proton beam with energy of 50 GeV. 2. The possibility of generation of gamma radiation was studied in the secondary electron beam with energy of 7 GeV. In both cases, promising preliminary data were obtained.

INTRODUCTION

Important in the physics of interactions of charged particles with single crystals was E. Tsyganov's proposal [1] to use bent single crystals to rotate positively charged particles. It turned out that the processes of interaction of particles with bent single crystals differ from processes in straight crystals. Thus, the so-called phenomenon of volume reflection [2.3] of a particle beam from bent crystallographic planes was discovered. In addition, the radiation of electrons and positrons in the plane fields of bent single crystals was predicted [4] and then measured [5], which accompanies the process of volume reflection. These two phenomena were the basis for our experimental study.

The physics of the process consists in the fact that at certain angles of entry of particles into the crystal with respect to the crystallographic planes, these particles are reflected from these planes. However, even under optimal conditions, the mean reflection angle (the mean angle of volume reflection) does not exceed 1.5 critical channeling angles (i.e., relatively small). Despite this fact, the process of volume reflection is of some interest because it has a high efficiency of reflection. When the reflected particle moves, its transverse coordinate in the plane of the bend undergoes apereodic oscillations. Due to this character of motion, the electron (positron) involved in the process emits gamma quanta. A theoretical description of this radiation process can be found in the papers [6, 7]. The first experiment to detect such radiation was performed at electron energy of 10 GeV [8] and showed satisfactory agreement with the calculations.

The present experiment is devoted to the study of scattering (volume reflection) of 50 GeV protons and radiation losses of energy by 7 GeV electrons in a multistrip crystal deflector.

MULTISRIP CRYSTAL DEFLECTOR

The appearance of the prepared multistrip crystal device is shown in Figure 1. The device comprises 24 bent crystals in the form of bent strips. The method of bending several strips in one holder was developed in experiments on volume reflection of proton and negative pion beams [9]. Six strips along a beam of 2.5 mm each reinforce the radiation effect, and four layers of 0.5 mm across the beam provide the necessary transverse dimension of 2 mm (thick crystals cannot bend to the required angles, so a sandwich is needed). After optical verification, the device was placed in a two-axis goniometer . The bending angle of each strip is 1.1 mrad. It is larger than the Coulomb scattering angle of electrons with energy of 7 GeV on a chain of six crystals, which is equal to 0.8 mrad.

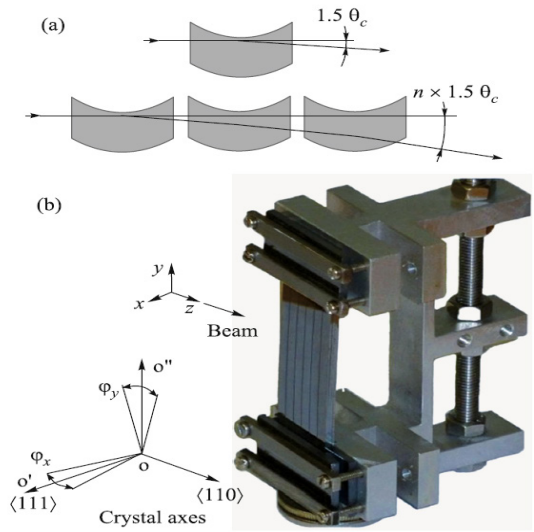

Figure 1: Multilayer crystal radiator for the beam: (a) the schematic of operation and (b) the appearance and arrangement with respect to the beam.

For each individual strip, its characteristics for deviation and ability to radiation were calculated. So according to these calculations, the average reflection angle of

ISBN: 978-3-95450-197-7 doi:10.18429/JACoW-RUPAC2018-WEPSB51

DEVELOPMENT OF HIGH POWER S-BAND KLYSTRON

A. Barnyakov, A. Levichev[1], S. Samoylov, D. Chekmenev, BINP SB RAS, Novosibirsk, Russia.

[1]also at Novosibirsk State University, Novosibirsk, Russia

Abstract

The design and scheme of the model of the S-band klystron model developed at Budker Institute of Nuclear Physics are described. The results of simulation and preliminary results of the tests are presented. Parameters of the klystron: operating frequency is 2856 MHz, output power is about 50 MW, pulse length is 3.5 μs. The tests of the output vacuum windows were carried out. The cathode node and collector are tested at a voltage of 200 kV and beam current of 140 A. A klystron buncher is prepared for measurements and tuning.

INTRODUCTION

Taking into account the necessary to develop new linear S-band accelerators in BINP SB RAS, the development of the own klystron is very important. Presently, the klystrons 5045 (SLAC) [1] are used at BINP injection complex VEPP-5 [2], and the lifetime of these klystrons is coming to the end. We are planning that new klystrons will replace old klystrons 5045 produced at SLAC. So new klystron should have the same main characteristics: frequency is 2856 MHz, pulse input RF power is not more than 350 W, pulse output RF power is about 50 MW, pulse duration is 3.5 μs, pulse repetition rate is not less than 25 Hz.

SIMULATION

To calculate the basic parameters of the geometry of the klystron elements and klystron characteristics the CST Studio software package was used [3]. Figure 1 shows the beam dynamics and the energy spectrum of the electron beam in the klystron. Figure 2 shows the signal from the output waveguide of the klystron.

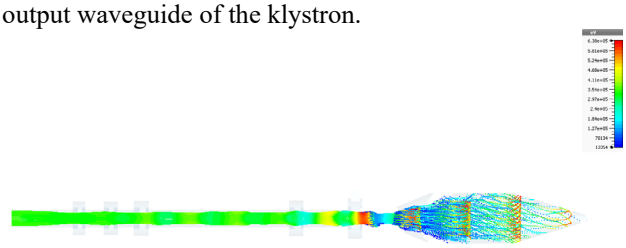

Figure 1: Dynamics of a beam in a klystron.

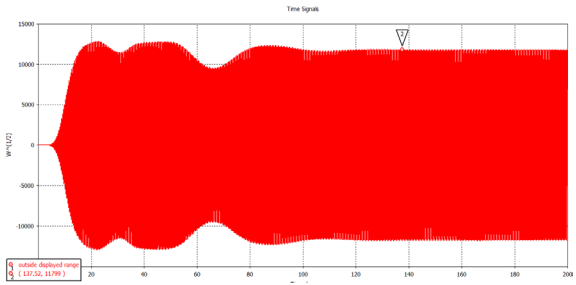

Figure 2: Output signal.

The initial energy of the electron beam is 350 keV, current is 400 A. The output RF power is about 69 MW.

COMPONENTS

The model without bunching cavities was created to test the cathode node and the collector (Fig. 3).

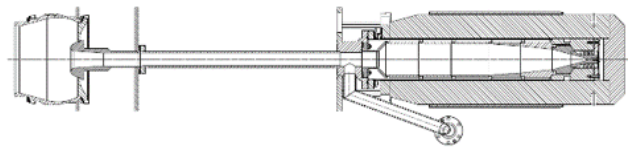

Figure 3: Model for testing the cathode node and collector.

A working version of the solenoid for focusing the electron beam was also created. Figure 4 shows the measured magnetic field on the klystron axis.

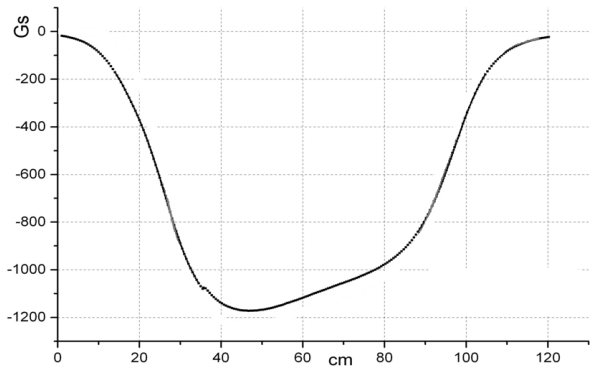

Figure 4: Magnetic field on the axis of the solenoid.

Dispenser cathode with a peak current density of 7.8 A/m^2 is shown on Fig. 5.

Figure 5: Cathode.

ISBN: 978-3-95450-197-7 doi:10.18429/JACoW-RUPAC2018-WEPSB52

AMPLITUDE-PHASE CHARACTERISTICS OF A THIN DIAPHRAGM IN A RECTANGULAR WAVEGUIDE

Yu. D. Chernousov†, ICKC SB RAS, BIC SB RAS, Novosibirsk, Russia
S.E. Erokhin, NSU, BIC SB RAS, Novosibirsk, Russia

Abstract

A model of a thin diaphragm in a rectangular waveguide is discussed. Expressions for determining the amplitude-phase characteristics of the diaphragm are presented. The position of the diaphragm nearest basic reference plane is determined, where the reflection coefficient is a real negative number. The basic reference plane is shown theoretically and experimentally to be on the right side of the diaphragm, i.e. outward from the generator. The obtained relationships are shown to allow the amplitude-phase characteristics of the diaphragm to be experimentally determined using the measuring line.

INTRODUCTION

Diaphragm is an orifice plate mounted transversely to the axis of a waveguide to blank off it. Diaphragms are used as inlet and outlet units of resonators, filters, accelerating systems [1, 2]. Diaphragm characteristics or, in other words, loads with complex reflection coefficient usually are considered in terms of the method of equivalent circuits by treating the diaphragm as the reactivity across the line (waveguide) [3, 4]. Physically adequate description of interference phenomena in the waveguide at wave scattering from inhomogeneities is allowed by the method of incident and reflected waves [5]. This method was used for considering the thin diaphragm. The reflection from the diaphragm produced a standing wave in the waveguide. The minimum position was determined using the measuring line, and the measurement results were used for calculation of modules and phases of reflection and transition coefficients of the diaphragm.

BASIC RELATIONSHIPS

Thin Diaphragm in a Rectangular Waveguide

We give relationships to determine amplitude-phase characteristics of a thin diaphragm in plane of its geometrical arrangement in a rectangular waveguide.

Let wave with amplitude a falls to the diaphragm. When so, another two waves emerge in the waveguide; these are reflected and transmitted waves of respective amplitudes Γa and Ta, where in-plane coefficients Γ and T can be shown in complex form:

$$\Gamma = |\Gamma| e^{i\psi}, \mathrm{T} = |\mathrm{T}| e^{i\theta} \quad (1)$$

Here $|\Gamma|$ and ψ are module and phase of the reflection coefficient; $|\mathrm{T}|$ and θ are module and phase of transition coefficient. In the absence of losses, the following equations can be written for the thin diaphragm [4, p. 144; 6]:

$$1 + \Gamma = \mathrm{T} \quad (2)$$

$$|\Gamma|^2 + |\mathrm{T}|^2 = 1 \quad (3)$$

The first equation follows from boundary conditions on the diaphragm, the second from the energy conservation law. Complex coefficients **Γ** and **T** can relate to radius-vectors on the complex plane. Relations (2) and (3) also are valid for these vectors **Γ** and **T**. In equality (2), if move **Γ** to the right and square all the expression, then the scalar product of vectors **Γ** and **T** with regard to (3) gives:

$$(\mathbf{\Gamma}, \mathbf{T}) = 0 \quad (4)$$

Move the origin of radius-vector **Γ** to point (1,0) in the complex plane. In accordance with expressions (2), (3), (4) we have diagram [6] that characterizes the amplitude-phase properties of the diaphragm:

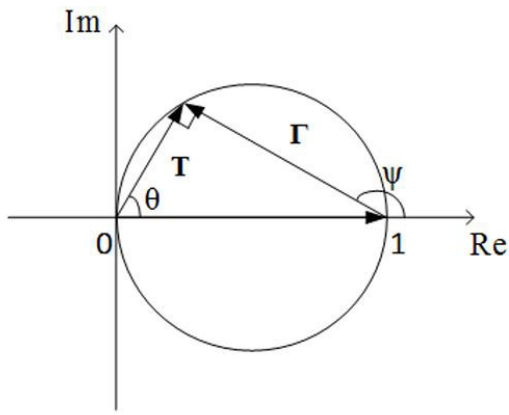

Figure 1: Amplitude-phase diagram of the diaphragm.

Diaphragms are classified into inductive, capacitive and resonant. In Figure 1, points in the unit diameter circumference correspond to multitude of inductive and capacitive diaphragms in the waveguide. The further consideration will concern inductive diaphragms because they are used for connection of inlet resonators of accelerating structures with the fill line. The points in the upper semiplane of the circumference correspond to the inductive diaphragms: $\pi \geq \psi \geq \frac{\pi}{2}$ and $\frac{\pi}{2} \geq \theta \geq 0$. Geometrically, Fig. 1 allows the following relationships:

$$\psi - \theta = \frac{\pi}{2} \quad (5)$$

† email address: chern@catalysis.ru

ISBN: 978-3-95450-197-7 doi:10.18429/JACoW-RUPAC2018-WEPSB53

START OF OPERATION OF A STANDING WAVE DEFLECTING CAVITY WITH MINIMIZED LEVEL OF ABERRATIONS

V. Paramonov*, INR of the RAS, 117312, Moscow, Russia
K. Floettmann, DESY, 22607, Hamburg, Germany
V. Danielyan, A. Simonyan, V. Tsakanov, CANDLE SRI, 0400, Yerevan, Armenia

Abstract

A family of deflecting structures with improved RF efficiency and minimized level of aberrations in the deflecting field distribution was presented at RuPAC 2016 [1]. The first cavity proposed in that paper has been designed for the diagnostics of the longitudinal distribution of the unique bunches generated at the REGAE facility. A short deflecting cavity was constructed, tuned and is now installed in the REGAE beam line. The cavity has been tested at the operational level of RF power. We describe main distinctive features of the cavity and report first results on beam operation.

INTRODUCTION

Periodical Deflecting Structures (DS's) were introduced for the deflection and separation of charged particle in the 1950s and 1960s. Here the bunch crosses the DS synchronously with the deflecting field Ed on the phase $\phi = 0°$, so that all particles gain a similar increment in the transverse momentum p_t.

Today DS's find new applications for the purpose of diagnostics of the longitudinal distribution, emittance exchange and luminosity improvements in colliders by introducing a correlated transverse momentum, i.e. a streak. For these applications the DS operates in another mode - the central particle of the bunch crosses the DS at the phase $\phi = 90°$, so that the transverse field E_d is zero for the bunch center, but downstream and upstream particles achieve opposite increments in p_t. In these applications a DS should produce a minimal distortion of the original distribution of the particles in the 6D phase space.

PHYSICAL BASE

Transverse emittance growth during the passage of a DS is related to coupling and to aberrations, i.e. nonlinear additives in the distribution of the deflecting field E_d, which appear due to a non-relativistic energy of the particles, additions from higher multipole modes, and higher spatial harmonics in the distribution of the dipole field E_d. The analysis of the deflecting field distribution was performed in [2,3]. The main attention should be drawn to the higher spatial harmonics in the E_d distribution. To estimate the level of higher spatial harmonics and as a criterion for the optimization of the DS shape the parameters $\delta\psi_j(z)$ and Ψ_j on the DS axis have been introduced:

$$\delta\psi_d(z) = \psi_d(z) + \frac{\Theta_0 z}{d}, \quad \Psi_d = max(|\delta\psi_d(z)|). \quad (1)$$

The physical sense of the parameters is the deviation and the maximal deviation of the phase of the equivalent traveling wave E_d distribution from the synchronous harmonics. Here Θ_0 is the operating phase advance, d is the DS period length and $\psi_d(z)$ is the phase distribution for the equivalent traveling wave E_d.

By minimizing Ψ_d we keep the bunch close to the DS axis, where the nonlinear field of the higher spatial harmonics is minimal. Simultaneously the level of higher spatial harmonics in E_d will be reduced.

For conventional iris loaded DS's [4] the minimization of Ψ_d represents an additional limitation and can be achieved only at the expense of a reduction in the effective shunt impedance Z_e. To combine a high RF efficiency and a high field quality a decoupled DS was proposed [5]. Later on the decoupled DS was investigated and optimized more thoroughly, showing very high rates in RF efficiency together with high field quality [1].

CAVITY DESIGN PARAMETERS

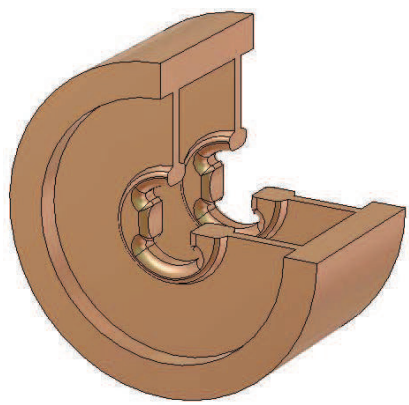

Figure 1: Geometry of the a decoupled structure which was selected for the deflecting cavity in the REGAE facility.

For implementation of a deflecting cavity for diagnostics of the longitudinal particle distribution at REGAE (Relativistic Electron Gun for Atomic Exploration) [6], a decoupled DS's option was selected as a compromise of RF parameters, low beam energy and other extreme beam parameters, and appreciation of construction effort and available space. The geometry of the selected decoupled DS is shown in Fig. 1. Operating in the standing wave mode, the short

* paramono@inr.ru

ISBN: 978-3-95450-197-7 doi:10.18429/JACoW-RUPAC2018-WEPSB54

SELECTION OF MATERIALS FOR TARGET STATION EQUIPMENT AT CYCLOTRON CYCLON-70*

E.N. Savitskaya†, M.A. Maslov, S.A. Nikitin, V.N. Peleshko, N.V. Skvorodnev,
Institute for High Energy Physics of the National Research Centre "Kurchatov Institute"
(NRC KI – IHEP), Protvino, Moscow Region, Russia

Abstract

A Radioisotope Centre of Nuclear Medicine for commercial production of radioisotopes is under construction now in Protvino. It is based on IBA (Belgium) Cyclone-70 proton cyclotron with proton energy up to 70 MeV and beam current up to 750 μA. The proton beam is split into two halves to provide simultaneous operation of two target stations. NRC KI – IHEP develops the design of the target station to produce nuclides Sr82 and Ge68 by the 70 MeV proton beam with current up to 375μA ($2.3 \cdot 10^{15}$ proton/s).

The present work is devoted to selection of target station materials to minimize the induced radioactivity of equipment during isotopes production. The main source of this radioactivity is a flux of secondary neutrons created from proton-nuclear interactions with target materials. The nucleon-nucleus interactions and the transport of particles in substances were simulated by package of Monte Carlo codes HADR99 and FAN15 specially adapted for this task. Time dependence of the activity of nuclides accumulated in surrounding equipment and the effective dose rate after the end of bombardment (EOB) was calculated. Several alloys were considered and aluminum alloy AMg2 was chosen as most promising base material.

INTRODUCTION

The wide use of radioactive isotopes in medical practice needs the increase of their industrial production. The manufacturing of radioisotopes Sr82 and Ge68 by the 70 MeV proton beam with current up to 375μA will be organized in Protvino on the base of cyclotron Cyclone-70 (IBA). Sr82 and Ge68 will be generated by irradiating rubidium (or RbCl) and gallium respectively. Wide peak in cross section of reaction $^{nat}Rb(p,xn)^{82}Sr$ lies in the energy range 40 – 70 MeV. The energy range of maximum yield of reaction $^{nat}Ga(p,xn)^{68}Ge$ is 12 – 30 MeV. This makes it possible to irradiate the rubidium and gallium targets simultaneously.

In general, terms the target station is a pipe with bottom inserted into a vertical protective sleeve of transport shaft from the top floor. A guide is installed in the pipe. A carriage moves along the guide by means of a chain connected to the motor. The encapsulated targets are delivered by the carriage to the place of irradiation. On the side of the beam in the pipe there is a window with a thin membrane. The pipe is filled with water. Water serves both the target cooler and neutron shield in the transport shaft. The components of the target station are shown in Fig. 1.

* Work supported by the Ministry of Education and Science of the Russian Federation, the agreement ID 0000000007417P3I0002
† savitskaya@ihep.ru

The targets fixed in a duralumin holder will be irradiated for one session (10-14 days). Secondary neutrons from proton-nuclear interactions in target materials have a large penetrating power. Inelastic interactions of neutrons with nuclei of surrounding equipment lead to the accumulation of radionuclides in them. The holder will be disposed of after each session. The remaining details of the target station will be irradiated during a large number of sessions with short technological breaks between them. During the breaks the decline in activity of the details will occur mainly due to the decay of short-lived nuclides. Long-lived nuclides will be accumulated in the materials from the session to the session.

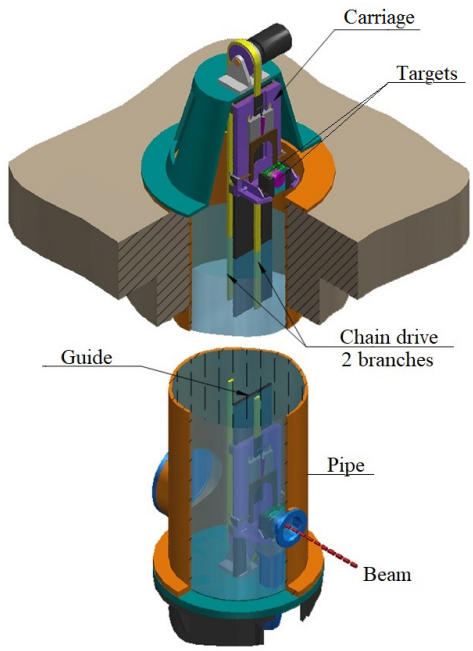

Figure 1: The target station.

Photons, electrons and positrons from nuclide decays form a radiation field in a target hall after the EOB. Photons make the main contribution to the dose rate. Maintenance of the target station involves periodic replacement of the membrane. Therefore, it is required to minimize the induced radioactivity of equipment and to determine what time is necessary for the decay of short-lived nuclides.

CALCULATION MODEL

The interactions of neutrons and protons with nuclei and the transport of particles in substances are simulated by package of Monte Carlo codes HADR99 [1] and FAN15 [2, 3]. A cascade-exciton model is used to describe the inelastic reactions of neutrons with energy above 20 MeV and protons. The interactions of neutrons ranging

ISBN: 978-3-95450-197-7 doi:10.18429/JACoW-RUPAC2018-WEPSB56

METHODICAL ISSUES OF THE USE OF DETECTORS FOR DOSIMETRY IN BEAMS OF THE CARBON NUCLEI OF THE ACCELERATOR U-70

A.G. Alexeev, E.V. Altuhova, I.I. Degtarev, V.A. Pikalov, O.V. Sumaneev, A.A. Yanovich, F.N.Novoskoltsev, NRC «Kurchatov Institute» – IHEP, Protvino
O. Kiryuhin, MSU, Moscow

Abstract

In the SRC "Kurchatov Institute"-IHEP are working on the project "Center for Ion Radiation Therapy". At present, the first stage of this project has been implemented is the creation of the Center Use "Radiobiological Stand on Carbon Beam of U-70 (RSU) [1]. RSU is used for radiobiological experiments. The research and testing of systems for radiotherapy by a carbon ions beam are tested at RSU. In this paper the result of methodologilal issue of the use of thermoluminescent detectors (TLD) and radiochromic films for dosimetry in a beam of carbon ions are used.

MEASURING INSTRUMENTS USED

In this work, 2 types of thermo luminescent detectors were used (DTG-4 and MMT-7). DTG-4 is single-crystal TLD, produced by the Angarsk branch of URALPRIBOR MMT-7 is polycrystalline, manufactured by RADCARD Poland (LiF). These TLD are specially designed for dosimeter for ions beam with large LET. The HARSHAW-4000 was used for the reading of TLD (NTC "Praktica-TL, Moscow).

Together with the TLD, the radiochromic EBT3 film was used [2]. All dissymmetric measurements were performed in a water phantom, which is a container with external dimensions of 590x360x375 mm. The material of the phantom walls is polycarbonate. The thickness of the front wall (relative to the direction of the beam) is 30 mm, the lateral - 15 mm. Inside the water phantom, an air chamber (caisson) is fixed with external dimensions of 130x240x265 mm. Detectors and dosimeters were placed in the caisson. The scheme of measurement is present on Fig. 1.

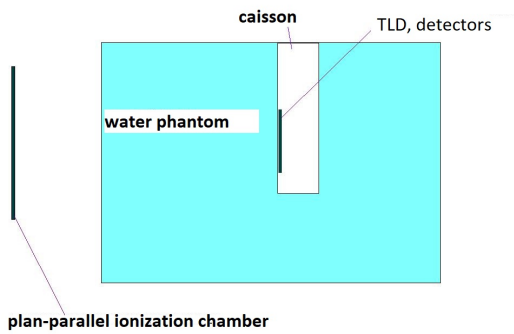

Figure 1: Measurement scheme.

CALCULATION OF THE BRAGG CURVE

The calculation of the Bragg curve and the estimation of the contribution of thermal neutrons to the TLD readings was made on the basis of calculations for 3 codes. MCNPX, FLUKA [3] and RT&T code system [4] were used for calculations. Absorbed dose (secondary charged particles contributions) in the water phantom is present on Fig. 2. The calculation is carried out by FLUKA. Carbon ions energy is 400 MeV/ nucleon. A comparison of the calculation of the Bragg peak and the experiment [5] is shown in Fig. 3. The calculation of the average LET value with the help of Fluke is shown in Fig. 4.

Neutron flux (thermal neutrons (En<0.4 eV) and in total energy range (TOTAL)) in the water phantom is present on Fig 5a, b. MCNPX, FLUKA and RT&T code system were used for calculations. A good agreement between the results of calculations for different codes is observed.

Estimation of contribution of thermal neutrons to the indication of DTG-4 (after the Bragg peak) is not more then 2 %.

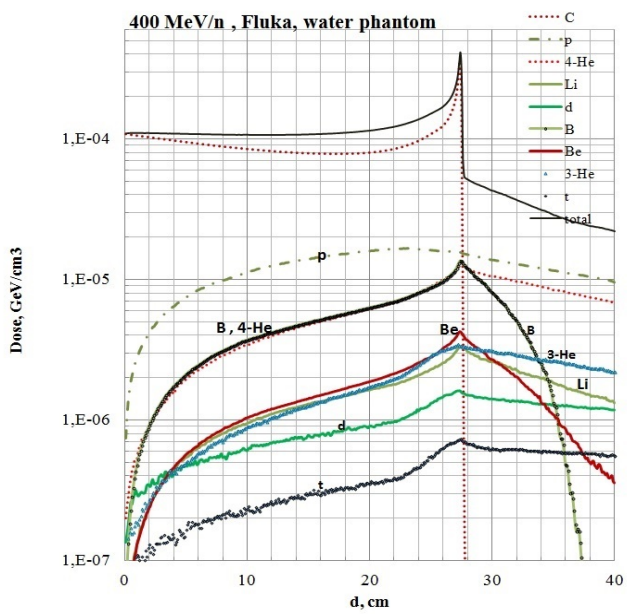

Figure 2: Absorbed dose (secondary charged particles contributions) in the water phantom.

ISBN: 978-3-95450-197-7 doi:10.18429/JACoW-RUPAC2018-WEPSB57

A STUDY ON IMPLEMENTATION OF MULTISTRIP CRYSTALS TO PROTECT THE SEPTUM-MAGNETS AND TO GENERATE THE GAMMA RADIATION ON THE U-70 ACCELERATOR

A.G. Afonin, E.V. Barnov, G.I. Britvich, Yu.A. Chesnokov, P.N. Chirkov, A.A. Durum, M.Yu. Kostin, I.S. Lobanov,V.A. Maisheev, I.V. Poluektov, S.F. Reshetnikov,Yu.E. Sandomirskiy, D.A. Savin, A.A. Yanovich, NRC "Kurchatov Institute" - Institute for High Energy Physics, 142281 Protvino, Russia

Abstract

Recently started studies on the application of volume reflection of particles in crystals for the steering beams (for extraction and collimation of a circulating beam in accelerators). Volume reflection is more efficient than channeling, but requires amplification of the deflection angle by applying multicrystals. The report discusses two new applications of multicrystals made like multistripe structures: 1). The property of effective deflection of particle beam was used to protect the septum-magnets of the U-70 in the process of extraction of the proton beam with energy of 50 GeV. 2). The possibility of generation of gamma radiation was studied in the secondary electron beam with energy of 7 GeV. In both cases, promising preliminary data were obtained.

INTRODUCTION

Important in the physics of interactions of charged particles with single crystals was E. Tsyganov's proposal [1] to use bent single crystals to rotate positively charged particles. It turned out that the processes of interaction of particles with bent single crystals differ from processes in straight crystals. Thus, the so-called phenomenon of volume reflection [2, 3] of a particle beam from bent crystallographic planes was discovered. In addition, the radiation of electrons and positrons in the plane fields of bent single crystals was predicted [4] and then measured [5], which accompanies the process of volume reflection. These two phenomena were the basis for our experimental study.

The physics of the process consists in the fact that at certain angles of entry of particles into the crystal with respect to the crystallographic planes, these particles are reflected from these planes. However, even under optimal conditions, the mean reflection angle (the mean angle of volume reflection) does not exceed 1.5 critical channeling angles (i.e., relatively small). Despite this fact, the process of volume reflection is of some interest because it has a high efficiency of reflection. When the reflected particle moves, its transverse coordinate in the plane of the bend undergoes apereodic oscillations. Due to this character of motion, the electron (positron) involved in the process emits gamma quanta. A theoretical description of this radiation process can be found in the papers [6, 7]. The first experiment to detect such radiation was performed at electron energy of 10 GeV [8] and showed satisfactory agreement with the calculations.

The present experiment is devoted to the study of scattering (volume reflection) of 50 GeV protons and radiation losses of energy by 7 GeV electrons in a multistrip crystal deflector.

MULTISRIP CRYSTAL DEFLECTOR

The appearance of the prepared multistrip crystal device is shown in Fig. 1. The device comprises 24 bent crystals in the form of bent strips. The method of bending several strips in one holder was developed in experiments on volume reflection of proton and negative pion beams [9]. Six strips along a beam of 2.5 mm each reinforce the radiation effect, and four layers of 0.5 mm across the beam provide the necessary transverse dimension of 2 mm (thick crystals cannot bend to the required angles, so a sandwich is needed). After optical verification, the device was placed in a two-axis goniometer . The bending angle of each strip is 1.1 mrad. It is larger than the Coulomb scattering angle of electrons with energy of 7 GeV on a chain of six crystals, which is equal to 0.8 mrad.

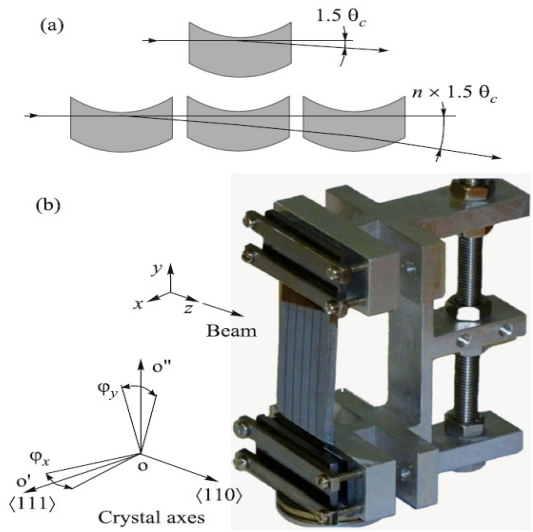

Figure 1: Multilayer crystal radiator for the beam: (a) the schematic of operation and (b) the appearance and arrangement with respect to the beam.

For each individual strip, its characteristics for deviation and ability to radiation were calculated. So according to these calculations, the average reflection angle of 50 GeV of the proton beam for the 2.5 mm silicon strip (in

ISBN: 978-3-95450-197-7 doi:10.18429/JACoW-RUPAC2018-WEPSB58

VERIFICATION OF THE WORLD EVALUATED NUCLEAR DATA LIBRARIES ON THE BASIS OF INTEGRAL EXPERIMENTS USING THE RTS&T CODE SYSTEM

I. I. Degtyarev, F. N. Novoskoltsev, E. V. Altukhova, Yu. V. Altukhov, R. Yu. Sinyukov, Institute for High Energy Physics named by A. A. Logunov of NRC "Kurchatov Institute", Protvino, Russia
A. A. Pryanichnikov, M. A. Belikhin, A. S. Simakov, P. N. Lebedev Physical Institute of the Russian Academy of Sciences, Physical Technical Center, Protvino, Russia
A. I. Blokhin, Nuclear Safety Institute of the Russian Academy of Sciences, Moscow, Russia
M. Yu. Smetanin, Federal State Unitary Enterprise "Mayak Production Association" State Enterprise "Rosatom", Ozersk, Russia

Abstract

The basis for validation and improvement of modeling algorithms and constant systems in the radiation transport problem is the procedure of comparing a calculated functionals obtained within the framework of high precision codes using a modern data libraries with high precision experimental data.

INTRODUCTION

Over the past decade, there has been a significant update of the world's evaluated nuclear data libraries. The paper presents selected results of testing the current versions of this evaluated nuclear data libraries such as ENDF/B VII.1, ENDF/B VIII.0, ROSFOND, BROND 2.2/3.1, JENDL4.0u +, JENDL-4.0/HE, JENDL/HE 2007, CENDL 4.0, TENDL 2015, FENDL 3.0, JEFF 3.2 based on the integral experiments included in the Shielding Integral Benchmark Archive and Database (SINBAD) [1] using the RTS&T [2] reference accuracy class code system. The RTS&T code uses continuous-energy nuclear and atomic evaluated data files to simulate of trajectories and discrete interactions of the particles in the energy range from thermal energy up to 20/150/3000 MeV. In current model development all data types provided by ENDF-6 format are takes account in the coupled multi-particle transport modelling. The PREPRO2017 [3], NJOY2016 [4], GRUCON [5] and CALENDF [6] pre-processing code systems are used to prepare a transport constant files.

BENCHMARKING

In this section of the paper, selective results of verification of the world evaluated nuclear data libraries written in the ENDF-6 format are presented on the basis of comparison of the results of calculations performed within the RTS&T high precision code using the PREPRO2017 pre-processing codes with experimental data [7] included in the SINBAD data bank. Unfortunately, a free version of the PREPRO2017 package does not include a procedure similar in purpose and functionality as the THERMR module of the NJOY code system, which calculates the integrated cross sections and energy-angular distributions of scattered particles in the interaction of neutrons on free or bound atoms in the thermal energy region with considering the temperature of the medium (using the FILE 7 of ENDF-6). To perform the functions similar to those of the THERMR module, the original procedure NTHERM2017 [8] (THERMRTST) was developed and tested. The module NTHERM2017 is included in the RTS&T general data pre-processing system (Fig. 1).

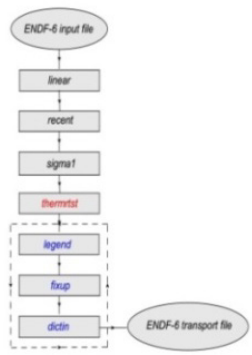

Figure 1: The sequence of procedures using for preparing the ENDF-6 transport file for the RTS&T code system.

A comparison of neutron leakage spectra from the surfaces of spherical assemblies is shown in Fig. 2. In Table 1 shows the values of $\chi 2$ / dof for all assemblies.

CONCLUSION

The analysis of a series of verification benchmark experiments taken from the international SINBAD database is carried out, selective results of calculated and experimental data comparison are presented. The results of the calculations of selected experiments show the acceptable agreement of the simulation with the experimental data.

ISBN: 978-3-95450-197-7 doi:10.18429/JACoW-RUPAC2018-THPSC03

THE TUNING OF THE ACCELARATING STRUCTURE UTILIZING ELECTROSTATIC UNDULATOR

N. V. Avreline, TRIUMF, Vancouver, B.C., Canada
S. M. Polozov, National Research Nuclear University -Moscow Engineering Physics Institute, Moscow, Russia

Abstract

The accelerating structure based on an electrostatic undulator is very attractive for bunching and acceleration of ribbon beams of light ions with beam current over 1 A. It also allows simultaneously accelerate two ion beams with positive and negative charged ions. This paper is presenting the analytical model of the accelerating structure. Also the paper is presenting the results of the simulation in ANSYS HFSS and the results of the experimental study of the mock-up of this structure that demonstrate the ways of tuning of the uniform transverse electrical RF field in its accelerating channel.

INTRODUCTION

At 1972 R. B. Palmer proposed to utilize magnetic undulator for acceleration electron beams [1]. Later E. S. Masunov showed that this idea are working and for acceleration of ions [2] and even better working better for accelerating ions utilazing an electrostatic undulator [3].

The beam dynamics calculation [4] showed that combined waves composed of the field of electrostatic undulator and the first harmonic of RF field in 0 mode can accelerate ribbon ion beams. The current limit of this structure with the aperture 8 mm by 200 mm is 1 A [5]. This type of accelerating structure also allows simultaneously accelerate two beams having positive and negative ions.

This article describes the development of equivalent circuits of this structure. The study of model of this structure with the uniform accelerating channel in ANSYS HFSS and the investigation of the mock-up of this structure showed the technique of tuning of the structure.

ACCELERATING CHANNEL

The accelerating channel of the mock-up structure consists of 16 pairs of cylindrical electrodes that the same time belong to the electrostatic undulator and RF, i.e. we have the combined accelerating structure. Electrostatic potentials $+U_0$, $-U_0$ were applied to the undulator and RF potentials also were applied to the same electrodes of the undulator $+\widetilde{U}_{rf}$, $-\widetilde{U}_{rf}$ (Fig. 1).

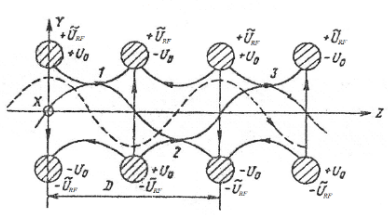

Figure 1: The accelerating channel of the accelerating structure with the electrostatic undulator.

The dash line shows the typical trajectory of the ions without FR field. The solid line shows the trajectory of the ion with RF field, if this ion injected in structure in zero phase of RF field. The deflection of beam caused by the RF field into the regions, where the combined wave of the electrostatic field and the first spatial harmonic of RF field has z-component of an electrical field makes conditions for acceleration of beam in the z-direction.

DESIGN OF MOCK-UP OF ACCELERATING STRUCTURE

The accelerating structure consist of two coupled RF subsystems A (inside green oval in the Fig. 2) and B (inside blue oval in the Fig. 2). Every of this system is DC insulated from the chamber. There is DC voltage between these two systems for the electrostatic undulator.

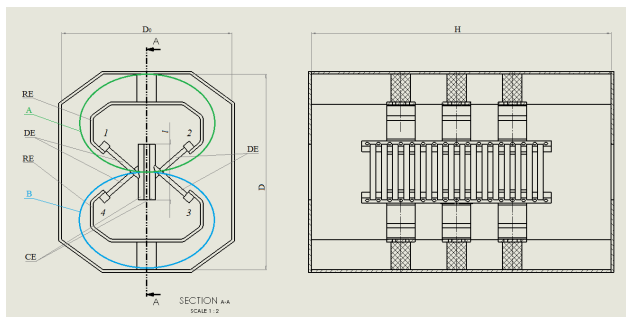

Figure 2: The design of the accelerating structure.

This mock-up has uniform accelerating channel composed of $N = 16$ pairs of cylindrical electrodes 10 mm of diameter, 100 mm of height. The aperture of the accelerating channel is 10 mm by 100 mm. The distance between centers of pair electrodes of accelerating channel in z-direction is 20 mm.

Every subsystem of structure based on three half wave of resonance elements the left ends of which and the right ends of which are joined by copper bars.

DEVELOPMENT OF EQUIVALENT CIRCUITS OF THE STRUCTURE

To minimize capacitive load of the accelerating channel the structure has used the synchronous phase type of excitation, where resonance elements excited in the half wave mode, bar 1 and bar 4 have the same potential that is opposite polarity of RF potentials of bar 2 and bar 3.

To compose equivalent circuits of structure in the synchronous and non-synchronous type of excitation, we present resonance elements as pieces of strip lines and calculate capacitance of accelerating channel. Figure 3 shows partial capacitances of the accelerating channel.

ISBN: 978-3-95450-197-7 doi:10.18429/JACoW-RUPAC2018-THPSC04

NEW SUPERCONDUCTING WIGGLERS FOR KSRS

A.Valentinov, V.Korchuganov, V.Ushakov
NRC Kurchatov Institute, Akademika Kurchatova Sq., 1, Moscow, 123182 Russia
S.Khrushchev, N.Mezentsev, V.Shkaruba, V.Tsukanov
Budker Institute of Nuclear Physics, Akademika Lavrentieva Prospekt, 11, Novosibirsk, 630090 Russia

Abstract

Presently a program of incorporation of two new superconducting wigglers into main ring of Kurchatov synchrotron radiation source is implemented in NRC Kurchatov Institute. The wigglers are intended for new experimental stations "Belok-2" (biology studies) and "VEU" (exploration of materials in extreme conditions). The wigglers are designed for maximal magnetic field 3 T with 48 mm period and contain 50 pairs of poles with maximum field. Technical details of wigglers' construction are presented in the report along with a description of testing and mounting procedures. An influence of the wigglers on beam dynamics is described.

INTRODUCTION

At present BINP (Novosibirsk) are producing two superconducting wigglers (SCW) with maximal magnetic field 3 T for Kurchatov Synchrotron Radiation Source (KSRS) [1]. This work is included in Federal Program for KSRS modernization. Magnetic measurements of the wigglers are planned to fulfil at the end of 2018. In the middle of next year they will be installed on main storage ring of KSRS.

BINP has wide experience in construction and producing of such wigglers [2] with different field levels and field periods. They are installed and put into operation on many SR facilities. For every machine follows parameters must be taken into account:

- Required synchrotron energy range.
- Dimensions of a straight section for SCW.
- Parameters of an electron beam at SCW azimuth, operational modes of given machine.
- Vacuum condition and vacuum chamber construction.
- Influence and geometry of SR from previous bending magnet.
- Convenient installation and maintenance of SCW.

SCW MAGNETIC SYSTEM

The magnetic system of SCW is optimized to get maximal flux of SR in spectral range between 10 and 35 keV. Wiggler's magnet consists of 54 poles: 50 central poles with nominal field 3 T and 4 side poles. Field period is equal to 48 mm; the field is oriented in vertical direction and changes by sinusoidal law. Magnet gap between top and bottom poles is 14 mm. Poles with magnetic field ¼ and ¾ from nominal value are situated on both side of the SCW. Its geometry and field distribution provide coincidence of wiggler and machine straight section axes. Zero values of first and second field integrals along the wiggler axe are maintained by regulation of currents in coils of the side poles. Scheme of the wiggler prototype with 4 central poles and beam trajectory inside the wiggler are presented on Fig.1.

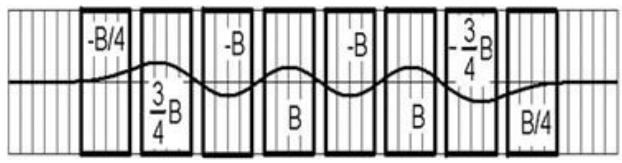

Figure 1: An electron beam trajectory in horizontal plane inside the wiggler prototype. B is nominal vertical magnetic field.

Every pole consists of pair of iron yokes of racetrack type with superconducting coils on them. The yokes are situated symmetrically (above and below) with respect to vacuum chamber. A conductor of the coil is NbTi alloy wire in copper matrix. The wire is coated by varnish isolation layer. The coils are wide enough to provide homogeneity of the magnetic field in horizontal direction not less than 10^{-3} inside ±6 mm.

The coils of central poles have two sections with different currents inside them (4 layers of the wire in both section, 62 turns per section). The coils of side poles have only one section with 2 or 8 wire layers. Outer section of the central pole is fed by greater current than inner one because it is situated in lower magnetic field.

VACUUM CHAMBER

Vacuum chamber aperture is equal to 10 mm in vertical plane and 60 mm in horizontal plane. Minimal thickness of the chamber is 0.5 mm. The chamber has elliptical form in central region of the wiggler and widens to the ends of the wiggler in order to provide smooth transition to machine vacuum chamber. The chamber was produced from aluminum alloy 6063 by extrusion procedure.

The vacuum chamber has temperature at the range between 10 K and 20 K and is thermally isolated from magnetic system of the wiggler. Stainless steel flanges are used at both sides of the chamber to connect it with machine vacuum chamber. Maximal energy inflow from synchrotron radiation and electron beam image currents is estimated to be less than 10 Watt for normal operation of cryosystem.

ISBN: 978-3-95450-197-7 doi:10.18429/JACoW-RUPAC2018-THPSC05

SUPERCONDUCTING 7 TESLA WIGGLER FOR DELTA SYNCHROTRON RADIATION SOURCE: TEST RESULTS

N. Mezentsev, A. Bragin, S. Khrushchev, A. Safronov, V. Shkaruba, O. Tarasenko, V. Tsukanov, A. Volkov, A. Zorin, V. Lev, Budker IInstitute of Nuclear Physics, Novosibirsk, 630090, Russia
S. Khan, Technische Universität Dortmund, 244227, Germany

Introduction

The multipole superconducting wiggler was designed, fabricated and successfully installed and tested on DELTA Synchrotron Radiation (SR) Source. The wiggler represents a multipole magnet with alternating high magnetic field of 7 Tesla along movement of particles in storage ring. The magnet is immersed into liquid helium of a special cryostat with working temperature of ~4.2K.
The wiggler consists of 22 pairs of poles superconducting magnet with 18 full field poles, 2 with a three-quarter field strength and 2 with one-quarter field poles. The magnet array produces a sin-like magnetic field variation on the magnetic axis of the device with first and second field integrals close to zero.

The Dortmund Electron Accelerator (DELTA, Germany) operated at 1.5 GeV synchrotron radiation source requires a superconducting wiggler as an insertion device for three x-ray beamlines with photon energies up to more than 30 keV. The wiggler has a period of 127 mm, magnetic field of 7 Tesla and the length from flange to flange of 2.2 m operated with zero boil-off mode [7]. The conception and main approaches for the design of the magnetic and cryogenic system as well as the main parameters and the test results of new 7 Tesla superconducting wiggler for DELTA synchrotron light source are presented.

MAIN PARAMTERS OF THE WIGGLER

The magnetic structure of the superconducting wiggler for the DELTA synchrotron radiation source is a sequence of superconducting magnets with transverse, alternating magnetic field with amplitude of 7tesla in the operating mode. The main parameters of the wiggler are given in Table 1. The magnet assembled and ready for installation into the cryostat is shown on Figure 1.

Figure 1: Superconducting 7 Tesla wiggler for DELTA SR Source.

Table 1 Main Parameters of the Wiggler

Period	125 mm
Nominal magnetic field	>7 T
Maximum peak on-axis field	7.2 T
Full vertical aperture	10 mm
Full horizontal aperture (entry/exit)	90/120 mm
Magnetic length	1408 mm
Maximum length flange-to-flange	2500 mm
Pole scheme	-1/4,3/4,-1,1…-3/4,1/4
Transverse field homogeneity $\Delta Bz/Bz$ at x=±20 mm, z=0	$\leq 2*10^{-3}$
Max. stray field on axis at each end of the cryostat	0.001 T
Maximum Ramping Time	< 15 min
Power supply stability $\Delta Bz/Bz$	$< 2*10^{-5}$
Field stability (2 week), 0.5-7 T	10^{-4}
Period for LHe refill with beam	>6 month

The cryostat, in which the magnet is placed, is a vacuum volume, in which there are 2 thermal screens with temperatures of 50K and 20K, a helium volume with a magnet inside [3,5,6]. To achieve zero liquid helium consumption the cryostat is equipped with cryocoolers to intercept and remove heat from the screens, from a copper liner, which is a heat shield from the heat coming from the electron beam, and with two copper fingers, which are connected to 4K cold heads of the cryocoolers to re-condense the evaporated liquid helium and return it to the helium volume. Figure 2 shows the assembled cryostat ready for site acceptance testing. In July 2018 elements of the superconducting wiggler was delivered in the hall of the DELTA SR source, assembled, tested for vacuum, cooled to helium temperature and subjected to acceptance tests.

COOLING DOWN OF THE WIGGLER

After assembling of the wiggler, pumping out of insulating vacuum and conducting leak test the wiggler magnet was cooled down by two steps:

- Cooling down with liquid nitrogen.
- Cooling down with liquid helium.

It was required about 300 liters of liquid nitrogen for preliminary cooling down of the wiggler magnet. Simultane-

ISBN: 978-3-95450-197-7 doi:10.18429/JACoW-RUPAC2018-THPSC06

NEW AUTOMATED CONTROL SYSTEM FOR THE KURCHATOV`S SYNCHROTRON RADIATION SOURCE

N.I. Moseiko, A.G. Valentinov, V.N. Korchuganov, Yu.V. Krylov, E.V. Kaportsev, K.N. Kuznetsov, L.A. Moseiko, K.V. Moseev, A.S. Smygacheva, E.A. Fomin, A.V. Shirokov, NRC Kurchatov Institute, Moscow, Russia
Yu.V. Efimov, RTSoft, Moscow, Russia

Abstract

The paper describes the new automated control system (ACS) for the Kurchatov syncrotron radiation source (KSRS), which is based on the modern servers and network equipment, VME equipment, National Instruments modules, time server, power equipment with built in intelligent controllers. The new system includes around 2300 control channels and 5900 measuring channels. Control programs that provide user interfaces, monitoring of the system operation, data acquisition, data processing and data storage, were developed using Citect SCADA 7.2, SCADA Historian Server, LynxOS Runtime, LabVIEW-2013, OC ARTX166, PCAN-Evaluation. The new ACS KSRS has allowed to increase the number of control and measuring channels, to increase the speed and accuracy of the measurements, to increase the speed of data processing and data transmitting. As a result, the main parameters of the KSRS have been improved and its work efficiency increased.

NEW AUTOMATED CONTROL SYSTEM AT KURCHATOV SYNCHROTRON RADIATION SOURCE

The description of new automated control system of Kurchatov`s synchrotron radiation source which is realized at the present time is presented in the paper. The necessity of automated control system modernization is explained by the equipment replacement in which we take state of art hardware decisions for facility control and increase the processing and transmitting data speed are considerably increase and the requirements to measurement accuracy are become more strict.

The paper [1] presents the detailed description of all control levels (lower, server and upper) of new automated control system and integration of SCADA system CitectSCADA v.7.2 into facility control system which provides the facility control, alarms notify, detailed reports preparation, acquisition and storage of historical data et al.

New automated control system essentially differs from previous system. New control system has multilevel equipment structure and uses a distributed control system instead of centralized used in the previous system. This allowed to increase the reliability of the control system, reduce the time and hardware resources on any data operation (read, write, processing), increase a flexibility and improve a performance of new control system. All equipment involved into facility control system (operator's work stations, servers, crates with single-board computers, microcontrollers, oscilloscopes) are connected to a local network divided hardware on 3 levels: lower, server and upper level (see Fig. 1). The organization of such a three-level local network allows to restrict access to the execution units thereby increasing reliability of the accelerator facility.

Lower Level

At the lower level of new control system acquisition of diagnostic data, execution of local and global facility technological systems control algorithms are carry out. The main part of the equipment used at this level are VMEbus standard equipment. The main units performing the required algorithms are VME single-board computers Emerson MVME5500 based on the PowerPC MPC7457 processor and the Marvel GT-64260B host bridge with a dual PCI interface and memory controller. On singleboard computer real-time operation system LynxOS v.4.2 and special software are operated. In some cases, we will be use the equipment of such companies as National Instruments, Tektronix, I-Tech, B&R etc. or an unique equipment of our own design.

There are 8 subsystem at this level. Each subsystem controls only a certain part of the accelerator complex.

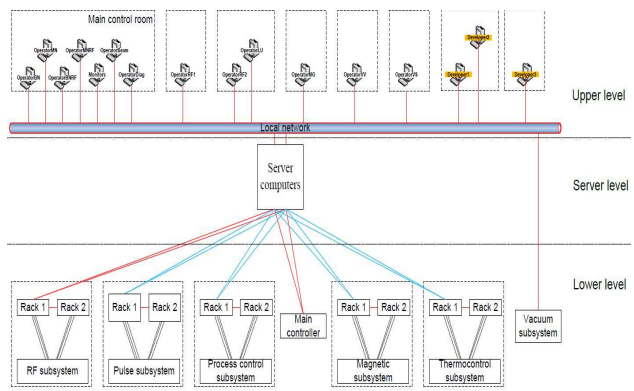

Figure 1: The layout of new automated control system at Kurchatov`s synchrotron radiation source.

SYSTEM OF THERMOMONITORING AND TERMOSTABILIZING

The modern system of thermomonitoring and thermostabilizing of KSRS is described [2,3]. The system provides: a monitoring of temperatures of the magnets and RF resonators of KSRS; the informing of operator on the violations of the technological process course; the data protection from an illegal access; the archiving and the

ISBN: 978-3-95450-197-7 doi:10.18429/JACoW-RUPAC2018-THPSC07

VEPP-5 INJECTION COMPLEX CONTROL SYSTEM BASE SOFTWARE UPGRADE

D. Bolkhovityanov*, F. Emanov, BINP SB RAS

Abstract

VEPP-5 Injection Complex control system software is based on CX framework. In the course of 2015-2016 it was upgraded to version 4. K500 transport channel (delivering e+/e- beams to VEPP-2000 and VEPP-4) has switched to CXv4 in 2017-2018. CXv4 is a redesign from the ground up, built in a modular fashion with maximum flexibility in mind. CXv4 server is easily configurable via plaintext files. Additionally, server configuration can be autogenerated from a database containing high-level information on the facility. CXv4 server supports artificial "mailbox" channels, which are used by high-level facility management software for inter-communication. For client-level access, a high-performance binding for Python exists, and visual programming tools are being developed.

BACKGROUND

VEPP-5 Injection Complex [1] operates at the Budker Institute of Nuclear Physics in Novosibirsk, Russia. It feeds BINP colliders VEPP-4M and VEPP-2000 with e+ and e- beams via K500 transport channel.

CX control system framework was developed at BINP in 1990s specifically for VEPP-5 [2]. Later it was also employed at several small- and middle-size facilities.

Its initial task was to serve CAMAC hardware. Later CAN-bus hardware support was added. Since CAMAC controllers used at VEPP-5 had changed several times during CX first years, its driver architecture was made modular since early days.

The 32-bit integer was hardwired as a datatype and it was adequate for most hardware. Digital oscilloscopes, CCD cameras and similar "vector-data" hardware were served in a special way. However, in mid-2000s new hardware appeared at BINP facilities, including that which natively operates with floating-point data. Thus, it became obvious that a broader datatype support is required.

Taking into account the accumulated experience of CX operation, including its benefits and shortcomings, a decision was made to create a new version from the ground up, reusing fragments of existing code, and this work started in late 2000s.

In 2015 the new CX version 4 (CXv4) was deployed at VEPP-5 for basic controls (magnetic and vacuum system, thermostabilization etc.) [3]. Digital oscilloscopes and CCDs followed the suit in 2016. Finally, K500 transport channel has switched to CXv4 in 2017–2018, as well as VEPP-5 RF-synchronization and modulators' controls.

* D.Yu.Bolkhovityanov@inp.nsk.su

CXv4 GENERAL STRUCTURE

CX is based on a classic 3-layer model (Fig.1a).

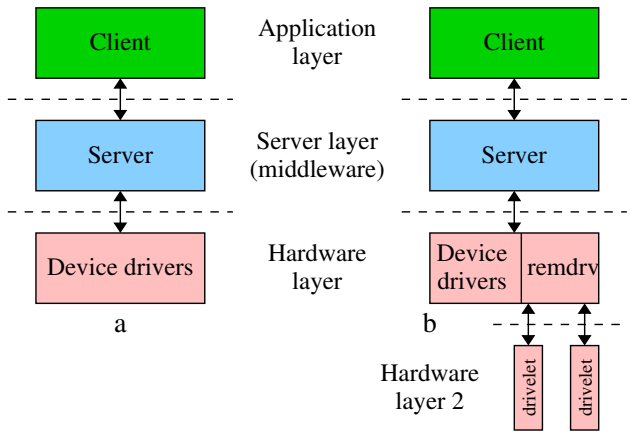

Figure 1: (a) Classic 3-layer architecture; (b) CX with 2-part hardware layer.

However, the lower layer can be split into two parts, if peripherial low-performance intelligent controllers are used (such as for CAMAC, CANbus or VME). In this case only a "low-weight" driver (called "drivelet" in CX) runs in such a controller and communicates with CX server (running on a more productive node) via network (Fig.1b).

Data Exchange Paradigm

As opposed to many other control systems, CX uses completely asynchronous data interchange at all levels — from device drivers up to operator screens.

The *"Read"* and *"Write"* requests don't suppose immediate result, but are rather treated as messages. Thus, a read request can be left without any answer at all. On the other hand, data can arrive without any request, on the initiative of the device (which is usual in case of externally-triggered devices). So, this is more of a publish/subscribe model rather than a client/server one.

CXv4 NEW FEATURES

Modularity

From the very beginning CXv4 was designed in a modular fashion [3]. Technology of "plugins" is used instead of a fixed implementation (see Fig.2).

Modules can be either statically linked or loaded at runtime (via `dlopen()`; this is taken care of by a dedicated "cxldr" component).

- Client library doesn't interact with server directly but rather via plugins. The library core provides clients

ISBN: 978-3-95450-197-7 doi:10.18429/JACoW-RUPAC2018-THPSC08

DEVELOPMENT OF HARDWARE AND SOFTWARE PRODUCTS OF SLOW-EXTRACTION SYSTEM BY MEANS OF CRYSTALLINE DEFLECTORS ON SYNCHROTRON U-70

S. Reshetnikov, A. Afonin, E. Barnov, A. Levin, M. Ukhanov,
Institute for High Energy Physics (IHEP) of "Kurchatov Institute",
142281 Protvino, Moscow Region, Russia

Abstract

S. Reshetnikov et al. The review is devoted to hardware and software products developed to serve working complex of extraction system by means of crystalline deflectors on the synchrotron U-70 IHEP.

INTRODUCTION

The system of high energy charged-particle beam's slow-extraction by means of crystalline deflectors (hereafter referred to as a "System") constitutes a part of IHEP synchrotron U-70 extraction system.

The slow-extraction by means of crystalline deflector has a number of strong points, which makes it popular with a number of physical units [1]. Practical implementation of this injection mode in IHEP synchrotron set up in 1997 and was based on baseline design of crystalline deflectors' stations and their control systems. To meet demands in new physical experiments, the development of managements systems of crystalline deflectors' stations for a long period was based on technical solutions previously adopted and slightly improved.

By today's standards, the system is obsolete and worn-out. New approaches and innovative solutions are required for maintenance, management and further development. This investigation reports on baseline design (pilot model) of crystalline deflectors' station, upon which the modernization of the System is planned.

THE UPGRADED CRISTALLINE DEFLECTORS' STATION

There are 11 varied crystalline deflectors' stations (hereafter referred to as CDS) now in the synchrotron U-70, which are operated by a number of control systems.

We worked out an advanced CDS.

For horizontal and angular movement we affirmed a unique type of stepper motor FL39ST38 manufactured by "Electroprivod"[2]. The engine rig tests confirmed that the power performance of the motor ensures mechanical operation of upgraded CDS.

Here are some of technical characteristics of upgraded CDS:

1. Radial and horizontal carriage drives - stepper motor FL39ST38- 0504A. Phase current I = 0.5 A; motor torque = 0.29 Nwm.
2. Carriage radial range – 150mm.
3. Cristal angular excursion range – 40 mrad.
4. To measure and to display the radial movements of the carriage and angular excursions of the crystal, varied potentiometers with resistance value of 10 kiloohm are used.
5. Extreme positions of the carriage and the crystal are fixed by microswitches.
6. The CDS is placed in standard vacuum box with inside diameter of 203mm and associated length of 520mm.
7. The electric connection of the CDS to the command equipment is effected by multicore radio-frequency cables.

Here on Figure 1, you may find the first sample of upgraded CDS which is equipped with two carriages. This first model of the upgraded CDS is manufactured by IHEP development design office.

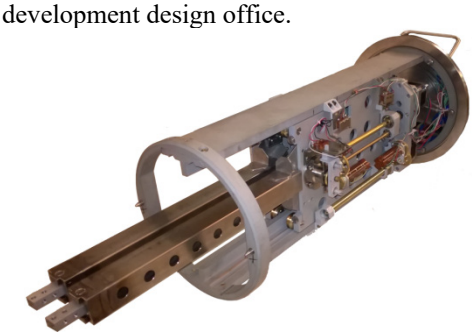

Figure 1: Crystalline deflectors' stations (CDS) with two carriages.

THE CONTROL SYSTEM

The CDS control system developed in IHEP is an entirely automated system. It consists of two functional parts: the **command part** which is located on panel of extraction system (and includes IBM PC), and the **peripheral part** which is located in the tunnel of U-70 close to CDS, where the radiation exposure is considerably less than on the orbit of U-70.

The automated control system (ACS) while managing the CDS, resolves the following tasks:

1. Selection of one of the CDSs, which are placed on synchrotron U-70.
2. Selection of the carrier among those two on the CDS.
3. Parameters of radial and angular movements of the carriage.

ISBN: 978-3-95450-197-7 doi:10.18429/JACoW-RUPAC2018-THPSC09

MEDIA SERVER FOR VIDEO AND AUDIO EXCHANGE BETWEEN THE U-70 ACCELERATOR COMPLEX CONTROL ROOMS: CURRENT STATUS AND PERSPECTIVES

I.V. Lobov, V.G. Gotman, IHEP, Protvino, Russia

Abstract

The dispatching system for audio and video exchange between various U-70 technological subsystems has been developed. The system architecture employs the original approach to the online streaming using the method of progressive download over HTTP. The system can be built on the basis of any one-pass decoding media container. Ogg format with Theora/Vorbis codecs has been chosen as an appropriate container.

The system is designed as a distributed software complex and consists of several executive components: Retransmitter, a number of Media Stream Coders and a number of clients. All the components can run either on separate computers or on the same computer. Media stream Coders consume streams from media sources, turn it into Ogg stream and send it out to Retransmitter. The possible media sources are: IP-cam, web-cam, computer screen along with microphone. A client is able connect to Retransmitter using any web-browser with Ogg Theora/Vorbis support. The range of values 250-350 ms has been achieved for the latency between real action and client video. The developed software is a framework for diverse media exchange systems that could be built on it's basis. Several possible applications are discussed in the scope of the U-70 Accelerator Complex technological needs. This could play an important role in personnel safety system while perform maintenance tasks in an extreme work environments such as the Beam Channel.

INTRODUCTION

The aim of the work is to develop a Media Server system for audio and video exchange between U-70 Accelerator Complex technological subsystems. The requirements for Media Server:

- the client software can run on different operation systems;
- the system software must use open-source free algorithms and libraries;
- do not use any special designed programs (plug-ins) on the client side;
- low latency between actual presentation action and the action coming up to a client screen;
- simultaneous communication between several clients.

The Media Server software employs the original approach to the online streaming. This approach uses the progressive download feature of HTML5 [1] standard for getting a media stream [2] through the tag <video>. Considering particular features of progressive download, only stream-oriented media container should be used. In other words, there must be one pass decoding stream container with no seeking. All in all, Ogg with Theora /Vorbis codecs [3] has been chosen.

The first report on the Media Server was reported at RuPAC 2014 [4]. Since then the software has endured significant changes in ***system structure*** and ***client software***.

To date the Media Server [5] has transformed into distributed dispatch system which consists of two separate executives – the central module called Retransmitter and several programs called Media Coders. Both Retransmitter and Media Coders can run on separate computers or on the same computer, they communicate with each other through Windows socket gear.

THE SYSTEM STRUCTURE STATUS: THE DISTRIBUTED EXECUTIVES

The dispatching system as a whole consists of several components, as follows:

- Media Sources;
- Media Stream Coders;
- Retransmitter;
- a set of web-pages for client.

DBMS SQL is used to control the system workflow, web server allows clients to download the web pages.

The structure of the dispatching system is shown in Fig.1. The scheme depicts the case of three presentations being viewed by four clients. Client 1 is connected to presentation 1, client 2 is watching presentations 1 and 3, client 3 is watching presentation 3, client 4 is watching the archive. Presentation 2 is being watched by no one.

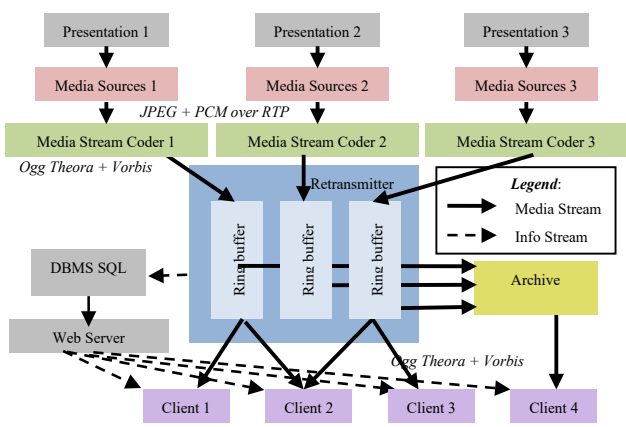

Figure 1: The structure of the dispatching system.

ISBN: 978-3-95450-197-7 doi:10.18429/JACoW-RUPAC2018-THPSC10

DEVELOPMENT OF MODERN DIGITAL SYNCHRONIZATION MODULES AT BINP

Ya.M. Macheret†, M.Yu. Vasilyev[1], G.A. Fatkin[1], E.S. Kotov[1], A.N. Selivanov,
Budker Institute of Nuclear Physics SB RAS, Novosibirsk, Russia
[1]also at Novosibirsk State University, Novosibirsk, Russia

Abstract

Modern digital synchronization system for big physical facilities is developed at BINP. It allows synchronizing the spatially distributed control devices with an accuracy of ±125 ps and low jitter (< 100 ps). Accurate time distribution and delay compensation is provided, as well as an ability to react to external events with a determined latency. Two modules are used in this subsystem: S-Timer and L-Timer. S-Timer provides a synchronized 250 MHz clock signal with embedded events data through the optical link to nine L-Timers or S-Timers. L-Timer decodes the signal from the optical link and provides synchronization pulses to final control devices.

INTRODUCTION

One of the important elements for the control of big physical facilities is the synchronization system. The tasks of synchronization systems are transmission of the operating frequency and the transmission of trigger events. The digital synchronization system is developed at BINP that is based on modern principles. It consists of two types of modules: S-Timer and L-Timer. These modules allow synchronizing the spatially distributed control devices with an accuracy of ±125 ps and low jitter (< 100 ps) as shown in Fig. 1. Special VME-BINP [1] synchronization lines are used for communication between modules in the same crate.

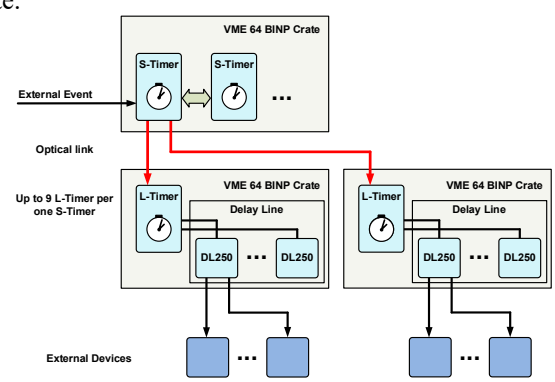

Figure 1: Synchronization structure using S-Timer and L-Timer modules.

S-Timer (Fig. 2) provides a synchronized 250 MHz clock signal with embedded events data through the optical lines to up to 9 L-Timers. The S-Timer has an input to receive a precise external clock or external events. Several S-Timers can be united in one crate. The L-Timer decodes the signal from the optical line and provides all necessary synchronization pulses to the modules of the crate. Both modules use the same PCB with different montage.

S-TIMER

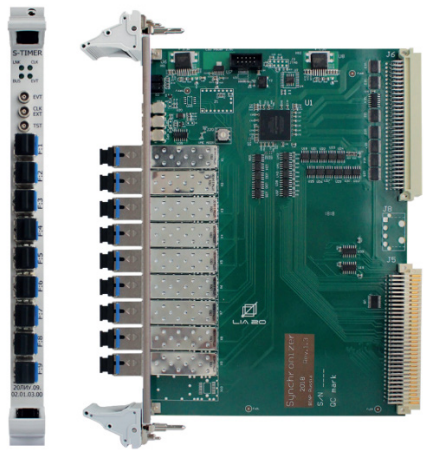

Figure 2: S-Timer module.

The main characteristics of S-Timer are:

- 9 output optical lines
- 2 synchronization inputs
- 250 MHz clock in optical lines
- ±125 ps Delay measurement error
- Jitter < 100 ps
- Up to 256 Events
- 512 Words Event Sequencer
- 512 Words Timestamp

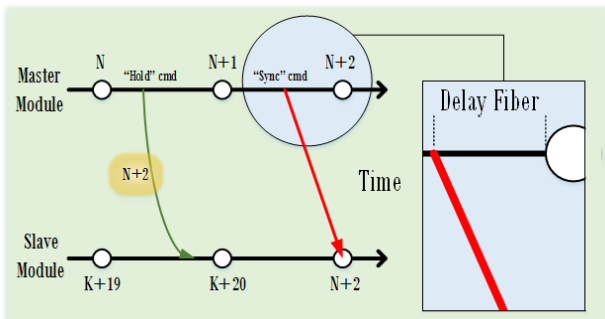

Figure 3: Common time diagram.

One of the main tasks of S-Timer (Master module) is to provide a common time in L-Timers (Slave module). To adjust the time it is necessary to determine the delays of the transmitting path, and then provide this information to the L-Timer. The special procedure is used to synchronize the clocks of S- and L-Timers that shown in Fig. 3. Master module fixes the L-Timer's current time by the command "Hold". Next step is to add 2 seconds to the fixed Master

ISBN: 978-3-95450-197-7 doi:10.18429/JACoW-RUPAC2018-THPSC11

PRESENT STATUS OF VEPP-5 INJECTION COMPLEX IT INFRASTRUCTURE

F. A. Emanov*, D.Yu. Bolkhovityanov, P.B. Cheblakov, Ya.V. Pisarev,
The Budker institute of nuclear physics, 630090 Novosibirsk, Russia

Abstract

VEPP-5 injection complex (IC) is an electron and positron beam source for VEPP-4 and VEPP-2000 experimental facilities. Continuous IC operation requires its control system infrastructure to provide high availability to all services. In order to make high availability possible and increase flexibility of control system, networks and servers were built from scratch, modern virtualization technologies being applied. The injection complex control system infrastructure is based on OS Linux and other open source software. The paper presents the architecture and implementation of the injection complex computer infrastructure.

INTRODUCTION

VEPP-5 injection complex (IC) [1–3] is an electron and positron beam source for BINP colliders VEPP-4 [4] and VEPP-2000 [5]. Layout of injection complex with colliders is shown on Fig. 1.

Since IC is a part of few continuous experiments care should be taken to avoid or reduce downtime. One of required steps is to build highly available control system infrastructure with simple maintenance for all involved accelerator facilities.

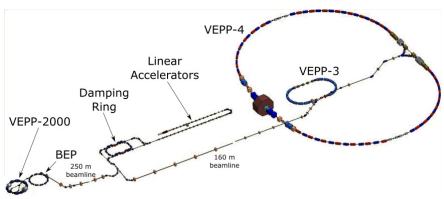

Figure 1: Injection complex and colliders layout.

Most of IC control system devices are connected to Ethernet and CAN networks [6]. CAN is mainly used at magnetic system power supply control. Modern or performance demanding devices like BPM processors, fast ADCs, embedded computers/controllers usually use Ethernet. High availability is required for server applications controlling Ethernet and CAN devices since their state is rapidly changing during routine operation.

In order to provide high availability and reduce management and maintenance efforts we developed IT infrastructure for IC and collider facilities using the same hardware and software basis [7]. Proposed infrastructure project includes redundancy for servers, server power, server network connections, storage devices and CAN connections. Injection complex control system infrastructure has been rebuilt by the moment and is able now to provide high availability for all server applications including CAN hardware control.

* f.a.emanov@inp.nsk.su

INFRASTRUCTURE DESCRIPTION

Injection complex control system currently includes 80 Ethernet and 128 CAN end devices, 8 servers, 3 control room workstations and 6 service room terminals. All servers are joined to virtualization environment cluster which is able to provide high availability for virtual machines. In order to have backup hardware for any particular task servers are organized in pairs. A number of pairs and its roles was selected to conveniently distribute services over computers

Each server of a pair has the same hardware and connections and is able to run all the pair tasks. Servers Rack has two UPSs. Some servers have redundant power supplies which are plugged in different power sources. In other cases at least paired servers have different power sources.

Network and infrastructure services are deployed to "infra" servers. Outside services, NAT and firewall are hosted on "firewall" servers. Database, control services, development machines are located on "HW" servers. In order to control CAN devices two servers with 6 PCI/PCI-E CAN adapters (each having two lines) are used. CAN lines have been rebuilt by the moment and now all devices are connected to 8 lines. We have chosen hardware from Supermicro vendor during server solution analysis. The resulting injection complex software structure is shown on Fig. 2.

In order to ensure reliable operation of control devices they should have separated network from general purpose computers. Also separation is required for management interface network and outside networks. IC network has been rebuilt by the moment using stack of three HPE 1950-24 switches as core and HPE 1920 series switches as peripheral. Network separation is implemented with VLANs. HPE 1950-24 switches support true stacking over 10GB ports which is used for server connection failover in case single switch is out of service.

HA Cluster Setup

Injection complex HA cluster is powered by Proxmox Virtualization Environment. Proxmox VE [8] is an open source server virtualization management solution based on QEMU/KVM [9] and LXC [10]. Injection Complex control system uses Centos 7 Linux for most applications thus we usually run it in KVM machines. In some special cases LXC containers are used. We use Open vSwitch as bridge for virtual machines [11]. Each server has 2 or more Ethernet ports which are connected to different central switches and bonded with LACP to make automatic failover and increase

ISBN: 978-3-95450-197-7 doi:10.18429/JACoW-RUPAC2018-THPSC12

UPGRADE OF APPLICATION-LEVEL SOFTWARE OF VEPP-5 INJECTION COMPLEX

F. A. Emanov*, D.Yu. Bolkhovityanov, V.V. Balakin, D.E. Berkaev, Yu.A. Rogovsky
The Budker institute of nuclear physics, 630090 Novosibirsk, Russia

Abstract

VEPP-4 and VEPP-2000 experimental facilities are fed with e+e- beams from VEPP-5 injection complex(IC). Application-level software of IC control system is based on CXv4 framework. This software includes a set of engineering and debugging tools for all the hardware, a database with high-level information and configuration tools, machine mode manipulation system, automatic control and data analysis programs. The software architecture and implementation is described.

INTRODUCTION

VEPP-5 injection complex (IC) [1–3] is an electron and positron beam source for BINP colliders VEPP-4 [4] and VEPP-2000 [5]. Beams are transferred to colliders by K-500 channel. Layout of injection complex with colliders is shown on Fig. 1.

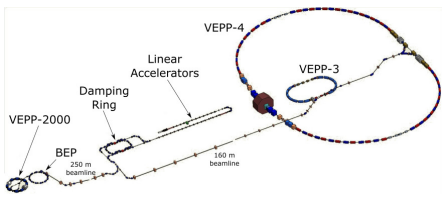

Figure 1: Injection complex and colliders layout.

Injection complex had had a long period of serving as test facility until 2015. During this time injection complex control system software was based on CX and EPICS frameworks and application level software mostly consisted of engineering GUI programs. This software set allowed us to run injection complex as test facility but was not acceptable for routine operation with beam users. It was required to create centralized configuration and operation tools and automatize frequent processes. Since two frameworks were applied it was needed to support both of them in our software. Some of required software was implemented earlier [6]. At the end of 2017/2018 experimental season we decided to fully migrate base control system software to CX since this framework served more than 90% of injection complex control hardware. By the time most of migration work has been completed. Current state of injection complex software is described bellow.

SOFTWARE DEVELOPMENT TOOLS

Software development is carried out in C/C++ and Python. In order to simplify application-level software development we created fast Cython bindings to CX client libraries called pycx4. Currently pycx4 can operate in CX event-loop or Qt4 or Qt5 ones. We use PyQt for joined CX and EPICS programs and for GUI software development. We use cothread.catools for EPICS devices access. In order to be able to use cothread in modern environment we added PyQt5 support and Qt version auto selection to cothread.

A set of PyQt4/5 widgets with embedded CX access was developed to simplify GUI programs creation. Since we are using Qt Designer for rapid software prototyping, designer plugins for CX widgets also implemented. We are currently considering possibility to bind CX to Taurus SCADA.

CONFIGURATION AND ACCELERATOR MODE DATABASES

Large experimental facilities like injection complex require lots of configuration information. In general this configuration information is structured data about machine. Therefore it can be presented in form of graph of some accelerator elements and their relations. Several attempts of implementation configuration tools in a control system agnostic way were made [7, 8]. But to our consideration these tools have not been developed to production-level. So we decided to develop our own configuration tools without solving too general problems. Databases are an appropriate engine to solve problems of configuration and storage for accelerator data like operation logs and modes. We have been using Postgresql since it is the most advanced open source database and it is suitable for all our needs. Currently we migrated to Postgresql 10 since native table partitioning was introduced in this version.

We designed databases and configuration tools in order to reach the following goals:

- to create configuration source for accelerator mode management system and operation logs.
- to create configuration generation scripts for CX.
- to minimize database deployment efforts.
- to create effective storage for accelerator mode data.
- to make mode data tolerant to software and hardware changes.

In order to store control system structure we designed "line" of objects: namespace, device, devtype, channel. Namespace, device and channel are significant parts, and devtype serves for reduction amounts of object relations. We believe logical accelerator systems can be formed to tree structure. Device can be a part of few different systems. Sometimes there is some information about device which is not common to all devices. In this case we can store

* f.a.emanov@inp.nsk.su

ISBN: 978-3-95450-197-7 doi:10.18429/JACoW-RUPAC2018-THPSC13

CONTROL SYSTEM USER INTERFACE FOR THE CYCLOTRON DC-280

V. Aleinikov, V. Badmatsyrenova, S. Pachtchenko, K. Sychev, FLNR JINR, Dubna, Russia

Abstract

At the end of 2018 new isochronous cyclotron DC-280 will be put into operation at the FLNR, JINR. The distributed control system consists of about 10000 process variables and has developed using LabVIEW DSC module. Based on our experience of many similar projects it was developed the technology to build interface for effective operation and control of the machine. This paper describes basic principles and functions that we applied for user interface.

INTRODUCTION

To simplify design and ease of maintenance the control system was divided into three subsystems: **Injection** (ECR source, axial injector), **Accelerator** (cyclotron, extraction, transport) and **Low level RF**. Each of them describes certain tasks. They are simply as follow: produce, inject, accelerate, extract and transport the beam to the target. The distribution of tasks between several computers gives fast response and allows debugging and running the subsystems independently of each other.

Every subsystem has unique human to machine interface (HMI) that can be executed on any project node.

TECHNOLOGY

All control signals are described by process variables. The variables of each subsystem are deployed on a dedicated host. LabVIEW provides fast and reliable data transmission for large and small applications, called Publish-Subscribe Protocol (PSP). It manages **shared variables** (See Fig. 1) that publish data over a network through a software component called the Shared Variable Engine (SVE).

INTERFACE LAYOUT

The user interface screen is divided into several functional areas (See Fig. 2). The top part contains information about the name of the accelerator, the version of the program, general parameters and the date and time. The central part of the screen is occupied by the front panel, which is divided into two main parts: a smaller left and a large right one, each of which has several tabs. Switch between tabs by using the buttons on the left side of the user interface screen. They switch the tab or combination of tabs of several panels. When the object under the mouse cursor next to it pops up a line with the name of the operating variable and the context information window that located at the bottom of the screen displays the name of the control and the path to the associated hardware variable. The lower part of the screen is reserved for system events and alarms.

Each control object image is represented in accordance with the actual device. The state of the object is displayed by color: black means that the device is off, green that it is on, grey means the device goes from one state to another and red indicates an alarm. And in some cases object state is displayed by shape of the its image. The user interface was developed taking into account the possibility of using a computer with two screens and works regardless of the position of the program window.

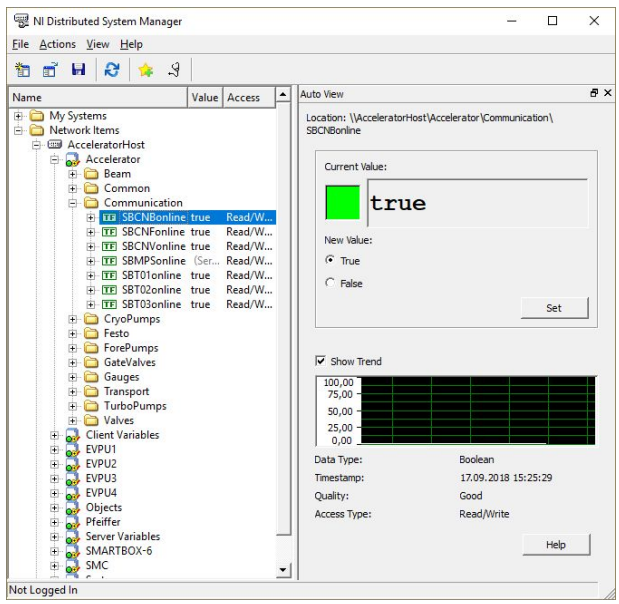

Figure 1: Shared variables.

To exchange data on the network HMI uses shared variables. All user interfaces are clients or subscribers to the SVE [1,2].

TOOLTIPS

For safety reason the interlocking system has a lot of signals blocking the operation of object. To simplify troubleshooting and identifying the causes of malfunctioning of the device, operator can view the list of all interlocks using the context menu on the selected object. Popup window that appears next to the object provides information about all interlocks that can affect the operation of the object. It contains information about the name of the interlock and the path to it. The triggered interlocks are indicates by red color (See Fig. 3). The number of popup windows is unlimited and there is a possibility to move them on the screen of the interface. When a driver loses connection to its device, all controls and indicators that represent this device become disabled and its image greyed out (See Fig. 4).

To quickly launch all control system software, a Program Manager was developed. With its help, operator can run and stop the entire software package with just one click.

ISBN: 978-3-95450-197-7 doi:10.18429/JACoW-RUPAC2018-THPSC16

LOW-LEVEL RF CONTROL AT LIGHT IONS INJECTOR FOR NICA

S. Barabin†, T. Kulevoy, D. Liakin, A. Lukashin, Institute for Theoretical and Experimental Physics of NRC Kurchatov Institute, Moscow, Russia
K. Levterov, Joint Institute for Nuclear Research, Dubna, Moscow Region, Russia

Abstract

Light ion injector for future NICA project contain several resonator: buncher, RFQ, Alvarez-type linac LU-20, and possibly debuncher, that all work on same resonant frequency 145.2 MHz. Base frequency for all resonators in injector produced by LU-20 linac, worked in self-excited loop mode. Low-level RF control system of injector should capture RF signal from LU-20 linac within front of signal and generate output RF signals with same frequency on others resonators, with regulated phase difference between channels. Additionally, low-level RF control system should tune resonant frequencies of RFQ, buncher and debuncher. Presented LLRF system was successively work within several years. LLRF controllers design, possibilities, and key stabilization techniques are presented.

INTRODUCTION

The NICA (Nuclotron-based Ion Collider fAcility) is accelerator facility, which is now under construction at Joint Institute for Nuclear Research (JINR, Dubna) [1]. It was used the Alvarez-type linac LU-20 as an injector for light ions, polarized protons and deuterons. Old HV fore-injector of the LU-20, which operated from 1974, was replaced by the new RFQ accelerator, which was commissioned in spring 2016 [2] and successfully works within 2016-2018 years.

Light Ions Injector RF Control

An injector for light ions, polarized protons and deuterons consists from next main parts [2]: SPI or LIS ion source, Low Energy Beam Transport (LEBT) Channel, 4-wane 3-section RFQ, Buncher, LU-20 and possibly Debuncher.

In 2016-2018 years Radio Frequency (RF) system of light-ion injector of Nuclotron was successfully work with Low-Level RF (LLRF) controller, developed in ITEP in 2015-2016. Figure 1 shows second generation of RF system of injector, with new LLRF Controller.

The RF power system is designed to excite an electromagnetic field in the accelerating structure at a frequency of 145.2 MHz, stable in amplitude, frequency and phase. RF amplifier stages and anode voltage modulator operate in a pulsed mode, with a maximum pulse repetition rate of 1 pulse/sec, and with more frequently used repetition rate of 7-10 sec/pulse. The duration of the RF pulse is about 150 μs.

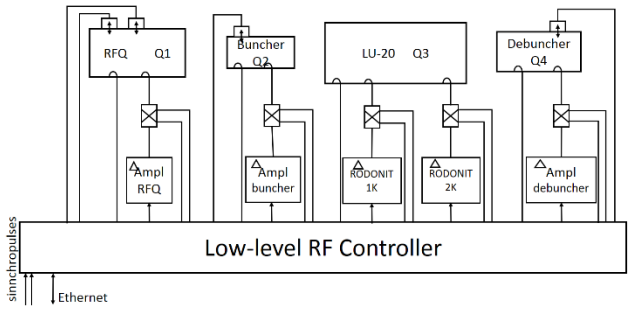

Figure 1: Injector of Nuclotron RF system.

In main mode the Alvarez-type linac LU-20 works in self-excited loop (SEL) mode, and his resonant frequency, equal to 145.2±0.1 MHz, and relative phase slowly changed from pulse to pulse. In the new proposed mode of operation, the LU-20 linac also should be excited from external RF generator. Accordingly, second generation LLRF controller should:

- Generate RF signals to the amplifiers of RFQ, buncher and debuncher resonators, whose frequency should be equal to the natural frequency of LU-20, if LU-20 works in SEL mode; additionally to generate RF signals to LU-20 resonator, if LU-20 works in external generation mode.
- In the commissioning mode, provide independent excitation of the LU-20, RFQ, buncher and debuncher with independent phasing of the channels and the possibility of simultaneous setting of different excitation frequencies for each of the channels.
- Synchronize the high-frequency fields in the resonators and to measure and control the phase difference in the resonators.
- Automatically adjust the own frequency of RFQ, buncher and debuncher resonators; in the case that the resonator LU-20 operates in the external excitation mode, determine the value of the resonant frequency of the resonator LU-20.
- Synchronize the operation of the controller by an external timer signal.
- Receive commands from the high-level control system and transmit diagnostic information via the Ethernet interface.

The differences between the frequencies of the RF field in the resonators and the resonator's natural frequencies are measured by the phase differences method, for the input and output signals of the resonators. For each resonator, three input RF signals are required: from the resonator loop, and also from the pin and from the loop of the input reflectometers. The own resonance frequency of RFQ,

† barabin@itep.ru

ISBN: 978-3-95450-197-7 doi:10.18429/JACoW-RUPAC2018-THPSC17

EMITTANCE MEASUREMENTS OF POLARIZED ION BEAMS USING A PEPPER-POT EMITTANCE METER

S. Barabin†, A. Kozlov, T. Kulevoy, D. Liakin, A. Lukashin, D. Selesnev, Institute for Theoretical and Experimental Physics of NRC Kurchatov Institute, Moscow, Russia
V. Fimushkin, Joint Institute for Nuclear Research, Dubna, Moscow Region, Russia
A. Belov, Institute for Nuclear Research of the Russian Academy of Sciences, Moscow, Russia

Abstract

A Source of Polarized Ions (SPI), developed at JINR, produces pulsed beams of polarized protons and deuterons for NUCLOTRON accelerator. The accelerated polarized ion beams will be injected into future NICA collider. In order to reconcile requirements of a RFQ fore-injector of the Alvarez type linear accelerator LU-20, it is necessary to measure a transverse emittance of the ion beams produced by the SPI. The emittance of beams of polarized deuterons and polarized protons was measured by the pepper-pot method. The results of measurements of the emittance and profile of the polarized ion beams are presented.

INTRODUCTION

The NICA (Nuclotron-based Ion Collider fAcility) is accelerator facility, which is now under construction at Joint Institute for Nuclear Research (JINR, Dubna) [1]. A study of spin physics with extracted and colliding beams of polarized deuterons and protons at the energies up to 12.6 GeV (for protons) is foreseen with the NICA facility. A proposed program allows to search for possible signs of the nuclear matter phase transitions and critical phenomena as well as to shed light on the problem of nucleon spin structure [2].

Initially, it was intended to use the Alvarez-type linac LU-20 as an injector for light ions, polarized protons and deuterons for NUCLOTRON and NICA accelerator complex. Now a possibility of LU-20 replacement by a new linac of 30 MeV energy for protons and ≥7.5 MeV/nucleon for deuterium beam is discussed. SPI has been developed at JINR as a source of polarized protons and deuterons for the LU-20 injector. The maximum permissible emittances of the beam at the input to the RFQ-based for-injector, are 4 π mm mrad for q/A= 1 and 2 π mm mrad for q/A= 0.5 [3]. To match the output beam from the SPI source with the injector acceptance, it is necessary to measure the emittance of the source.

Source of Polarized Ions

The SPI is an atomic beam-type polarized ion source with nearly resonant charge-exchange plasma ionizer and storage cell in the charge-exchange region [4]. Schematic diagram of the SPI is shown in Fig. 1.

The main parts of the source are the atomic beam section (on the left in Fig. 1), the plasma ionizer (on the right in Fig. 1) and the spin rotator [5]. The atomic beam section includes a pulsed RF discharge dissociator of molecular hydrogen or deuterium, sextupole separating magnets and RF transition units to get the nuclear polarized hydrogen or deuterium atomic beam.

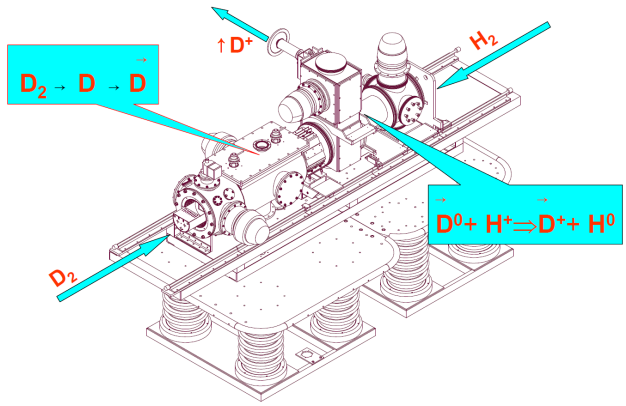

Figure 1: SPI source.

Polarized deuterons or polarized protons are produced in the source via nearly resonant charge-exchange in plasma between polarized atoms and unpolarized ions of the isotope relatively the polarized atoms:

$$H^0 \uparrow + D^+ \rightarrow H^+ \uparrow + D^0,$$
$$D^0 \uparrow + H \rightarrow D^+ \uparrow + H^0.$$

The polarized ions then accelerated to the energy of 25 keV together with unpolarized plasma ions. Spin rotator extraction system include: 90^0 bending magnet, electrostatic Einzel lens, 90^0 electrostatic deflector and output spin precessor solenoid. In the spin rotator extraction system polarized ions change the spin orientation from horizontal to vertical, separate from unpolarized plasma ions and are extracted from the source by turning first in a vertical direction by magnet and later deflecting in the horizontal plane by an electrostatic deflector.

The source worked in pulsed mode with repetition rate of 0.2 Hz and pulse duration of ~100 μs.

EXPERIMENTAL SETUP

The emittance meter was mounted on the output flange of the SPI source (see Fig. 1, near $\uparrow D^+$ row). The emittance meter is a pepper-pot meter device [6]. Its main parts are a copper mask with a pattern of holes, and a scintillator behind it. Both the mask and the scintillator are

† barabin@itep.ru

ISBN: 978-3-95450-197-7 doi:10.18429/JACoW-RUPAC2018-THPSC18

PEPPER-POT EMITTANCE MEASUREMENTS

S. Barabin†, A. Kozlov, T. Kulevoy, D. Liakin, A. Lukashin, D. Selesnev, Institute for Theoretical and Experimental Physics of NRC Kurchatov Institute, Moscow, Russia

Abstract

The pepper-pot emittance measuring device was developed to determine the parameters of the ion source beam. It includes a "pepper-pot" mask, a scintillation screen, a charge-coupled device (CCD) recorder, a personal computer (PC), software for data processing, calculation of beam profile and emittance. Measurements of emittance by pepper-pot method have been successfully carried out on several ion sources, at ITEP and JINR. The pepper-pot measurement method, the emittance meter design, and the emittance calculation technics are presented.

PRINCIPLES OF PEPPER-POT MEASUREMENTS

The measurement of emittance by the pepper-pot method consists of processing an image from a scintillator excited by an investigated beam passing through a mask with a rectangular grid of holes [1].

The copper mask takes the investigated beam, and round holes in the mask break the beam into several beamlets, which hit the scintillator and cause a flash of light from it. The scintillation pattern consists of a rectangular set of spots. This pattern is recorded and stored by the recorder and then processed by the software package for emittance calculation.

The process of emittance calculation from the registered image of the scintillator consists in plotting the beam image on the phase spaces x-x' and y-y' and then calculating the area occupied by the beam in these phase spaces. Images of the investigated beam in the phase spaces x-x' and y-y' are constructed by folding the graphs of the total radiation intensity for each column or row of spots and, respectively, for each column or row of holes in the mask. From the beam images on the phase planes, the areas occupied by the beam in the phase space, i.e. emittances are calculated. The most common method for calculating emittance is the statistical method. This method consists in constructing an envelope of the ellipse of the beam image on the phase planes, and calculating the characteristics of this ellipse, namely the area (this is emittance) and the ratio of the lengths of the ellipse's axes and the angle of their inclination with respect to the coordinate axes (these are TWISS parameters) [2].

The process of constructing a beam profile from an image of scintillation radiation consists in summing the radiation intensity for each spot in the image and, respectively, for each hole in the mask.

EMITTANCE METER

The emittance meter was used for several emittance measurements, in particular in [3] and [4]. It is a pepper-pot meter device. Its main parts are a copper mask with a pattern of holes, and a scintillator behind it (Fig.1).

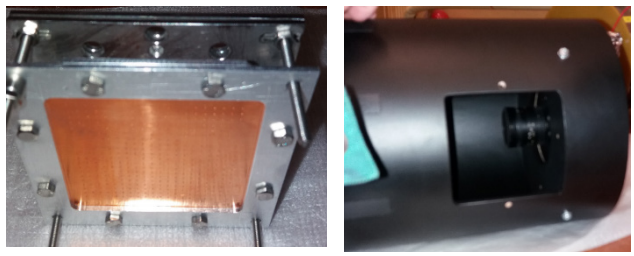

Figure 1: Emittance meter equipment.

The copper mask has a thickness of 100 μm. It contains a rectangular pattern of 20x20 holes with an average diameter of about 0.19 mm and a distance between the holes of 2.5 mm along the horizontal and vertical axes. It is mounted in a mandrel with external dimensions of 80x80 mm and with an internal window size for the passing a beam through an array of holes in a mask equal to 56x56 mm.

In this emittance meter equipment, several types of scintillators can be used. The first type is the standard P43 (Gd_2O_2S:Tb) round (52 mm diameter) scintillator from ProxyVision manufacture. Since scintillators are consumables that need to be replaced after each measurement, we need a relatively cheap scintillator. The second is a homemade $Y_2O_3:Eu$ [5] scintillator, which manufactured in ITEP on 56 mm round glass, and more frequently is used in measurements. The scintillator is mounted in a mandrel with external dimensions of 80x80 mm and an inner window with a diameter of 48 mm, which is mounted together with the mask holder. The distance between the mask and the scintillator is adjustable from 8 to 45 mm.

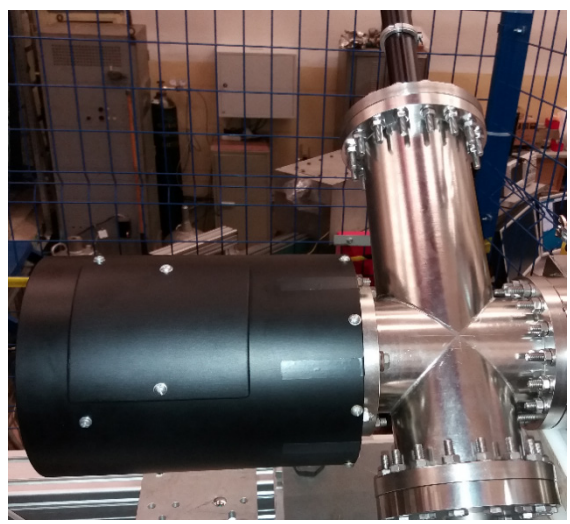

Figure 2: Emittance meter.

ISBN: 978-3-95450-197-7 doi:10.18429/JACoW-RUPAC2018-THPSC19

THE BUNCH SIZE MEASUREMENTS IN THE STORAGE RING SIBERIA-2

A.S. Smygacheva, A.I. Stirin, V.N. Korchuganov
NRC «Kurchatov Institute», Moscow, Russia

Abstract

An interaction of particles with each other and electromagnetic fields produced by an external source and the bunch in the vacuum chamber defines the electron bunch sizes in the storage ring. To research the influence of the bunch-chamber interaction on the longitudinal motion of electrons and to estimate the relative contribution of the observed effects, the measurements of bunch sizes and a bunch current spectrum were carried out in the storage ring SIBERIA-2. Results of measurements and analytical estimations are presented at this article.

INTRODUCTION

The SIBERIA-2 works in the multi-bunch mode at the beam energy 2.5 GeV. The injection energy of electrons is 450 MeV. It is at this energy the effects of the particles interaction and the beam-chamber interaction are manifest due to weak radiation damping. Therefore research of longitudinal beam dynamics was started when there is a single bunch at the energy 450 MeV in the storage ring.

The bunch size measurements were carried out with the help of the optical observation station [1]. The beam spectrum was measured by a digital spectrum analyzer. The analytical estimations of the bunch sizes due to the multiple intra-beam scattering (IBS) and the potential well distortion effect were done in addition to measurements. Calculation of bunch sizes given by the IBS was made in ZAP [2].

EFFECTS AND BUNCH SIZES

The electron bunch has the Gaussian stationary distribution of particles in the synchrotron and betatron phase spaces. Bunch sizes are defined by a set of effects such as the quantum excitation, the radiation damping, the IBS and interaction with the wake-fields.

Classical and statistical approaches to consideration of the synchrotron radiation give the expressions to define zero current rms bunch sizes in the longitudinal and horizontal directions, respectively:

$$\sigma_{lo} = \frac{c\eta}{\omega_{so}} \frac{\sigma_{E\gamma}}{E}, \tag{1}$$

$$\sigma_x = \sqrt{\beta_x \epsilon_x + \left(D_x \frac{\sigma_{E\gamma}}{E}\right)^2}, \tag{2}$$

where $\frac{\sigma_{E\gamma}}{E}$ and ϵ_x – the equilibrium relative energy spread and the horizontal emittance given by the radiation damping and quantum fluctuations of the radiation [3], β_x и D_x – the horizontal beta-function and the dispersion of the storage ring, $\eta = \alpha - 1/\gamma^2$, α – the momentum compaction factor, E – the particle energy, ω_{so} – the incoherent synchrotron frequency given by the accelerating RF-field.

Weak collisions of particles inside the bunch lead to the excitation of betatron and synchrotron oscillations, to an increase of the energy spread and sizes of the bunch. The balance between the radiation damping and the IBS limits the growth of the bunch parameters. The effect depends on the number of electrons in the bunch. The current dependence of the energy spread and bunch sizes can be found numerically, because of the calculation formulas have the complicated form. One of the basic approaches to solving the problem of the IBS proposed by J.D. Bjorken and S.K. Mtingwa [4] and developed by M. Conte and M. Martini [5] was used by M.S. Zisman and his colleagues in ZAP.

The electromagnetic (EM) fields induced in the vacuum chamber by the electron bunch distort the shape of the potential well created by the external accelerating field and can lead to the significant increase of an amplitude of coherent oscillations and to the loss of stability of the particles motion, to the microwave instability and the turbulent increase of the bunch sizes.

The consequence of the potential well distortion is the change of the longitudinal size of the bunch. It can increase or decrease with increasing the number of electrons in the bunch, depending on the spectrum of interacting fields. As a rule, the longitudinal size increases with increasing the electron current in the storage rings, what is determined by the high frequency spectrum of the EM-fields. Their wavelengths are comparable and larger than the length of the bunch. In this case, the dependence of the longitudinal size on the bunch current is usually found from the system of equations [6]:

$$\begin{cases} \omega_s^2 - \omega_{so}^2 = \frac{e\eta\omega_o}{\beta^2 T_o E} I_b \frac{\sqrt{2\pi}}{(\omega_o \sigma_\tau)^3} Z_{eff}, \\ \sigma_\tau \, \omega_s = \sigma_{\tau o} \, \omega_{so} \end{cases} \tag{3}$$

where ω_s and σ_τ – the incoherent synchrotron frequency and the rms longitudinal duration given by the potential well distortion effect, $\sigma_{\tau o} = \sigma_{lo}/c$, I_b – the average bunch current, Z_{eff} – the effective longitudinal broadband impedance, T_o and $\omega_o = \frac{2\pi}{T_o}$ – the period and the circular frequency of the revolutions, $\beta = v/c$ – the relativistic velocity factor.

The second equation in (3) is written based on the assumption that the energy spread is constant under the potential well distortion. However, the dependence of the energy spread on the number of particles is given at least by the IBS. Then the relation between the longitudinal size of the bunch and the energy spread has the form similar to formula (1), but ω_{so} is replaced by ω_s, and $\frac{\sigma_{E\gamma}}{E}$

ISBN: 978-3-95450-197-7 doi:10.18429/JACoW-RUPAC2018-THPSC20

SOME ASPECTS OF DEVELOPMENT OF CONTROL AND DIAGNOSTIC SYSTEMS FOR THE FOURTH-GENERATION RUSSIAN SYNCHROTRON RADIATION SOURSE*

S. Barabin, T. Kulevoy, D. Liakin†, A. Orlov, Institute for Theoretical and Experimental Physics of NRC Kurchatov Institute, 117218 Moskva, Russian Federation
M. Saratovskikh, NRC Kurchatov Institute, 123182 Moskva, Russian Federation

Abstract

A fourth-generation synchrotron radiation source assumed as a powerful instrument of mega science program in Russia. Recently several divisions of Kurchatov institute are involved into this project for detailed study of parameters of the beam diagnostics and the supervision control system. The actual status of this study is presented.

INTRODUCTION

The fourth-generation Specialized Synchrotron Radiation Source (SSRS-4) is the new radiation facility based on both synchrotron and FEL radiation. The project aims to create a fundamentally new specialized X-ray source - a specialized synchrotron radiation source of the 4th generation (SSRS-4) with extremely high spatial coherence corresponding to that of laser radiation, a record high brightness and temporal structure.

Both synchrotron and XFEL based on top-up injection linac are proposed to construct in SSRS4 complex. Suggested prototype of the injector initially will include 10 MeV RF photo-gun and 50 MeV regular section.

Main preliminary parameters of the SSRS4 synchrotron are [1]:

- Beam energy in synchrotron 6 GeV.
- Beam current up to 300 mA.
- Transverse emittance <100 pm·rad (two schemes are under simulation today: "user machine" with emittance of 70-100 pm·rad and "record machine" with 20-50 pm·rad).
- Top-up injection from linac or booster.
- MBA magnet structure with SR length ~1300 m and 40 superperiods
- Four groups of RF cavities (3 or 4 cavities/group) in fully symmetries periods, solid-state RF power sources, operation frequency 500 or 700 MHz.

CONTROL AND DIAGNOSTIC SYSTEMS

Main parts of SSRS-4 synchrotron, dependent of selected scheme, are medium or full energy LINAC, compact or full-scale Booster, Main Ring of Synchrotron and Beam Transfer Lines. Main control systems (Fig. 1) are:

- RF systems for LINACs, Booster and Synchrotron.
- LINACs, Booster Synchrotron and Beam Transfer Lines magnet systems, which include slow elements control, ramping elements control, fast correction control, injector and extractor elements control, with servomechanisms control.
- Timing system.
- Vacuum systems.
- Water flow control and temperature control.
- Area access control and dosimetry control.
- Beam diagnostic systems, such as beam position monitors (BPMs), Beam Current monitors, Beam profiles and emittance measurements, Beam Loss monitoring system and so on.

Control system core, TANGO [2] or similar, should include: set of operator's terminals, configuration database server, History server(s), set of Event servers.

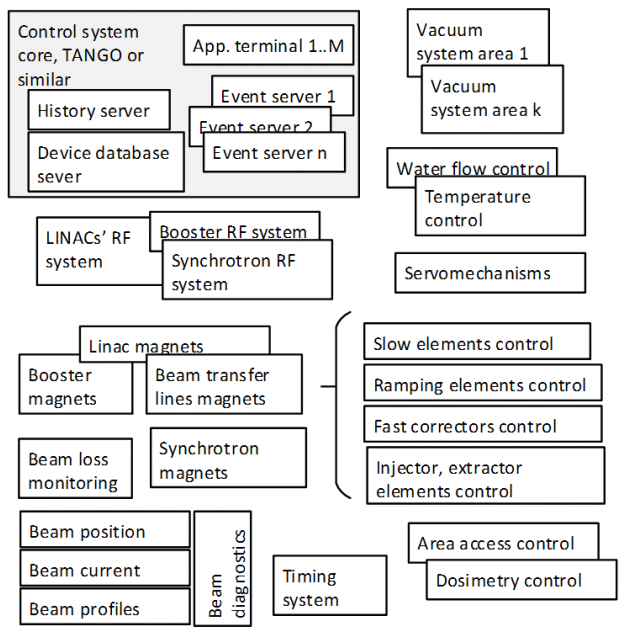

Figure 1: SSRS-4 systems.

CONTROL SYSTEMS DEVELOPMENT

To develop software for the SSRS-4 CS, a development model was chosen in accordance with the Rapid Application Development (RAD) rules [3]. RAD is the concept of creating software development tools, focusing on the speed and ease of programming, creating a technological process that allows the programmer to create computer programs

†liakin@itep.ru
* - work supported by the Ministry of Education and Science of the Russian Federation. Agreement 14.616.21.0088 from 24\11\2017. ID RFMEFI61617X0088. (Federal Targeted Program "Research and development on priority directions of scientific-technological complex of Russia in 2014 -2020 year"

ISBN: 978-3-95450-197-7 doi:10.18429/JACoW-RUPAC2018-THPSC22

LONGITUDINAL BEAM MEASURUMENTS ON DAMPING RING BINP'S INJECTION COMPLEX WITH NEW RESONATOR

V. V. Balakin†, F. A. Emanov[1], D. E. Berkaev, O. I. Meshkov[1], V. M. Borin
Budker Institute of Nuclear Physics, 630090, Novosibirsk, Russia
[1]also at Novosibirsk State University, 630090, Novosibirsk, Russia

Abstract

Injection Complex VEPP-5 feeds two BINP's colliders – VEPP-4M and VEPP-2000 with the electron and positron beams. 700 MHz 64-harmony damping ring resonator was replaced with 10.94 MHz first harmonic one in 2017. The key parameters for IC damping ring are particles storage rate and extraction beam parameters. In order to figure out how collective beam effects influence them with the new resonator we explore longitudinal beam distribution during the injection and storage, length during the extraction and effects, which influences on them. The results of research are presented at this paper.

INTRODUCTION

VEPP-5's injection complex (IC) is the electron and positron beam source for the VEPP-2000 and VEPP-4M colliders. It was introduced in 1994 and turned into regular operation in 2015 [1]. VEPP-2000 upgraded his injection chain in 2014-2015 [2], VEPP-4M switched into IC in summer 2016 [3]. The BINP's accelerator facilities layout is presented on Fig. 1. Beam Transportation Chanel K-500 connects injection complex and colliders.

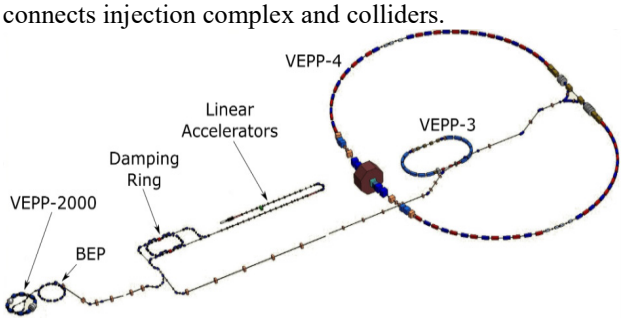

Figure 1: BINP's accelerator facilities layout.

The key parameters of injection complex are presented in Table 1.

Table 1. IC Key Parameters

Parameter	Value
Energy (2016/17 run)	385-420 MeV
Electron storage rate	$2*10^{10}$/s
Positron storage rate	$2*10^{9}$/s
Repetition time	up to 12 Hz
Maximum e- extraction	up to $1.2*10^{11}$
Maximum e+ extraction	up to $1.2*10^{11}$

BUNCH LENGTHENING THEORY

Beam interaction with electro-magnetic fields, emitted by it in vacuum chamber, leads to beam lengthening and shape-distortion effects, which depends on number of particles inside the ring. It efficiently decreases the RF voltage and called potential well distortion. It is possible to observe the influence of this effect from small beam current.

Potential Well Distortion

It is well known that for Gaussian beam with sigma σ_z the peak current I_p depends from average I_b current as $I_p = \frac{\sqrt{2\pi}R}{\sigma_z} I_b$ (R is an average accelerator radius) beam length vs. current is defined by formula:

$$\left(\frac{\sigma_z}{\sigma_{z0}}\right)^3 - \left(\frac{\sigma_z}{\sigma_{z0}}\right) - \frac{e}{\sqrt{2\pi}} \frac{\alpha I_b}{E Q_{s0}^2} Im\left(\frac{Z_{||}}{n}\right)\left(\frac{R}{\sigma_{z0}}\right)^3 = 0, \quad (1)$$

where $Q_{s0}^2 = \left(\frac{\omega_s 0}{\omega_0}\right)^2 = \frac{neV_0|cos\varphi_s|}{2\pi E}$, E is a particle energy and α – momentum compactor factor [4].

In addition, synchronous beam phase shift is occurred [5]:

$$\Delta\varphi = \frac{2\pi I_b}{V_0 \cos(\varphi_s)} \frac{\sqrt{2\pi}}{\omega_0 \sigma} Re\left(\frac{Z_{||}}{n}\right). \quad (2)$$

Potential well distortion leads not only beam lengthening, but longitudinal beam profile distortion, too. The beam density along longitudinal coordinate z in case of resistive impedance (with the wake-function $W'_0(z) = S\,\delta(z)$,) is determined by:

$$\rho(z) = \frac{\sqrt{2/\pi} e^{-\frac{z^2}{2\sigma_z^2}}}{\theta\sigma_z\left[\coth\left(\frac{\theta N}{2}\right) - \mathrm{erf}\left(\frac{z}{\sqrt{2}\sigma_z}\right)\right]}, \quad (3)$$

where $\theta = r_0 S/\alpha\sigma_\delta^2\gamma C$, $\mathrm{erf}(x) = \frac{2}{\sqrt{\pi}}\int_0^x e^{-t^2} dt$, C – accelerator circumference, σ_δ - rms beam energy spread. Full description of this process is shown in [6].

STREAK-CAMERA MEASUREMENTS

For measuring damping ring (DR) beam parameters during the injection and after it, we used the PS-1/S1 streak-camera (SC).

SC was synchronized with inflectors trigger, and it allowed tracking the beam injection process in the damping ring RF bucket and measurement the longitudinal beam size dependences with precision about 1 turn.

IC VEPP-5 linear accelerator produces the beam, which consists from 16 bunches (Fig. 2).

† balakinvitalyv@gmail.com.

ISBN: 978-3-95450-197-7 doi:10.18429/JACoW-RUPAC2018-THPSC23

LOW ENERGY "PEPPER-POT" EMITTANCE MEASURING DEVICE

V.S. Klenov, S.E. Bragin, O.M. Volodkevich, V.N. Zubets, Institute for Nuclear Research of the Russian Academy of Sciences, Moscow, Russia

Abstract

The device which includes the "pepper-pot" mask, the quartz screen, and the CCD camera was used for measure the transverse emittances of beam at the exit of H-minus ion source for 7-15 keV beam energy. Emittance measuring at such low ions energy required low-level signals from quartz screen to be recorded and processed, while the intense glow of the gas discharge plasma created a spurious illumination of the quartz screen. The issues of obtaining sufficient signal level at such low ions energy, methods of subtracting the signal of non-ion-beam illumination of quartz screen from the full amplitude of the signal as well as issues of data processing and presentation of phase portraits are discussed.

INTRODUCTION

The advantage of "pepper-pot" emittance measuring device is that the device allows, in principle, to get the phase portraits simultaneously in XX' and YY' planes in a single shot or a small number of pulses of beam current in quasi real time mode.

This type device which includes the "pepper-pot" mask, the quartz screen, the CCD camera, PC, the software for camera data processing and beam phase portrait formation was implemented at the 400 keV H-minus LEBT channel of the INR RAS linac and the possibility to measure the emittance of the ion beam in a single shot beam pulse was demonstrated [1]. However, when measuring the emittance close to the output of an ion source for a beam with an energy of about 15 keV, the level of the useful signal from the quartz screen is much lower, and the spurious illumination of the CCD-matrix by the radiation of the gas discharge plasma from the ion source may be much higher than the useful signal. Direct light illumination from gas discharge plasma is the most critical when measuring the emittance of a source with "direct" ion beam extraction without the use of a bending magnet. It is for this geometry of the ion source that measurements were made, which are discussed later in the report.

EQUIPMENT SELECTION

The disadvantage of the "pepper-pot" method is the need for constructive selection of the measurement step (step between holes) and this step cannot be changed during the measurement. The choice of the "pepper-pot" mask parameters was determined by the expected characteristics of the measured ion beam – its sizes and angular divergences as well as the distance to the screen and the intensity of the screen glow.

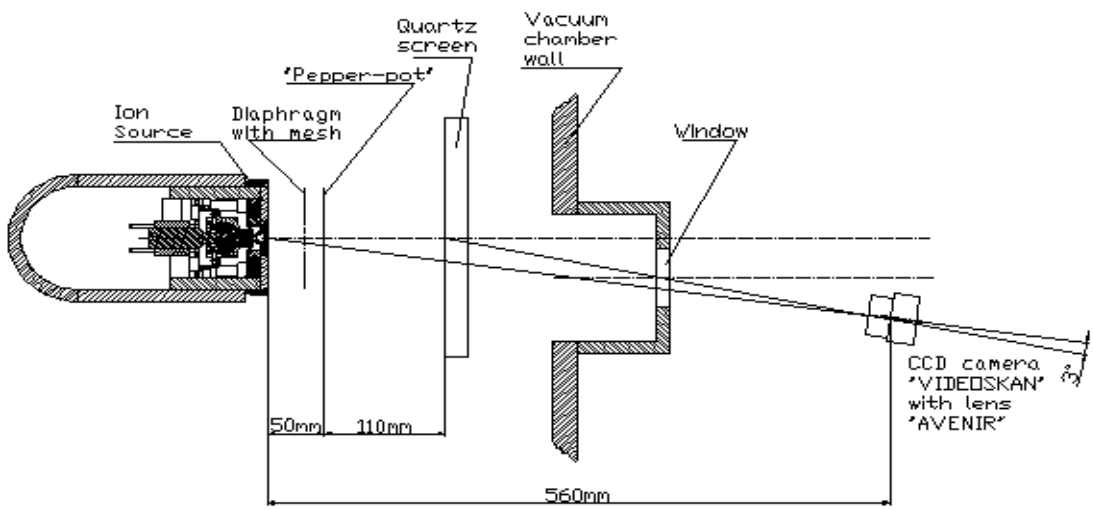

Figure 1: Scheme of the emittance measuring device.

ISBN: 978-3-95450-197-7 doi:10.18429/JACoW-RUPAC2018-THPSC24

FAST WIRE SCANNERS FOR U-70 ACCELERATOR OF IHEP

V. T. Baranov†, V. N. Gorlov, D. A. Savin, V. I. Terekhov, Institute for High Energy Physics in National Research Centre "Kurchatov Institute", 142281 Protvino, Russia

Abstract

The fast wire scanners are used for the transverse beam profile measurement in horizontal and vertical planes at the IHEP U-70 Accelerator. They cover the total range of operating beam intensities and energies of the circulating of proton and ion beams. The scheme of the scanners is based on a rotary brushless servomotor produced by the "Faulhaber" company. The speed of the fork with the carbon fiber is 16 m/s. The rotation mechanism and the control electronics was done to take into account the available radiation levels at the locations of the wire scanners. This report gives the mechatronic design of the wire scanners and provides a system overview.

INTRODUCTION

For the operational work of the U-70 accelerator the measuring of transverse circulating beam profiles in both planes is necessary. Initially the ionization beam profile monitors with industry television components were used for these purposes [1]. That was very bulky and provided a poor resolution. The measuring targets are also used to determine the beam transverse boundaries. During the last 30 years new techniques based on wire scanners were developed at many labs: CERN, FNAL, BNL and others. At IHEP the several types of wire scanners were built and tested at the real beam with the speeds 1 m/s [2] and 10 m/s [3]. An alternative method has been proposed and tested: the beam is guided by a deflecting magnetic field on a fixed carbon wire. In the case of the using standard equipment for the beam was put spilled on the absorber the speed of 3 m/s was obtained [4]. However, these devices were not highly reliable and had large errors in the measuring profile. The estimated resolution was of 0,1 mm and a low speed of the wire motion caused the overheating and destruction of fibers at full beam intensity. That is why the new wire scanners at U-70 were designed and put in pilot operation to measure the profiles of the circulating beam all over the machine cycle and over a full operational range of intensity and energies of the protons and ions.

PRINCIPLE OF OPERATION OF WIRE SCANNER

The U-70 wire scanners are based on a circle movement of a thin carbon fiber through the circulating beam at a speed of 10÷20 m/s. Such parameters insure the fiber saving because of weak heating when they move through the beam. Beam profile data are provided due to a radiation generated by the interaction of protons or ions with the material of the carbon fiber. The radiation is registered in a scintillation detector located in the downstream of ~ 5 m. The movement of the wire occurs an arc. When calculating the beam profile it is necessary to take this circumstance into account.

At the first wire scanners control of electric motors was carried out by analog signals in combination with mechanical devices and organization of movement through bellows. At CERN a new generation of devices in which the rotor of the servomotor is isolated from the stator by vacuum has recently been developed [5], [6]. This project stimulated our development of the wire scanners, in which the entire motor was located inside the vacuum chamber of the accelerator. The work was started in 2014 and contained the choice of the servomotor and control electronics [7], the mechanical design, manufacture and installation of these wire scanners at U-70.

COMPONENTS OF WIRE SCANNER FOR ACCELERATOR U-70

Servomotors

The servomotor shaft with a U-shaped fork is mounted on the boundary of the vacuum chamber. The device is characterized by the presence of a trapezoidal operating mode of a fast servomotor. The U-shaped fork with the carbon fiber is accelerated to the required speed during ¼ turn, then there is an area of ½ turn for a steady motion of the wire when crossing the ion beam and then the fork slows down and returns to its original position for the remaining ¼ turn.

A general approach to the development of such a device implemented in IHEP using servomotors is described in [7]. We chose a brushless high-performance servomotor 4490H024BS, developed by the company "Faulhaber". The advantages of this type of motors are a wide range of operating speeds, high overload capacity and good dynamic features. A high unit torque and lack of a core in the winding are its special features. The dynamically balanced rotor and light-weight also positively affect the ability of the motor to accelerate and maintain the speed in the prescribed limits.

An additional advantage of this servomotor is the ability to operate under pressure up to 10^{-7} Torr when a special option is used. This allows to install the motor inside the vacuum chamber of the U-70 accelerator. When selecting this series it was taken into account that it is possible to produce a motor with two shaft ends on both sides of the motor, with an extended shaft length of one of the ends. At the extension of the shaft an electromagnetic brake "Faulhaber" series MBZ is mounted for fixing the frame position when the power is off. We further mounted on the shaft a resolver RE-10-1-C64 by "LTN Servotechnik" which contains no active elements, the radiation hardness of the resolver being much higher than the radiation hardness of Hall sensors.

ISBN: 978-3-95450-197-7 doi:10.18429/JACoW-RUPAC2018-THPSC27

LONGITUDINAL BEAM PROFILE DIAGNOSTIC SYSTEM AT BOOSTER OF ELECTRONS AND POSITRONS BEP

M. Timoshenko*, Yu. Zharinov, E. Perevedentsev, Yu. Rogovsky, D. Shwartz
BINP SB RAS, Novosibirsk, Russia

Abstract

The longitudinal beam profile measurement system based on optical dissector was upgraded at booster synchrotron BEP during VEPP-2000 collider complex 2017/2018 data taking run. New RF cavity of 13-th harmonic was installed during the booster upgrade in 2013-2015 to increase top energy to 1 GeV. The complex work on synchrotron radiation output modernization was performed, and measurement system was commissioned. The system was tested and calibrated, the resolution was studied. The bunch length dependence was measured for different RF cavity voltages while beam current changes and compared with the potential well distortion model. Good agreement with theory proved system operability. In addition the results of bunch length current dependence obtained by dissector at VEPP-2000 collider were compared with streak-camera measurements being in a good agreement. The synchrotron tune dependence on RF cavity voltage was measured both at BEP and VEPP.

INTRODUCTION

The VEPP-2000 is a collider complex which mean parts are electron-positron booster BEP and collider VEPP-2000 with two detectors CMD-3 and SND [1]. After modernization BEP energy range began to be from 200 MeV to 1 GeV. It and BEP parameters are described in [2]. The experiments at the collider VEPP-2000 has become possible at this energy range without energy increasing in it.

Before this work longitudinal beam distribution monitoring system wasn't used. Observation of this distribution can give more full understanding of beams nature in the booster and collider of VEPP-2000 complex.

MEASUREMENT SYSTEM AT BEP

Electron and positron booster BEP are needed for portioned storaging of particles supplied by Injection complex VEPP-5 [3] at 395 MeV energy. At the accelerating regime BEP works at the energy range from 200 MeV to 1 Gev. Operating with different sort of particle is possible due to polarity reverse of magnet systems.

BEP synchrotron radiation spectrum contains optical range and beam motion is strictly periodical. These factors allow to use synchrotron radiation in optical diagnostic system. BEP have several outputs of synchrotron radiation but all of them are used. For this reason one of them has been upgraded.

The longitudinal beam charge distribution measurement system (dissector) has been installed and tested at BEP at first.

Optical Table Modernization

The task of modernization concluded in to save current beam transverse position monitor (CCD-camera) functional. Duplication light of synchrotron radiation has been applied by semitransparent mirror set in optical table tract. Yellow part of table (with some mirrors cube and dissector components) at the Fig. 1 has been added during modernization.

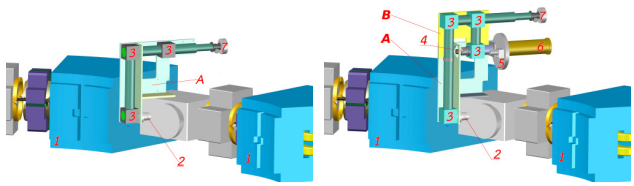

a) b)

Figure 1: Concept of modernization. Optical table before a) and after b) modernization.
1 – bending magnet, 2 – sync. rad. output, 3 – cubes with moving mirrors inside them, 4 – calibration light source, 5 – light filters, 6 – dissector, 7 – CCD-camera.

Alignment of Optical Table

After production necessary details and realization of optical table concept it has been aligned outside BEP room with using portable CCD-cameras. The task was to precisely pointing and focusing[1] of light from simulation of synchrotron radiation source on the places where the real devices (CCD-camera and dissector) should be set.

After preliminary alignment the optical table with both devices have been installed to BEP synchrotron radiation output and the final tuning has been completed with very low intensity beam (around 100 μA) in the BEP.

DISSECTOR

Dissector is a optical stroboscopic device. One of the way of applying it is registration of longitudinal distribution of beam charge in a circular accelerators.

Operation Principles

Dissector is the vacuum tube consisting of mean components:

- photo-cathode

* email address: tim94max@gmail.com

[1] There are system of lenses in the optical tract

ISBN: 978-3-95450-197-7 doi:10.18429/JACoW-RUPAC2018-THPSC28

A SYSTEM FOR MONITORING BEAM LOSSES AT THE IHEP U-70 ACCELERATOR

V. Terekhov†, G. Antonichev, V. Baranov, Yu. Bardik, D. Savin, E. Syshchikov , Institute for High Energy Physics of NRC "Kurchatov Institute", 142281 Protvino, Russia
V. Kokovin, State University "Dubna", branch "Protvino", 142281 Protvino, Russia.

Abstract

Updated beam monitor system executes continuous monitoring surveillance beam losses around the IHEP U-70 accelerator. The system consists of 120 detectors. One is located upstream of each bending magnet in the median plane outside of the beam-pipe at 60 cm apart. The detectors are cheap ion chambers filled with air under barometric pressure and 1.8 liter volume. Chamber signals processing is based on digital integration and done in the framework of the U-70 Control System. Acquired data are used to facilitate tuning of the accelerator, minimize beam losses at any point of the machine circumference and consequently decrease damage for accelerator equipment. This report gives a brief description of the system and the result of run experience as an example.

INTRODUCTION

During beam circulating at high energy accelerators many possibilities exist for the beam to be lost, partially or even as a whole. Probable beam loss causes are:

- Steering errors at the injection
- Closed orbit distortion
- Erroneous transition crossing
- Improper tuning of the extraction
- Gas scattering because of poor vacuum
- Aperture restrictions
- Equipment malfunctions.

Operational intensities of proton beam at the IHEP U-70 Accelerator are typically around $9*10^{12}$ protons per cycle at the same time full design intensity is $3*10^{13}$ protons. It is then mandatory to operate with the smallest beam losses to minimize damage of accelerator equipment and personnel exposure while maintenance. Time and position distribution of the losses is the very useful diagnostic aid for facilitating tuning the machine. A beam loss monitor (BLM) system for continuous detecting radiation levels around the U-70 accelerator had been developed and put in operation for the first time in 2000 [1,2]. After a seven year experience the main drawbacks have been exposed:

- Used miniature ionization chambers (IC) of 0.16 liter volume produced low level currents in range from tens of pA to hundreds of nA [3]. Their transmission via long (up to 1000 m) coaxial cables to a surface building under high industrial noises caused deficient SNR for many locations. This fact was usually an obstacle for researches at the low intensities.
- The obsolete and very bulky data acquisition means. That cased often errors of data traffic and impeded the maintenance service.

That is why the system was improved by replacing the small IC`s with new chambers and developing a new electronics.

The new BLM system was installed in 2012 and has been operating successfully since the start. It has been included in the U-70 control system [4] and provides the qualitative information about beam losses in each straight section over the accelerator cycle with 100 mc time resolution, or not less than 10 mc for short time intervals at the range of the intensities from $3*10^{10}$ to $3*10^{13}$ protons. The beam loss distribution is given by a histogram. This report presents monitor design, their mounting and the processing electronics.

BEAM LOSS MONITOR

The monitors are home-made IC's filled with 1800 cm^3 air at local barometric pressure. They are inherently slower devices, but this feature is not a significant drawback in our practice. Figure 1 shows a photograph of the new monitor. It is an electrode assembly, consisting of 31 plane-parallel 0.2 mm thick stainless steel foils, 6 mm apart, alternatively connected to the collector voltage and signal buses. The operating volume is about 1800 cm^3. The assembly is packed into a stainless steel cylinder 100 mm diameter and 43 cm length. Connectors are placed on the end of the cylinder, two ones connected in parallel (for daisy chain connection) are used for applying the bias voltage and third one is the signal output.

The main electrical characteristics of the chamber are next:

- The bias voltage 750 V
- The positive ion transit time ≤ 0.2 mc
- The interelectrode and electrode to ground resistance ≥ 1 TΩ
- The interelectrode capacity 0.65 nF
- Output typical current 200÷6 mkA
- The sensitivity 500 nC/rad

Long-term observations during operation of the U-70 in different modes did not detect a saturation of the monitors. Their gains are all practically identical and do not change with age.

The total charge collected in the monitor is highly depends on its relative position to a loss source. For the sake of homogeneity the IC's are mounted close to each of 120 bending magnets in the median plane outside of

ISBN: 978-3-95450-197-7 doi:10.18429/JACoW-RUPAC2018-THPSC29

MEASUREMENTS OF ENERGY SPREAD AT VEPP-4M

V. M. Borin, V. L. Dorokhov, V. A. Kiselev, O. I. Meshkov[1], S. A. Nikitin, P. A. Piminov, S. V. Sinyatkin, Budker Institute of Nuclear Physics, Novosibirsk, Russia
A. V. Smirnov, General Physics Institute, Moscow, Russia
[1]also at Novosibirsk State University, Novosibirsk, Russia

Abstract

The unique feature of the VEPP-4M electron-positron collider is wide energy range (1 - 4.75 GeV) available for experiments in high-energy physics. Energy spread value of the beam is an important parameter in a choice of energy step during measurement of e+e- -> hadrons cross sections as well as it has a strong influence on the statistic collection time required for the scanning of narrow resonances like planned for the nearest future scan of Upsilon(2s) meson. Thus, it is important to control energy spread of the beam and measure it operatively and reliably. The paper presents measurements of the beam energy spread at the VEPP-4M electron-positron collider in its complete energy range. Energy spread was calculated from bunch length measured by PS-1/S1 streak camera with picosecond temporal resolution. In order to exclude the influence of collective effects on bunch length, we measured length of low-intensity bunch. Values of energy spread calculated from bunch length were cross-checked by the measurements of energy spread based on registration of a beam decoherence. The impact of the Touschek effect in the beam energy spread at low energy range (1.0 - 1.5 GeV) is discussed.

ENERGY SPREAD

Natural Energy Spread

Neglecting an influence of collective effects the energy spread in circular accelerator is determined by equlibrium between quantum excitation and radiation damping of synchrotron oscilations. The value of equlibrium energy spread is determined by an accelerator lattice and can be calculated using Eq. 1:

$$\left(\frac{\sigma_E}{E}\right)^2 \approx 0.9923 \frac{\lambda_E <1/r_0^2>}{J_E <1/r_0^3>}\gamma^2, \qquad (1)$$

where σ_E is the energy spread, E is the bunch energy, λ_E is the Compton wavelength of the electron, J_E is the longitudinal damping partition number (Eq. 2), r_0 is the bending radius, γ is the Lorentz factor.

$$J_E = 2 + \frac{\oint\left(\frac{1}{r_0^2} + \frac{2G}{H_0 r_0}\right)\frac{D}{r_0}\mathrm{d}s}{\oint \frac{\mathrm{d}s}{r_0^2}}, \qquad (2)$$

where G is a vertical magnetic field gradient, H_0 is a vertical magnetic field. Value of second term of Eq. 2 is limited by -2 and 1 by conditions of stable beam motion.

A presence of bending magnets with focusing sections at the lattice of VEPP-4M leads to values of second term of Eq. 2 out of its limits. In order to get the conditions of stable motion a special Robinson damping wigglers are installed at the VEPP-4M. Altering their strength, we can control the value of energy spread in a wide range. It is very important to know the value of energy spread during the scanning of narrow resonances, because the luminosity integral required for the measurements of the resonance cross section with certain precision is proportional to third degree of the energy spread of the beam.

Intrabeam Scattering

Another significant effect that we should consider during the operations of the VEPP-4M at the low energy range (below 1.5 GeV) is the intrabeam scattering (IBS of multiple Touscheck effect), which causes energy spread increase as the beam current increases. The effect is based on transferring of momentum from the transverse plane of motion to the longitudinal one, boosted by Lorentz factor [1,2].

The energy spread growth is not correlated with the quantum excitation. Thus, the total energy spread is determined by the quadratic sum of natural energy spread and the IBS term.

BEAM DIAGNOSTICS

Bunch Length Measurements

The main method we used to determine bunch energy spread is the measurements of its length:

$$\frac{\sigma_E}{E} = \frac{\sigma_s \omega_s}{\alpha c}, \qquad (3)$$

where σ_s is the bunch length, ω_s is the synchrotron revolution frequency, c is the speed of light, α is the momentum compaction factor.

For the measurements the PS-1/S1 streak camera was installed into optical diagnostics of the VEPP-4M [3, 4] The camera has a temporal resolution about 3 ps. The example of longitudinal profile of the bunch acquired by the camera is shown in the Fig. 1.

The method can be used only with low intensity beams. In case if beam is intense enough, then collective effects affect the relation between bunch length and energy spread [5]. In order to avoid it, all measurements were conducted with beam current about 0.2 mA at which all collective effects are negligible. Choice of current is based on studies of collective effects conducted earlier [6].

ISBN: 978-3-95450-197-7 doi:10.18429/JACoW-RUPAC2018-THPSC33

RADIATION INSTALLATION AND ACCELERATOR UELV-10-10-C-70 BEAM PARAMETERS CONTROL, MANAGEMENT AND REGISTRATION SYSTEM

P. A. Bystrov, Yu. S. Pavlov, A. A. Kozlov, IPCE RAS, 199071 Moscow, Russia
I. Yu. Yakupov, A. V. Prokopenko, MEPhI, 115409 Moscow, Russia
N. E. Rozanov, MRTI RAS, 117519 Moscow, Russia

Abstract

The design of radiation technological installation operation parameters recording system for accelerator UELV-10-10-S-70 is presented. Proposed the design of the sensor, which makes possible roughly evaluate the energy spectrum of accelerator beam. Solutions are proposed for data transfer from the accelerator equipment to the computer for former analysis and recording data in journal, as well as preventing supernumerary situations.

INTRODUCTION

Irradiation of medical products on radiation installations based on electron beam requires a careful, responsible approach. To increase the quality of irradiation, continuous monitoring of the installation operation is necessary. The design of the system for monitoring and recording parameters of a radiation-technological installation at IPCE RAS was presented earlier [1]. The developed monitoring system is able to collect data in real time with number of sensors, perform its analysis and registration, inform about errors and emergency situations. System uses a simple solution for collecting and transferring data from sensors to a computer, which traditionally remains a bottleneck in technology.

An important task remains to develop a sensor able to determine the parameters of the accelerator beam, such as pulse current and energy spectrum and transfer them to recording system in real time. Various methods, based on simple equipment, for determining the energy spectrum of accelerator beam, which can be used for continuous monitoring without interrupting the production process, were proposed [2].

This paper concerns developing a technique for evaluating the beam energy spectrum of an industrial accelerator UELV-10-10-S-70 by methods based on standard equipment, which does not interrupt the process of irradiation on accelerator. For this problem, the beam spectrum sensor based on the Faraday cup is proposed, using the control system. The sensor measures the current of the part of the deflected beam. It uses that part of the beam which is not utilized in standard accelerator operation.. The measurement accuracy can be increased by using long-term collecting and mathematical post processing of the collected data.

The method is simulated using the "Beam Scanning" code. A computational model is being developed for processing the results of measurements in these methods, using the computer code "Beam Scanning".

MATERIALS AND METHODS

Irradiation center at IPCE RAS is based on radiation-technological installation with electron accelerator UELV-10-10-S-70 which is mounted in radiation-safe bunker and designed to perform irradiation by electron beam with electron energy up to 8 MeV, beam power up to 10 kW.

Figure 1: Radiation installation at IPCE RAS center.

Radiation-technological installation consists of linear electron traveling wave accelerator with beam scanning system attached to it and circular conveyer, which moves objects before the output window of accelerator, one meter far from output window. The conveyer with boxes and accelerator with beam scanning system of this installation are presented on Fig. 1. Installation is used in different research, technological and commercial applications. Installation has an open beam, which makes possible to work with the beam using different instruments.

To collect information about installation operation and to control the process of irradiation, recording system was implemented. This system consists of measurement and signal conversion blocks for collecting the following data: the data on conveyer movement, the data on conveyer motor power supply and the data on deflection magnet beam scanning system power supply. In current version of the system the data about the conveyor movement, scanning system deflecting magnet current and accelerator

ISBN: 978-3-95450-197-7 doi:10.18429/JACoW-RUPAC2018-THPSC34

MODERN BEAM MONITORING SYSTEMS DURING SEE TESTING ON ISDE&JINR HEAVY ION FACILITY

A.T. Issatov†[1], I. Kalagin, A. Krylov, S.V. Mitrofanov, Yu.G. Teterev, Flerov Laboratory of Nuclear Reactions, Joint Institute for Nuclear Research, Dubna, Russia
P. Chubunov, ISDE, Moscow, Russia
V.S. Anashin, United Rocket and Space Corporation, Moscow, Russia
[1] also at L.N. Gumilyov Eurasian National University, Astana, Kazakhstan

Abstract

Diagnostic systems of ion beam parameters were modernized at beam-lines for electronic tests at FLNR accelerator complex. Scintillation detectors based on flexible optical fibers, multichannel and 15-channel beam profile detectors and energy measurement system for the high energy beam-line based on U400M were created.

INTRODUCTION

Beams of accelerated ions of low intensity are required for applied research, e.g., research of radiation resistance of electronics [1] or in biology.

Three beam-lines have been built in the accelerator complex of the FLNR JINR for testing electronic components: two low energy beam-lines (3-9 MeV/nucleon) and one high energy beam-line (15-60 MeV/nucleon) [2]. For testing, it is necessary to know the following parameters of heavy ion beams: ion energy, flux density and uniformity of beam distribution. To determine these parameters during the tests, a system for diagnosing ion beams based on scintillation detectors was developed. But this system does not meet all requirements. First, online flow density control is conducted away from the test sample. Secondly, on the high-energy channel, there is no direct measurement of energy at the location of the sample. Third, there are no ion beam profile detectors on the low energy channel.

Diagnostics systems of ion beam parameters were modernized to eliminate shortcomings. A multichannel ion beam profile detector, scintillation detectors on flexible fibers, and a system for measuring ion energy at the location of the test sample were created.

SCINTILLATION DETECTORS BASED ON FLEXIBLE OPTICAL

Detectors are designed to online flux measurement near DUT. Detectors are consist of PMT H10721 (Hamamatsu), wavelength shifting fibers Y-11 (200) (Kuraray) and plastic scintillator. The area of plastic scintillator is 1 cm^2. There are up to 8 detectors to each beam-line. Detectors are mounted on vacuum flange DN-63 and installed on the test chamber. Photo of detectors is shown on Fig. 1.

† issatov@jinr.ru

The detectors are calibrated with polycarbonate or polyethylene terephthalate track detectors. Some results of the calibration are presented in the Table 1.

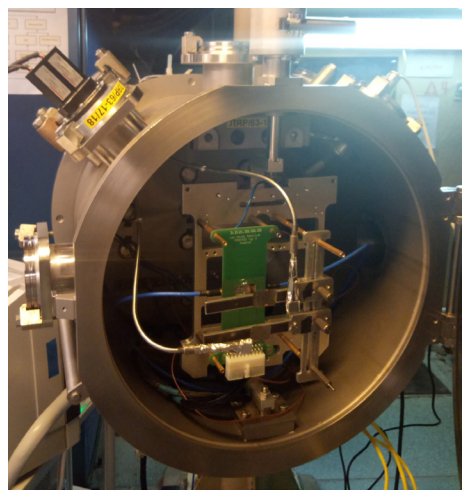

Figure 1: Photo of detectors.

Table 1. Results of Detector Calibration

№	№ of detector	The scint. detector fluence	The track detector fluence	k
83	1	5.50E+07	5.90E+07	1.07
	2	5.11E+07	5.60E+07	1.10
84	1	5.41E+07	5.50E+07	1.02
	2	4.96E+07	5.60E+07	1.13
85	1	5.38E+07	5.70E+07	1.06
	2	5.11E+07	6.10E+07	1.19
86	1	5.57E+07	5.85E+07	1.05
	2	5.29E+07	5.90E+07	1.12
87	1	1.98E+07	2.10E+07	1.06
	2	1.85E+07	1.80E+07	0.97
88	1	1.98E+07	2.10E+07	1.06
	2	1.83E+07	2.30E+07	1.26

ISBN: 978-3-95450-197-7 doi:10.18429/JACoW-RUPAC2018-THPSC35

INFLUENCE OF MECHANICAL VIBRATION ON BUNCH SHAPE MONITOR PHASE RESOLUTION

D. Chermoshentsev†[1,2,3], A. Feschenko[2], S. Gavrilov[1,2]
[1] Moscow Institute of Physics and Technology, Moscow Russia
[2] Institute for Nuclear Research of the Russian Academy of Sciences, Moscow, Russia
[3] Skolkovo institute of Science and Technology, Skolkovo, Russia

Abstract

Bunch Shape Monitor with three changeable deflectors was designed and manufactured for UNILAC, CW LINAC and proton linac of GSI-FAIR project. The length of BSM RF-deflector for UNILAC was large, that increased the influence of external mechanical vibrations on the BSM operation. The model for mechanical and electrical analysis of BSM RF-deflector and design solutions for vibration damping are presented.

INTRODUCTION

Bunch shape monitor (BSM) [1] uses the technique of a coherent transformation of a temporal bunch structure into a spatial charge distribution of low energy secondary electrons through RF-modulation. The main part of BSM is a RF-deflector. The RF-deflector electric field is a superposition of electrostatic focusing and steering fields and RF-deflecting field, thus enabling simultaneous focusing and RF-scanning of the electrons. Typically, BSM deflectors are RF-cavities based on parallel wire lines with capacitive plates. After the deflector intensity of secondary electrons beam registered by electron multiplier. Electrical length of the deflectors is usually quarter-wave (QW) or half-wave (HW) (Fig. 1).

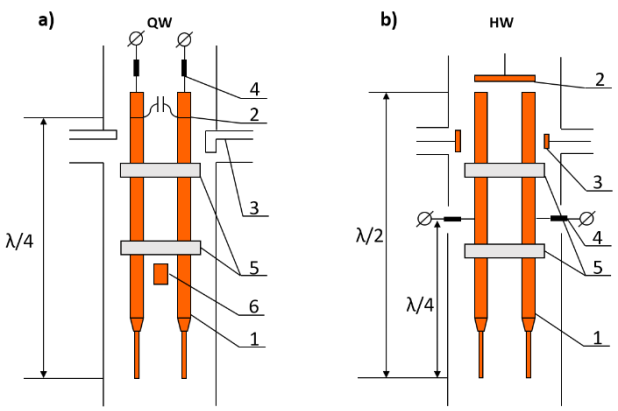

Figure 1: Scheme of a) QW-type and b) HW-type RF-deflectors. 1 – electrodes, 2 – main tuning, 3 – RF - feedthrough, 4 – HV - feedthrough, 5 – isolating holders, 6 – extra tuning.

BSM with three changeable deflectors was fabricated for GSI linacs: UNILAC, CW linac and Proton linac.

At lower frequencies, length of the RF-deflector increases that makes the device more unstable to external mechanical vibrations. One of possible reasons causing such vibrations can be vacuum pumps, located near the BSM. The problem of external vibrations was faced for the first time during the tests of BSM GSI UNILAC. Since operation RF-field frequency for UNILAC is low – 108.408 MHz, the RF-deflector is long – 610 mm.

The external vibrations can lead to instability of electrical operational frequency of RF-deflector, which is crucial problem for measurements.

The mechanical and electrical analysis of the BSM was provided to find a solution how to eliminate this effect.

EXPERIMENTAL RESULTS

The oscillations of the registered secondary emission electrons beam intensity were obtained. Usually, phase measurements are provided with the phase steps from 1° to 5°, that seems sufficient for typical bunch lengths.

In the Fig. 2a-c the results of BSM measurements are shown for different phase steps. Experimental points were taken for each beam pulse with 3.6 Hz repetition rate. The curve clearly shows modulation with the period equal to about 3.2 s. The amplitude of modulation can be estimated from Fig. 2a and is equal to 4÷5°. The fluctuations of the secondary electron beam intensity disappear with increasing of a phase step (Fig. 2b, c). Obviously, that the oscillations appear during the experiment if the average time of the electric field phase adjustment inside the deflector is more times less than the characteristic vibrations period. For the period of oscillation, about 3.2 s and the amplitude about 5°, the modulation of 2.5° is completed at the quarter of the period, i.e. about 0.8 s. The phase of RF-field is adjusted by 0.29° during this time.

The Fig. 2a-c shows that the modulation decreases with the phase step 0.5° and disappear completely with the phase step 2°.

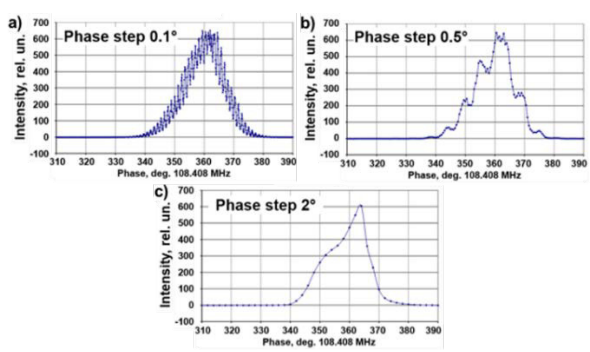

Figure 2(a -c): Experimental bunch shape measurements. Displacements of the vacuum pump changed the effect quantitively but did not remove it completely.

† dmitriy.chermoshentsev@phystech.edu

ISBN: 978-3-95450-197-7 doi:10.18429/JACoW-RUPAC2018-THPSC36

EXPERIMENTAL STUDY OF THE TRANSVERSE BEAM SIZE USED A FAST WIRE SCANNER IN THE U70 AT IHEP

V. Kalinin, V. Baranov, O. Lebedev, G. Khitev, Institute for High Energy Physics (IHEP) of NRC "Kurchatov Institute", Protvino, Moscow Region, 142281, Russia

Abstract

Results of experimental study of the transverse beams size in the U70 synchrotron based on a fast wire scanner are given. Measurements of the transverse beam size were carried out at three special points of the U70 synchrotron magnetic cycle: on the injection flat top (1.3 GeV proton, 0.455 GeV/u carbon); in the region of the transition energy (7.959 GeV proton); on the main flat top (49 GeV proton). Results of the fast wire scanner approbation for determination of transverse injection errors and evaluating transverse feedback efficiency are presented.

INTRODUCTION

The goal of this work is to study the transverse dimensions of light-ion beams (protons and carbon) in various operating modes of the accelerator. The implementation of such studies contributes to an increase in the efficiency of the accelerator and to the improvement of the quality of the output beam. The possibility of such work is due to the commissioning of vertical and horizontal fast wire scanner. The horizontal scanner is located in vacuum chamber with a length of 600 mm in a 104 rectilinear gap. The vertical scanner is located in a 550 mm long vacuum chamber in a 94 rectilinear space. Betta functions for these sections are equal to β_R = 26.8 m, β_Z = 27.6 m. Scanners are developed on the basis of servomotor and servo controller and are described in [1]. The speed of intersection of the beam with a carbon filament in them was V = 16 m / sec. Stages of development of measurement systems for the profile of a circulating beam in IHEP are also presented in [2].

REGISTERING EQUIPMENT

Two secondary scintillation detectors with plastic scintillators with a high gain and with a time resolution of ~ 8-10 ns (SSDI-8 based on the SNFT3 photomultiplier and detectors based on the photomultiplier tube PMT-30) have been installed near the vacuum chamber to detect secondary radiation arising from the crossing of the circulating beam with a carbon filament. The use of such detectors allowed recording beam profiles along a coaxial cable up to 400 m long directly on an oscilloscope or ADC for a load of 50 Ohms and to observe each bunch as well as the entire beam profile. Taking into account the need to perform measurements both at the injection energy and with the carbon beam, we chose a carbon filament with a diameter of ~ 200 μm. The installed filament consists of a bundle of stranded 5 μm filaments. The created equipment allows detecting profiles of the proton beam in the energy range (1.3 ÷ 70 GeV) and intensities (10^{10}÷10^{13}), as well as beam of carbon nuclei in the energy range (0.455 ÷ 35 GeV/ nucleon) and intensity (10^9÷10^{10}) $^{12}C^{+6}$.

STUDY RESULTS

Measurements on the Injection Flat Top Magnetic Field 355 G

Measurements of the transverse dimensions of the beam on the injection plateau make it possible to estimate and correct such important parameters of the accelerator complex as: the dimensions of the output beam from U1.5; bug input errors from U1.5; stability of the magnetic field plateau; work of orbit corrections; position of the working point on the plane (Q_R, Q_Z); work of corrections of quadratic and cubic nonlinearities; analog narrow-band and digital broadband transverse feedback systems works, etc. The results of measuring the vertical and horizontal dimensions of the proton beam at an intensity I=5·10^{12} protons are shown in Fig. 1.

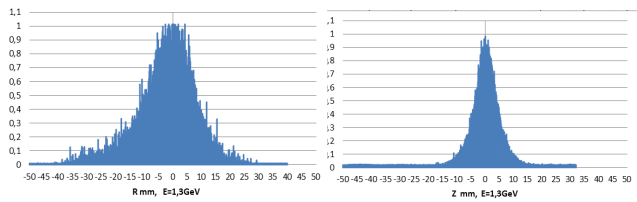

Figure 1: Transverse profiles of the proton beam (left – horizontal, right – vertical), 1.3 GeV and 5·10^{12} ppp.

The results of measuring the vertical and horizontal dimensions of the carbon beam (455 MeV/u) at an intensity I=3·10^9 $^{12}C^{+6}$ are shown in Fig. 2.

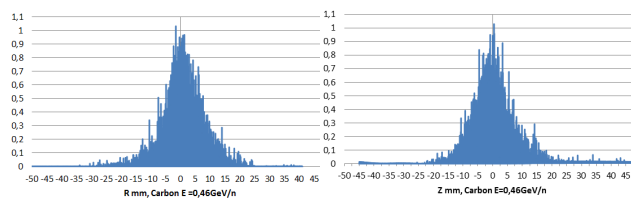

Figure 2: Transverse profiles of the carbon beam (left – horizontal, right – vertical), 455 MeV/u injection flat top magnetic field 355 G.

Measurements at the Transition Energy

The transition energy of a particular point in the acceleration of particles in a synchrotron is described in detail in [3]. The acceleration through transition can be accompanied by an increase in the transverse dimensions of the beam. The main factors influencing the beam size: an increase momentum dispersion associated with longi-

ISBN: 978-3-95450-197-7 doi:10.18429/JACoW-RUPAC2018-THPSC37

PHOTO-ACTIVATION METHOD FOR DETERMINATION ELECTRON ENERGY OF LINEAR ACCELERATOR*

S.V. Mitrofanov†, V.G. Shabratov, Yu.G. Teterev, V.V. Kobets, A.E. Brukva, JINR, Dubna, Moscow region, Russia
T.V. Tetereva, MSU SINP, Moscow, Russia
M. Krmar, University Novi Sad, Novi Sad, Serbia

Abstract

Unknown energy of electron beam of linear accelerator LINAC-200 was estimated by photo activation of only one activation detector – foil of natural indium. Four different photonuclear reactions were considered: ^{115}In(γ, γ')^{115m}In, ^{115}In(γ, n)^{114m}In , ^{115}In(γ, 2n)^{113m}In and ^{113}In(γ, 2n)^{111}In. Ratio of saturation activities R(^{113m}In)/R(^{115m}In), R(^{114m}In)/R(^{115m}In) and R(^{111}In)/ R (^{115m}In) were determined by standard gamma spectroscopy in electron energy region of interest (10 MeV – 23 MeV) using indium foils exposed in the FLNR Microton MT25 bremsstrahlung beam. The choice of cyclic accelerator MT25, as a reference machine, was made due to the fact, that the energy of its electrons is known with accuracy not worse than 1%. Same ratios of saturation activities were determined after exposition of In activation detectors in photon beam of linear accelerator. The fact that both irradiations, by Microton MT25 and accelerator LINAC-200, were performed in identical geometry using same target (3 mm of Tungsten) allowed us to estimate electron energy of accelerator by comparison of ratios of saturation activities obtained by both machines. Small variation in accelerator electron current was taken in consideration [1].

INTRODUCTION

The energy of electrons accelerated in linear accelerator wave guide (and maximal energy of bremsstrahlung produced as well) is one of the most important parameters. Although the principle of electron acceleration by EM wave is well known, determination of maximal accelerating potential and electron energy is not straightforward. The photoactivation reactions are usually method of choice for energy calibration of bremstrahlung endpoint energy. Direct measurement of energy spectra of accelerated electrons using some solid state detector (BGO or LaBr) can be very fast and confident method for linear accelerator monitoring. However, accurate energy calibration of detectors in MeV region is a problem that cannot be ignored.

In this work we would like to present simple method developed at JINR for fast determination of electron energy of linear accelerator LINAC-200. Method consists of three stages:

i) determination of ratios of saturation activities of several products of photonuclear reactions on selected target exposed to photon beam of Microtron MT25. Obtained ratios of saturation activities of several products of photonuclear reactions determined in the broad region of Microtron photon energies were used as calibration ones considering that energy of electrons accelerated in MT25 is known with accuracy up to 1%;

ii) exposition of same activation detectors in photon beam of linear accelerator. It is very important to underline that photon beam of LINAC-200 is produced in Tungsten target of Microtron. Ratios of obtained saturation activities obtained were determined and used to estimate energy of accelerated electrons by comparison with Microtron derived ratios of saturation activities

iii) measurement of single electron spectra by the use of BGO detectors positioned directly in the electron beam of linear accelerator. Estimated electron energies were used to calibrate BGO detectors in high energy region.

DESCRIPTION OF METHOD

The yield of products of photonuclear reaction can be described by the saturation activity R:

$$R = \int_{E_{th}}^{E_{max}} \sigma(E) \cdot \Phi(E) \cdot dE \qquad (1)$$

where σ (E) is cross section for observed nuclear reaction Φ (E) is flux of photons, E_{th} is the energy threshold for nuclear reaction and E_{max} is the maximal energy of photons. The activity of the isotopes after the exposure was measured by the HPGe spectrometer. The saturation activity can be experimentally determined using the intensity of a single gamma line in recorded gamma spectra as:

$$R = \frac{N_\gamma \lambda M}{m N_{Av} \varepsilon \eta p_\gamma e^{-\lambda \Delta t}\left(1-e^{-\lambda t_{irr}}\right)\left(1-e^{-\lambda t_m}\right)} \qquad (2)$$

where N_γ is the number of detected gamma photons of chosen energy, λ is the decay constant, M and m are the mass number and the mass of the activation detector used, N_{Av} is Avogadro number, ε is the efficiency of the detector at the chosen energy, η is the natural abundance of activated isotope, p_γ is the quantum yield of detected photons, Δt, t_{irr} and t_m are cooling, irradiation and measurement time respectively.

It was chosen to use ratios of saturation activities of two or more products of photonuclear reactions for energy calibration. In this case a number of parameters related to exposition and measurements of activation detector disappear. Due to the difference in the energy dependences of the cross sections for different photonuclear reactions, ratio of saturation activities is still function of bremsstrahlung endpoint energy. Natural Indium, in the form of tiny discs was chosen to be activation detector because four photonuclear reactions can be followed

ISBN: 978-3-95450-197-7 doi:10.18429/JACoW-RUPAC2018-THPSC38

OPTICAL FIBER BASED BEAM LOSS MONITOR FOR THE BINP E-E+ INJECTION COMPLEX

Yu.I. Maltseva*, V.G. Prisekin,
Budker Institute of Nuclear Physics SB RAS, Novosibirsk, Russian Federation

Abstract

A distributed optical fiber based beam loss monitor has been implemented for the Budker INP Injection Complex designed to accelerate and store electron and positron beams up to 500 MeV. The principle of the device operation consists in detecting the Cherenkov radiation generated in an optical fiber by relativistic charged particles produced in an electromagnetic shower when beam hits the accelerator vacuum chamber wall. Single optical fiber section can cover the entire accelerator instead of using a large number of local beam loss monitors. Timing of optical signal gives the location of the beam losses along the beamline. In this paper summary of the monitor application at the BINP Injection Complex is given. Methods to improve monitor spatial resolution are discussed.

INTRODUCTION

Since 2016 Injection Complex [1–3] supplies two BINP colliders with high energy electron and positron beams (up to 500 MeV). In order to control beam losses along beamline during the Complex operation we proposed to use a distributed beam loss monitor based on the Cherenkov effect in an optical fiber [4].

This type of beam loss monitor has been developed at several facilities such as FLASH (DESY), SPring-8 (RIKEN/JASRI), CLIC Test Facility (CERN) [5–7]. The monitor overview is given by T. Obina [8].

Compared with other distributed beam loss monitors such as long ionization chamber and scintillating fiber, optical fiber beam loss monitor (OFBLM) has the following advantages: fast response time (< 1 ns), near zero sensitivity to background signal (mainly gamma radiation) and synchrotron radiation, unlike scintillating fiber. Optical fiber is insensitive to magnetic field, but it is susceptible to radiation damage (except quartz fiber), which limits fiber lifetime. Another disadvantage of the OFBLM is its signal calibration.

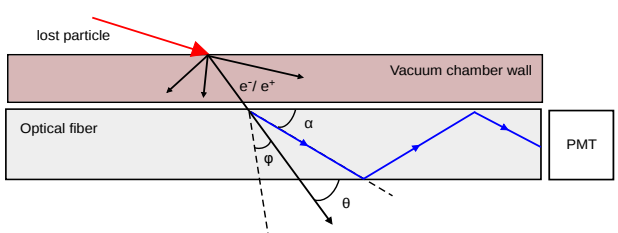

Figure 1: Scheme of beam loss monitor.

The basic idea behind the OFBLM is to detect a burst of the Cherenkov radiation (CR) generated in the optical fiber (OF) by means of relativistic particles created in electromagnetic shower after highly relativistic beam particles (electrons or positrons) hit the vacuum pipe. Some of the Cherenkov photons propagate in the fiber and can be detected by photomultiplier tube (PMT) (Fig. 1). For electromagnetic shower simulation G4beamline code [9] was used.

CHERENKOV RADIATION GENERATION

To generate the CR the kinetic energy of charged particle propagating through a dielectric medium must satisfy the condition: $E_k > E_0(n/\sqrt{n^2-1}-1)$, where E_0 – particle rest energy, n – medium refractive index. According to our simulations, for the CR to be generated kinetic energy of lost particles hitting the vacuum pipe must be greater than 5 MeV for electron or positron beam. The CR is emitted in a cone around the moving charged particle with cone semi-angle, $\cos\varphi = 1/(\beta n)$. Since the average kinetic energy of the electron component of the shower is about 15 MeV, the CR photons are emitted with 48°.

The number of the CR photons generated by single electron or positron per unit radiation wavelength λ per unit path length x of the particle in a medium is given by:

$$\frac{d^2N}{d\lambda dx} = \frac{2\pi \sin^2\varphi}{137\lambda^2} \quad (1)$$

According to eq. (1), the greater part of the CR photons is emitted in the ultraviolet (UV) range of the spectrum. For relativistic electron passing through the plastic OF (n = 1.49) the number of the CR photons generated in UV-visible spectrum (300 nm < λ < 700 nm) per mm is equal to 50.

CHERENKOV LIGHT PROPAGATION IN OPTICAL FIBER

Main Principle

The emitted CR propagates in the OF by means of total internal reflection with angles $\alpha \le \alpha_{max} = \sin^{-1}(NA/n_c)$ relative to the fiber axis (see Fig. 1), where NA – OF numerical aperture, n_c – refractive index of the OF core. For plastic OF with typical values of NA = 0.47 and n_c = 1.49, $\alpha \le 18°$. For quartz one with NA = 0.22 and n_c = 1.46, $\alpha \le 9°$. Thus, the greater NA, the higher the number of propagating photons.

Neglecting attenuation effects, the portion of total CR photons to be transmitted in the fiber by guided rays is given by [10]:

$$P = \frac{1}{\pi}\cos^{-1}\left(\frac{\beta n_c \cos\alpha_{max} - \cos\theta}{\sin\theta\sqrt{\beta^2 n_c^2 - 1}}\right) \quad (2)$$

* yu.i.maltseva@inp.nsk.su

ISBN: 978-3-95450-197-7 doi:10.18429/JACoW-RUPAC2018-THPSC39

LUMINESCENT DIAGNOSTICS OF LOW INTENSITY PROTON BEAMS AT INR RAS LINAC

A. I. Titov†, S. A. Gavrilov, Institute for Nuclear Research of the Russian Academy of Sciences, Moscow, Russia and Moscow Institute of Physics and Technology (State University), Moscow, Russia

Abstract

INR RAS linear accelerator is a high-intensity accelerator, mostly used for rare isotopes production and neutron experiments. However low-intensity beam research is also presented at INR linac and requires appropriate diagnostics, such as luminescent diagnostics, which is implemented at a new proton irradiation facility. Important experimental results of beam position, size and intensity measurements during accelerator run are discussed.

INTRODUCTION

INR RAS linear accelerator is a high-intensity accelerator mostly used for isotopes production and neutron experiments. However low-intensity experiments such as irradiation of materials and proton therapy are also presented and require diagnostics that can provide information about beam parameters such as position, size and pulse charge (C/pulse) (or pulse intensity measured in particles/pulse). System of luminescent diagnostics is an appropriate one.

Luminescent diagnostics is one of the oldest methods of obtaining beam position and size and is already used for more than a century as a particle detector [1]. At INR linac system of luminescent diagnostics is implemented at the proton irradiation facility and consists of luminescent screen, CCD camera and software designed for image processing. Figure 1 shows a layout of its components.

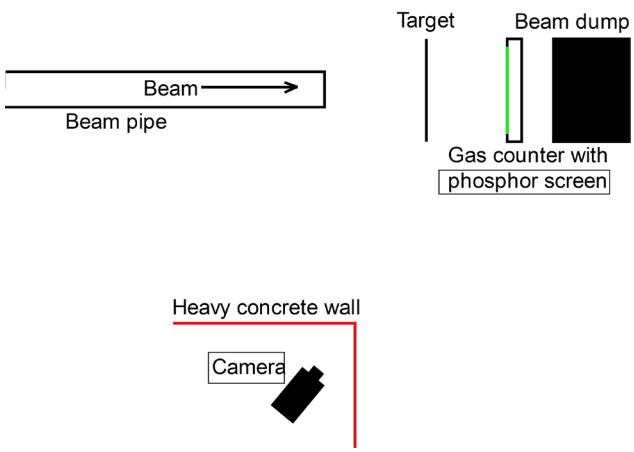

Figure 1: Layout of luminescent diagnostics components at INR PIF.

While passing through the scintillator screen, beam particles interacts with luminophore molecules which emit light. This makes feasible to measure beam position and size. Moreover, for many scintillators amount of emitted light is linear to pulse charge in a wide range of beam intensities, which makes luminescent diagnostics appropriate for measuring beam charge.

DESIGN FEATURES

Phosphor screen is a P43 luminophore molten with Kapton™ which is attached to multianode gas counter, another diagnostics method on proton irradiation facility (Fig. 2). Phosphor screen is 100*100 mm^2 and has coordinate grid on it.

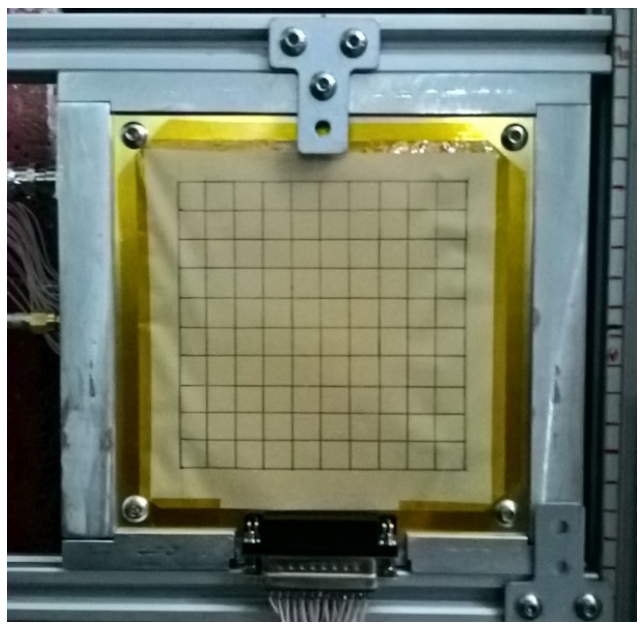

Figure 2: Phosphor screen.

CCD camera which is used for image registration is hidden behind heavy concrete wall to decrease camera irradiation during PIF operation. Basler acA780-75gm [2] monochrome camera with 75 mm focal length lens is used for image registration. Camera is connected with a PC in a control room by a GigE standard cable. There is an interesting fact that cable length is 130 m, which is considered inappropriate for Gigabit Ethernet standard, however camera still works correct with this limit exceed.

SOFTWARE FEATURES

Camera is displaced non-perpendicularly to luminescent screen plane and luminophore image is distorted. To solve this problem a LabVIEW [3] program was written to make an image correction. It uses several

† aleksandr.titov@phystech.edu

ISBN: 978-3-95450-197-7 doi:10.18429/JACoW-RUPAC2018-THPSC40

MULTIANODE GAS COUNTER FOR LOW INTENSITY BEAM DIAGNOSTICS AT THE INR LINAC

A.Melnikov†, S. Gavrilov,
Institute for Nuclear Research of the Russian Academy of Sciences, Troitsk, Moscow, Russia and
Moscow Institute of Physics and Technology (State University), Moscow, Russia

Abstract

Multianode gas counter is used to measure beam intensity in ionization mode and profiles in proportional mode at a new INR RAS proton irradiation facility. A special model is created in COMSOL to simulate operational characteristics of this counter. A program for data acquisition and processing is based on LabVIEW. Operational characteristics of the counter and experimental results of beam measurements are presented. Upgrade of the existing software and hardware is discussed.

INTRODUCTION

A proton irradiation facility (PIF) at INR RAS linac is used to study radiation effects in electronic components. This facility is characterized with working parameters: proton energy - 20÷210 MeV; particles per pulse - 10^7÷10^{12}; pulse duration - 0.3÷180 μs; pulse repetition rate - 1÷50 Hz.

Partially diagnostics was realized with a beam current transformer (BCT) installed in the beam pipe. It provides absolute nondestructive measurements of beam pulse current with the amplitude > 25 μA. The BCT is not applicable for less intensive beams and for measurement of beam profiles. In this case induced field detectors do not work. Detectors based on gas ionization are widely used for low intensity beams. One of the ways to measure beam current and profiles is to collect ionization particles.

MULTIANODE GAS COUNTER

Multianode gas counter (MGC) consists of 5 plates (Fig. 1) which are printed-circuit boards made of FR4 with 0.5 mm width. The metal covering is 18 μm nickel, plated with 0.5 μm immersive gold.

Three central plates, which collect electrons of primary ionization at the middle anode in a quasi-uniform electrostatic field, form dual gap ionization chamber. This part of the detector allows to measure beam current in an ionization mode.

Lateral regions are proportional chambers for beam position and profile measurements. Electrons come to the anodes of a multichannel structure, which consists of 25 stripes with 100 μm width, 100 mm length and 4 mm spacing. Strong nonuniform field around stripes leads to electron avalanches, increasing the signal.

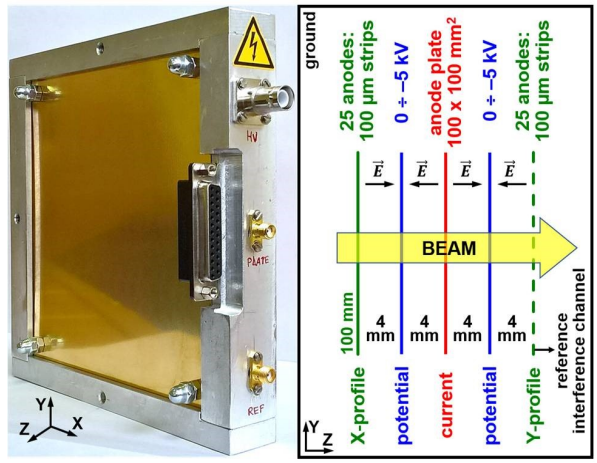

Figure 1: MGC photo and layout.

Modeling of this detector helps to find out operational characteristics of this counter, voltage range of power supplies and suitable gain of read-out electronics.

IONIZATION CHAMBER

The filling gas is atmospheric air: 80% N_2 and 20% O_2 molecules at standard conditions. The amount of primary ionization electrons was calculated according to [1, 2], (Fig. 2).

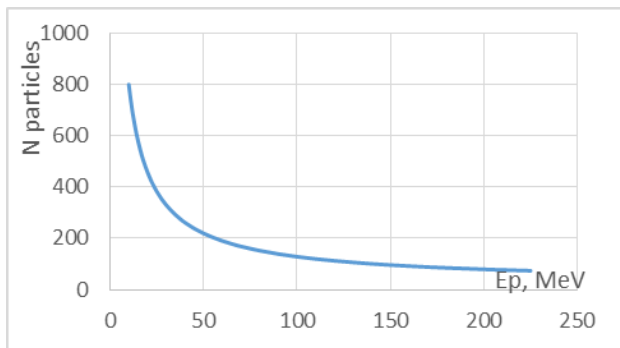

Figure 2: Number of primary electrons produced by an incident proton depending on its energy in the 4 mm gap.

Primary particles drift in the electric field undergoing various types of collisions with N_2 and O_2 molecules [3] (Fig. 3).

† aleksey.melnikov@phystech.edu

ISBN: 978-3-95450-197-7 doi:10.18429/JACoW-RUPAC2018-THPSC42

NUMERICAL INVESTIGATION OF THE INFLUENCE OF THE MAGNETIC FIELD IN THE ION SOURCE WITH THE PENNING DISCHARGE OF A GAS-FILLED NEUTRON TUBE ON THE ION CURRENT PULSE*

D. S. Stepanov†, E. Ya. Shkolnikov, National Research Nuclear University (MEPhI), 115409, Moscow, Russian Federation
A. V. Agafonov, The Lebedev Physical Institute of the Russian Academy of Sciences (LPI RAS), 119991, Moscow, Russian Federation

Abstract

The report examines the influence of the distribution and intensity of a magnetic field in the ion source with the Penning discharge of a gas-filled neutron tube on the shape and amplitude of the ion current pulse. The study was carried out by means of numerical modelling using the KARAT code. The ion source has a length of 1.1 cm, the length of the anode is 0.6 cm with its diameter of 1.1 cm. Atomic deuterium is used at a pressure of 1 mTorr as the residual gas. A ring-shaped hot cathode with an internal diameter of 4 mm and an external diameter of 6 mm with an electron current of 10 mA is considered as the discharge trigger. The anode voltage pulse has an amplitude of2.5 kV and a front of 0.5 μs. The magnetic field is created by a 1.1 cm long solenoid with a diameter of 2.3 cm, the magnetomotive force of which ranged from 2 kA to 4 kA. The change in the distribution of the magnetic field was achieved by moving the solenoid along the longitudinal axis. The base case with respect to which the magnetic field ranged has an ion current pulse amplitude of 700 μA at a rise time of 2.5 μs. The displacement of the solenoid towards the cathode entails an increase in the ion current pulse amplitude up to 1 mA, but at the same time it leads to its spreading. The transfer of the solenoid toward the anticathode shortens the front of the ion current pulse, but leads to a decrease in its amplitude to 350 μA. At the low magnetic field intensity, the current pulse front becomes steeper, but the pulse itself has a more sinusoidal shape with an amplitude of 600 μA. An increase in the magnetic field intensity entails an increase in the duration of the pulse front and an increase in its amplitude up to 450 μA, while retaining a pulse shape close to rectangular.

INTRODUCTION

At present time, the method of the neutron logging of oil-and-gas wells requires the new generation of gas-filled neutron tubes capable of generating the neutron pulses with the short fronts [1]. The form of the neutron pulse in the modern gas-filled neutron tubes (GNT) is determined mainly by the operating mode of the ion source that generates and delivers the directed deuterium ions beam towards the neutron-generating target. The rising front of the ion current pulse is bound to be less than 1 μs, and the value of the ion current is to be of the order of 400 μA. It is appropriate to search for methods of an achievement of such an operating mode of GNT with the help of the numerical simulation.

SETTING A NUMERICAL MODEL

The numerical simulation has been conducted by means of code KARAT [2] in the axially symmetric geometry with the dimension 2.5D. Figure 1 shows the model of a gas-filled neutron tube with the ion source of the Penning type [3] for code KARAT and the ion current pulse, generated with it. The cylindrical anode voltage is equal to 2.5 kV and its front duration is 0.5 μs. The cone-shaped electrode in the right part of the model has potential equal to –2.5 kV and simulates potential of the accelerating electrode that has potential equal to –100 kV. The coil 1.1 cm long creates the magnetic field and 2.3 cm in average diameter, which magnetomotive force varies from 2 to 4 kA that corresponds to the average value of the magnetic field induction equal to 1 – 2 kGs. The source is filled with the atomic hydrogen at the pressure 1 mTorr. The ring electron beam, emitted from the cathode surface that is enclosed by circles with radii equal to 2 and 3 cm, is used as the initiator of discharge.

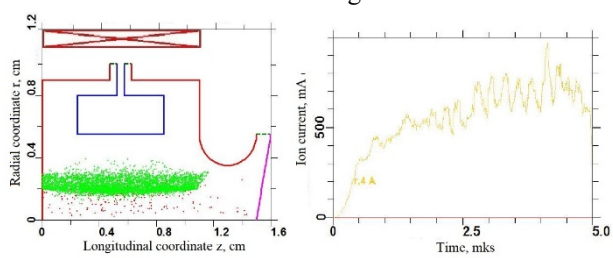

Figure 1: Model of the ion source of the Penning type (on the left) and extracted ion current (on the right).

At the numerical simulation of the plasma processes, the crucial issue is the spatial mesh size. A numerical model has to take into account the action of the electromagnetic field on the plasma particles; therefore, the size of the computation cell has to be much less than the Debye layer or the skin depth. The Debye radius is determined only for the thermalized plasma whereas the skin depth is the dynamic parameter. Initiation of discharge takes place due to the directed electron beam; the continuous generation and loss of ions and electrons occur. At the same time, when the volume density of the charged particles is equal to $10^{10} – 10^{11}$ cm^{-3} and their energies are

* Work supported by Ministry of Science and Education of the Russian Federation under the agreement No. 14.575.21.0169 (RFMEFI57517X0169).
† DSStepanov@mephi.ru

ISBN: 978-3-95450-197-7 doi:10.18429/JACoW-RUPAC2018-THPSC47

CHARACTERISTICS OF LASER-PLASMA ION SOURCE BASED ON A CO_2-LASER FOR HEAVY ION ACCELERATORS AT ITEP

A.A. Losev, A. Balabaev, I. Hrisanov, T. Kulevoy, Yu. Satov, A. Shumshurov, A. Vasilyev
NRC «Kurchatov Institute» - ITEP, 117259 Russia, Moscow

Abstract

The design of laser-plasma heavy ion source is described. This ions source is supposed to operate at I-3 and I-4 accelerators at ITEP. Characteristics of ion component of plasma produced by pulses of the CO_2 laser were studied, when irradiating a solid carbon target at power density of $10^{11} \div 10^{12}$ W/cm^2. Time-of-flight technique using a high-resolution electrostatic energy analyzer was applied to explore charge state and energy distribution as well as partial currents of carbon and tungsten ions. Some results of investigation of influence of cavern formation on charge state of generated ions are presented. This work is of considerable interest in a wide area of applications of accelerated particle beams, including fundamental studies of state of matter in particle colliders (NICA project at JINR), radiation damage simulation and hadron therapy for cancer treatment. The goal of this work is to investigate characteristics of ions in expanding laser plasma and find optimal conditions of target illumination and ion beam extraction. This research is valuable for adapting an intensive beam from laser ion source to the accelerator, improving acceleration efficiency and rising the amount of accelerated particles.

SCHEMATIC DIAGRAM OF THE HIGH CURRENT ION INJECTOR

Schematic diagram of the high current heavy ion I-4 (ITEP) is shown on Fig. 1.

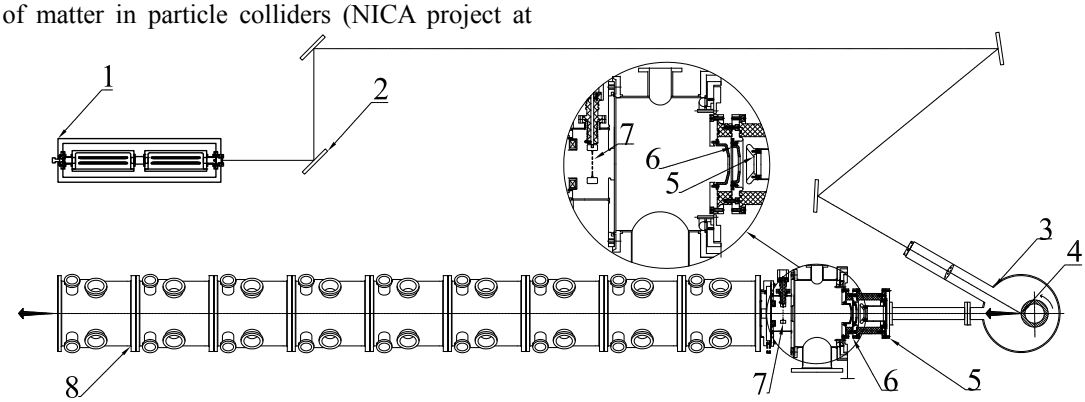

Figure 1: Schematic diagram of ion injector I-4.

It consists of two-modules CO_2 pulsed laser generator *1* which radiation is transported by copper mirrors *2* to the entrance tube of the vacuum chamber *3* that has the internal diameter of 350 mm. Then the laser beam is focused to the target *4* with the spherical lens. The target rotates around the geometrical axis and shifts up and down during operation to avoid a crater formation in the target material. The laser beam falls on the target angularly (30º) but the surface normal coincides with the time of flight tube axis and laser plasma expansion direction. The extraction system consists of three electrodes: positive *5*, negative *6* and grounded (interelectrode distances are 40 and 20 mm, accordingly). Positive extraction electrode is placed at the distance 1680 mm from the target. Its passage opening of 40 mm is closed by the grid. Gridded lens *7* is used to match the ion beam with the RFQ section *8* entrance. The RFQ section main characteristics are frequency–81.36 MHz, z/A≥1/3, injection energy–0.02 MeV/u, output energy–1.6 MeV/u, maximum ion current–100 mA. The system operates in repetition rate mode up to 0.2 Hz.

CHARACTERISTICS OF LASER BEAM

CO_2 laser setup [1] operates at a high level of the specific energy deposition into a self-sustained discharge. It provides laser beam with high quality of spatial and temporal characteristics:

- pulse energy – 7 J
- peak power – up to105 MW
- FWHM duration – 30 ns
- Beam divergence – close to diffraction limit

These parameters are reproduced during long term operation.

Flat mirrors transport the laser beam into the vacuum chamber. Then laser radiation is focused on the target surface by exchangeable spherical lenses with different focal length to vary power density in the range of $8 \cdot 10^{10} \div 8 \cdot 10^{11}$ W/cm^2. A typical shape of the spatial distribution of the energy density in the focal spot is close to Gaussian and its width is between 200 ÷ 600 μm.

ISBN: 978-3-95450-197-7 doi:10.18429/JACoW-RUPAC2018-THPSC48

MAGNETRON PROTON SOURCE

O.K. Belyaev, B.A. Frolov, E.A. Konoplev, A.M. Korotkov
NRC«Kurchatov Institute», IHEP, 142281, Protvino, Moscow region, Russia

Abstract

The design and preliminary experimental results for magnetron proton source with a cold cathode are presented. To produce nonuniform magnetic field at the emission aperture the permanent circular NdFeB magnets with opposed polarity placed outside the ceramic chamber of source have been used. 110 mA impulse beam current with the energy of 100 keV at 1Hz frequency and 25 μs pulse duration has been received. Normalized emittance equals to 0.8 π mm·mrad .

INTRODUCTION

The most important question of linear accelerator LU-30 with the radio-frequency quadrupole focusing (RFQ) reliability operation is the operational integrity of its injection system. The injection system includes an ion gun with a protons source and an extraction system of ions from the plasma and focusing lenses. From the injection system the beam enters in the initial part of accelerator (RFQ linac). The beam capture, formation and acceleration to 2 MeV happen in the RFQ. At the present time the source of duoplazmotron type with a cold-cathode developed by V.V. Nizhegorodsev over 35 years ago is applied as the source of protons [1]. The long-standing practice of using the source with a non-glow cathode showed its high reliability and cathodes long service life. This source has proven good performance for many years of its operation. Proton beam phase characteristics generated by this source meet the linear accelerator LU-30 source requirements. It provides the beam necessary quality requirements, but its construction is critical in many parameters and it is difficult in adjustment and operation.

During the LU-30 operation it was investigated that the breakdowns frequency in the RFQ linac is not less, but often more than the breakdowns frequency in the main part of the LU-30 accelerator with the spatially periodic quadrupole focalization followed by the RFQ linac. It should be noted that the electrical field strength on the RFQ linac electrodes is 225 kV/cm and on the electrodes of the main part of accelerator it is 380 kV/cm. The RFQ linac electric strength reduction process increases in time due to the high content of impurities in the generated ion beam. This is explained by the contamination of the RFQ linac electrodes by the work products used in the construction of a proton source in which PTFE, organic glass and vacuum rubber are widely applied. Contamination process is irreversible and removing impurities by the cleanup is not possible. The only way out of the situation is the RFQ linac electrodes replacement and application of a new proton or ion source H-minus source.

It should be noted that there are two ways to increase the proton source emission ability and to receive plasma with high density at the design stage: either to increase the number of particles bombarding the emission surface or to increase the emission surface. When designing the source V.V. Nizhegorodtsev chose the first approach. As a result the hydrogen supply in discharge chamber source is done impulsively at relatively high pressure, which causes significant gas inleakage into the accelerator. In pulsed mode of source work with high pulse repetition rate (16.7 Hz) the vacuum pumps of high efficiency are required to provide source electric strength and to prevent beam scattering on residual gas which reduces phase density.

At the present time IHEP is developing a proton source of magnetron type with simpler and more reliable design. In the developed protons source of magnetron type with inverted cathode the surface area emitting electrons is increased substantially, and the application of the above mentioned materials is limited. As a prototype the ion source with a cold magnetron cathode and magnetic plasma contraction developed in the Sukhumi Physics-Technical Institute was selected [2,3].

SOURCE CONSTRUCTION

The main elements of the magnetron protons source with a cold cathode and magnetic contraction of plasma are shown in Fig. 1. The discharge source chamber is installed in a longitudinal magnetic field and it can be divided into three areas: auxiliary discharge area (magnetron cathode area), general discharge area (the main anode and magnetic plasma contraction area) and plasma expansion area (expander with conical insert) [2].

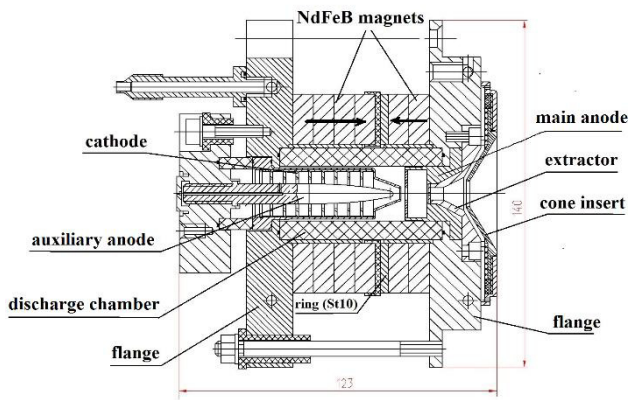

Figure 1: Magnetron proton source.

ISBN: 978-3-95450-197-7 doi:10.18429/JACoW-RUPAC2018-THPSC50

METHODS FOR PRODUCTION OF INTENSE METAL ION BEAMS AT THE DC-60 CYCLOTRON

V.N. Loginov, A.E. Bondarchenko, K.I. Kuzmenkov†, S.L. Bogomolov, V.E. Mironov,
FLNR, JINR, Dubna, Moscow Region, Russia
I.A. Ivanov, M.V. Zdorovets, E.K. Sambayev, V.V. Alexandrenko, A.E. Kurakhmedov, S.G. Kozin,
M.V. Koloberdin, D.A. Mustafin, Astana Branch of Institute of Nuclear Physics, Astana,
Kazakhstan

Abstract

The paper is devoted to the description of research conducted in 2017-2018 at the accelerator complex DC-60 of the Astana branch of INP, on production and acceleration of intense ion beams of solids.

The main purpose of this work was to develop techniques for obtaining accelerated ions using evaporation method and the volatile compounds (MIVOC) method. The development of these techniques will significantly expand the range of accelerated ions, which gives particular relevance to the purpose of the study. With the increase in the spectrum of accelerated elements, the possibilities of posing, searching for and solving new problems and experiments in the field of experimental nuclear physics, solid-state radiation physics, and various applied problems will increase.

INTRODUCTION

The DC-60 cyclotron [1] is designed for acceleration of ions from Li to Xe with A/Z in the range from 6 to 12. The accelerator is equipped with the normally-conducting 14-GHz DECRIS-3 ion source [2]. The main parameters of the source are: magnetic fields at the injection and extraction sides of the source are 1.3 and 1.1 T respectively, the hexapole field at the wall is 1.0 T, the source chamber length is 20 cm, and the chamber diameter is 6.4 cm. Microwaves are injected into the source through the coaxial waveguide along the source axis. The extraction voltage of the source is up to 25 kV.

We use three different methods for metal ion production: evaporation of material from large volume crucible heated by microwaves in the source chamber, evaporation from a filament-heated oven, and injection into the source of volatile compounds that contain the desired atoms.

When producing ions of the solid elements, thin cylindrical tantalum sheet is inserted into the source chamber to facilitate atom recycling from the walls [3]. As a support gas, we always use helium, which was found to be the best choice for production of moderately charged ions requested by the DC-60 cyclotron.

MIVOC PRODUCTION OF IONS OF SOLID ELEMENTS

MIVOC (Metal Ions from Volatile Compounds) method is based on use of metal compounds that have a high vapor pressure at room temperature [4]. Ferrocene Fe $(C_5H_5)_2$ has a vapor pressure of 2.6×10^{-3} Torr at 20 °C, and dicarba-*closo*-dodecaborane compound $C_2B_{10}H_{12}$ has a vapor pressure of about 1-2 Torr. Using these compounds, intense beams of B and Fe ions were obtained for the first time at the DC-60 cyclotron of Astana Branch of INP.

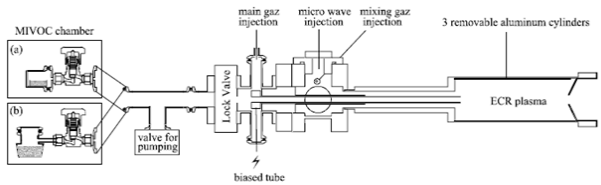

Figure 1: Schematic view of MIVOC chamber connection to ECR ion source.

Compound is placed into a glass container connected to the gas transport line at the injection side of the source. No extra heating of the container is needed, and the gas flow into the source is regulated by a needle valve. (Fig.1)

Up to 25 μA of $^{56}Fe^{10+}$ ions were extracted at the optimized conditions (Fig.2) with Fe consumption of 0.8 mg/h.

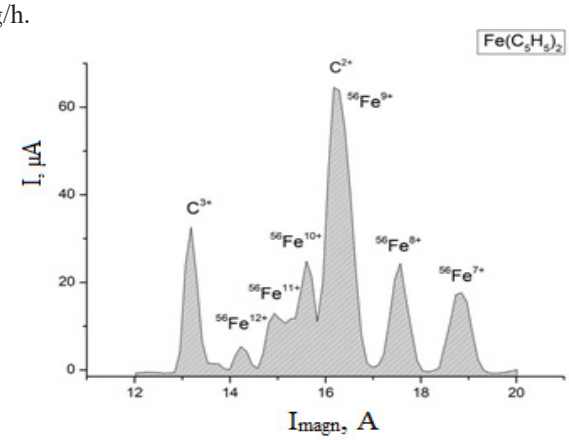

Figure 2: Charge state distribution of the extracted Fe ions.

The maximum current of $^{11}B^{2+}$ is up to 60 μA. Spectrum of the extracted boron ions is shown in Fig. 3. Consumption of the compound is about of 1.2-1.4 mg/h.

† e-mail: k.i.kuzmenkov@gmail.com

ISBN: 978-3-95450-197-7 doi:10.18429/JACoW-RUPAC2018-THPSC53

TEST STAND RESULTS OF CW 100 mA ELECTRON RF GUN FOR NOVOSIBIRSK ERL BASED FEL*

V. N. Volkov†, V. Arbuzov, E. Kenzhebulatov, E. Kolobanov, A. Kondakov, E. Kozyrev, S. Krutikhin, I. Kuptsov, G. Kurkin, S. Motygin, A. Murasev, V. Ovchar, V.M. Petrov, A. Pilan, V. Repkov, M. Scheglov, I. Sedlyarov, S. Serednyakov, O. Shevchenko, S. Tararyshkin, A. Tribendis, N. Vinokurov, BINP SB RAS, Novosibirsk, Russia

Abstract

Continuous wave (CW) 100 mA electron rf gun for injecting the high-quality 300-400 keV electron beam in Novosibirsk Energy Recovery Linac (ERL) and driving Free Electron Laser (FEL) was developed, built, and commissioned at BINP SB RAS. The RF gun consists of normal conducting 90 MHz rf cavity with a gridded thermionic cathode unit. Bench tests of rf gun is confirmed good results in strict accordance with our numerical calculations. The gun was tested up to the design specifications at a test bench that includes a diagnostics beam line. The rf gun stand testing showed reliable work, unpretentious for vacuum conditions and stable in long-term operation. The design features of different components of the rf gun are presented. Preparation and commissioning experience is discussed. The latest beam results are reported.

INTRODUCTION

Recent projects of advanced sources of electromagnetic radiation [1] are based on the new class of electron accelerators where the beam current is not limited by the power of rf system – energy recovery linacs (ERLs). Such accelerators require electron guns operating in continuous wave (cw) mode with high average current. The only solution is an rf gun, where the cathode is installed inside the rf cavity. There are no back bombardment ions in rf guns so there are no cathode degradation, and vacuum condition does not important there. The most powerful Novosibirsk FEL [2] can be more powerful by one order on magnitude with this rf gun [3-5] (see Table 1).

RF GUN AND DIAGNOSTIC STAND

The rf gun and diagnostic stand are presented in Fig. 1.

The RF gun cavity is made on the base of standard bimetallic cavity of Novosibirsk ERL. Detailed information can be found in [3-5]. Only the insert with the thermionic cathode-grid unit is built into the cavity. The gridded thermionic dispenser cathode is driven by special modulator with GaN rf transistor. The insert focusing electrode executes the strong rf focusing on the beam just near the cathode that ensures the beam emittance compensation at the relatively low electric field at the cathode. Also it ensures the absolute absence of dark currents in the beam.

* Work supported by Russian Science Foundation (project N 14-50-00080)

† v.n.volkov@inp.nsk.su

There are in the stand: 30 kW water cooled beam dump with 5 cm lead radiation shield, wideband Wall Current Monitor (WCM2) inserted into the replaceable target, Transition Radiation Sensor, the pair of standard WCM, three focusing solenoids, and the testing cavity.

Table 1: Measured rf Gun Characteristics

Average beam current, mA	≤100
Cavity Frequency, MHz	90
Bunch energy, keV	100 ÷ 400
Bunch duration (FWHM), ns	0.06 ÷ 0.6
Bunch emittance, mm mrad	10
Bunch charge, nC	0.3 ÷ 1.12
Repetition frequency, MHz	0.01 ÷ 90
Radiation Doze Power, mR/h	100/2m
Operating pressure, Torr	10^{-9}…10^{-7}
Cavity RF loses, kW	20

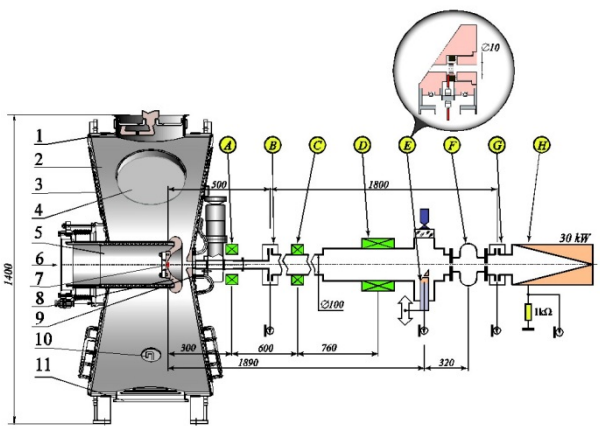

Figure 1: Rf gun and stand layout: 1-Power input coupler; 2- Cavity shell; 3-Cavity back wall; 4-Sliding tuner; 5-Insert; 6-Cathode injection/extraction channel; 7-Thermionic cathode-grid unit; 8-Concave focusing electrode; 9-Cone like nose; 10-Loop coupler; 11-Vacuum pumping port; A-Emittance compensation solenoid; B-First Wall Current Monitor (WCM); C, D - Solenoids ; E-Wideband WCM and transition radiation target; F – Test Cavity; G-third WCM; H-Faraday cup and Water-cooled beam dump.

STAND TESTING RESULTS

Beam Current Regulation

There are some methods of beam current increasing: decreasing of the grid bias voltage (V_{bias}), increasing of

ISBN: 978-3-95450-197-7 doi:10.18429/JACoW-RUPAC2018-THPSC56

CODE FOR SIMULATION OF DIFFRACTION RADIATION FROM FLAT FINITE SURFACES

D. A. Shkitov, Tomsk Polytechnic University, Tomsk, Russia

Abstract

In this report a description of developed diffraction radiation simulation code is presented. This code is suitable for calculating the diffraction radiation characteristics (angular and spectra distributions) from flat finite surfaces (compound targets) for charge particles with different energies and for wavelength range from optics to mm. The code can be used for transition radiation simulation too.

INTRODUCTION

Nowadays practically all investigations and developments in physics content the simulation as one of the big part of research. The simulation allows predict many characteristics of objects in the physical investigations and saves a time as well. The accelerator physics is not an exception.

The large and important part of this science area is diagnostics. Practically all accelerators must be constructed with special diagnostic tools. One of the phenomena which apply in order to control the accelerator is the diffraction radiation (DR) which already has a long history [1]. The application history of DR for the beam diagnostics counts a little bit more than 20 years [2]. At the moment DR has several fields of application such as transversal sizes [3], bunch length [4], and emittance [5] diagnostics. And until now a new idea how to use DR in diagnostics is proposed [6].

This radiation occurs when charged particles move close to a target [7]. There are several DR calculation methods which were developed in the past. But all of them are analytical [8] and contain series assumptions, for example, infinite target size, far field zone approximation [9] and so on. We know only one theory with analytical solution in near field zone but for transition radiation (TR) case [10].

However, until now there are no special codes for DR simulation from different types of targets. All researchers have to develop their own numerical codes to calculate DR characteristics for their cases (target size, geometry of task, detector location, optical system presence and other) or have to use the analytical formulas. This is the general way how the most researchers do.

It is need to be noted that there are codes which can be used to calculate DR properties: *CST* [11] and *KARAT* [12]. *CST* is a well-known commercial 3D electromagnetic (EM) code. *KARAT* is 3D EM code based on particle-in-cell (PIC) solver which belongs to the state institute. With all advantages of these codes, they require large experience from the users in order to start simulation the DR characteristics (as practically all big computational program).

Mentioned that code *ZEMAX* [13] can also be applied for working with DR. But this code was developed for optics and, based on our knowledge, require to preliminary calculate the DR field which should be input into *ZEMAX* [14]. It may be only additional tool in diagnostics approach development based on DR.

In this report we present the code for DR characteristic calculations from metal targets with finite dimensions and finite distance to detector. Our code is written on *Wolfram Language* (WL) [15]. It represents a set of files which contain the internal and custom functions. These functions allow to calculate the EM fields of DR from arbitrary finite flat surfaces. Despite the fact that *Wolfram Mathematica* (WM) is also commercial product, on our knowledge almost all academic institutions have and use it.

Our mathematical model is the integration equations and is based on the exact solution of Maxwell's equations. That's why this code is implemented, in other world, on the semi analytical approach in comparison with fully numerical *CST* [16] and *KARAT* [17]. Moreover, mentioned that it is need significantly less time to obtain the results to use our code.

CODE AND TARGETS DESCRIPTION

Developed code is just two main files (**.m* format) written on WL. First file contains the custom functions which calculate all three EM component and intensity of DR. Second file contains the custom functions which allow to create the geometry of the targets. These two files should be launched after starting WM session and before the simulation. The files structure is divided into 2 parts: the function description and functions themselves.

The schematic view of the process simulated in the code depicts on Fig. 1, where θ_0 is the target rotation angle and η is the observation angle. Charge particle EM field interacts with the target surface and after this the radiation is produced which is registered by the detector.

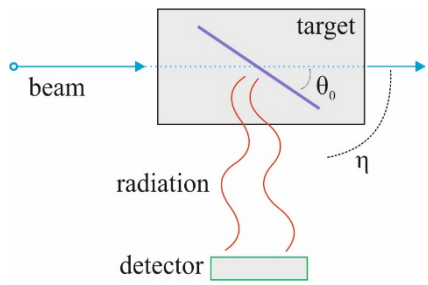

Figure 1: A schematic view of charge particle interaction with a target and radiation registration by a detector.

Email address: shkitovda@tpu.ru